THE UNIVERSITY *of* EDINBURGH

Lewis acidic metal complexes with polydentate ligands for the preparation of biorenewable polymers

Sergio A. Gamboa

The University of Edinburgh

Submitted for the degree of Doctor of Philosophy

30th September 2013

Declaration

The work described in this thesis is entirely my own, except where I have either acknowledged help from a named person or given reference to a published source. Text taken from another source will be enclosed in quotation marks and a reference given. This thesis has not been submitted, in whole or in part, for any other degree.

Signature:

Acknowledgements

I would first like to thank Prof. Polly Arnold for her support and guidance before and during my studies. The Mexican Consejo Nacional de Ciencia y Tecnología (CONACYT), the Engineering and Physical Sciences Research Council (EPSRC) and the University of Edinburgh are thanked for their financial support.

I would also like to acknowledge everyone who directly or indirectly contributed to my formation as a chemist, especially past and present members of the Arnold and Love groups.

I thank God for the opportunity to work and learn during these studies; the support offered by my wife, family and friends was very valuable to me, too.

Lay Summary

The present document states the experiments carried out for the study of the reactivity of chemical compounds containing metal ions supported by intricate alcohols or by similar species rich in electrons. Given the generalised interest to store or utilise the excess amount of carbon dioxide in the atmosphere, these compounds were studied for their interaction with such a molecule. Furthermore, the compounds were preliminarily probed as catalysts for the formation of polycarbonates, which are plastics with better strength and transparency than the ubiquitous PET and PS. The production of polycarbonates requires the combination of cheap and reactive molecules with carbon dioxide. Finally, the compounds were also used to initiate the formation of biodegradable plastics from renewable molecules found in corn and wood. The utilisation of some of these compounds aiding the manufacture of useful plastics may provide another way to preserve our planet by creating useful everyday materials from renewable (non-fossil) sources and by making use of the greenhouse gas carbon dioxide.

Abstract

Due to the ever increasing necessity to reduce our dependence on fossil fuels as feedstocks for polymeric materials, the work presented herein describes the investigation of new metal complexes as initiators for the formation of polyesters and polycarbonates from renewable monomers. These polymers are regarded as biodegradable and have the properties required to replace traditional plastics in applications such as food packaging, electronic devices, and medical biomaterials.

Chapter one introduces previous literature relevant to the research on which this study focuses; ligands based on alkoxides, phosphine oxides and *N*-heterocyclic carbenes with alkoxide or amino pendant groups, as well as the metal complexes in which they are used. Current methods of polymerisation and copolymerisation and the initiators utilised are also examined.

Chapter two contains the design and synthesis of $[M(L^R_n)]_m$ metal complexes where L^R is $[(R)_2P(O)CH_2CH(^tBu)O]^-$ and R is Ph or ^{t}Bu. Divalent metal centres such as Co^{II} and Zn^{II} have been used for the formation of the studied compounds. Studies on their reactivity as initiators for polymerisations are also described.

Chapter three presents the utilisation of di- and tridentate ligands, with one or two NHC species respectively, for the synthesis of $[M_x(L^Y_n)]$, where M is Cu^I, Zn^{II} or Ti^{III} and L^Y is an alkoxy-tethered NHC species or a 'CNC' tridentate ligands with an amino derivative as bridge. Their reactivity and ability to act as initiators for polymerisation reactions was also examined.

Chapter four comprises overall conclusions of this work and the impact of these investigations.

Chapter five outlines the experimental details and data for the compounds presented.

Table of contents

CHAPTER 1. INTRODUCTION

1.1 The need for renewable monomers

In recent years, the environmental problem of greenhouse-gas pollution caused by human activity has received much attention in both political and scientific arenas. Governments have found little success in the arriving at sensible agreements that make scientific sense because the setting of environmental laws and caps for the emission of carbon dioxide is generally viewed as detrimental to the economy. Hence, the current trend is not ecological; for instance, about 6 millions of plastic bottles are used in the UK every hour,[1] leading to the consumption of high quantities of fossil fuels and energy, thus producing more greenhouse gases of which the most abundant is carbon dioxide.

The energy required for the execution of human activities is mainly harvested from the combustion of fossil fuels, which are largely made up of hydrocarbons. The complete oxidation of these hydrocarbons results in the inevitable formation of water and carbon dioxide. These molecules are key for the subsistence of life given that the autotrophs, and hence all other living beings, rely on them as nutrients; unfortunately, the amount of carbon dioxide in the atmosphere surpasses what is required by nature. According to reports offered by the Intergovernmental Panel on Climate Change (IPCC),[2] more than 40 gigatonnes of carbon dioxide are released to the atmosphere each year, which is equivalent to 77% of the total anthropogenic greenhouse gas emissions. As the production of carbon dioxide and other greenhouse gases grows with time, societies are forced to utilise their resources to minimise their effect on the environment and to reduce their emissions; these initiatives are called ‘adaptation to global warming’ and ‘mitigation’, respectively. It is thought that to avoid the point where adaptation to the climate change will no longer be feasible, a peak of 1800 gigatonnes of total CO_2 should not be exceeded by the end of the 21st century.[2] Two general approaches can be used to address the resulting environmental problem. These are:

(1) to reduce the emissions of CO_2 through the use of alternative energy sources such as hydrogen and nuclear energy; and

(2) to convert it back into useful feedstock molecules – returning it to the carbon cycle.

The most convenient approach is (2) since it requires fewer changes in our industrial technologies and also in our lifestyle. However, carbon dioxide is a thermodynamically stable molecule with a bond dissociation energy of 532.2(4) kJ/mol (comparable to $H_3C–CH_3$ with 368 and $H_2C=NH$ with 644(21) kJ/mol).[3] For instance, the enthalpy of the generation of hydrogen from carbon monoxide and water is a clear example of the thermodynamic stability of carbon dioxide, as seen in Scheme 1.1.

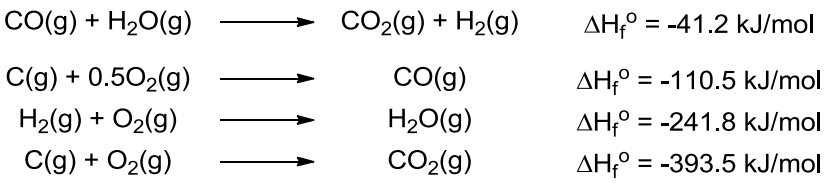

Scheme 1.1. Calculation of the enthalpy for the formation of hydrogen from carbon monoxide.[4]

The thermodynamics of the various conversions of carbon dioxide are well-understood, and for its conversion to other useful molecules and feedstocks to be energetically feasible, it must react with high-energy molecules such as hydrogen, unsaturated compounds, small-membered ring compounds or organometallics, to form mainly oxygen-containing products such as lactones, esters, carboxylic acids, carbamates and carbonates.[5] The use of a catalyst, to lower the activation energy of the process, speed up the reaction, and control the products is the final important key to the energy-favoured and chemoselective conversion of CO_2 back into useful products such as the ones mentioned above and their polymers. In addition to carbon dioxide, for the preparation of valuable polymers, there are other useful and biorenewable monomers readily available such as lactide, glycolide and diverse epoxides. As mentioned before, suitable catalysts, especially metal complexes, are essential for efficient polymerisations.

1.2 Overview of metal complexes of alkoxides, carbenes and other ligands for catalysis and asymmetric synthesis

The study of metal alkoxides began in the late 1870s, when the first examples for titanium and aluminium were published.[6] Among the numerous types of reactions for the formation of alkoxides and aryloxides (see Scheme 1.2) the reaction of metal disubstituted amides is advantageous because the liberated amine is generally highly volatile, which facilitates purification of the metal alkoxide.[7] Generally bound as two-electron donors, alkoxides may contain a variety of functional groups or include chiral centres, which increase their versatility as catalysts. Among the first claims of chiral metal alkoxides assisting reactions are the works of Landor *et al.*[8] in which complexes based on lithium aluminium hydride and glucose derivatives catalyse a hydrogenation process from carbonyls to enantiomerically pure alcohols (see Equation 1.1). Other metal alkoxides have been used in polymerisation catalysis; for instance, the aluminium and yttrium alkoxides of a ligand featuring a hybrid between 2,2'-bis(diphenylphosphino)-1,1'-binaphthyl (BINAP) and N,N'-ethylene bis(salicyl-imine) (salen) (**II**) was probed for the polymerisation of lactide (LA) resulting in heterotactic and syndiotactic polymers (see Figure 1.1).[9]

$$M^0 + nROH \longrightarrow M(OR)_n + (n/2)H_2$$

$$M^{n+} + nRO^- \longrightarrow M(OR)_n$$

$$M(vapour) + 2ROH \longrightarrow M(OR)_n + H_2$$

$$MCl_n + (x+y)ROH \longrightarrow MCl_{n-x}(OR)_x(ROH)_y + xHCl$$

$$n{:}B + nROH + MCl_n \longrightarrow M(OR)_n + n(BH)^+Cl^-$$

$$M(OH)_n + nROH \longrightarrow M(OR)_n + nH_2O$$

$$M(OR)_n + xR'OH \longrightarrow M(OR)_{n-x}(OR')_x + xROH$$

$$M(OR)_n + nMeCOOR' \longrightarrow M(OR')_n + nMeCOOR$$

$$M(NR_2)_n + xR'OH \longrightarrow M(OR')_x(NR_2)_{n-x} + xHNR_2$$

$$M(OCOR)_n + nNaOR \longrightarrow M(OR)_n + NaOCOR$$

Scheme 1.2. Main reactions for the preparation of alkoxides and aryloxides

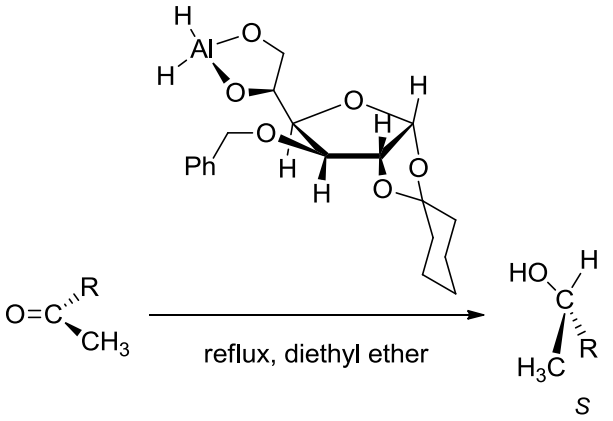

Equation 1.1. Reduction of ketones to enantiomerically pure alcohols using a chiral metal alkoxide.[8]

Other species that also show high enantioselectivity in alkyl additions are catalysts containing *N*-heterocyclic carbenes (NHC).[10] In particular, Rix *et al.* found that these catalysts have higher selectivity when the stereogenic centre is located within any or both of the two *N*-side chains, instead of in the backbone of the *N*-heterocyclic ring.[11] In addition, a catalyst containing a stereogenic centre in the α-position relative to the alkoxide, instead of in the β-position as previously presented by Arnold *et al.* (see Scheme 1.3 for a comparison of NHC ligands bearing a chiral *tert*-butyl in different positions),[12] gives enantiomeric selectivity of up to 97% enantiomeric excess (*ee*) for related conjugate additions (Scheme 1.3c shows the conjugated addition of diethylzinc to 2-cyclohexenone, which results in a lower *ee* than the addition of a Grignard reagent to 3-(1-propenyl) 2-cyclohexen-1-one).[13]

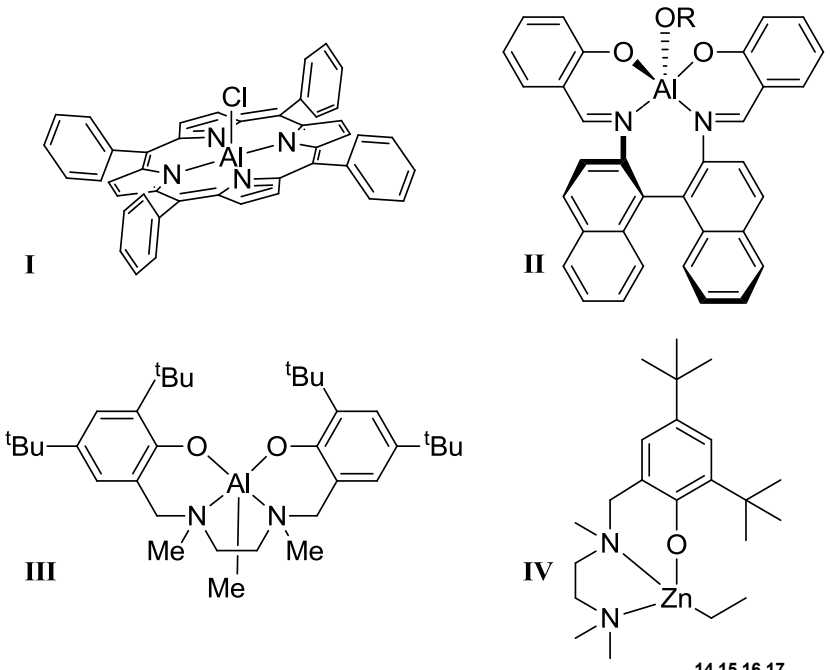

Figure 1.1. Catalysts based on porphyrins and alkoxides.[14,15,16,17]

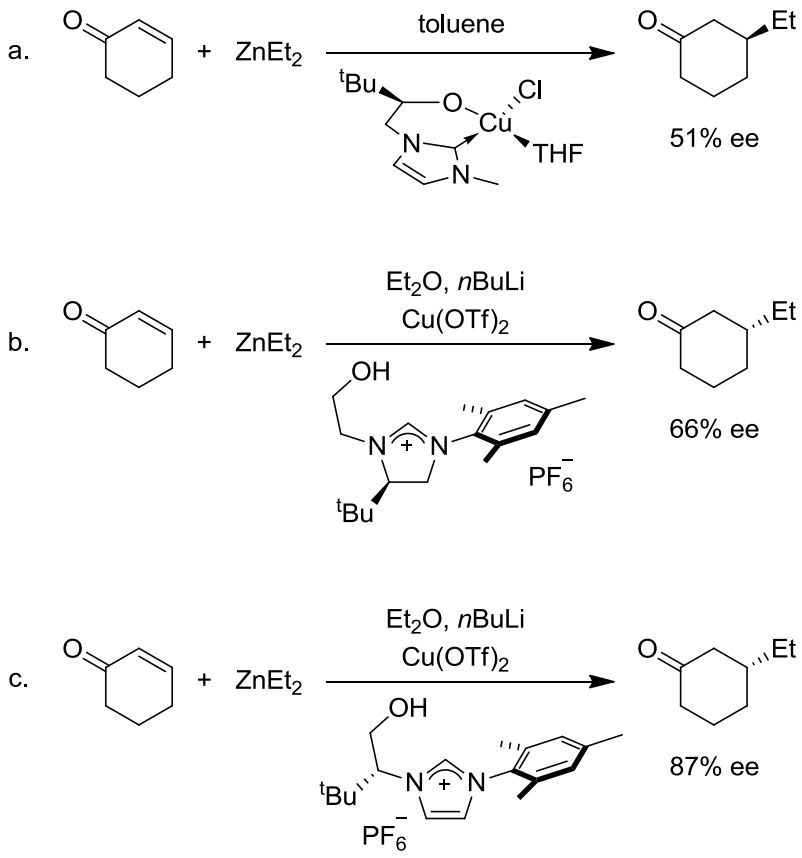

Scheme 1.3. Examples of copper-catalysed asymmetric conjugate addition. Insight into the influence in enantioselectivity of the position of a chiral *tert*-butyl group in the alkoxy-tethered NHC ligands

NHCs generally require the activation or deprotonation of a precursor for their coordination to metal centres, although many of them can persist as free carbenes.[18,19] NHCs are very electron-rich ligands, especially when compared to other more traditional ligands such as phosphines. Furthermore, NHCs in general have similar electron-donating character, whereas phosphines, depending on the substituents on the phosphorus atom, can present a significant difference in their abilities to donate electrons.[20] Ligands containing phosphines, which have a relatively soft character (less basic) according to the Pearson acid-base concept,[21] can be more versatile when they also feature harder groups;[22] such is the case of an alkoxide/diphenylphosphine ligand that formed stable complexes of a wide range of soft and hard cations, from copper(I) (compound **V**) to rhodium(III) (compound **VI** in Figure 1.2). On the one hand, if the Lewis acid is softer, the metal-oxygen bond will be relatively labile for further chemistry; on the other hand, it is expected that the phosphine-metal interaction is weaker in complexes of harder Lewis acids.[23]

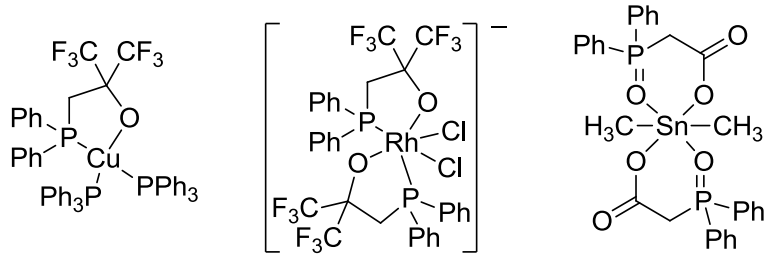

V VI VII

Figure 1.2. Metallic complexes containing phosphines and alkoxides as ligands.[23,26]

Another option is the oxidation of the phosphine group to phosphine oxide (or phosphinoyl) which, being a weak base, shows an intermediate hardness between phosphine and alkoxide. Phosphine oxide as a functional group provides a more robust ligand with similar tuneability to phosphines and the potential for hemilability when combined with other groups in the same ligand (compound **VII** in Figure 1.2).

1.3 Bidentate alkoxide/phosphine oxide ligands

In spite of being studied since the 1860s as ligands,[24] interest in the coordination chemistry of phosphine oxides grew only after they were found to be an essential part of effective solvents for the selective extraction of valuable metals such as uranium and zirconium during the 1950s.[25] The selective oxidation of phosphine ligands in compounds such as **V** and **VI** in Figure 1.2 produce phosphine oxides as part of bifunctional ligands. In order to understand their role in bifunctional ligands with carboxylic acid, Ng and Zuckerman treated a triorganotin(IV) borate with diphenylphosphinoyl acetic acid (see Scheme 1.4a) expecting to form triphenyltin(IV) (diphenylphosphinoyl)acetic acid tetraphenylborate. Instead, the tin-phenyl bond was cleaved and diphenyltin bis(diphenylphosphinoyl acetate) was formed (Scheme 1.4b), showing that it is likely that both donating agents (carboxylic acid and phosphine oxide) have similar tendency to bind to the Lewis acid. The analogous dimethyl complex (**VII**) was prepared from dimethyltin(IV) oxide and the corresponding acid (Scheme 1.4c); a neat structural analysis is reported using a variety of characterisation methods from infrared to Mösbauer spectroscopy (compound **VII** in Figure 1.2).[26]

a. $[(C_5H_6)_3Sn]^+[B(C_6H_5)_4]^- + (C_6H_5)_2P(O)CH_2CO_2H \longrightarrow [(C_5H_6)_3Sn\{(C_6H_5)_2P(O)CH_2CO_2H\}]^+[B(C_6H_5)_4]^-$

b. $(C_5H_6)_3Sn^+B(C_6H_5)_4^- + (C_6H_5)_2P(O)CH_2CO_2H \longrightarrow (C_6H_5)_2Sn[O_2CCH_2P(O)(C_6H_5)_2]_2$

c. $(CH_3)_2SnO + 2(C_6H_5)_2P(O)CH_2CO_2H \longrightarrow (CH_3)_2Sn[O_2CCH_2P(O)(C_6H_5)_2]_2$ (**VII**) $+ H_2O$

Scheme 1.4. Attempted reactions to understand the role of phosphine oxide in bidentate ligands

In the search for effective oxidation catalysts with the ability to enantiomerically resolve the oxidation products, chirality was introduced to the system along with metals in high oxidation state. 2-(Diphenylphosphinoyl)propanoic acid (Hdpop) was treated with V^{III}, Cr^{III}, Fe^{III}, Sn^{IV} and Mo^{VI} to give bis- and tris(dpop) complexes; structural data of vanadium tris(dpop) show only the homochiral (*R*,*R*,*R*) and (*S*,*S*,*S*) complexes in the racemic product. The Ti(IV) complex **VIII** and Mo(VI) complex **IX** of the chiral 2-(diphenylphosphoryl)-1-alkylethanol (Hdpoxeo) ligand (see Figure 1.3) were reported at the same time by Cross *et al*.[27]

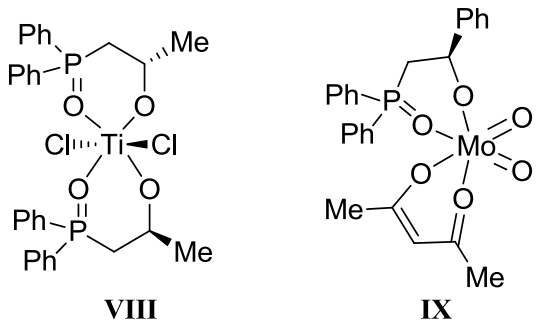

Figure 1.3. Examples of metal complexes from Hdpomeo (VIII) and Hdpopeo (IX) ligands.[27]

In 1962, Keough and Grayson reported reactions between various cyclic olefin carbonates with secondary and tertiary alkyl phosphines, which resulted in oxidation of the phosphine and liberation of the olefin from the carbonate in the presence of catalyst. Using secondary phosphines they invariably obtained the alkylene bis(phosphine oxide) corresponding to the carbonate used. Unexpectedly, when reacting diphenyl phosphine oxide with propylene carbonate in the presence of heptamethylbiguanide the product was 1-(diphenyl phosphinoyl)-propan-2-ol (Scheme 1.5**a**), or a mixture of it with the expected propylene-1,2-bis(diphenylphosphine oxide) depending on temperature.[28] At the same time, a study of the chemistry of bis(dialkylphosphinoyl)methanes was undertaken because of their importance as extractants of metal ions. Synthesis of these compounds ($R_2P(O)CH_2P(O)R'_2$) began with the lithiation of the corresponding dialkylmethyl phosphine oxide followed by the addition *in situ* of disubstituted phosphine oxide chlorides. Reaction of other species such as CO_2, aldehydes, ketones, and esters with the lithiated phosphine oxides resulted in new difunctionalised ligands with some activity as extractants of metal ions. Particularly, the reaction of the lithium salt of the methyl(diphenyl)phosphine oxide with aldehydes afforded β-hydroxyphosphine oxides similar to the one reported by Keough and Grayson (Scheme 1.5**a**).[29]

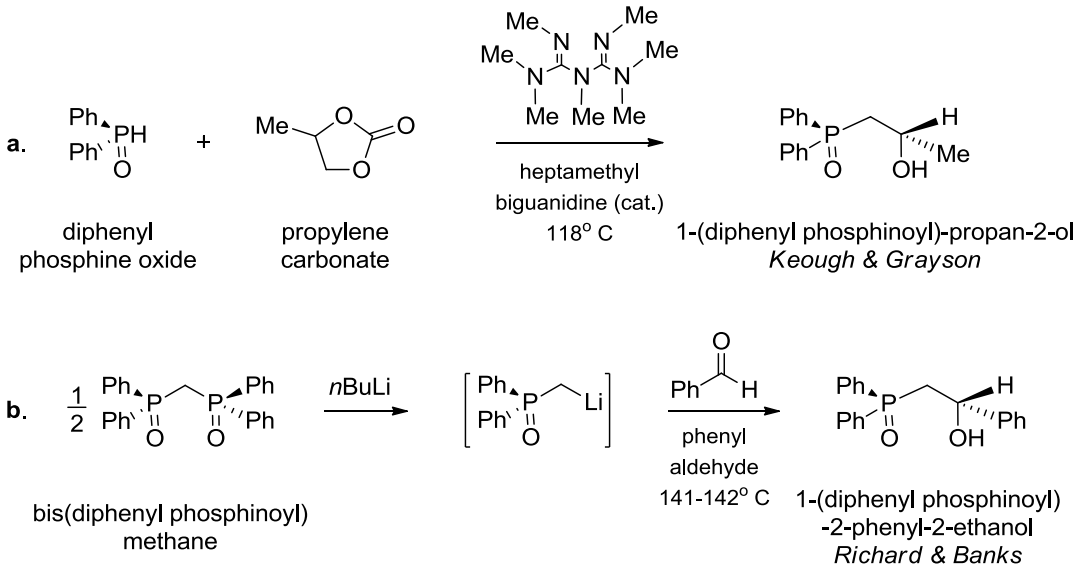

Scheme 1.5. Comparison between the first procedures for the synthesis of chiral proligands containing alkoxides and phosphine oxide[28,29]

The same procedure was followed to obtain unsaturated phosphine oxides through the method of Santelli-Rouvier[30,31] and to understand the different conformations of the β-hydroxyphosphine oxide compound in solution and solid state. Genov *et al.* found that these compounds form inversion-centre-related cyclic dimers and polymeric chains in the solid state due to hydrogen bonding. In solution, β-hydroxyphosphine oxides show a monomer-dimer equilibrium featuring intramolecular hydrogen bonding between the hydroxyl and the phosphinoyl group, especially favoured by the bulkiness of the alkyl groups on the phosphorus and the β-carbon.[32]

Arnold *et al.* improved the method reported by Cross *et al.*[27] for the synthesis of this type of ligands. Furthermore, the Arnold group studied their complexation around lanthanide ions. In these studies, the chiral character of the ligands was exploited for the preparation of homochiral metal complexes with potential applications in asymmetric catalysis, as shown in Equation 1.2.[33]

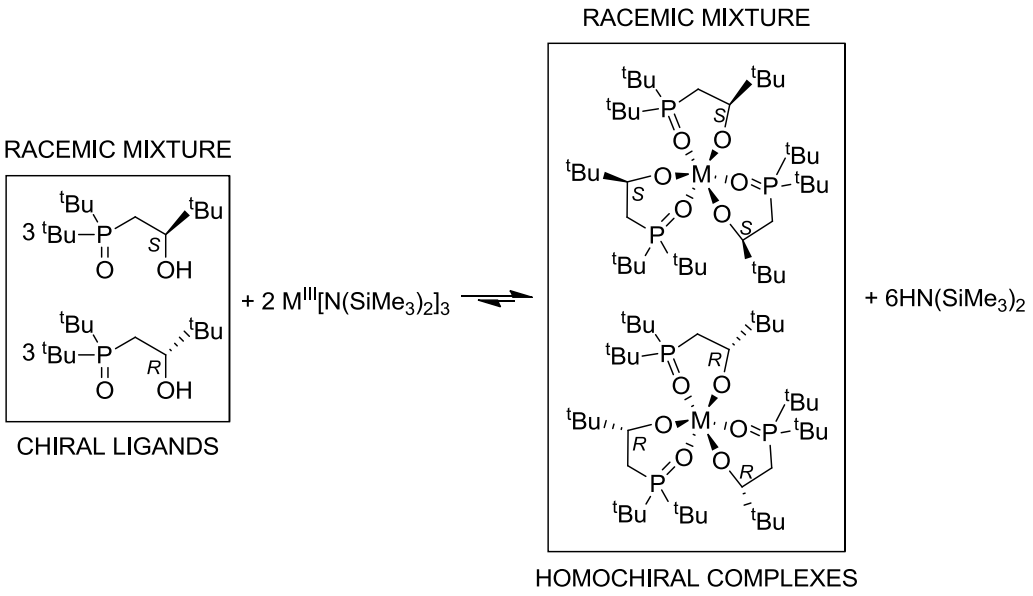

Equation 1.2. Spontaneous resolution of chiral proligands into homochiral metal complexes

A new family of homochiral complexes based on lanthanides was synthesised and tested as catalysts for ring-opening polymerisation. Homochirality was favoured when reacting a racemic mixture of the alkoxide ligand with lanthanides. The catalysts were identified as *rac*-Ln(L^{tBu})$_3$, where Ln = Y, Er, Eu; L^{tBu} = [(^{t}Bu)$_2$P(O)CH$_2$CH(^{t}Bu)O]$^-$.[33] The synthesis of the catalyst, using HL^{tBu} (**X**) and Ln[N(SiMe$_3$)$_2$]$_3$ as reagents, yielded 80% of the racemic mixture of *RRR*- and *SSS*-Ln(L^{tBu})$_3$ and 20% of the diastereomer (*RRS*)-/(*SSR*)-[Ln(L^{tBu})$_3$] showing the remarkable spontaneous resolution of the ligands. The ligands used to form the homochiral catalyst result in 'self-resolution' because they are rigid, sized to fit the correct number around the metal centre, project chirality, and assemble to generate the most compact structure.[34] This system has been used for the formation of complexes with other divalent and trivalent metals, for instance, the homochiral complex *rac*-Sn(L^{tBu})$_2$ (**XI** in Figure 1.4) with a square pyramidal geometry.[35] An analogous complex, **XII**, was prepared previously by Ionkin *et al.* fully oxidising the alkoxide/phosphine ligands already in the tin complex to alkoxide/phosphine oxide ligands as shown in Equation 1.3.[36] An account of the reactivity of this kind of complexes is found in Chapter 2.

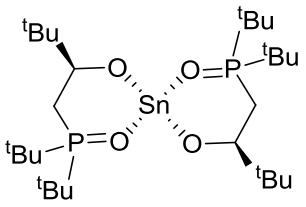

XI

Figure 1.4. Homochiral *R*,*R*-SnL$_2$

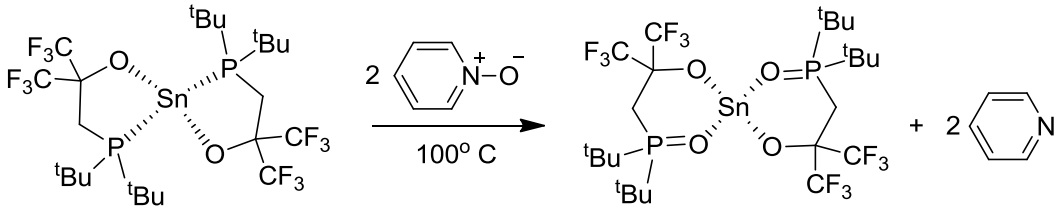

XII

Equation 1.3. Oxidation of the alkoxide/phosphine ligand into alkoxide/phosphine oxide ligand

1.4 Bidentate alkoxide/NHC ligands

Carbenes, in their ground state, have two non-bonding electrons that may be located in the same orbital with antiparallel spin, singlet state, or in separate orbitals with parallel spins, triplet state. The first example of an identified carbene was reported in 1954, with the first carbene in a metallic complex published ten years later.[37] There are two general categories for carbenes in a metal complex: Fischer carbenes which are mostly electrophilic due to their strong π acceptor character, and Schrock carbenes which show nucleophilicity and a π-donor character. These categories also correspond to the singlet and triplet state of the non-bonding electrons, respectively; these states are shown in Scheme 1.6. The singlet carbene, for instance, has a bent shape with nearly sp^2 geometry caused by one filled orbital and another empty one. The triplet carbene, on the contrary, presents a linear sp geometry in which the p_y and p_z orbitals are occupied and have parallel spins.

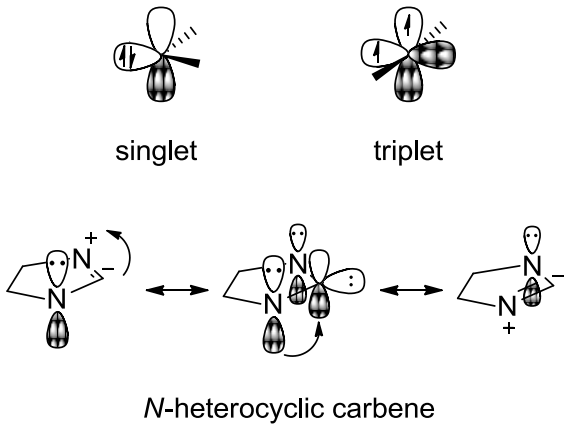

N-heterocyclic carbene

Scheme 1.6. Classes of carbenes and resonance structures of NHC

In *N*-heterocyclic carbenes, the singlet carbene is stabilised by the existing interaction of the lone pairs of electrons in the neighbouring nitrogen atoms and its empty p orbital, as is shown by the resonance structures in Scheme 1.6.[20] These resonance structures help understand why NHCs are electron-rich, present nucleophilicity, and have strong σ-donor properties and little or no π-acceptor character. In addition, these characteristics give rise to structural features such as the increase of the C2–N bond lengths and the decrease of the N–C2–N angle of an imidazolium salt when it is transformed into an NHC due to an increased σ-bond character (see Scheme 1.7).[20] Examples of NHCs are found binding practically to all metals in the periodic table; chemically, they react in a very similar way to tertiary phosphines because of their behaviour as strong σ-donor ligands and their poor backbonding character.[38]

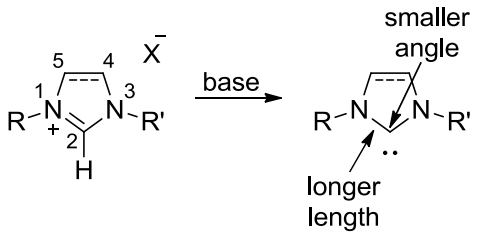

Scheme 1.7. Structural comparison of imidazolium salt and NHC.[20]

N-Heterocyclic carbenes have been used as organocatalysts in reactions such as olefin metathesis, carbon–carbon and carbon–nitrogen cross-coupling, hydrogenation and hydrosilylation. The uncommon characteristics of NHCs were reported by Wanzlick and further investigated by Öfele, describing their potential as ligands in metal complexes.[39] Twenty years later, Arduengo *et al.* isolated the first stable NHC which provoked much interest in this type of ligand.[19] There are numerous pathways for the synthesis of NHC-metal complexes with some of the most common being: the Lappert method, which involves the inclusion of a metal into the double carbon-carbon bond of bis(imidazolidin-2-ylidene) group in alkenes;[40] the generation of a free carbene by deprotonation of an imidazole by a base and the subsequent addition to the metal centre;[41,42] the transmetallation of a silver-NHC complex already synthesised by the addition of an imidazolium species with silver oxide;[43] the oxidative addition by activation of the C2-X (X=Me, I, H) bond of an imidazolium cation at low valent or metal hydride species; the direct metallation of an imidazolium salt with a basic metal precursor; and the thermal elimination of H-X from an NHC-alcohol or NHC-chloroform protected carbene.[44]

Inclusion of alkoxides into *N*-heterocyclic carbene ligands ensures stronger bonding toward Lewis acidic metal centres; in addition, the steric properties of the bifunctional ligand can be tuned by the presence of chiral centres in the original alkoxide ligand. One procedure for the synthesis of alkoxy-NHC ligands requires the regioselective reaction of a substituted 1,2-epoxide in its less hindered carbon centre with a monosubstituted imidazole as shown in Equation 1.4.[45]

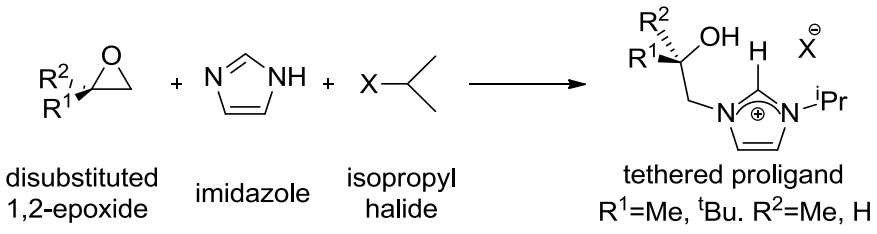

Equation 1.4. Synthesis of alkoxy-tethered proligands

Among the advantages of this system are that the ligands are electron rich and sterically tuneable; they also have simultaneous soft-hard character, they give the opportunity of having optically pure compounds by the choice of the epoxide precursor, and they can be tuned by varying the alkyl or aryl groups on the other N atom of the imidazole. The first NHC bearing a hard anionic donor in a metallic complex was reported by Arnold *et al.*;[45] similar complexes were probed for the catalysis of conjugate addition to cyclohexenone with considerable enantiomeric selectivity (51% *ee*).[12] Metal complexes of tridentate ligands including one NHC group have been studied; for instance, nickel salicylaldimine/NHC complexes were tested as catalysts for the polymerisation of styrene, as shown in Figure 1.5 **XIII**,[46] whereas similar palladium complexes with longer linkers between the imine and the NHC groups functioned for the Suzuki-Miyaura cross-coupling reaction (Figure 1.5 **XIV**).[47] Given that nickel complexes might offer economic and ecological advantages over palladium complexes as catalysts in cross-coupling reactions, Lee and his group synthesised a series of bis-bidentate nickel complexes with NHCs tethered by amido groups, as shown in Figure 1.5 **XV**.[48] These complexes proved more active than palladium analogues for the Suzuki-Miyaura reaction of certain aryl chlorides. The reactivity of these complexes has been studied by other groups using similar ligands based on NHCs for cross-coupling reaction (mainly Suzuki-Miyaura and Kumada-Corriu), the Michael addition reaction,[49] polymerisation of olefins,[46,50] and polymerisation of renewable monomers.[51]

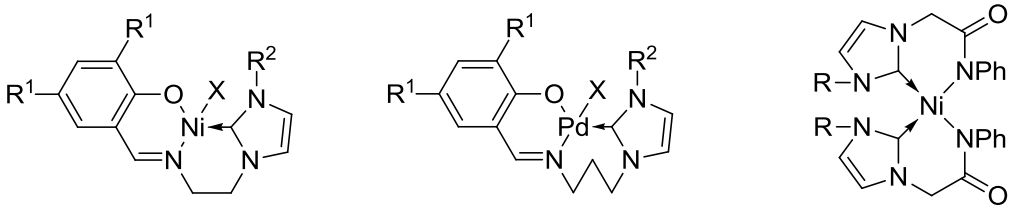

XIII **XIV** **XV**

Figure 1.5. NHC metal complexes as effective catalysts

1.5 Tridentate amine/NHC ligands

The Arnold group synthesised the first NHC-based tridentate ligand with an alkoxide functional group. This ligand was used to form copper complexes in its monovalent and divalent forms (see compounds **XVI** and **XVII** in Figure 1.6).[12,45] Meyer and his group synthesised other multidentate complexes in which the tetradentate ligands consist of three NHCs joined by a single anchoring centre resulting in a trigonal-planar geometry with a weak axial metal/donor interaction (See Figure 1.7 **XIX**).[52] The architecture of the ligands described was inspired by the work of Fehlhammer, who exchanged pyrazolyl groups from "scorpionates" for NHCs in the syntheses of iron complexes in which the metal centre has an octahedral coordination as shown in Figure 1.7 **XX**.[41] Similarly to Meyer's work, NHCs with multiple carbene groups were synthesised by Douthwaite *et al.* In this case the carbenes were anchored by an *N*-donor group. For the synthesis of the ligand, it is necessary to protect the secondary amine, used as backbone, with a benzyl moiety in order to avoid oligomerisation (see Scheme 1.8). Palladium complexes of this system were probed successfully for the catalysis of the Heck reaction and hydroamination of alkenes.[53]

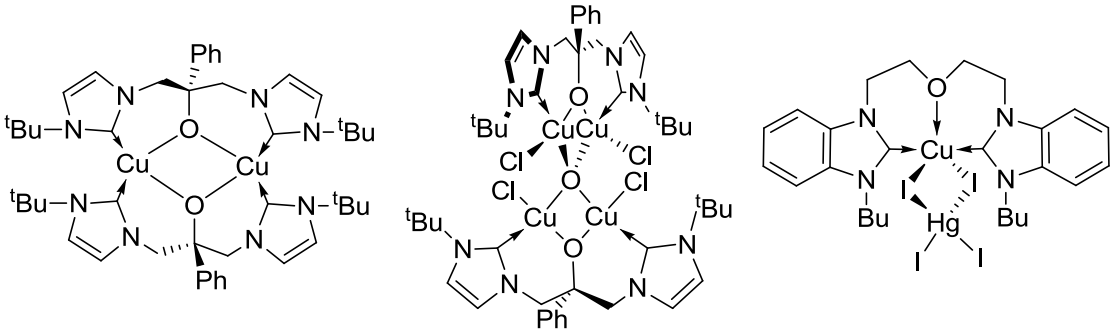

XVI **XVII** **XVIII**

Figure 1.6. Copper complexes of tridentate alkoxide bis(NHC) ligands.[12,45,54]

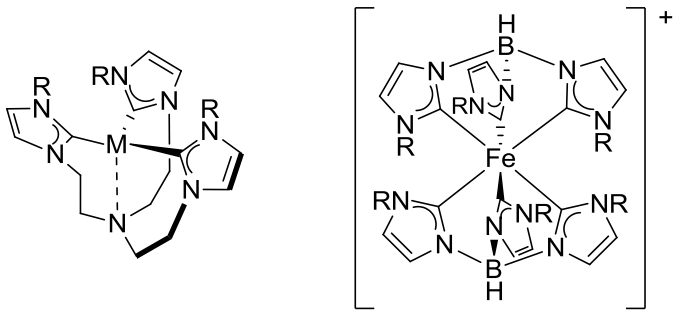

XIX **XX**

Figure 1.7. Tripodal systems with NHCs based on "scorpionates".[41,52]

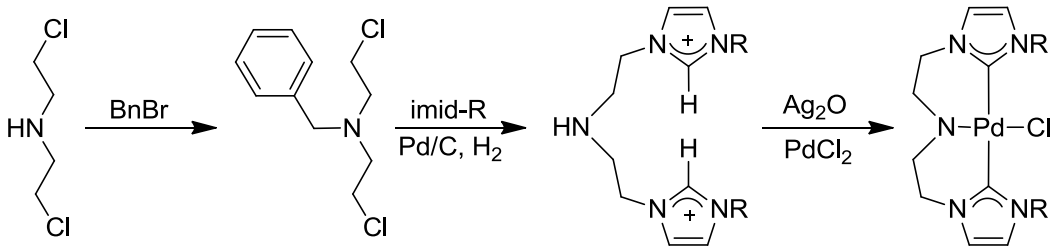

Scheme 1.8. Synthesis of tridentate CNC Pd complex with two NHC ligands.[53]

Following the work of the Douthwaite group,[53] Arnold *et al*. synthesised Y, Ti, Zr and Mg complexes using analogous ligands. These complexes show the variety of chelating modes that a flexible tridentate ligand can offer such as trigonal bipyramidal and octahedral geometries of the metal centres (compounds **XXI**, **XXII** and **XXIII** in Figure 1.8)[55] or the formation of coordination pockets for clusters of nuclei (compounds **XXIV** and **XXV** in Figure 1.9).[56] Other examples of tridentate bis(NHC) ligands were reported by Liu *et al*. in which imidazole is replaced by benzimidazole and the amino backbone is changed for ethers (compound **XVIII** in Figure 1.6). In **XVIII**, for example, the benzene rings of the carbenes help to promote the crystal packing by formation of intermolecular π-π stacking interactions.[54]

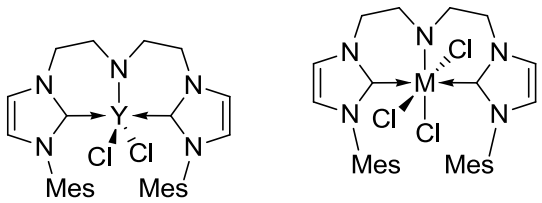

XXI **XXII**, **XXIII**

Figure 1.8. Examples of tridentate amido-bis(NHC) early-transition-metal complexes.[55]

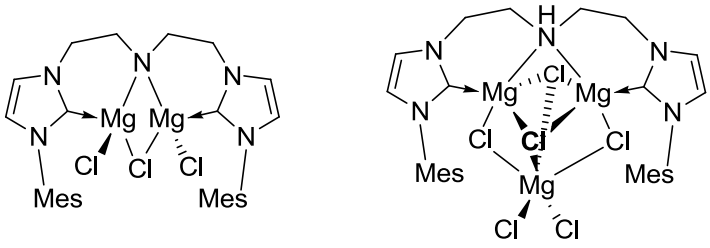

XXIV **XXV**

Figure 1.9. Magnesium complexes of tridentate *N*-bridged bis(NHC) ligands.[56]

1.6 Poly(lactic acid), polycarbonates and other biorenewable polymers *via* ring-opening polymerisation

Ring-opening polymerisation (ROP) is an effective route for the synthesis of polyesters because it enables living polymerisation, which requires a linear relation between the number average molar mass (M_n) and the rate of conversion, resulting in a steady growth of the polymer chains (low polydispersity index) and favouring control on the physical properties of the resulting polymer. This occurs because termination and transfer reactions are virtually non-existent, producing a molecular weight directly proportional to the monomer-to-initiator ratio. ROP is thermodynamically driven by the relief of ring strain, although it provides negative entropy as for every polymerisation. When producing a polyester, in addition to aiming for a high molecular weight and low polydispersity, it is important to prepare polymers with stereochemical control, low toxicity and cost, and controllable physical appearance. Furthermore, it is necessary to carefully distinguish the transesterification rates and mechanisms, and the potential secondary structures of the formed polymer.

1.6.1 Poly(lactic acid)

Poly(lactic acid), PLA, is enjoying a boost in popularity due to its potential for numerous applications in the fields of biomedicine, food packaging and fibres.[57] Due to its biodegradable characteristics and the renewable nature of its feedstock (corn starch, maize, sugar or wheat), poly(lactic acid) has been targeted as an eco-friendly material. The formation of six-membered ring lactide requires several steps which include: the fermentation of D-glucose by *Lactobacillus*, *Streptococcus* and *Pediococcus* bacteria; the condensation polymerisation to poly(L-lactic acid) in low molecular weight chains; and its depolymerisation, with consequent loss of optical purity (see Scheme 1.9).[58]

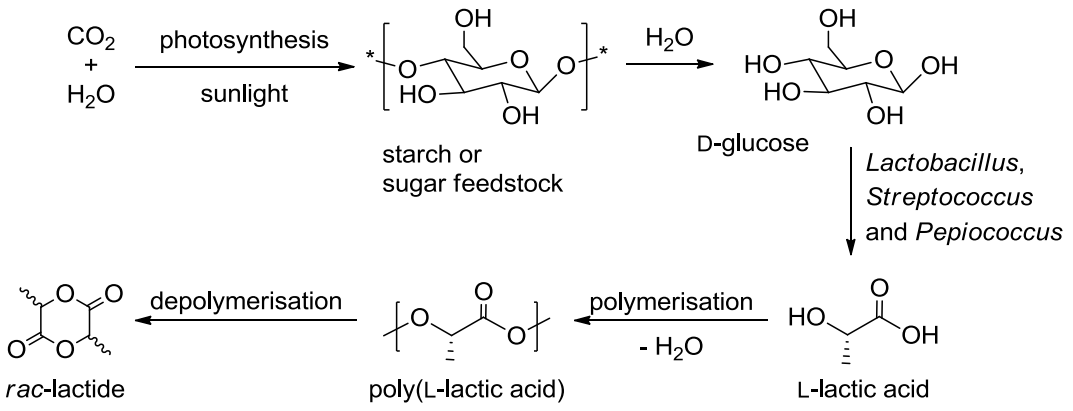

Scheme 1.9. Process for the formation of *rac*-lactide

Given that it bears two chiral centres, there are three stereoisomers of lactide: L-lactide, its enantiomer R-lactide and the diastereomer *meso*-lactide. Poly(lactic acid) chains of

diverse tacticities will result depending on the starting material and the stereoselectivity of the catalyst used. For instance, if only one of the enantiomers L-lactide or R-lactide is present in the polymerisation mixture, an isotactic polymer is expected to form in the absence of epimerisation. If the starting material is pure *meso*-lactide, it is expected that a selective catalyst will generate a syndiotactic polymer. Alternating series of blocks of isotactic chains are characteristic of heterotactic polymers, whilst an atactic polymer has an irregular arrangement of building units on its chains. These examples are shown in Scheme 1.10.

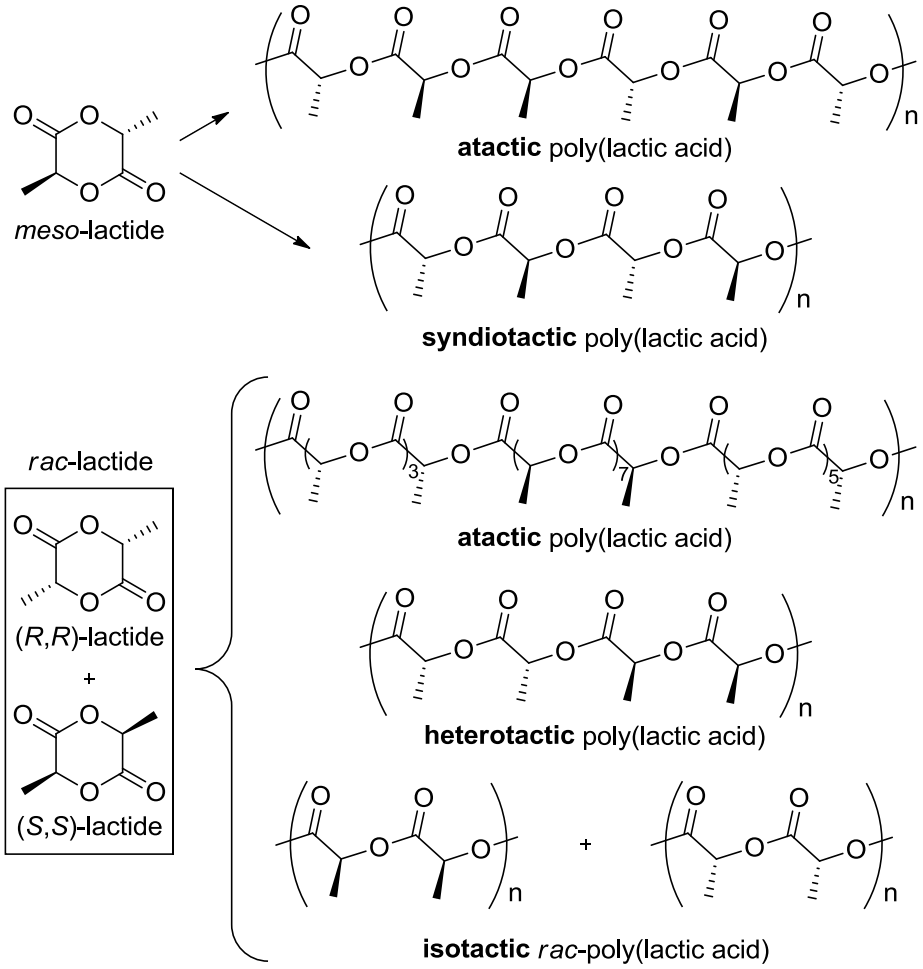

Scheme 1.10. Common microstructures from the polymerisation of lactide diastereo- and enantioisomers

In addition, the formation of stereocomplexes can be achieved if enantiomeric isotactic chains are able to intertwine given their opposite chirality; see Scheme 1.11. These stereocomplexes are interesting and industrially useful because their higher melting points confirm the stability and strength of the polymer.[59] In order to classify polymeric chains according to their microstructure ^{1}H nuclear magnetic resonance (NMR) spectroscopy of the methine groups is utilised.

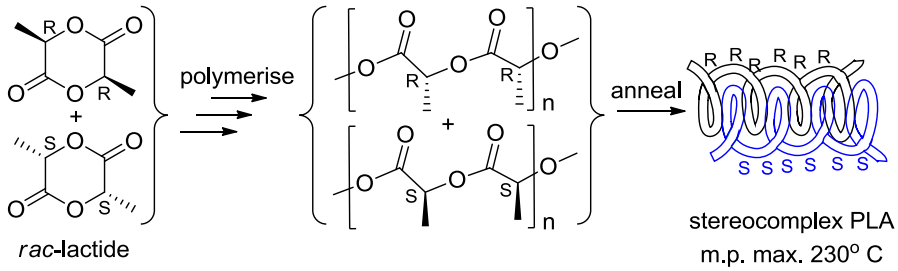

Scheme 1.11. Polymerisation of *rac*-lactide into isotactic chains of PLA which form a stereocomplex with high melting point.[33]

Chiral centres in poly(lactic acid) can be studied at the molecular level by assigning tacticity to diads in NMR spectroscopy. One of the methods currently used was mainly developed by the Thakur and Munson groups in 1997.[60] After their work, Chisholm *et al.* refuted their findings and proposed a different assignment.[61] Finally, Thakur and Munson took it upon themselves and published another article on the matter, rebuking Chisholm's work on the basis of probability.[62] An example of the resonance assignments for different tetrads in poly(lactic acid) is shown in Figure 1.11.[60] In summary, the sensitivity of the NMR equipment dictates the amount of chiral centres interacting with the studied chiral centre. Thus, if the NMR spectrometer is very sensitive (with a magnetic field >11.7 T), it might account for hexad or even octad stereosequences; on the contrary, when the NMR device is not as sensitive, it will be reliable for tetrad stereosequences such as *iii*, *isi*, *sii*, *iis*, and *sis* when the polymer is formed from *rac*-lactide (see Figure 1.10). Given that the *iis* and *sii* stereosequences for poly(lactic acid) from *rac*-lactide have the same probability from Bernoullian statistics, they will present the same chemical shift. In these tetrads, *s* and *i* refer to syndiotactic and isotactic, which means that a resonance accounts for four chiral centres (hence, tetrad) in which each consecutive pair of centres (dyad) is denominated either syndiotactic (contiguous *R* and *S*) or isotactic (either *RR* or *SS*). Another common nomenclature for the identification of dyads uses *m* (*meso*) and *r* (*racemic*) to state that a pair of chiral centres has the same or different chirality, respectively. This system is not convenient when the monomer is a dimer such as lactide because polymers from *meso*-lactide will have a majority of *r* dyads and polymers from *racemic*-lactide will have a majority of *m* dyads making the assignment of tacticity counterintuitive.

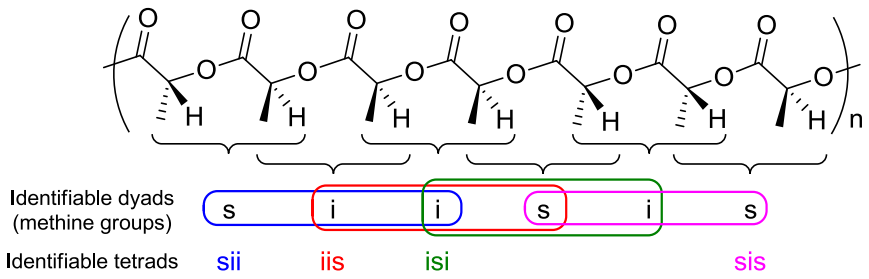

Figure 1.10. Polymeric tetrads identifiable by ^{1}H NMR spectroscopy

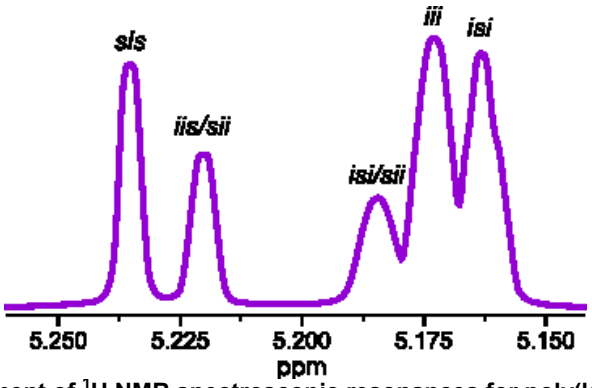

Figure 1.11. Assignment of ^{1}H NMR spectroscopic resonances for poly(lactic acid) from *rac*-lactide.[60]

It has been proposed that the mechanism followed by single-site metallic catalysts in the polymerisation of lactide includes the coordination of one carbonyl oxygen to the Lewis acid of the catalyst, followed by the insertion of the alkoxide group originally bound to the Lewis acid. Then, the selective cleavage of the acyl-oxygen bond of the ring opens it forming a pendant chain which contains the nascent polymer (see Scheme 1.12).[63]

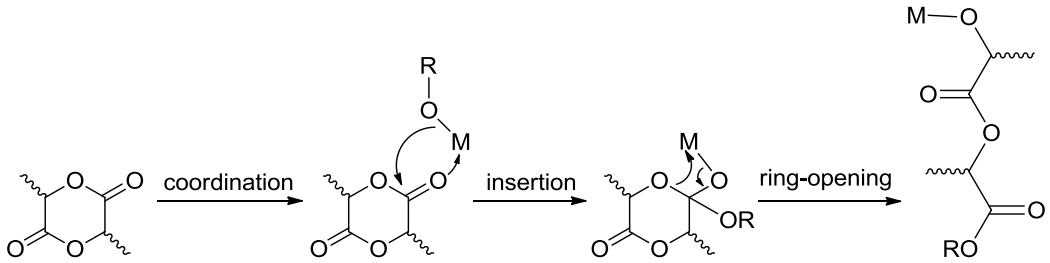

Scheme 1.12. Proposed mechanism for the polymerisation of lactide by a single-site metallic catalyst.[63]

It is noteworthy that, given that five- and six-membered rings are stable, the ring strain found in lactide arises from the planarity of the carbonyl groups; such a strain is not very significant and, hence, the newly formed polymer chain can become an oligomer or return to its monomeric state, especially at high temperatures.[64]

Currently, there are several companies focused on the industrial production of poly(lactic acid); notably, NatureWorks LLC has released a catalogue of products based on poly(lactic acid) such as clothes, furniture covers, electronic devices, cups currently used in the canteens at the University of Edinburgh, and medical commodities like drug-loaded devices, surgical sutures, stents and implants using the trade name Ingeo®.[65] The most common catalyst used for the industrial synthesis of this plastic is tin(II) bis(2-ethylhexanoate), also called tin octoate, tin octanoate or $Sn(oct)_2$ (**XXVI**), which provides high activity but is suspected as a highly toxic agent. Other industrially used catalysts are

aluminium isopropoxide, Al(O-^{i}Pr)$_3$ (**XXVII**), and zinc lactate, Zn(lact)$_2$ (**XXVIII**), with opposite advantages in activity and stereoselectivity, with the aluminium catalyst being the least active (see Figure 1.12). Among the metal complexes that have been used for the polymerisation of lactide, those containing sodium, lithium and potassium alkoxides are effective, but favour side reactions such as the epimerisation of the chiral centre of the ester due to their high basicity.[64]

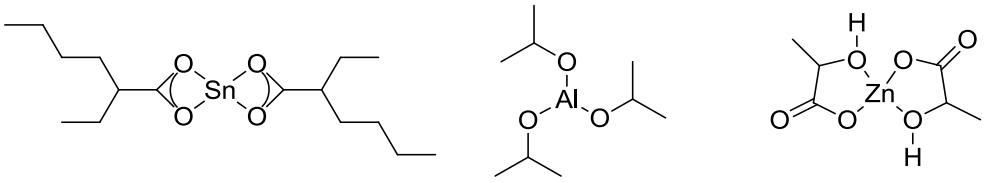

tin(II) octanoate
$Sn(oct)_2$
XXVI

aluminium(III) isopropoxide
$Al(OiPr)_3$
XXVII

zinc(II) lactate
$Zn(lact)_2$
XXVIII

Figure 1.12. Catalysts utilised in the industry for the polymerisation of lactide.[57]

One of the first catalysts used was developed by Inoue and his co-workers having alkoxide among other species as end chain and achieving low polydispersities (Figure 1.1 **I**).[14] Another interesting initiator was synthesised by the Spassky group[66] making use of the chiral binap and the ubiquitous salen framework used for the oxidation of olefins (Figure 1.1 **II**).[15] This initiator preferred D-lactide for the formation of the polymeric chains at low conversions; later, it was reported to form the racemic mixture of isotactic chains.[67] The formation of purely isotactic chains of poly(lactic acid) was later disputed in favour of the production of a stereoblock polymer with isotactic portions in the chain.[68] Ovitt and Coates obtained syndiotactic and heterotactic chains along with stereoblocks with higher molecular weight than the enantiomeric isotactic chains.[9,68,69]

Salan ligands are the amino analogues of the imino-containing salen; aluminium catalysts based on salan ligands, such as **III** in Figure 1.1, were found to be easily tuned to deliver a variety of microstructures (degrees of isotacticity and heterotacticity) by small changes in remote ligand substituents.[16] In addition, a zinc complex of a half salan (**IV** in Figure 1.1) was deemed the most active, at the time of the report, for the polymerisation of lactide, although without any stereoselectivity when polymerising *rac*-lactide.[17] Metal complexes with triamidoamines and diamidoamines (Figure 1.13 **XXXI**) were prepared using transition and main-group metals, but again aluminium-containing catalysts had the most activity towards lactide polymerisation resulting in high molecular-weight chains with low polydispersity (M_w/M_n = 1.23).[70] Also, zinc complexes from a combination of primary amines and 2,4-pentanedione forming a β-diimine ligand were utilised for the formation of heterotactic poly(lactic acid) from *rac*-lactide (**XXIX**).[71] Tris(pyrazolyl) and

tris(indazolyl)borates complexated with magnesium and zinc were also probed resulting in the magnesium catalysts being of the most active, and showing preference to polymerise *meso*- over *rac*-lactide (diastereoselectivity) with polydispersity indices between 1.1 and 1.3 (Figure 1.13 **XXX**).[72]

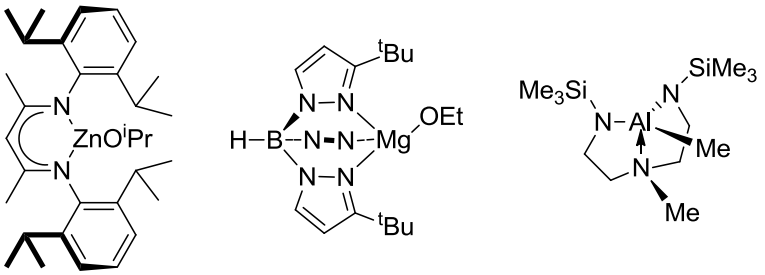

XXIX **XXX** **XXXI**

Figure 1.13. *N*-donor catalysts prepared for the polymerisation of lactide.[70,71,72]

More recently, other metal complexes have been used for the polymerisation of lactide, some very simple like those synthesised by the collaborative efforts between the Hillmyer and Tolman groups using iron alkoxides such as ethoxide and 1,1-dimethyl benzyloxide (Figure 1.14 **XXXII**) which result in pseudo-living polymerisations with polydispersity indices as low as 1.17.[73] Coates *et a*l. also prepared dinuclear catalysts (Figure 1.14 **XXXIII**) as a second generation of their previous catalyst **XXIX** shown in Figure 1.13. The new magnesium and zinc complexes facilitate the polymerisation of *rac*-lactide into highly heterotactic chains with at least 90% of enantiomeric alternation at low temperatures.[74]

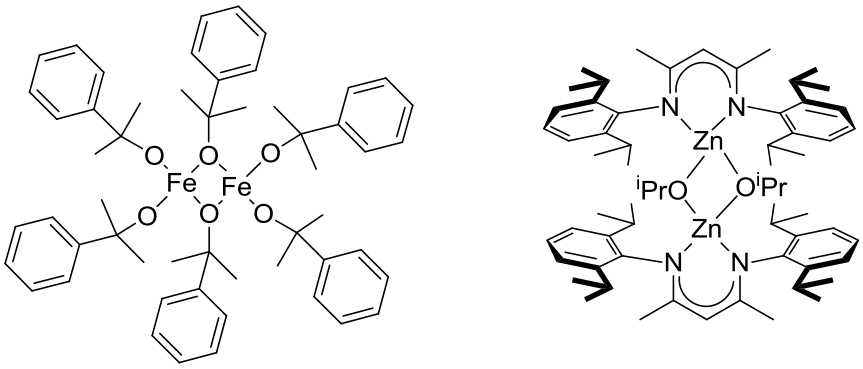

XXXII **XXXIII**

Figure 1.14. Dinuclear catalysts prepared by Hillmyer and Tolman (XXXII) and Coates (XXXIII).[73,74]

The Carpentier group has been working simultaneously with different ligands for the formation of catalysts for polymerisation of olefins, lactones and lactide. Some of the structural features of the catalysts prepared are shown in Figure 1.15. The variety of ligand

systems also results in a diversity of outcomes when it comes to the polymerisation process and products. For instance, a tetradentate amino/alkoxide lanthanide catalyst **XXXIV** produces a highly heterotactic poly(lactic acid) comparable to that produced by Coates's compound **XXXIII**. Also, **XXXIV** has been used for the block copolymerisation of *rac*-lactide and ε-caprolactone.[75] Given that it is comparably less rigid than the previously mentioned compounds, a tridentate amido/pyrazole transition-metal catalyst **XXXV** did not show any stereospecificity; however, the zinc and magnesium catalysts are efficient initiators of the atactic polymerisation of *rac*-lactide with polydispersity indices as narrow as 1.28.[76] Finally, a combination of salen ligand and a fluorinated alkoxy-imino ligand, previously reported by the Carpentier group (**XXXVI**),[77] was used for the preparation of aluminium and yttrium catalysts. These complexes produce isotactic polymers (80%) with very low polydispersity indices (PDI) during living polymerisation.[78] Other recent reports show the use of even simpler catalysts such as indium chloride, which in the presence of benzyl alcohol and various amines produces >90% heterotactic poly(lactic acid) from *rac*-lactide (Equation 1.5).[79]

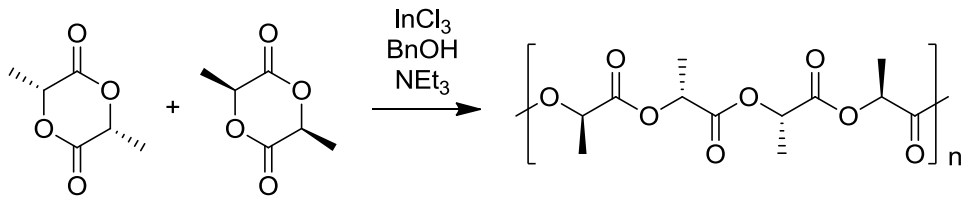

rac-lactide heterotactic poly(lactic acid)

Equation 1.5. Preparation of heterotactic poly(lactic acid) using indium chloride.[79]

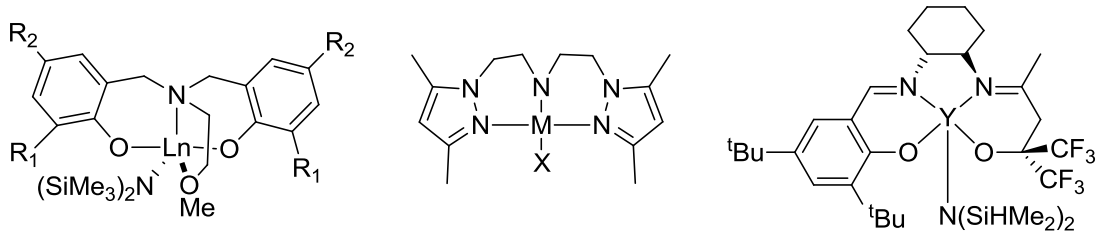

XXXIV **XXXV** **XXXVI**

Figure 1.15. Catalysts prepared by the Carpentier group.[75,76,77]

The use of organocatalysts other than enzymes deserves a special mention, with *N*-heterocyclic carbenes as the most active and effective catalysts, followed by amines and phosphines, with the former generating polymers with narrow PDI and tuneable molecular weight and the latter prone to undesirable transesterification side reactions and equilibrium between polymerisation and oligomerisation.[80] Nucleophiles as catalysts require the presence of an alcohol or another protic agent as an initiator. The mechanism proposed

includes a nucleophilic attack to a carbonyl group followed by reaction of a protic species (primary or secondary alcohol) with the short-lived monomer-catalyst arrangement (as in Scheme 1.13).[80] The original nucleophile is liberated and the chain, which is now an alcohol itself, may react with another monomer-catalyst complex. In summary, the nucleophilic catalyst only activates the monomer and opens the ring, contrary to metallic complexes which remain in the polymeric chain. Interest in these species comes from the advantage of not using metals in the polymerisation when aiming for applications in the areas of biology or medicine because of their potential higher toxicity and cost.[81] The work on organocatalysts for the formation of poly(lactic acid) has been almost single-handedly carried out by scientists at the IBM Almaden Research Center in California with other groups having minor input to the area. A recent investigation presented the possible structural features needed in a nucleophile to successfully produce polymers with low polydispersity indices, high rate of reaction and low rate of transesterification as a combination of rigidity between the distance of the nucleophilic agents and their efficiency to interact with the propagating alcohols giving them a more basic character.[82] Figure 1.16 shows some of the most effective organic compounds for the ring-opening polymerisation of lactides: the natural products (–)-sparteine (**XXXVII**) and cinchona alkaloids (**XXXVIII**),[83] tris[2-(dimethylamino)ethyl]amine (**XXXIX**), *N*-heterocyclic carbenes (**XL**),[80,84] thiourea amines (**XLI**),[85] and phosphazene bases (**XLII**) which have delivered highly isotactic chains from *rac*-lactide at low temperatures.[86]

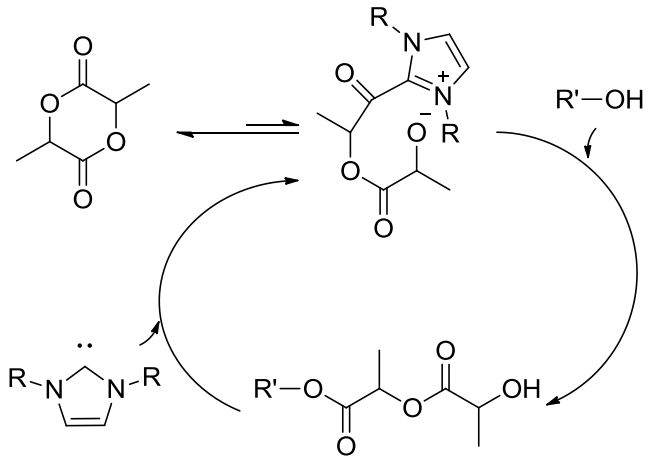

Scheme 1.13. Mechanism of ring-opening polymerisation of lactide mediated by an NHC

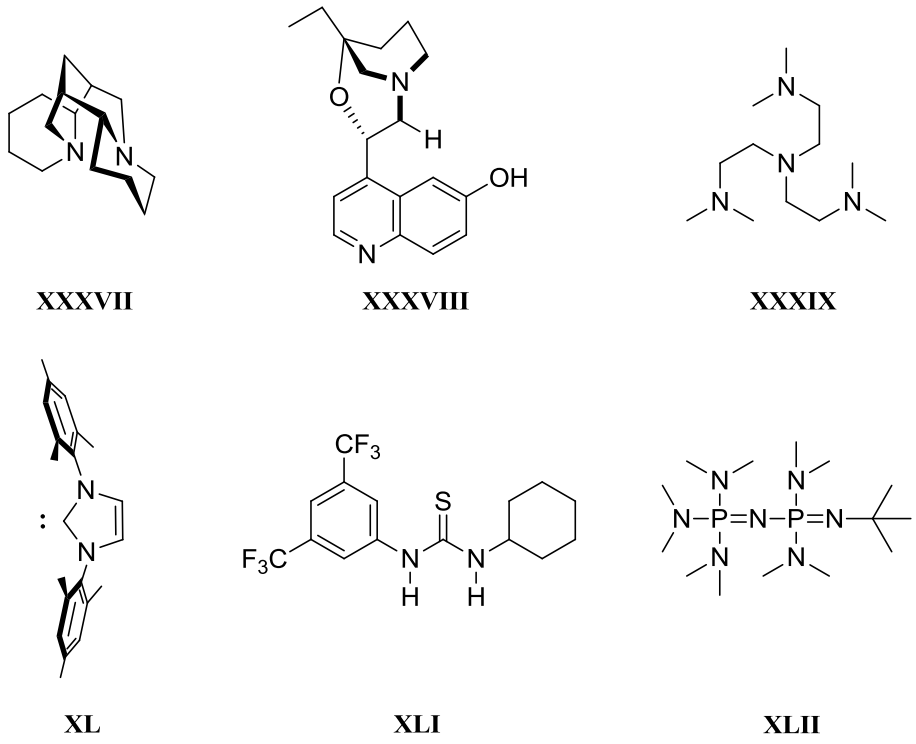

XXXVII XXXVIII XXXIX

XL XLI XLII

Figure 1.16. Organocatalysts for the formation of poly(lactic acid). [80,83,84,85,86]

1.6.2 Polycarbonates

Currently, the largest applications of CO_2 in the production of new chemicals are the formation of urea, salicylic acid, inorganic carbonates, ethylene/propylene carbonates, polycarbonates and methanol in combination with carbon monoxide.[87] Interestingly, in the production of polycarbonates from epoxides and carbon dioxide, these two cheap and abundant species are intended to replace the reagents phosgene, a warfare agent, and the infamous bisphenol A (BPA). Other applications of CO_2 can be further optimised in industry, such as the production of formic acid, formic acid methyl ester and dimethylformamide; dimethyl carbonate and urethanes; 2-pyrone, and diphenyl carbonate.[5]

For the synthesis of cyclic and acyclic carbonates, the reaction between epoxide and carbon dioxide has been catalysed with diverse metal complexes containing, for instance, chromium, cobalt and zinc;[88] those based on salen ligands are highly active as catalysts for this kind of reactions.[89] The first report of the ring-opening copolymerisation of epoxides and carbon dioxide was by Inoue *et al*. in 1969 in which a mixture of diethylzinc and water proved efficacious for the copolymerisation of propylene oxide and carbon dioxide at 50 bar and room temperature.[90] After that, numerous catalysts have been developed, many of them based on the complexes used for the ring-opening polymerisation of esters such as lactide. For instance, catalyst **I** (Figure 1.1) coupled with onium salts as cocatalyst produced full consumption of the epoxide, in this case cyclohexene oxide, and a copolymer with up to 63% of carbonate from 50 bar of CO_2 (Equation 1.6).[91]

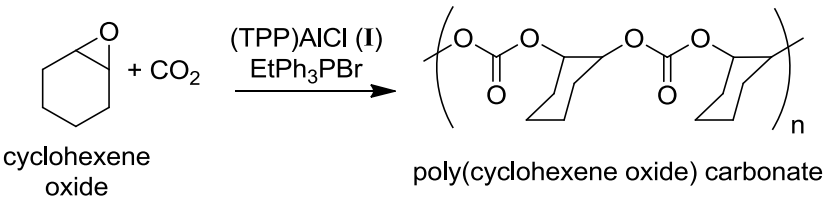

Equation 1.6. Copolymerisation of cyclohexene oxide and carbon dioxide initiated by I and an onium salt.[91]

The Coates group used a β-diiminate zinc analogue to **XXXIII** for the copolymerisation of CO_2 and limonene oxide (*trans*-limonene oxide is LO in Equation 1.7), a derivative of the main component of the citrus peel oil. To produce poly(limonene oxide) carbonate (PLC in Equation 1.7) with a balanced selectivity and activity there were required 2 h and a pressure of 100 psi at 25° C with catalyst **XLIII** (see Equation 1.7) at a 0.4 mol % concentration.[92] Although limonene oxide is an attractive monomer due to its character as a renewable material coming from waste, it has not been studied as extensively as propylene oxide, which is a teratogen and carcinogen, or cyclohexene oxide.

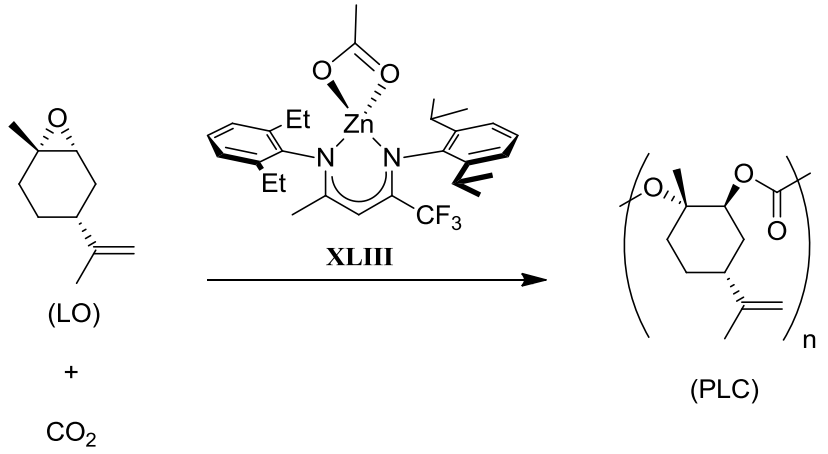

Equation 1.7. Copolymerisation of limonene oxide and carbon dioxide using Coates's catalyst.[92]

Along with zinc and aluminium, many chromium and cobalt complexes have been studied for this copolymerisation. The Coates group, using a salcy ligand (analogous to the typical salen ligand but with cyclohexenediamine as a bridge between the salicylate groups), probed the first cobalt(III) complex (**XLIV** in Figure 1.17) with success especially in terms of selectivity towards the poly(propylene oxide) carbonate against the cyclic carbonate and a high content of carbonate linkages (>90%) at ~50 bar of CO_2 pressure and 40° C.[93] The use of nucleophilic salts, as mentioned before, and the variation of the ligand axial to the metal centre were necessary to double the activity of the catalyst at pressures as low as 2 bar.[94] The use of free onium salts was later avoided by the inclusion of a pendant piperidinium

group as part of the salcy ligand (**XLV** in Figure 1.17). This catalyst resulted consistently in the production of polycarbonate with low polydispersity indices (1.06 – 1.28) instead of the cyclic carbonate from propylene oxide at relatively low temperatures.[95a] This and other work using a pendant onium salt on the salcy ligand were compared for their viability in the industrial setting.[95b] Sugimoto and Kuroda later reported their studies on another highly selective catalyst, a cobalt porphyrin (**XLVI** in Figure 1.17), for the formation of polycarbonates from propylene oxide and cyclohexene oxide under only one bar of CO_2 and room temperature. As cocatalyst, they used dimethylaminopyridine (DMAP) over other species such as triethylamine, onium salts and phosphines.[96]

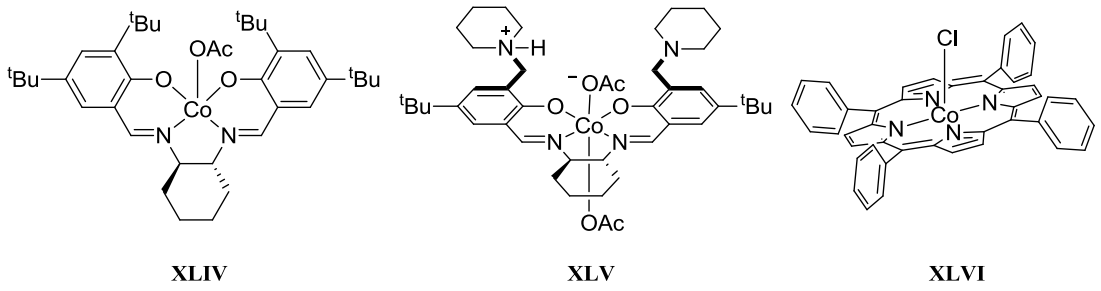

Figure 1.17. Some catalysts selective for the production of polycarbonate over cyclic carbonate

Other examples of the pendant nucleophilic group in a salen-type cobalt complex include a methyl-imidazolium salt (**XLVII** in Figure 1.18) and an imidazole (**XLVIII**), which were not successful for the copolymerisation of oxirane and CO_2; nevertheless, they are interesting due to their potential as secondary ligands when deprotonated for the formation of carbenes.[97]

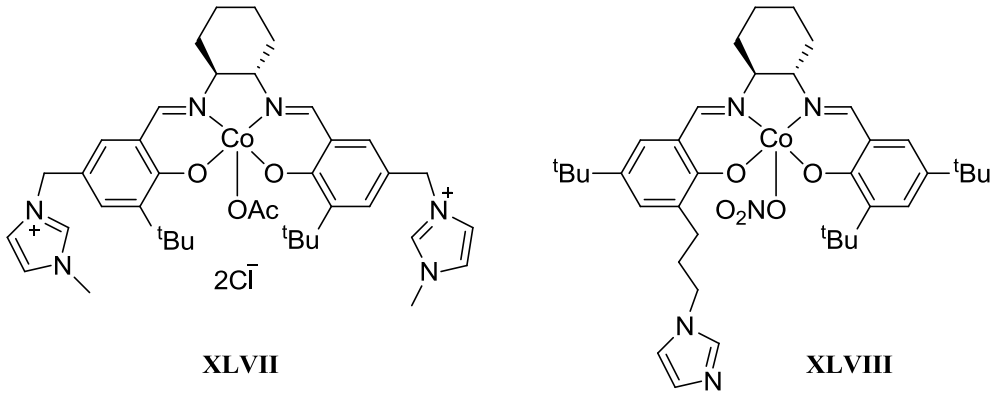

Figure 1.18. Cobalt(III) complexes with imidazole-like pendant groups

The previous catalysts were mainly used for the coupling of propylene oxide (PO) and carbon dioxide given that the epoxide is cheap, small and easy to purify and identify; unfortunately, it is a known carcinogen and teratogen. Cyclohexene oxide (CHO) was then

utilised because it is not as toxic and still remains easy to handle; in addition, it is easier to selectively convert it to its polycarbonate given the additional strain of forming a five-membered ring carbonate over the six-member ring of the cyclohexane group. Darensbourg *et al*. reported the reaction coordinate diagrams for the formation of polycarbonate and cyclic carbonate from propylene oxide and cyclohexene oxide. It is possible to compare in Figure 1.19 the energy profiles for the coupling of carbon dioxide and polypropylene oxide *versus* cyclohexene oxide. In this example, the activation energies for the formation of cyclic carbonate and polycarbonate are very similar when the comonomer is propylene oxide, whereas there is a larger difference and, consequently, a higher selectivity for the formation of polycarbonate when cyclohexene oxide is the comonomer. The reported energies of activation using a chromium(III) salcy complex are: for the formation of polypropylene carbonate (PPC) 67.6 kJ/mol, of cyclic propylene carbonate (PC) 100.5 kJ/mol, and the enthalpy of formation of PC is -54 kJ/mol. For the formation of polycyclohexene carbonate (PCC) the activation energy is 46.9 kJ/mol, for cyclic cyclohexene carbonate (CC) it is 133.0 kJ/mol and the energy gained when CC is formed is 34.03 kJ/mol.[98]

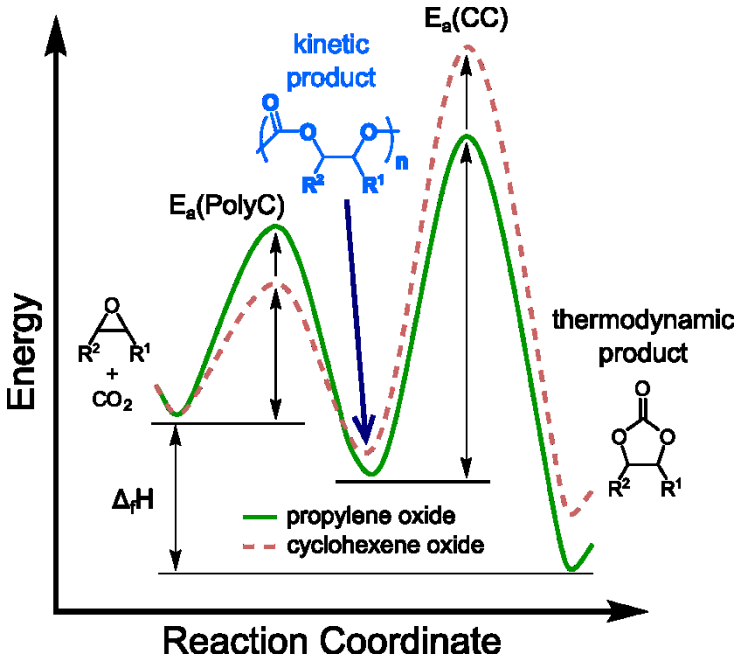

Figure 1.19. Reaction coordinate diagrams for the coupling of CO_2 and PO or CHO.[98]

A different kind of ligand was developed by Williams *et al*. based on the Hillmyer and Tolman's catalysts (see **IV** in Figure 1.1) and the work of the Robson group.[99] Complexes of this ligand proved highly active catalysts for the selective copolymerisation of epoxide and carbon dioxide under mild conditions. The macrocyclic ancillary ligand studied supports a pair of metal centres which are coordinatively bridged by acetates (**XLIX**) that participate in the copolymerisation mechanism proposed in Scheme 1.14. Thorough studies were performed on this complex to show that the activation energy for the formation of the

copolymer is double that of the chromium-salcy complex mentioned above (96.8 kJ/mol); nevertheless, it was found that the energetic barrier to obtain cyclohexene carbonate is still very high and comparable to Darensbourg's studies (137.5 kJ/mol).[100]

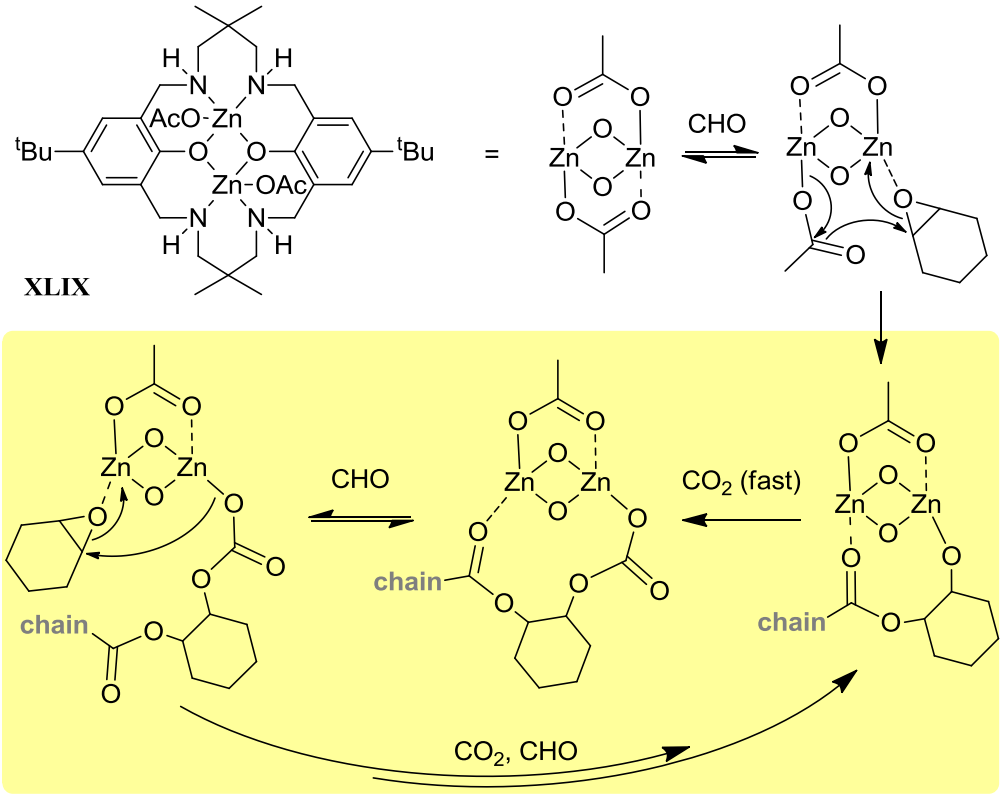

Scheme 1.14. Zinc complex for the CHO/CO_2 copolymerisation and proposed mechanism.[100]

In recent years, the scope of the copolymerisation of epoxides and carbon dioxide have widened and more catalysts and epoxides have been tested to create more durable and still degradable polymeric materials. For instance, uncommon metals for this reaction have been used, such as iron catalysing the regioselective copolymerisation of *cis*-CHO with CO_2,[101] other oxiranes have also been coupled to carbon dioxide such as indene oxide using a cobalt-salcy catalyst resulting in a very high glass-transition temperature of 134° C,[102] or styrene oxide with high content of carbonate linkages using the same type of catalysts.[103] As observed, cobalt has been one of the most prolific nuclei for the coupling of epoxides and carbon dioxide especially using salcy ligands, which are related to the Jacobsen's catalyst. Before their utilisation for the formation of polycarbonates, Co(II) complexes were used for the preparation of cyclic carbonates from ethylene oxide and even copolymerisation of oxetane with carbon dioxide; always using an onium salt as cocatalyst. Then, Co(III) complexes were probed for the synthesis of polycarbonates and there is a long list of catalysts and studies in this matter, highlighted here and elsewhere.[104] Although it is widely

accepted that Co(II) salen-type complexes are inactive for the copolymerisation of oxiranes and carbon dioxide, Williams and her coworkers reported an ancillary macrocycle analogous to **XLIX** with two Co(II) nuclei (**L**) that was active for the copolymerisation of CHO and carbon dioxide. They also synthesised a mixed-valence Co(II)/Co(III) (**LI**) complex and a Co(II)/Co(II)/Co(II) trinuclear (**LII**) complexes with similar activity toward the formation of polycarbonates. **L** and **LI** were compared in activity at 1 bar of CO_2 with **XLIX**, showing more activity and more selectivity for the copolymerisation over the formation of cyclic carbonate at 80° C. Analogous complexes with halides have been tested with comparable results.[105] The positive outcome of using Co(II) nuclei is not completely surprising given that there is a previous report of a Co(II) acetate being used for the coupling of epoxide and carbon dioxide;[106] nevertheless, the prominence of the salen-type complexes in the development of this area dimmed the interest for using Co(II) as an effective metal centre for these particular reactions.

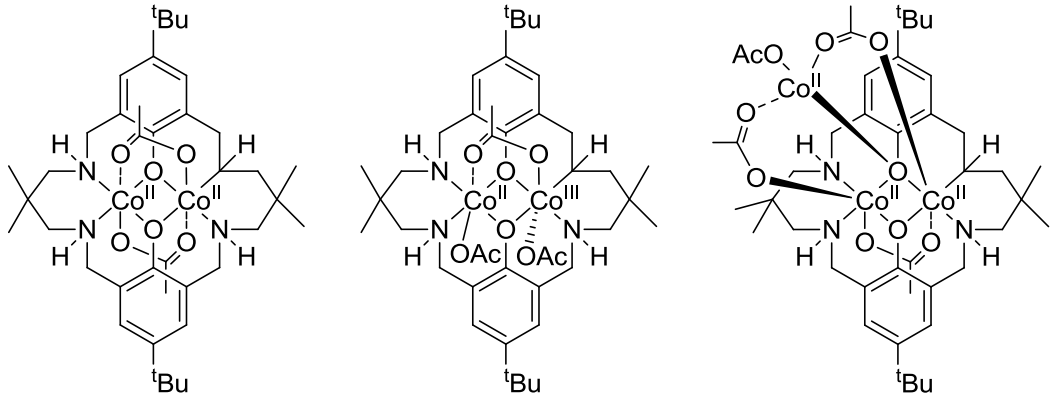

L **LI** **LII**

Figure 1.20. Cobalt(II) complexes for the copolymerisation of CHO and CO_2 by Williams *et al*.[105]

Lately, the crystallinity of the prepared polymers has received more interest because it induces a higher glass transition temperature and, thus, a polymer more attractive to industry and a possible real competitor to polycarbonates made of phosgene and BPA. In this case, the catalyst should be effective not only by favouring the formation of polycarbonate and cyclic carbonate, but also by being regioselective (adding the monomer in a consistent head-to-tail mode) and stereoselective (adding the correct enantiomer as designed). Nozaki and coworkers prepared an "iso-enriched" poly(propylene carbonate) that starts with an almost isotactic *S*-PPC and ends with an almost isotactic *R*-PPC; this chain is known as stereogradient polymer. The term "iso-enriched" is defined as a chain highly isotactic, but not perfectly so. The best catalyst for the designed alternation of enantiomers in this study has an acetate group and a pendant quaternary ammonium salt in the typical cobalt(III)-salcy complex (see **LIII** in Figure 1.21).[107] Then, Lu *et al*. proposed catalysts based on similar cobalt(III)-salcy complexes, but with unsymmetrical substituents in the salicyl group such as

binaphthyl, adamantyl (**LIV**), silane and a perhydrofuran in conjuction with bis(triphenylphosphine)iminium chloride (PPNCl). These complexes delivered terpolymers with up to 98:2 ratio of *RR*:*SS* pairs when reacting a mixture of *meso*-CHO and *S*-PO at 15 bar of CO_2 . The best polymer reached a melting point of 216° C.[108] Another example is a β-ketoiminate aluminium complex (**LV**) that allowed a higher concentration of carbonate linkages in the polymeric chains, although it did not improve the enantioselectivity in the presence of only two monomers, in this case CHO and CO_2. The catalyst was generally used together with tetraethylammonium acetate. More studies using the same catalyst, now in the presence of a dimeric Lewis base (bis-*N*-methylbenzimidazole) and the Lewis acid methylaluminium bis(di*tert*butylmethylphenoxide) (MAD), resulted in a much higher enantioselectivity of up to 82%, but with a lower percentage of carbonate linkages (37%).[109]

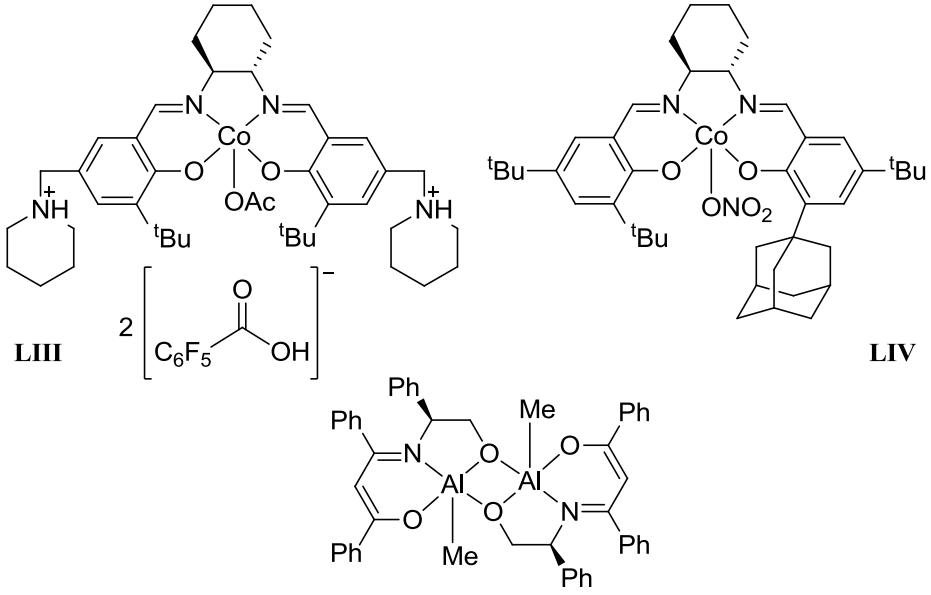

Figure 1.21. Examples of catalysts for the enantioselective copolymerisation of epoxide and CO_2.

Furthermore, no account of organocatalysts aiding the formation of polycarbonates from CO_2 and epoxides was found. There is, though, a report by Makiguchi *et al*. utilising a phosphine oxide for the tuneable ring-opening polymerisation of trimethylene carbonate.[110] This work, in addition to accounts of NHCs activating epoxides[111] and even coupling them with carbon dioxide to form cyclic carbonates,[112] opens the door to cleaner processes using renewable materials.

1.7 Strategy for the design of new systems for the polymerisation of renewable monomers

Building from the success of the alkoxide/phosphine oxide ligand system in lanthanide metal complexes for the polymerisation of *rac*-lactide discussed in Section 0, we wanted to use similar ligands to synthesise new complexes for this and other polymerisations using transition metals, because of their availability and diversity of oxidation state, toxicity and ecological impact.

1.7.1 Alkoxide/phosphine oxide as ligands

As already mentioned, the proligand, HL^{tBu}, used by Arnold *et al*. has the characteristic ability to form homochiral complexes spontaneously and is prepared by the oxidation of the condensation product of an epoxide and a phosphine.[33] We aim to use this and an analogue with phenyl groups on the phosphorus atom: $Ph_2P(O)CH_2CH(^tBu)OH$, which is abbreviated as HL^{Ph}, **1** (see general synthesis in Scheme 1.15).[35]

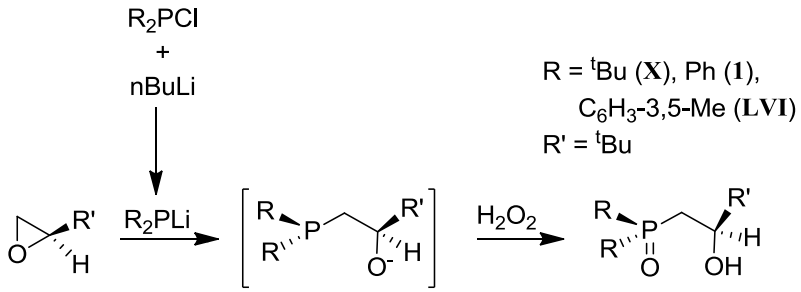

Scheme 1.15. Synthesis of the proligand HL^{alkyl}

Because these ligands have been used with success for the polymerisation of *rac*-lactide, ε-caprolactone and even copolymerisations, we aim to explore the spectroscopic characteristics of these ligands and their known complexes to ultimately design, with confidence, new complexes for more effective polymerisations. Table 1.1 shows chosen complexes of **X** and their spectroscopic data, which will be helpful for comparison with our results in the next chapters. Complexes with **1** and analogues and their spectroscopic data are tabulated in Table 1.2.

Table 1.1. Previously reported compounds containing the alkoxy/di(*tert*-butyl)phosphine oxide ligand

Metal	Structure	Spectroscopic and physical data
(**X**)	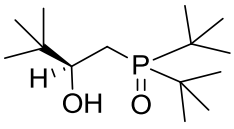	m.p. 98° C ^{31}P NMR (C_6D_6): 63.7 ppm. (C_7D_8): 63.8 ppm.[33]
Sn (**XII**)	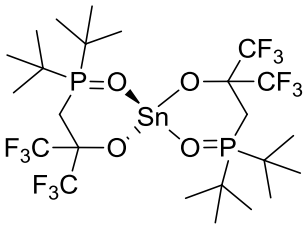	^{31}P NMR (C_7D_8): 60.7 ($^2J_{SnP}$=255.6 Hz) ppm.[36]
Bi, Er, Eu, In, La, Lu, Sc, Y	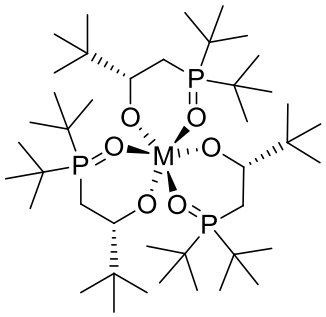	^{31}P NMR (C_6D_6): 68.9 (Bi, Y), 69.4 (In), 66.6 (La), 69.9 (Lu), 67.7 (Sc), ppm.[35,113] Some of these complexes catalyse the polymerisation of *rac*-lactide
In (**LVII**), Lu, Y	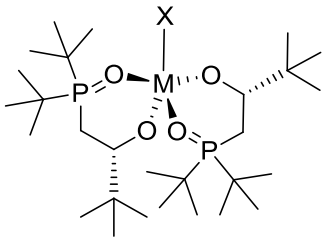	X = nucleophilic group v(P=O) = 1104s cm^{-1} (M=In, X=N(SiMe$_3$)$_2$) ^{31}P NMR (C_6D_6): 70.5-72.9 ppm.[35,113] **LVII** catalyses polyester formation and copolymerisations
Ca, Sn (**XI**), Zn (**LVIII**)	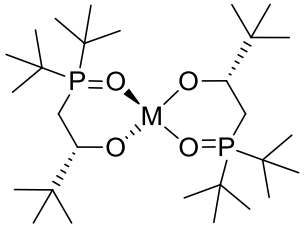	^{31}P NMR (C_6D_6): 78.9 (Ca), 66.7 ($^2J_{SnP}$=255.6Hz), 72.2 (Zn) ppm.[35] These complexes catalyse the polymerisation of *rac*-lactide
Al, In	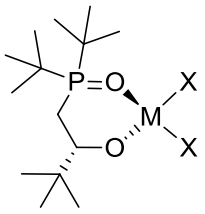	^{31}P NMR (C_6D_6): 73.0-78.8 ppm.[35]

Table 1.2. Previously reported compounds containing alkoxy/di(phenyl)phosphine oxide ligands

Metal	Structure	Spectroscopic and physical data
– (**1**)	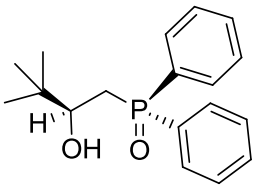	^{31}P NMR (C_6D_5N): 33.6 ppm.[32]
Na	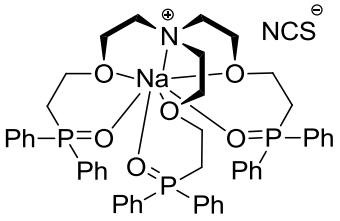	^{31}P NMR ($CHCl_3$): 30.02 ppm.[114]
Bi, In, Lu, Sc, Y	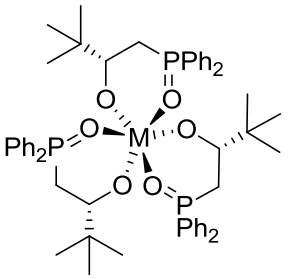	^{31}P NMR (C_6D_6): 34.0 (Bi), 46.96 (In), 43.5 (Lu), 42.0 (Sc), 42.9 (Y) ppm.[35]
Sn	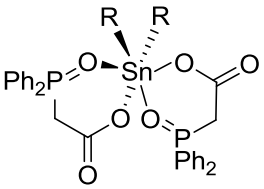	R = methyl or phenyl m.p. 75-78° (Me, **VII**), 182-183° (Ph) C. v(P=O): 1190s (Me), 1216m (Ph) cm^{-1}.[26]
Ti	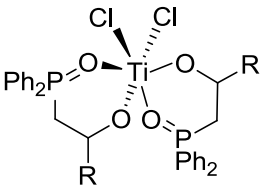	v(P=O): 1176m (Me, **VIII**), 1194m (Ph) cm^{-1}. ^{31}P NMR ($CDCl_3$): 44.3 (Me), 45.1 (Ph) ppm.[27a]
In	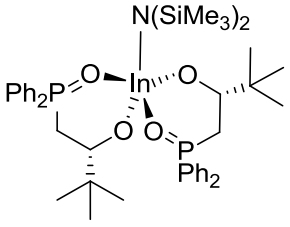	^{31}P NMR (C_6D_6): 48.0 ppm.[35]
Mg (**LIX**),Co (**LX**), Sn (**LXI**)	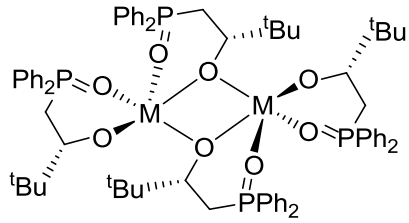	^{31}P NMR (C_6D_6): 40.1 (Mg), 34 (broad, Co), 37.5 ($^2J_{SnP}$=198.0 Hz) and 38.5 ($^2J_{SnP}$=241.2 Hz) ppm.[35]

Prior to this work, no complex with a bidentate alkoxy/phosphine oxide ligand has been used as a catalyst for the copolymerisation of epoxides and carbon dioxide. Examples of the reactivity of these compounds with carbon dioxide are presented in Chapter 2.

1.7.2 Tethered *N*-heterocyclic carbenes as ligands

An alternative to the alkoxy/phosphine oxide ligand system is the use of *N*-heterocyclic carbenes with tethered nucleophilic groups. Table 1.3 and Table 1.4 summarise the spectroscopic data of a number of alkoxy-tethered NHCs and some of their precursors for comparison to the species presented in this work. Table 1.4 specifically presents complexes with two NHC ligands.

Table 1.3. Previously reported compounds containing tethered NHCs and their precursors

Metal	Structure	Spectroscopic data
–	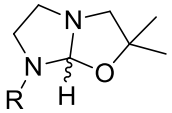	^{1}H NMR (C_6D_6) N-C(O)*H*-N: 5.47 (^{i}Pr), 5.79 (Mes) ppm; N-C*H*$_2$: 3.13 2.85 2.64 (^{i}Pr), 3.42 3.21 3.02 (Mes) ppm; ^{13}C N-*C*H-N: 107.8 (^{i}Pr), 108.6 (Mes) ppm.[115]
–	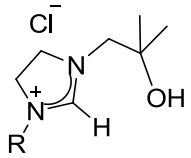	^{1}H NMR ($CDCl_3$) N-C*H*-N: 9.71 (^{i}Pr), 9.33 (Mes) ppm; backbone: 4.33, 4.05 (^{i}Pr), 4.42, 4.13 (Mes) ppm; O*H*: 5.25 (^{i}Pr), 5.20 (Mes) ppm; ^{13}C N-*C*H-N: 158.5 (^{i}Pr), 160.8 (Mes) ppm.[115]
– (**LXII**, **LXIII**)	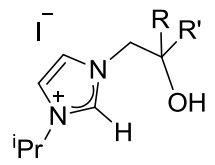	For R=Me, R'=Me (**LXII**). ^{1}H NMR (D_2O) N-C*H*-N: 8.85, backbone: 7.63 7.51 ppm. ^{13}C N-*C*H-N: 134.9 ppm. For R=H, R'=^{t}Bu (**LXIII**). ^{1}H NMR ($CDCl_3$) N-C*H*-N: 9.58, backbone: 7.58 7.42 ppm. ^{13}C N-*C*H-N: 135.2 ppm.[12]
Mg, Zn	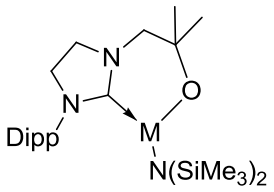	^{1}H NMR (C_6D_6) backbone: 3.18 (Mg), 3.11-2.85 (Zn) ppm; ^{13}C carbene: 196.1 (Zn) ppm; *C*-O: 70.4 (Zn) ppm.[51c]

Table 1.4. Previously reported compounds containing alkoxy-tethered NHCs

Zn	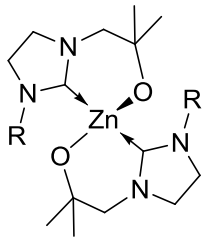	^{1}H NMR (C_6D_6) backbone: 2.80, 2.64-2.46 (^{i}Pr), 2.89-2.80 (Mes) ppm; ^{13}C carbene: 203.6 (^{i}Pr), 205.7 (Mes) ppm; *C*-O: 71.7 (^{i}Pr), 71.1 (Mes) ppm.[51c]
Cu^{II},[12] Zn	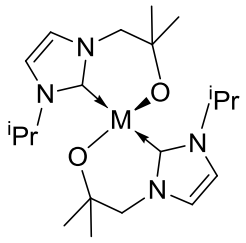	^{1}H NMR (C_6D_6) backbone: 6.39, 6.33 (Zn), ppm; ^{13}C carbene: 179.0 (Zn), ppm; *C*-O: 71.1 (Zn), ppm.[51c]
Mg, Zn	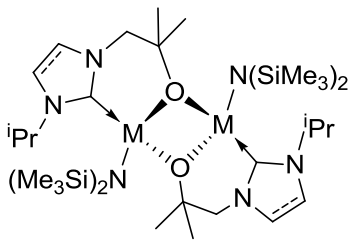	^{1}H NMR (C_6D_6) backbone: 6.26, 6.12 (Mg, unsat), 2.88, 2.78, 2.64, 2.63 (Mg, sat), 2.90, 2.72, 2.64, 2.62 (Zn, sat) ppm; ^{13}C carbene: 185.9 (Mg, unsat), 210.2 (Mg, sat), 204.8 (Zn, sat) ppm; *C*-O: 70.5 (Mg, unsat), 71.4 (Mg, sat), 72.5 (Zn, sat) ppm.[51c]

Furthermore, tridentate ligands and others with higher coordination sites generally present a more rigid environment for metal nuclei either blocking the active site or forming a selective point for catalysis. The use of multidentate ligands in catalysts for the copolymerisation of epoxides and carbon dioxide is promising, taking into account examples of high stereoselectivity with tetradentate ligands such as salen[98] and of effective catalysts at low pressures and temperatures with multidentate ligands.[100]

1.8 References

[1] "Plastics Recycling." British Plastics Federation. 7 August 2013. < http://www.bpf.co.uk/Sustainability/Plastics_Recycling.aspx>. Note: Data from 2009; a plastic bottle currently weighs about 10 g.

[2] Core Writing Team, Pachauri, R.K. and Reisinger, A. (Eds.) "Climate Change 2007. Synthesis Report." Intergovernmental Panel on Climate Change. Geneva, Switzerland. 27 November 2007. pp. 104.

[3] Weast, R. C. (Ed.) "Properties of Atoms, Radicals, and Bonds." Handbook of Chemistry and Physics. CRC Press, Inc. USA. 61st Edition. 1980-1981. pp. F-233 – F-239.

[4] Petrucci, R. H.; Harwood, W. S.; Herring, G. E.; Madura, J. General Chemistry: Principles and Modern Applications. Prentice Hall, USA. 9th Edition. 2006.

[5] Sakakura,T.; Choi, JC.; Yasuda,H. *Chem. Rev.* **2007,** *107,* 2365-2387. 10.1021/cr068357u. Omae, I. *Catal. Today* **2006,** *115,* 33-52. 10.1016/j.cattod.2006.02.024.

[6] Demarçay, M. E. *Compt. Rend.* **1875,** *80,* 51-53. Gladstone, J. H.; Tribe, A. *J. Chem. Soc.* **1876,** *29,* 158-162. Jennings, J. S.; Wardlaw, W.; Way, W. J. R. *J. Chem. Soc.* **1936,** 637-640. 10.1039/jr9360000637.

[7] Bradley, D. C.; Mehrotra, R. C.; Rothwell, I. P.; Singh, A. "2 – Homometallic Alkoxides." Alkoxo and Aryloxo Derivatives of Metals. Elsevier, The Netherlands. 2001. pp. 3-181.

[8] Landor, S. R.; Miller, B. J.; Tatchell, A. R. *Proc. Chem. Soc.* **1964,** 227. *J. Chem. Soc. C* **1966,** 1822-1825. 10.1039/j39660001822 and 2280-2282. 10.1039/j39660002280.

[9] Ovitt, T. M.; Coates, G. W. *J. Am. Chem. Soc.* **2002,** *124,* 1316-1326. 10.1021/ja012052+.

[10] Gade, L. H.; Bellemin-Laponnaz, S. *Top. Organomet. Chem.* **2007,** *21,* 117-157. 10.1007/3418_028.

[11] Rix, D.; Labat, S.; Toupet, L.; Crévisy, C.; Mauduit, M. *Eur. J. Inorg. Chem.* **2009,** 1989-1999. 10.1002/ejic.200801243.

[12] Arnold, P. L.; Rodden, M.; Davis, K. M.; Scarisbrick, A. C.; Blake, A. J.; Wilson, C. *Chem. Commun.* **2004,** 1612-1613. 10.1039/B404614E.

[13] Clavier, H.; Coutable, L.; Toupet, L.; Guillemin, J.-C.; Mauduit, M. *J. Organomet. Chem.* **2005,** *690,* 5237-5254. 10.1016/j.jorganchem.2005.04.027. Martin, D.; Kehrli, S.; d'Augustin, M.; Clavier, H.; Mauduit, M.; Alexakis, A. *J. Am. Chem. Soc.* **2006,** *128,* 8416-8417. 10.1021/ja0629920. Hénon, H.; Mauduit, M.; Alexakis, A. *Angew. Chem. Int. Ed.* **2008,** *47,* 9122-9124. 10.1002/anie.200803735.

[14] Trofimoff, L.; Aida, T.; Inoue, S. *Chem. Lett.* **1987,** *16,* 991-994. 10.1246/cl.1987.991.

[15] Zhang, W.; Loebach, J. L.; Wilson, S. R.; Jacobsen, E. N., *J. Amer. Chem. Soc.* **1990,** *112,* 2801-2803. 10.1021/ja00163a052.

[16] Hormnirun, P.; Marshall, E. L.; Gibson, V. C.; White, A. J. P.; Williams, D. J. *J. Am. Chem. Soc.* **2004,** *126,* 2688-2689. 10.1021/ja038757o.

[17] Williams, C. K.; Breyfogle, L. E.; Choi, S. K.; Nam, W.; Young, Jr., V. G.; Hillmyer, M. A.; Tolman, W. B. *J. Am. Chem. Soc.* **2003,** *125,* 11350-11359. 10.1021/ja0359512.

[18] Viciano, M.; Mas-Marzá, E.; Poyatos, M.; Sanaú, M.; Crabtree, R. H.; Peris, E. *Angew. Chem. Int. Ed.* **2005,** *44,* 444-447. 10.1002/anie.200461918.

[19] Arduengo, III, A. J.; Harlow, R. L.; Kline, M. *J. Am. Chem. Soc.* **1991,** *113(1),* 361-363. 10.1021/ja00001a054.

[20] Glorius, F. *Top. Organomet. Chem.* **2007,** *21,* 1-20. 10.1007/3418_2006_059.

[21] Pearson, R. G. *J. Am. Chem. Soc.* **1963,** *85,* 3533-3539. 10.1020/ja00905a001.

[22] Myers, R. T. *Inorg. Chem.* **1978,** *17,* 952-958. 10.1021/ic50182a032. Fryzuk, M. D.; MacNeil, P. A.; Rettig, S. J.; Secco, A. S.; Trotter, J. *Organometallics* **1982,** *1,* 918-930. 10.1021/om00067a006. Civiš, S.; Podlahová, J.; Loub, J.; Ječný, J. *Acta Cryst.* **1980,** *B36,* 1395-1397. 10.1107/S0567740880006152.

[23] Boeré, R. T.; Montgomery, C. D.; Payne, N. C.; Willis, C. J. *Inorg. Chem.* **1985,** *24,* 3680-3687. 10.1021/ic00216a042.

[24] Pebal, L. *Ann.* **1861,** *120,* 194-206. 10.1002/jlac.18611200206. Pickard, R. H.; Kenyon, J. *J. Chem. Soc., Trans.* **1906,** *89,* 262-273. 10.1039/CT9068900262.

[25] Levitt, A. E.; Freund, H. *J. Am. Chem. Soc.* **1956,** *78,* 1545-1549. 10.1021/ja01589a010. Burger, L. L. *J. Phys. Chem.* **1958,** *62,* 590-593. 10.1021/j150563a017.

[26] Ng, S. W.; Zuckerman, J. J. *Organometallics* **1982,** *1,* 714-720. 10.1021/om00065a008.

[27] a) Cross, R. J.; Farrugia, L. J.; Newman, P. D.; Peacock, R. D.; Stirling, D. *J. Chem. Soc., Dalton Trans.* **1996,** 1087-1092 (10.1039/dt9960001087), b) 1637-1643 (10.1039/DT9960001637) and c) 4449-4458 (10.1039/dt9960004449). d) Cross, R. J.; Newman, P. D.; Peacock, R. D.; Stirling, D. *J. Mol. Catal. A: Chem.* **1999,** *144,* 273-284. 10.1016/S1381-1169(98)00371-9.

[28] Keough, P. T.; Grayson, M. *J. Org. Chem.* **1962,** *27,* 1817-1823. 10.1021/jo01052a082.

[29] Richard, J. J.; Banks, C. V. *J. Org. Chem.* **1963,** *28,* 123-125. 10.1021/jo01036a028.

[30] Fox, D. J.; Medlock, J. A.; Vosser, R.; Warren, S. *J. Chem. Soc., Perkin Trans. 1* **2001,** 2240-2249. 10.1039/b104436m.

[31] Santelli-Rouvier, C. *Synthesis* **1988,** 64-66.

[32] Genov, D. G.; Kresinski, R. A.; Tebby, J. C. *J. Org. Chem.* **1998,** *63,* 2574-2585. 10.1021/jo972036o.

[33] Arnold, P. L.; Buffet, JC.; Blaudeck, R. P.; Sujecki, S.; Blake, A. J.; Wilson, C. *Angew. Chem. Int. Ed.* **2008,** *47,* 6033-6036. 10.1002/anie.200801279.

[34] Arnold, P. L.; Buffet, JC.; Blaudeck, R; Sujecki, S.; Wilson, C. *Chem. Eur. J.* **2009,** *15,* 8241-8250. 10.1002/chem.200900522.

[35] Buffet, J.-C., PhD Thesis, The University of Edinburgh, UK (Edinburgh), **2009**.

[36] Ionkin, A. S.; Marshall, W. J.; Fish, B. M. *Organometallics* **2006,** *25(17),* 4170-4178. 10.1021/om060355c.

[37] Doering, W. von E.; Hoffmann, A. K. *J. Am. Chem. Soc.* **1954,** *76,* 6162-6165. 10.1021/ja01652a087. Fischer, E. O.; Maasböl, A. *Angew. Chem. Int. Ed.* **1964,** *3(8),* 580-581. 10.1002/anie.196405801.

[38] Herrmann, W. A. *Angew. Chem. Int. Ed.* **2002,** *41,* 1290-1309. 10.1002/1521-3773(20020415)41:8<1290::AID-ANIE1290>3.0.CO;2-Y.

[39] Wanzlick, H. W. *Angew. Chem. Int. Ed.* **1962,** *1(2),* 75-80. 10.1002/anie.196200751. Wanzlick, H. W.; Schönherr, H. J. *Angew. Chem. Int. Ed.* **1968,** *7(2),* 141-142. 10.1002/anie.196801412. Öfele, K. *J. Organomet. Chem.* **1968,** *12,* P42-P43. 10.1016/S0022-328X(00)88691-X.

[40] Hitchcock, P. B.; Lappert, M. F.; Terreros, P.; Wainwright, K. P. *J. Chem. Soc. Chem. Commun.* **1980,** 1180-1181. 10.1039/C39800001180.

[41] Kernbach, U.; Ramm, M.; Luger, P.; Fehlhammer, W. P. *Angew. Chem. Int. Ed. Engl.* **1996,** *35(3),* 310-312. 10.1002/anie.199603101.

[42] Poyatos, M.; Mata, J. A.; Falomir, E.; Crabtree, R. H.; Peris, E. *Organometallics* **2003,** *22,* 1110-1114. 10.1021/om020817w.

[43] Wang, H. M. J.; Lin, I. J. B. *Organometallics* **1998,** *17,* 972-975. 10.1021/om9709704.

[44] Arnold, P. L.; Pearson, S. *Coord. Chem. Rev.* **2007,** *251,* 596-609. 10.1016/j.ccr.2006.08.006.

[45] Arnold, P. L.; Scarisbrick, A. C.; Blake, A. J.; Wilson, C. *Chem. Commun.* **2001,** 2340-2341. 10.1039/b107855k.

[46] Li, W.; Sun, H.; Chen, M.; Wang, Z.; Hu, D.; Shen, Q.; Zhang, Y. *Organometallics* **2005,** *24,* 5925-5928. 10.1021/om050612y.

[47] Ulusoy, M.; Şahin, O.; Büyükgüngör, O.; Çetinkaya, B. *J. Organomet. Chem.* **2008,** *693,* 1895-1902. 10.1016/j.jorganchem.2008.02.017.

[48] Liao, C.-Y.; Chan, K.-T.; Chang, Y.-C.; Chen, C.-Y.; Tu, C.-Y.; Hu, C.-H.; Lee, H. M. *Organometallics* **2007,** *26,* 5826-5833. 10.1021/om700607m.

[49] Zhou, Y.; Xi, Z.; Chen, W.; Wang, D. *Organometallics* **2008,** *27,* 5911-5920. 10.1021/om800711g. Huynh, H. V.; Jothibasu, R.; *Eur. J. Inorg. Chem.* **2008,** 1926-1931. 10.1002/ejic.200801149. Berding, J.; van Dijkman, T. F.; Lutz, M.; Spek, A. L.; Bouwman, E. *Dalton Trans.* **2009,** 6948-6955. 10.1039/b905036a. Xi, Z.; Liu, B.; Lu, C.; Chen, W. *Dalton Trans.* **2009,** 7008-7014. 10.1039/b906242d. Kumar, S.; Narayanan, A.; Rao, M. N.; Shaikh, M. M.; Ghosh, P. *J. Organomet. Chem.* **2012,** *696,* 4159-4165. 10.1016/j.jorganchem.2011.09.007.

[50] Aihara, H.; Matsuo, T.; Kawaguchi, H. *Chem. Commun.* **2003,** 2204-2205. 10.1039/b305745c. McGuinness, D. S.; Gibson, V. C.; Steed, J. W. *Organometallics* **2004,** *23,* 6288-6292. 10.1021/om049246t.

[51] a) Jensen, T. R.; Schaller, C. P.; Hillmyer, M. A.; Tolman, W. B. *J. Organomet. Chem.* **2005,** *690,* 5881-5891. 10.1016/j.jorganchem.2005.07.070. b) Patel, D.; Liddle, S. T.;

Mungur, S. A.; Rodden, M.; Blake, A. J.; Arnold, P. L. *Chem. Commun.* **2006,** 1124-1126. 10.1039/b514406j. c) Arnold, P. L.; Casely, I. J.; Turner, Z. R.; Bellabarba, R.; Tooze, R. B. *Dalton Trans.* **2009,** 7236-7247. 10.1039/b907034f.

[52] a) Hu, X.; Castro-Rodríguez, I.; Meyer, K. *J. Am. Chem. Soc.* **2003,** *125,* 12237-12245. 10.1021/ja036880+. b) *J. Am. Chem. Soc.* **2004,** *126,* 13464-13473. 10.1021/ja046048k. c) *Chem. Commun.* **2004,** 2164-2165. 10.1039/b409241d.

[53] a) Douthwaite, R. E.; Houghton, J.; Kariuki, B. M. *Chem. Commun.* **2004,** 698-699. 10.1039/b314814a. b) Houghton, J.; Dyson, G.; Douthwaite, R. E.; Whitwood, A. C.; Kariuki, B. M *Dalton Trans.* **2007,** 3065-3073. 10.1039/b703248j.

[54] Liu, Q.-X.; Yu, J.; Zhao, X.-J.; Liu, S.-W.; Yang, X.-Q.; Li, K.-Y.; Wang, X.-G. *CrystEngComm* **2011,** *13,* 4086-4096. 10.1039/c1ce05134b.

[55] Edworthy, I. S.; Blake, A. J.; Wilson, C.; Arnold, P. L. *Organometallics* **2007,** *26,* 3684-3689 10.1021/om0701874.

[56] Arnold, P. L.; Edworthy, I. S.; Carmichael, C. D.; Blake, A. J.; Wilson, C. *Dalton Trans.* **2008,** 3739-3746 10.1039/b803253j.

[57] Drumright, R. E.; Gruber, P. R.; Henton, D. E. *Adv. Mater.* **2000,** *12,* 1841-1846. 10.1002/1521-4095(200012)12:23<1841::AID-ADMA1841>3.0.CO;2-E.

[58] Wheaton, C. A.; Hayes, P. G.; Ireland, B. J. *Dalton Trans.* **2009,** 4832-4836. 10.1039/b819107g.

[59] Ikada, Y.; Jamshidi, K.; Tsuji, H.; Hyon, S. H. *Macromolecules* **1987,** *20,* 904-906. 10.1021/ma00170a034.

[60] Thakur, K. A. M.; Kean, R. T.; Hall, E. S.; Kolstad, J. J.; Lindgren, T. A. *Macromolecules* **1997,** *30,* 2422-2428. 10.1021/ma9615967

[61] Chisholm, M. H.; Iyer, S. S.; Matison, M. E.; McCollum, D. G.; Pagel, M. *Chem. Commun.* **1997,** 1999-2000. 10.1039/A703676K

[62] Thakur, K. A. M.; Kean, R. T.; Zell, M. R.; Padden, B. E.; Munson, E. J. *Chem. Commun.* **1998,** 1913-1914. 10.1039/A708911B

[63] Kricheldorf, H. R.; Berl, M.; Scharnagl, N. *Macromolecules* **1988,** *21,* 286-293. 10.1021/ma00180a002. Dubois, Ph.; Jacobs, C.; Jérôme, R.; Teyssié, Ph. *Macromolecules* **1991,** *24,* 2266-2270. 10.1021/ma00009a022.

[64] O'Keefe, B. R.; Hillmyer, M. A.; Tolman, W. B. *J. Chem. Soc., Dalton Trans.* **2001,** 2215-2224. 10.1039/b104197p.

[65] "Product & Applications." NatureWorks LLC. 18 June 2013 <http://www.natureworksllc.com/Product-And-Applications.aspx>.

[66] Spassky, N. Wisniewski, M.; Pluta, C.; Le Borgne, A. *Macromol. Chem. Phys.* **1996,** *197,* 2627-2637. 10.1002/macp.1996.021970902.

[67] Radano, C. P.; Baker, G. L.; Smith, III, M. R. *J. Am. Chem. Soc.* **2000,** *122,* 1552-1553. 10.1021/ja9930519.

[68] Ovitt, T. M.; Coates, G. W. *J. Polym. Sci. Part A: Polym. Chem.* **2000,** *38,* 4686-4692. 10.1002/1099-0518(200012)38:1+<4686::AID-POLA80>3.0.CO;2-0.

[69] Ovitt, T. M.; Coates, G. W. *J. Am. Chem. Soc.* **1999,** *121,* 4072-4073. 10.1021/ja990088k.

[70] Emig, N.; Nguyen, H.; Krautscheid, H.; Réau, R.; Cazaux, J. B.; Bertrand, G. *Organometallics* **1998,** *17,* 3599-3608. 10.1021/om980401b.

[71] Cheng, M.; Attygalle, A. B.; Lobkovsky, E. B.; Coates, G. W. *J. Am. Chem. Soc.* **1999,** *121,* 11583-11584. 10.1021/ja992678o.

[72] Chisholm, M. H.; Eilerts, N. W.; Huffman, J. C.; Iyer, S. S.; Pacold, M.; Phomphrai, K. *J. Am. Chem. Soc.* **2000,** *122,* 11845-11854. 10.1021/ja002160g.

[73] O'Keefe, B. J.; Monnier, S. M.; Hillmyer, M. A.; Tolman, W. B. *J. Am. Chem. Soc.* **2001,** *123,* 339-340. 10.1021/ja003537l.

[74] Chamberlain, B. M.; Cheng, M.; Moore, D. R.; Ovitt, T. M.; Lobkovsky, E. B.; Coates, G. W. *J. Am. Chem. Soc.* **2001,** *123,* 3229-3238. 10.1021/ja003851f.

[75] Cai, C.-X.; Amgoune, A.; Lehmann, C. W.; Carpentier, J.-F. *Chem. Commun.* **2004,** 330-331. 10.1039/b314030j. Amgoune, A.; Thomas, C. M.; Roisnel, T.; Carpentier, J.-F. *Chem. Eur. J.* **2006,** *12,* 169-179. 10.1002/chem.200500856. Amgoune, A.; Thomas, C. M.; Carpentier, J.-F. *Pure Appl. Chem.* **2007,** *79(11),* 2013-2030. 10.1351/pac200779112013.

[76] Lian, B.; Thomas, C. M.; Casagrande Jr., O. L.; Lehmann, C. W.; Roisnel, T.; Carpentier, J.-F. *Inorg. Chem.* **2007,** *46,* 328-340. 10.1021/ic061749z. Lian, B.; Thomas, C. M.; Casagrande Jr., O. L.; Roisnel, T.; Carpentier, J.-F. *Polyhedron* **2007,** *26,* 3817-3824. 10.1016/j.poly.2007.04.022.

[77] Bouyahyi, M.; Grunova, E.; Marquet, N.; Kirillov, E.; Thomas, C. M.; Roisnel, T.; Carpentier, J.-F. *Organometallics* **2008,** *27,* 5815-5825. 10.1021/om800651z.

[78] Alaaeddine, A.; Thomas, C. M.; Roisnel, T.; Carpentier, J.-F. *Organometallics* **2009,** *28,* 1469-1475 10.1021/om8010273.

[79] Pietrangelo, A.; Hillmyer, M. A.; Tolman, W. B. *Chem. Commun.* **2009,** 2736-2737. 10.1039/b902968k. Pietrangelo, A.; Knight, S. C.; Gupta, A. K.; Yao, L. J.; Hillmyer, M. A.; Tolman, W. B. *J. Am. Chem. Soc.* **2010,** *132,* 11649-11657. 10.1021/ja103841h.

[80] Connor, E. F.; Nyce, G. W.; Myers, M.; Möck, A.; Hedrick, J. L. *J. Am. Chem. Soc.* **2002,** *124(6),* 914-916. 10.1021/ja0173324.

[81] Dechy-Cabaret, O.; Martin-Vaca, B.; Bourissou, D. *Chem. Rev.* **2004,** *104,* 6147-6176. 10.1021/cr040002s.

[82] Coady, D. J.; Engler, A. C.; Horn, H. W.; Bajjuri, K. M.; Fukushima, K.; Jones, G. O.; Nelson, A.; Rice, J. E.; Hedrick, J. L. *ACS Macro Lett.* **2012,** *1,* 19-22. 10.1021/mz2000048.

[83] Miyake, G. M.; Chen, E. Y.-X. *Macromolecules* **2011,** *44,* 4116-4124. 10.1021/ma2007199.

[84] Dove, A. P.; Li, H.; Pratt, R. C.; Lohmeijer, B. G. G.; Culkin, D. A.; Waymouth, R. M.; Hedrick, J. L. *Chem. Commun.* **2006,** 2881-2883. 10.1039/b601393g.

[85] Pratt, R. C.; Lohmeijer, B. G. G.; Long, D. A.; Lundberg, P. N. P.; Dove, A. P.; Li, H.; Wade, C. G.; Waymouth, R. M.; Hedrick, J. L. *Macromolecules* **2006,** *39,* 7863-7871. 10.1021/ma061607o.

[86] Zhang, L.; Nederberg, F.; Pratt, R. C.; Waymouth, R. M.; Hedrick, J. L.; Wade, C. G. *Macromolecules* **2007,** *40,* 4154-4158. 10.1021/ma070316s. Zhang, L.; Nederberg, F.; Messman, J. M.; Pratt, R. C.; Hedrick, J. L.; Wade, C. G. *J. Am. Chem. Soc.* **2007,** *129,* 12610-12611. 10.1021/ja074131c.

[87] Darensbourg, D. J. *Inorg. Chem.* **2010,** *49,* 10765-10780. 10.1021/ic101800d.

[88] Darensbourg, D. J.; Holtcamp, M. W. *Coordin. Chem. Rev.* **1996,** *153,* 155-174. 10.1016/0010-8545(95)01232-X.

[89] Coates, G. W.; Moore, D. R. *Angew. Chem. Int. Ed.* **2004,** *43,* 6618-6639. 10.1002/anie.200460442. Darensbourg, D. J. *Chem. Rev.* **2007,** *107,* 2388-2410. 10.1021/cr068363q.

[90] Inoue, S.; Koinuma, H.; Tsuruta, T. *Makromol. Chem.* **1969,** *130,* 210-220.

[91] Aida, T.; Ishikawa, M.; Inoue, S. *Macromolecules* **1986,** *19,* 8-13. 10.1021/ma00155a002.

[92] Byrne, C. M.; Allen, S. D.; Lobkovsky, E. B.; Coates, G. W. *J. Am. Chem. Soc.* **2004,** *126,* 11404-11405. 10.1021/ja0472580.

[93] Qin, Z.; Thomas, C. M.; Lee, S.; Coates, G. W. *Angew. Chem. Int. Ed.* **2003,** *42,* 5484-5487. 10.1002/anie.200352605.

[94] Lu, X.-B.; Wang, Y. *Angew. Chem. Int. Ed.* **2004,** *43,* 3574-3577. 10.1002/anie.200453998.

[95] a) Nakano, K.; Kamada, T.; Nozaki, K. *Angew. Chem. Int. Ed.* **2006,** *45,* 7274-7277. 10.1002/anie.200603132. b) Noh, E. K.; Na, S. J.; Sujith, S.; Kim, S.-W.; Lee, B. Y. *J. Am. Chem. Soc.* **2007,** *129,* 8082-8083. 10.1021/ja071290n. c) Ren, W.-M.; Zhang, X.; Liu, Y.; Li, J.-F.; Wang, H.; Lu, X.-B. *Macromolecules* **2010,** *43,* 1396-1402. 10.1021/ma902321g.

[96] Sugimoto, H.; Kuroda, K. *Macromolecules* **2008,** *41,* 312-317. 10.1021/ma702354s.

[97] Chang, T.; Jin, L.; Jing, H. *ChemCatChem* **2009,** *1,* 379-383. 10.1002/cctc.200900135. Ren, W.-M.; Liu, Z.-W.; Wen, Y.-Q.; Zhang, R.; Lu, X.-B. *J. Am. Chem. Soc.* **2009,** *131,* 11509-11518. 10.1021/ja9033999.

[98] Darensbourg, D. J.; Yarbrough, J. C.; Ortiz, C.; Fang, C. D. *J. Am. Chem. Soc.* **2003,** *125,* 7586-7591. 10.1021/ja034863e.

[99] Pilkington, N. H.; Robson, R. *Aust. J. Chem.* **1970,** *23,* 2225-2236.

[100] Kember, M. R.; Knight, P. D.; Reung, P. T. R.; Williams, C. K. *Angew. Chem. Int. Ed.* **2009,** *48,* 931-933. 10.1002/anie.200803896. Kember, M. R.; White, A. J. P.; Williams, C. K. *Inorg. Chem.* **2009,** *48,* 9535-9542. 10.1021/ic901109e. Jutz, F.; Buchard, A.; Kember,

M. R.; Fredriksen, S. B.; Williams, C. K. *J. Am. Chem. Soc.* **2011,** *133,* 17395-17405. 10.1021/ja206352x.

[101] Buchard, A.; Kember, M. R.; Sandeman, K.; Williams, C. K. *Chem. Commun.* **2011,** *47,* 212-214. 10.1039/c0cc02205e.

[102] Darensbourg, D. J.; Wilson, S. J. *J. Am. Chem. Soc.* **2011,** *133,* 18610-18613. 10.1021/ja208711c.

[103] Wu, G.-P.; Wei, S.-H.; Ren, W.-M.; Lu, X.-B.; Li, B.; Zu, Y.-P.; Darensbourg, D. J. *Energy Environ. Sci.* **2011,** *4,* 5084-5092. 10.1039/c1ee02566j.

[104] Lu, X.-B.; Darensbourg, D. J. *Chem. Soc. Rev.* **2012,** *41,* 1462-1484. 10.1039/c1cs15142h.

[105] Kember, M. R.; White, A. J. P.; Williams, C. K. *Macromolecules* **2010,** *43,* 2291-2298. 10.1021/ma902582m. Kember, M. R.; Jutz, F.; Buchard, A.; White, A. J. P.; Williams, C. K. *Chem. Sci.* **2012,** *3,* 1245-1255. 10.1039/c2sc00802e.

[106] Soga, K.; Hyakkoku, K.; Ikeda, S. *Makromol. Chem.* **1978,** *179,* 2837-2843. 10.1002/macp.1978.021791203.

[107] Lee, B. Y.; Cyriac, A. *Nature Chem.* **2011,** *3,* 505-507. 10.1038/nchem.1081. Nakano, K.; Hashimoto, S.; Nakamura, M.; Kamada, T.; Nozaki, K. *Angew. Chem. Int. Ed.* **2011,** *50(21),* 4868-4871. 10.1002/anie.201007958.

[108] Wu, G.-P.; Ren, W.-M.; Luo, Y.; Li, B.; Zhang, W.-Z.; Lu, X.-B. *J. Am. Chem. Soc.* **2012,** *134,* 5682-5688. 10.1021/ja300667y.

[109] Nishioka, K.; Goto, H.; Sugimoto, H. *Macromolecules* **2012,** *45,* 8172-8192. 10.1021/ma301696d.

[110] Makiguchi, K.; Ogasawara, Y.; Kikuchi, S.; Satoh, T.; Kakuchi, T. *Macromolecules* **2013,** *46,* 1772-1782. 10.1021/ma4000495.

[111] Zhou, H.; Campbell, E. J.; Nguyen, S. T. *Org. Lett.* **2001,** *3,* 2229-2231. 10.1021/ol0161110.

[112] Zhou, H.; Zhang, W.-Z.; Liu, C.-H.; Qu, J.-P.; Lu, X.-B. *J. Org. Chem.* **2008,** *73,* 8039-8044. 10.1021/jo801457r.

[113] Arnold, P. L.; Okuda, J.; Buffet, JC. *Inorg. Chem.* **2010,** *49,* 419-426. 10.1021/ic900740n.

[114] Solov'ev, V. P.; Baulin, V. E.; Strakhova, N. N.; Kazachenko, V. P.; Belsky, V. K.; Varnek, A. A.; Volkova, T. A.; Wipff, G. *J. Chem. Soc., Perkin Trans. 2* **1998,** 1489-1498. 10.1039/a708245b.

[115] Arnold, P. L.; Casely, I. J.; Turner, Z. R.; Carmichael, C. D. *Chem. Eur. J.* **2008,** *14,* 10415-10422. 10.1002/chem.200801321.

CHAPTER 2. SYNTHESIS OF METAL COMPLEXES USING DITOPIC ALKOXIDE/PHOSPHINE OXIDE LIGANDS AND THEIR ROLE AS POLYMERISATION INITIATORS

2.1. Introduction

Given the success of the phosphine oxide-tethered alkoxide ligands in the formation of homochiral rare earth metal complexes, which proved to be very active as catalysts in the formation of highly isotactic poly(lactic acid) chains, we chose to study similar systems using transition metals.[1] The proligands used are the previously reported *rac*-3,3-dimethyl-1-(*P*,*P*-ditertbutyl-phosphonyl)-butan-2-ol (**X**), and the *P*,*P*-diphenyl analogue, **1**. These ligands, especially **X**, are of a suitable size to allow the formation of octahedrally coordinated yttrium and other larger rare earth metal cations, but the hemilability of the P=O group can offer a flexibility that can still allow reactivity from even sterically saturated complexes of smaller metal cations.[2]

2.2. Synthesis and X-ray structure of HL^{Ph}

Because these complexes containing the L^{tBu} ligand are expensive and susceptible to degradation in the presence of oxygen and moisture, the analogous ligand L^{Ph}, containing phenyl instead of *tert*-butyl groups as substituents on the phosphine oxide donor, was synthesised, following the literature preparation.[1]

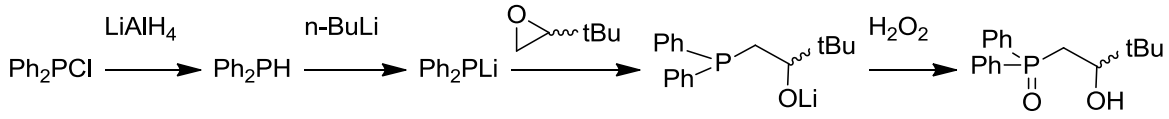

Equation 2.1. Preparation of proligand HL^{Ph}.

Reducing agent $LiAlH_4$ was added to a tetrahydrofuran (THF) solution of chlorodiphenylphosphine at 0 °C to form Ph_2PH after 12 h. The solution containing diphenylphosphine was filtered and *n*-butyllithium was added dropwise for half an hour at the same temperature. After, an equivalent of 3,3-dimethyl-1,2-epoxybutane was added and the solution stirred for 12 h at room temperature. Finally, hydrogen peroxide was added slowly to oxidise the phosphine at 0 °C. Crystallised proligand HL^{Ph} was obtained in 47% overall yield from a toluene solution at -4 °C.

Interestingly, single crystals of HL^{Ph} were grown from dichloromethane (DCM) solution and toluene solution at -30 °C, and show two very different polymorphs: one with an intramolecular hydrogen bond between the OH and P=O group, and one with an

intermolecular hydrogen bond between the OH and P=O group. The two structures are shown in Figure 2.1.

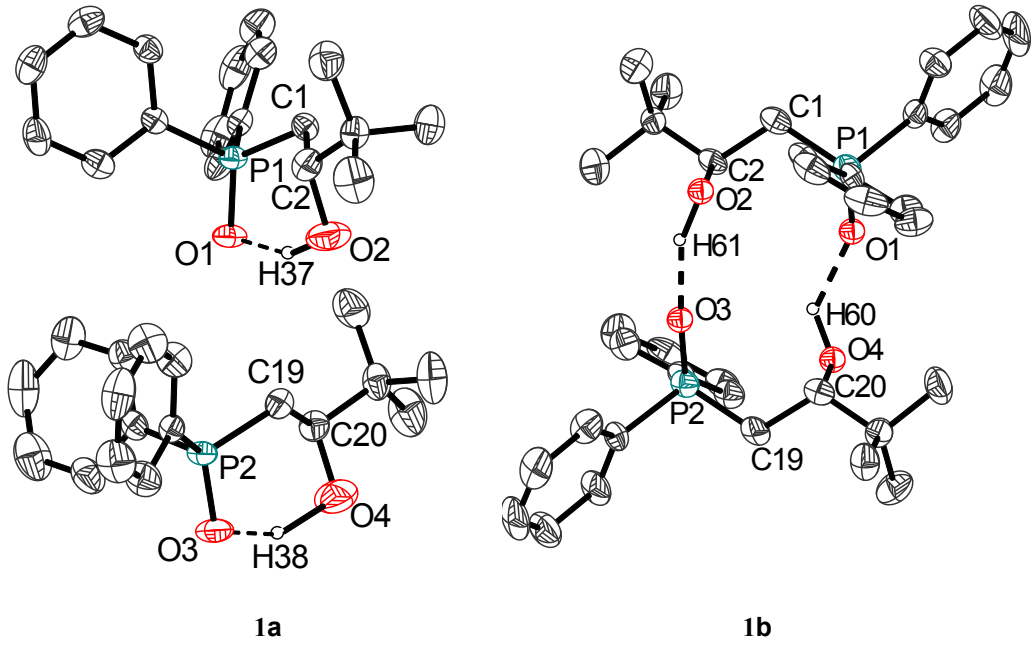

1a **1b**

Figure 2.1. Displacement ellipsoid drawing of two morphologies of HL^{Ph} (1). 50% probability ellipsoids. All hydrogen atoms, except those of the alcohol units, are omitted for clarity.

Selected distances (Å): for **1a** P1–O1 1.496(3), P2–O3 1.499(3), O2–H37 1.498(35), O4–H38 1.634(32), O1…H37 1.471(34), O3…H38 1.336(30), for **1b** P1–O1 1.477(5), P2–O3 1.496(5), O2–H61 1.138(31), O4–H60 1.085(44), O3…H61 1.604(39), O1…H60 1.805(33); selected angles (°): for **1a** C1–P1–O1 111.5(2), C19–P2–O3 112.4(2), C2–O2–H37 100.8(14), C20–O4–H38 103.6(12), O2–H37…O1 147.1(25), O4–H38…O3 147.7(23), for **1b** C1–P1–O1 113.4(3), C19–P2–O3 113.6(2), C2–O2–H61 99.3(26), C20–O4–H60 112.1(26), O2–H61…O3 152.6(26), O4–H60…O1 132.1(27).

Structural features of the colourless, needle-like crystals of **1** collected from a DCM solution at -30° C are shown in the left of Figure 2.1, as **1a**. The structure presents intramolecular hydrogen bonding and an alternately almost-orthogonal packing with respect to the planes formed by the P and O atoms (dihedral angle between planes: 81.3°). The hydrogen atoms in the alcohol group were refined manually according to the highest amount of electronic density between the oxygen atoms. Oddly, in both molecules of the asymmetric unit of **1a** the PO...H bond distance (1.471(34) and 1.336(30) Å) is slightly shorter than the H–OC bond distance (1.498(35) and 1.634(32) Å, respectively) due to the influence of a highly negative dipole moment in the phosphinoyl group. The angles C–O–H and P–O...H

are very similar in each molecule: 100.8(14) and 100.9(14)° for the top molecule and 103.6(12) and 102.0(14) for the bottom one, respectively.

Structural features of the colourless, block-like crystals of **1** collected from a toluene solution at -30° C are shown in the right of Figure 2.1, named **1b**. The structure presents intermolecular hydrogen bonding with parallel planes formed by P and O atoms in adjacent molecules. The hydrogen atoms in the alcohol group were refined manually according to the highest amount of electronic density between the neighbouring O atoms. In this case, the CO–H bond distances (1.138(31) and 1.085(44) Å) are shorter than the PO...H interactions (1.604(39) and 1.805(33) Å, respectively) with the C–O–H angles (99.3(26) and 112.1(26)°) more in agreement with the expected ~109° compared to the P–O...H angles (150.9(11) and 146.3(10)°, respectively). In contrast, the dipole moment in the phosphinoyl group in the molecular structures of **1a** has a bigger influence in its resulting geometry; this effect may be caused by the lower dihedral O–C...P–O angles in **1a** (20.5(2) and 9.3(3)°) compared to those in **1b** (95.0(3) and 92.5(3)°).

A third polymorph was previously reported by the Tebby group (crystallised from hexane/acetone at room temperature, called **1c** for reference; see Figure 2.2) with bond distances and angles similar to those of **1a** and **1b**: P1–O1 1.489(3) Å and C1–P1–O1 112.2(2)°.[3] The molecular structure in **1c** presents intramolecular hydrogen bonding with an O1...O2 distance of 2.838(5) Å compared to 2.848(4) and 2.854(5) Å in **1a** and 2.658(6) and 2.666(6) Å in **1b**; distances of intramolecular hydrogen bonds are longer than those of intermolecular hydrogen bonds in these examples. The O–C...P–O torsion angle of **1c** is relatively low (17.8(2)°) and is similar to those of **1a**, which also features intramolecular hydrogen bonding. No further comparisons will be made of the hydrogen atom in the alcohol group because its position was theoretically modelled.[3] It is interesting to note that the model of **1c** contains two carbon atoms, C6 and C16, in close proximity. Although no indications of problems with the molecular structure are given in the reported text or tables ($R[I > 2\sigma(I)]$ factor is 0.0463), there is an irregularity with the atoms C6 and C16: the distance between them, 0.797(6) Å, is shorter than the typical value for an alkyne (~1.21 Å) or even the theoretical assigned value for aryl hydrogen bonds (0.93 Å).[3]

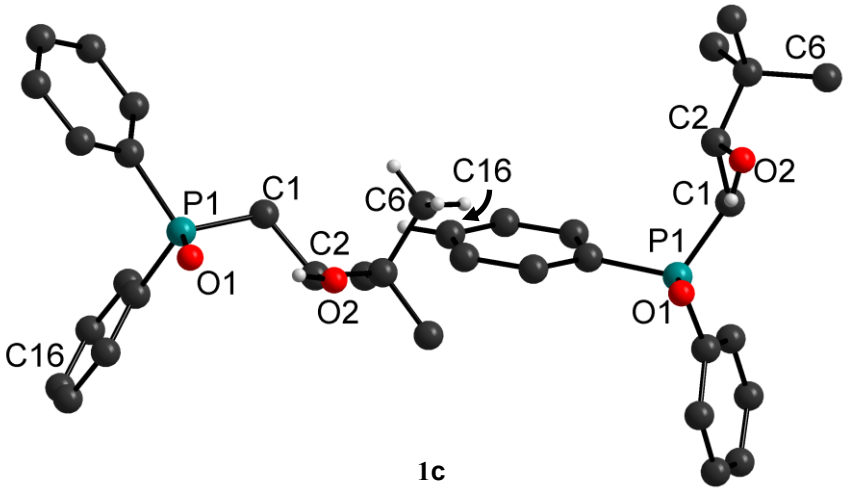

Figure 2.2. Two molecules of the reported polymorph of 1.[3]

2.3. M^{II} complexes of alkoxide/phosphine oxide ligands (M = Zn, Sn, Co)

The majority of the catalysts studied for the copolymerisation of carbon dioxide and epoxides reported in the literature are zinc or cobalt complexes; diethyl zinc was the first reported initiator for this reaction.[4] Buffet synthesised and structurally characterised Co^{II} and Sn^{II} complexes using the HL^{Ph} proligand **1** as shown in Equation 2.2.[2]

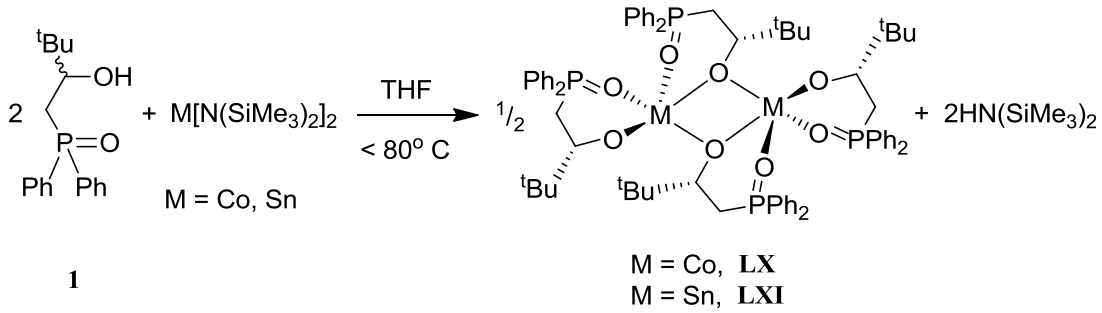

1

M = Co, **LX**
M = Sn, **LXI**

Equation 2.2. Synthesis of homoleptic $M(L^{Ph})_2$ complexes

The deep-blue cobalt complex presents a dimeric form of $Co(L^{Ph})_2$ (**LX**) in the solid state in which the cobalt atoms are bridged by two alkoxide groups and have a distance of 3.0437(9) Å.[2] The tin complex $[Sn(L^{Ph})_2]_2$ (**LXI**) shows activity for the polymerisation of *rac*-lactide.[2]

Using the **X** proligand, both homoleptic complexes $Zn(L^{tBu})_2$ (**LVIII**) and $Sn(L^{tBu})_2$ (**XI**) have been reported by Buffet and synthesised as shown in Equation 2.3.[2]

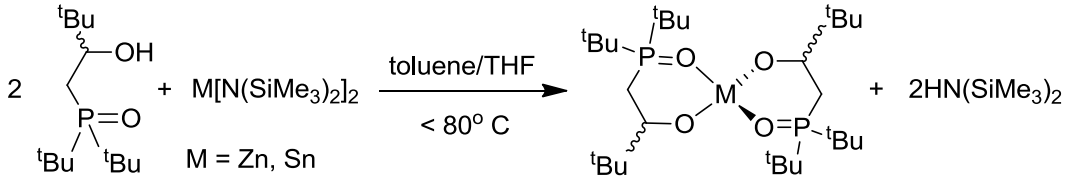

X

M = Zn, **LVIII**
M = Sn, **XI**

Equation 2.3. Synthesis of homoleptic $M(L^{tBu})_2$ complexes

Polymerisation studies performed by Buffet of **LVIII** catalysing the formation of poly(lactic acid) led to high conversion of lactide and polydispersity indices as low as 1.42 (see Table 2.1).[2] The tin complex bearing this ligand, $Sn(L^{tBu})_2$ (**XI**), was also reported to produce poly(lactic acid), although less effectively than the zinc analogue in terms of molecular weight and reaction temperature (see Table 2.1). The polymers made by the tin

complex in a reaction carried out at room temperature had good polydispersity indices at low conversions.[2]

Table 2.1. Previously reported polymerisation data of *rac*-lactide using Zn(L^{tBu})$_2$ (LVIII) and Sn(L^{tBu})$_2$ (XI).[2]

Complex	Cat:monomer :solvent ratio	T /°C	Time / h	Conv.[c] / %	$M_{n,\,exp}$[d] g/mol	$M_{n,\,theo}$[e] g/mol	PDI[f] M_w/M_n
LVIII	1 : 100 : 1000[a]	25	0.17	> 99	41 500	58 541	1.7
LVIII	1 : 200 : 10000[a]	25	16	98	82 000	115 327	1.4
XI	1 : 100 : 1000[a]	25	16	15	7 500	10 380	1.2
XI	1 : 200 : 1000[b]	60	16	93	65 000	60 098	1.5

a: Dichloromethane; **b**: toluene; **c**: conversion of LA monomer (([LA]$_0$-[LA])/[LA]$_0$) from integration of ^{1}H NMR spectra; **d**: measured by GPC, weight corrected by multiplication by 0.58; **e**: molecular weight theoretically calc. using $M_{n,theo}$ = Conv. × [Mono]/[Cat] × M_{Mono}; **f**: polydispersity index (M_w/M_n), PDI, measured by GPC.

2.3.1. Synthesis and X-ray structure of Co(L^{tBu})$_2$ (3)

Using the **X** proligand, the cobalt analogue of **LVIII** and **XI**, Co(L^{tBu})$_2$ (**3**), was synthesised by a similar procedure as shown in .

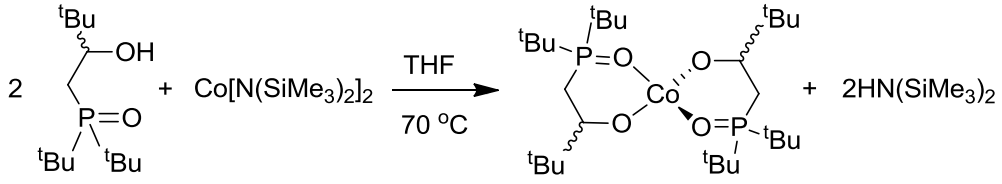

Equation 2.4. Synthesis of complex Co(L^{tBu})$_2$ (3)

The freshly prepared cobalt silylamide precursor was mixed in a THF solution with two equivalents of the proligand **X** immediately turning the green solution into a deep purple colouration. The crystallised product was obtained from a hexanes solution at -30 °C in a 71% yield. Bright green crystals of compound **3** were grown from a purple hexanes solution of the pure compound affording molecular structures from a single-crystal X-ray diffraction study as shown in Figure 2.3.

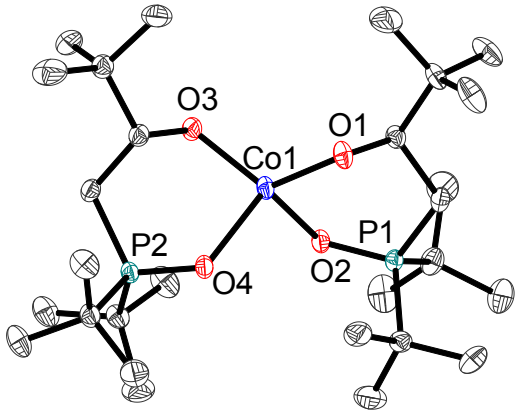

Figure 2.3. Displacement ellipsoid drawing of Co(L^{tBu})$_2$ (3). 50% probability ellipsoids. All hydrogen atoms are omitted for clarity.

Selected distances (Å): Co1–O1 1.897(2), Co1–O2 2.047(2), Co1–O3 1.897(2), Co1–O4 2.060(2), P1–O2 1.512(2), P2–O4 1.507(2); selected angles (°): O1–Co1–O2 93.6(1), O3–Co1–O4 93.8(1), O1–Co1–O4 127.7(1), O2–Co1–O3 128.0(1).

The metal cation in **3** has a distorted tetrahedral geometry. The distortion is derived from the cumbersome *tert*-butyl group. As a result, the biting angles of the ligand (93.6(1) and 93.8(1)°) are smaller in comparison to the angles between oxygen atoms from different ligands (127.7(1) and 128.0(1)°). The Co–OP average bond length (2.053 Å) is in the higher part of the range reported in the literature (1.87 to 2.16 Å) and it is longer than the reported lengths for tetrahedral Co(II) centres (1.911 to 2.035 Å).[2,5] In fact, the closest value, 2.035(6) Å, corresponds to **LXIV** (see Figure 2.4), a complex of the analogous proligand $(Ph)_2P(O)CH_2CH(^tBu)OH$ (**1**), bearing a carbonate moiety, which will be further commented from Section 2.4.1 onwards.[2] Complex **3** has also an average P–O bond distance (1.51 Å) well in the range for phosphinoyl-coordinated cobalt(II) complexes of 1.38 to 1.62 Å. In comparison to **LVIII** and **XI**, the molecular structure of **3** has bond distances that are very similar to those in the zinc analogue **LVIII** and consistently shorter than in the tin analogue **XI**, in accordance with their ionic radii for four-coordinated cations: r(Co^{2+}) = 0.72 Å, r(Zn^{2+}) = 0.74 Å and r(Sn^{2+}) = 0.93 Å.[6] For instance, the average M–OP lengths are 2.053, 2.027 and 2.372 Å for cobalt, zinc and tin, respectively. M–OR average distances for Co, Zn and Sn are 1.897, 1.873 and 2.048 Å, respectively.[2]

2.4. Comparison of homoleptic complexes of HL^{Ph} and HL^{tBu}

Table 2.2 presents an overview of the complexes obtained with divalent zinc, cobalt and tin and the phosphine oxide ligands mentioned. The synthesis of the zinc complex of **1** was attempted but not achieved; see Section 0 for more details.

Table 2.2. Zn, Sn and Co complexes of the phosphine oxide/alkoxide ligands.[2]

	substituents on P=O	
Metal	**^{t}Bu**	**Ph**
Zn	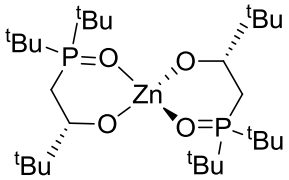 LVIII	See Section 2.5
Sn	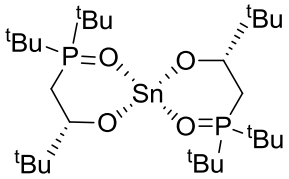 XI	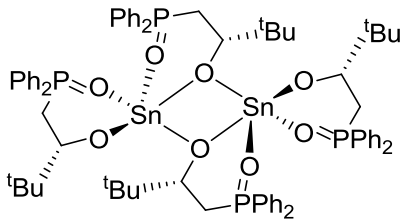 LXI
Co	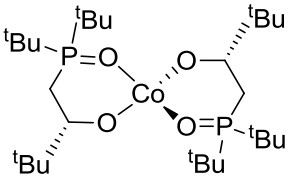 3	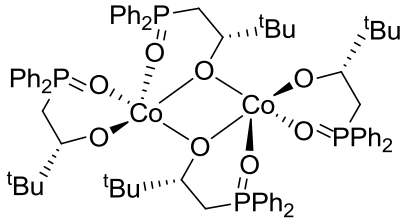 LX

Because of their catalytic activity for the formation of poly(lactic acid) and poly(caprolactone), it is of interest to investigate if metal complexes of phosphine oxide/alkoxide ligands can act as initiators for the copolymerisation of carbon dioxide and epoxides. In the first instance, their reactivity towards carbon dioxide at low pressures has been studied.

2.4.1. Reactivity of $M^{II}(L^{tBu})_2$ and $M^{II}(L^{Ph})_2$ complexes towards CO_2

Solutions containing the complexes **XI**, **3** and **LX** were exposed to an atmosphere of carbon dioxide at room temperature and 1 bar of pressure for 16 h. The anticipated product was the formation of carbonate from CO_2 insertion into the metal alkoxide bond in each case as shown in Equation 2.5.

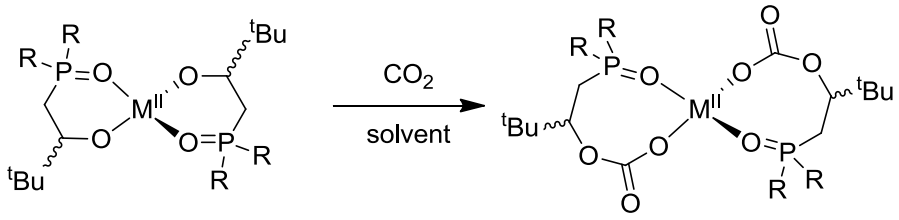

Equation 2.5. Expected reaction of a $M^{II}(L^{tBu})_2$ complex and carbon dioxide

2.4.1.1. Reaction of **XI** with CO_2 with and without added base

Analysis of the solution formed from exposure of a benzene solution of compound **XI** to CO_2 showed no reaction with carbon dioxide. The reaction was repeated with the addition of two equivalents of various Lewis bases, pyridine, triethylamine or 1,8-diazabicyclo[5.4.0]-undec-7-ene (DBU), and using different pressures and temperatures, according to the data in Table 2.3. The bases chosen have previously been shown in the literature to bind and activate CO_2, and also have the potential to compete with the bound phosphine oxide group of the ligand, facilitating its labilisation.

Table 2.3. Added base and reaction conditions for the reaction between XI and CO_2

Solvent	Pressure / bar	Added base	Time / h	Temperature / °C	Conversion / %
C_6D_6	1	-	18	80	0
C_6D_6	1	-	16	100	0
C_6D_6	1	-	16	110	0
C_6D_6	1	-	7	120	0
C_6D_6	1	pyridine	16	80	0
C_6D_6	1	triethylamine	16	80	0
C_6D_6	1	DBU	16	80	0
C_6D_6	1.5	-	16	80	0

In each case, the colour of the solution remained unchanged, and the mixture was analysed by ^{1}H NMR spectroscopy after the time given in Table 2.3. However, in each case, the only resonances observed were those due to starting materials, and no reaction was observed in any case.

2.4.1.2. Reaction of 3 with CO_2

Compound **3** was subjected to 1 bar of CO_2 at 80° C in deuterated benzene. After 36 h no noticeable change in colour was observed, and analysis of the paramagnetic ^{1}H NMR spectrum showed no change in the chemical shifts, indicating no reaction.

2.4.1.3. Reaction of LX with CO_2

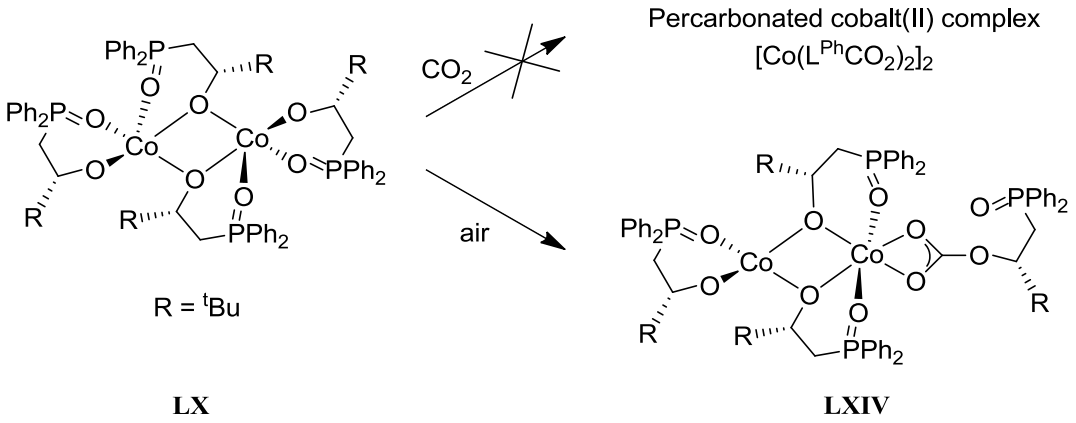

Equation 2.6. Reaction of $[Co^{II}(L^{Ph})_2]_2$ and carbon dioxide

According to Buffet, a Schlenk flask stored for a number of months containing **LX** in hexanes allowed formation of complex $[(CoL^{Ph})(Co(L^{Ph})_2(L^{Ph}CO_2)]$ (**LXIV**). The incorporated CO_2 was attributed to the reaction with adventitious atmospheric carbon dioxide and the new complex was characterised by X-ray diffraction studies.[2]

Accordingly, the insertion of carbon dioxide into all metal alkoxide bonds was expected for compounds of the type $[M^{II}(L^{Ph})_2]_2$ as shown in Equation 2.6. Complex $[Co(L^{Ph})_2]_2$ (**LX**) in deuterated benzene and in the presence of tetrahydrofuran (THF) was heated at 80° C for 50 h after 1.5 bar of carbon dioxide were added; this resulted in no apparent change in the paramagnetic ^{1}H NMR spectrum originally reported by Buffet.[2] In contrast, the structural features of compound **LXIV**, as shown in Figure 2.4, are varied and interesting: a) as expected, the carbonate moiety formed is in contact with the metal, instead of pendant; b)

Co2 is sterically more encumbered than **LX** due to the bidentate carbonate coordination mode towards the metal ion, hence forcing one phosphine oxide motif to become pendant; c) in the solid-state structure, the cobalt centre Co2 goes from a distorted square pyramidal geometry in **LX** to a distorted octahedral geometry in **LXIV** in which the bidentate coordination of the carbonate and an extra phosphine oxide from a neighbouring ligand are featured; d) thus, Co1 presents a tetrahedral geometry in **LXIV**. Unfortunately, given the unexpected nature of this result, the compound has not been reproduced and other characterising studies were not carried out.

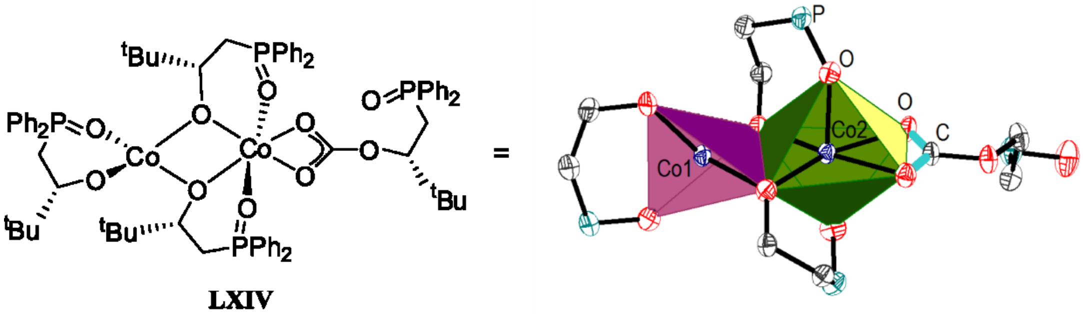

LXIV

Figure 2.4. [Co(L^{Ph})$_2$]$_2$CO$_2$ (LXIV) and the geometry of its cobalt cations taken from Buffet's work.[2]

2.4.2. Reactivity of [Co(L^{Ph})$_2$]$_2$ as an initiator of ring-opening polymerisation reactions

In the literature, propylene oxide (PO) and cyclohexene oxide (CHO) have been shown to form copolymers with carbon dioxide with high molecular weights and polydispersities as narrow as 1.04;[7] characterisation data on the polymers produced by complexes introduced in Section 1.6.2 such as tailored salcy ligands (**XLV**,[8] **LXV**,[9] **LXVI**[10] and **LXVII**[11]), porphyrins (**XLVI**)[12] and multidentate macrocycles (**LI**)[7] can be found in Table 2.4. The catalysts used most effectively in the copolymerisation of PO and CO_2 are depicted in Figure 2.5, whilst those preferred for the formation of PCC are shown in Figure 2.6. It is worthy to mention that the overwhelming interest in salcy-based catalysts for the coupling of epoxides and carbon dioxide is fundamentally based on their efficiency (measured as turnover frequency) and tuneability.[13] Although the great majority of the cobalt complexes used contain cobalt in its oxidation state of +3, at the time of our studies Co^{II}(acetate)$_2$, **LXVIII**, had also been shown to provide alternating copolymerisation of propylene oxide and CO_2 (see Table 2.4).[14] Furthermore, during the course of this investigation, Williams *et al*. reported the dinuclear cobalt(II) complex **L**, an analogue of **LI** with one less acetate group (Figure 1.20), which catalyses the copolymerisation of CHO and carbon dioxide at 1 bar of CO_2 and with low molecular weight and narrow polydispersity as seen in Table 2.4.[7]

Table 2.4. Selected epoxide/CO_2 copolymerisation results from the literature and from this work

catalyst	epoxide	monom/cat (molar ratio)[a]	pressure of CO_2 (bar)	temp. (°C)[b]	TOF (h^{-1})[c]	M_n[d]	PDI[e]
XLV[8]	PO	2000	14	25	NR[f]	23900	1.1
LXV[9]	PO	25000	20	50	650	75000	1.2
LXVII[10]	PO	5000	6	25	428	121600	1.1
XLVI[12]	CHO	500	1	25	NR[f]	1500	1.1
LXVII[11]	CHO	5000	20	50	1018	68700	1.1
LI[7]	CHO	1000	1	80	159	6300	1.0
LXVIII[14]	PO	42	80	80	0.03	17000	NR[f]
L[7]	CHO	1000	1	80	172	5100	1.3
LX (vi)[g]	CHO	500	50	80	2.5	39000	2.8
LX (vii)[g]	CHO	500	50	80	3.5	37000	2.8

Reaction conditions stated in the corresponding referenced publications. [a] Monomer-to-catalyst molar ratio. [b] Temperature. [c] Turnover frequency = number of moles of epoxide consumed per mole of catalyst per hour. [d] Number average molecular weight, determined by gel permeation chromatography. [e] Polydispersity index, from the weight average molecular weight-to-number average molecular weight ratio. [f] Not reported. [g] Polymerisation carried out for 24 h in 15 mL of neat CHO.

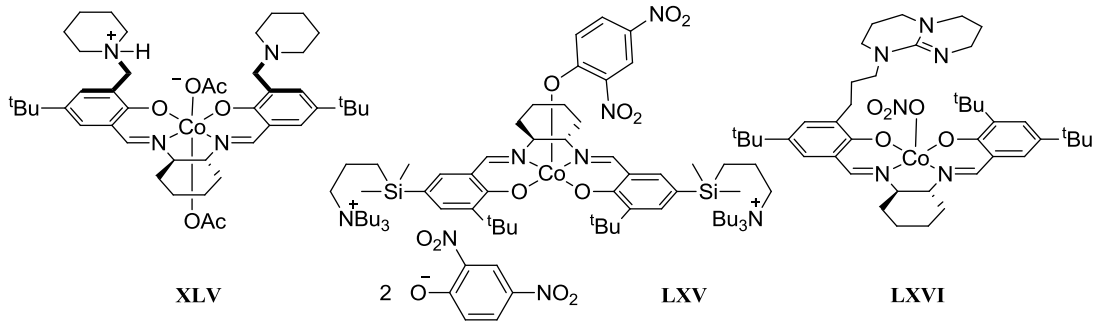

Figure 2.5. Efficient cobalt(III) catalysts for the copolymerisation of PO and CO_2.[8,9,10]

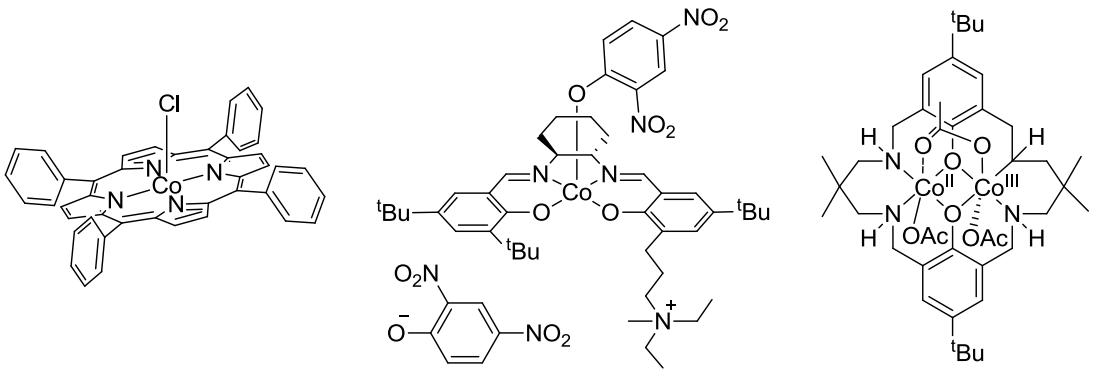

XLVI LXVII LI

Figure 2.6. Efficient cobalt catalysts for the copolymerisation of CHO and CO_2.[7,11,12]

2.4.2.1. Copolymerisation of propylene oxide and carbon dioxide using LX

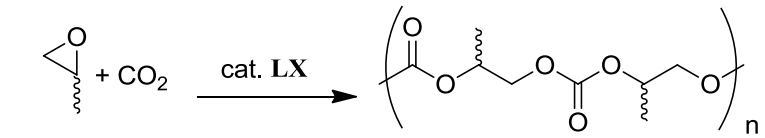

propylene oxide — poly(propylene oxide) carbonate

Equation 2.7. Attempted copolymerisation of propylene oxide and carbon dioxide by LX

In a typical reaction 1000 equivalents of PO are mixed with one of **LX** at 1 bar of CO_2 and 70 °C for 16 h. The conditions are summarised in Table 2.5.

Table 2.5. Reaction conditions for the copolymerisation of PO and CO_2 using LX as catalyst

Entry	LX (mg)	PO (g)	CO_2 (bar)	Molar ratio cat:epox:solv	Solvent	Temp. (°C)	Time (h)
i	30	1.3	1	1:1000:500	C_6D_6	70	16
ii	30	1.3	1	1:1000:3000	THF	70	16
iii	200	8.8	1	1:1000:400	THF	40	16

All reactions were unsuccessful for the conversion of PO

Using THF or deuterated benzene as solvent, and a catalyst loading of 0.1%, no product formation was observed by ^{1}H NMR spectroscopy. The reactions neither produced polycarbonates nor cyclic carbonates; only the decomposition products of the catalyst were found.

2.4.2.2. Copolymerisation of cyclohexene oxide and carbon dioxide using LX

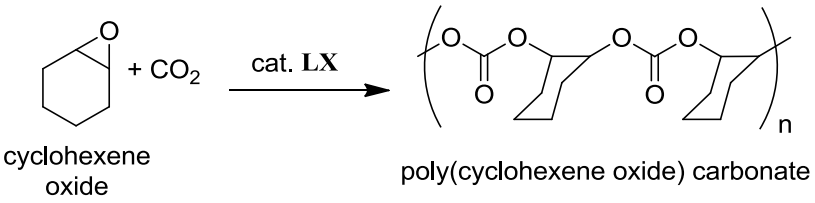

Equation 2.8. Copolymerisation of cyclohexene oxide and carbon dioxide initiated by LX

Compound **LX** was also probed for its reactivity towards cyclohexene oxide and carbon dioxide under a variety of conditions. In a typical reaction 500 equivalents of CHO were mixed with one of **LX** at 50 bar of CO_2 and 80 °C for 24 h. The conditions are summarised in Table 2.6.

Table 2.6. Reaction conditions for the attempted formation of PCC using LX as catalyst

entry	LX (mg)	CHO (g)	CO_2 (bar)	molar ratio cat:epox:solv	solv.	TOF (h^{-1})[b]	M_n[c]	PDI[d]
iv	50	0.3	1	1:80:500	DCM	0	-	-
v	100	0.6	8	1:80:500	DCM	0	-	-
vi	397	14.55	50	1:500:0	no solvent	2.5	39000	2.8
vii	397	14.55	50	1:500:1[a]	PPNCl[a]	3.5	37000	2.8
viii	100	1.48	8	1:200:0	no solvent	0	-	-

Reaction temperature: entry **iv** = 85 °C; entry **v** = 60 °C; entries **vi**, **vii**, and **viii** = 80 °C. Reaction time: entries **iv** and **v** = 16 h; entries **vi**, **vii**, and **viii** = 24h. [a] No solvent was used for reaction vii; instead, PPNCl was used as cocatalyst. [b] Turnover frequency = number of moles of epoxide consumed per mole of catalyst per hour. [c] Number average molecular weight, determined by gel permeation chromatography. [d] Polydispersity index, from the weight average molecular weight-to-number average molecular weight ratio.

The reaction under a 1 bar pressure of CO_2 and with a 1.2 mol % of catalyst loading in DCM at 85° C resulted in 0% conversion, similar to the reaction with PO. The readily-available glass autoclave (Figure 5.1) was used in order to increase the pressure of carbon dioxide to 8 bar for further reaction studied. The reaction was carried out at 60° C and with 1.2 mol % of catalyst loading in DCM with the same outcome, i.e. no coupling of the epoxide and carbon dioxide occurred. Since the majority of the catalysts reported in the literature utilise pressures of 40 bar or more of carbon dioxide, which require equipment and expertise that are not available in our laboratory, two further copolymerisation reactions were

attempted in the Williams Laboratory at Imperial College London with the help of Dr Emma Hollis, where a reactor is set up for procedures at up to 50 bar of carbon dioxide (Figure 5.2). The advantages of utilising this system are that the use of a set of conditions which have been successful for other catalysts,[7,15] and with effective CO_2 drying, are available.

In a typical reaction 500 equivalents of CHO are mixed with one of **LX** (0.2 mol % of catalyst loading) at 50 bar of CO_2 and 80° C for 24 h, which resulted in the formation of poly(cyclohexene carbonate) with a number average molecular weight of 39000 Da and a wide polydispersity index of 2.8 in a low yield of 12%. The addition of one equivalent of cocatalyst, in this case bis(triphenylphosphine)iminium chloride (PPNCl), only increased the yield marginally (17%) and delivered a polymer with similar characteristics in molecular weight and polydispersity (37000 Da and 2.8, respectively). The addition of PPNCl as a cocatalyst in cobalt(III) and chromium(III) tetradentate systems affects positively the copolymerisation of CO_2 and epoxides by the formation of a more active catalyst with a six-coordinated metal centre, $[PPN]^+[M^{III}(ligand)ClX]^-$.[16] The basis of the improved activity lies in the increase of nucleophilicity of the catalyst, initiating the copolymerisation more effectively.[17] In the case of **LX**, the presence of additional ligands to the metal centres would be impeded by the fluctuation of the L^{Ph} ligands in the binuclear structure (see proposed mechanism in Section 2.4.3).

Another copolymerisation reaction with 0.5 mol % of catalyst loading, 8 bar of CO_2 and 80° C for 24 h was attempted with no products forming.

2.4.3. Proposed mechanism of copolymerisation of CHO and CO_2 by LX

On the basis of the ability of **LX** to form copolymers from CHO and CO_2, the evidence of insertion of carbon dioxide in one of its metal alkoxide bonds in compound **LXIV** and of previous mechanisms reported for bimetallic catalysts,[15,18,19] we propose the following mechanism, as shown in Scheme 2.1. The first step, supported by the formation of **LXIV** and its structural characterisation, consists in the insertion of carbon dioxide into one metal alkoxide bond and the transference of a coordinating phosphinoyl group from one cobalt centre (Co1 in Figure 2.4) to the other in which the carbon dioxide insertion occurred (Co2 in Figure 2.4). The rearrangement of the ligands results in cobalt centres with different coordination geometries: one tetrahedral (Co1) and the other octahedral (Co2), as seen in **LXIV** in Scheme 2.1. Because of the phosphinoyl group coordinating to Co2 in **LXIV**, we suspect that the ligands are prone to switching coordination according to the electronic needs of the metal centres, therefore obstructing the action of cocatalysts such as PPNCl. We also suggest that the first insertion of carbon dioxide is slow because neither **LXIV** nor

any other example of **LX** with CO_2 insertion was obtained at shorter times of reaction (see Section 2.4.1). After the carbon dioxide insertion, one of the two phosphinoyl groups from Co2 transfers its coordination to Co1 and leave a coordination site for an incoming cyclohexene oxide molecule which, in time, will be subjected to a nucleophilic attack by the carbonate group. In turn, carbon dioxide insertion occurs in alternation with nucleophilic attacks to CHO resulting in the formation of a polymeric chain. Further kinetic studies would provide a better understanding on the speed of each step in the reaction and, hence, the opportunity to improve the catalytic activity of **LX**. However, it is possible that the CHO insertion is rate-determining in accordance with previous studies on bimetallic catalysts.[15,18] Examples of other bimetallic complexes for this copolymerisation report metal-metal distances in the range of 2.92 and 3.06 Å,[7,18,20] with the separation between Co1 and Co2 in **LX** at 3.0437(9) Å.

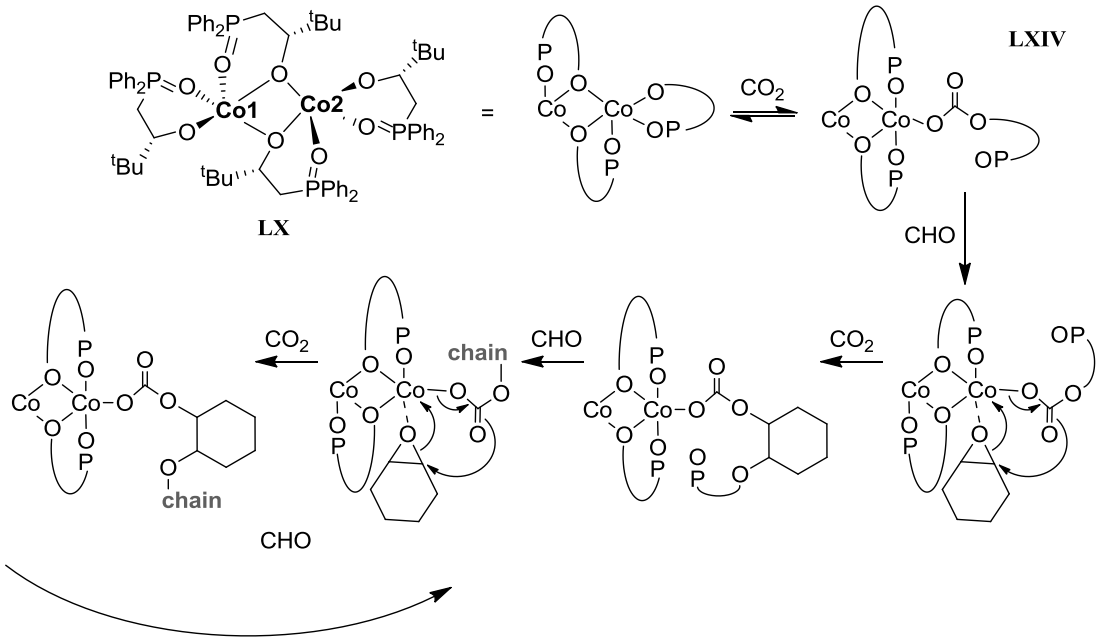

Scheme 2.1. Proposed mechanism for the copolymerisation of CHO and CO_2 by LX

2.4.4. Attempted oxidation of LX into a cobalt(III) species

Even when there was some copolymerisation catalysis using **LX**, it is thought that a cobalt(III) complex of the same ligand would increase the yield of the reaction and, possibly, alter the properties of the resultant polymers. In effect, the metals more used for the conversion of epoxides and carbon dioxide into copolymers are zinc(II), cobalt(III) and chromium(III).[21] Therefore, the oxidation of **LX** was attempted using mild oxidants. The oxidation of multidentate cobalt(II) complexes into cobalt(III) complexes is well documented

in the presence of air and an additional ligand, generally a pseudohalide.[7,8,9,10,11,12] Our aim was to synthesise a cobalt(III) complex without disturbing the homoleptic nature of **LX**. Thus, two equivalents of proligand HL^{Ph} in the presence of $AgBF_4$ or I_2 were mixed with **LX** in THF (Figure 2.7). The suspension treated with $AgBF_4$ did not react immediately and was heated for 16 h at 60° C. The expected silver mirror was formed but the ^1H NMR spectrum of the filtered solution revealed an intractable mixture of compounds in the diamagnetic region. The reaction with iodine, on the other hand, presented an immediate change of colour from purple to green. Its ^1H NMR spectrum only showed diamagnetic resonances of the proligand and paramagnetic signals in the same range as those of **LX**.

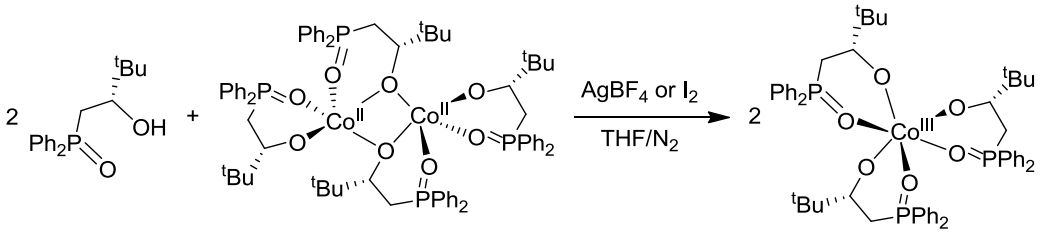

Figure 2.7. Attempted oxidation of LX to a homoleptic cobalt(III) complex

2.5. Dehydration of proligand HL^{Ph} by $Zn[N(SiMe_3)_2]_2$

As previously stated, the zinc complex of the proligand HL^{tBu} (**X**) can be used as a catalyst for the polymerisation of *rac*-lactide with positive results in terms of conversion and activity. The analogous complex with phenyl groups in the phosphine oxide (**1**) was thus targeted. Treatment of a toluene solution of **1** with either half or one equivalent of $Zn[N(SiMe_3)_2]_2$ was carried out at 70 °C for 16 h with the formation of a white precipitate. At the end of the reaction time, analysis of the reaction mixture by NMR spectroscopies suggested the ligand no longer had the same connectivity. For instance, the ^{1}H NMR spectrum of the product shows a single ligand environment with a resonance for a proton in the β position at 6.76 and the proton of the original CH group at 6.11 ppm, in great contrast with the frequencies of proligand **1** for the same protons at 2.30 and 3.60 ppm, respectively. The ^{13}C-{H} NMR spectrum of the product shows the frequency of the groups in the α and β positions at 133.5 and 131.8 ppm, respectively; whilst the same groups resonate at 30.8 and 74.2 ppm in the precursor **1**.

Colourless single crystals grew from the reaction mixture of a sufficient quality to allow X-ray structural analysis. The molecular structure, shown in Figure 2.8, presents the product as (*E*)-3,3-dimethyl-1-diphenylphosphinoylbut-1-ene (**4**), formally the dehydration product of **1**, (see Equation 2.9).

The asymmetric dehydration of comparable alcohols has been reported previously to afford similar compounds and is discussed below.[22]

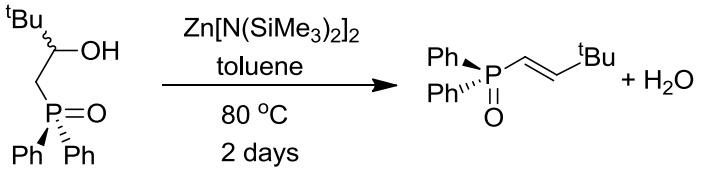

1 **4**

Equation 2.9. Dehydration of 1 using a zinc base

2.5.1. X-ray structure of (*E*)-3,3-dimethyl-1-diphenylphosphinoylbut-1-ene (4)

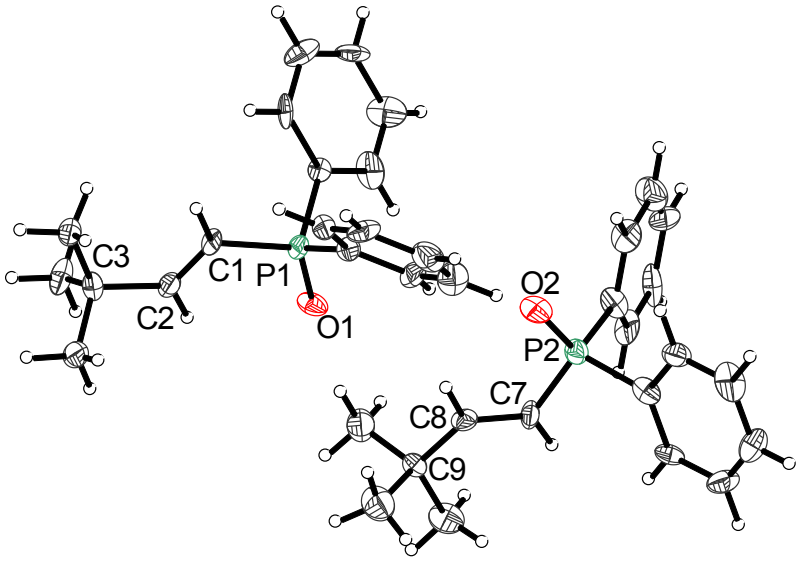

Figure 2.8. Displacement ellipsoid drawing of (*E*)-3,3-dimethyl-1-diphenylphosphinoylbut-1-ene (4). 50% probability ellipsoids.

Selected distances (Å): P1–O1 1.478(13), P2–O2 1.498(14), P1–C1 1.805(12), P2–C7 1.765(14), C1–C2 1.323(19), C7–C8 1.328(18), C2–C3 1.54(2), C8–C9 1.45(2); selected angles (°): P1–C1–C2 117.7(9), P2–C7–C8 121.0(11), C1–C2–C3 126.2(12), C7–C8–C9 132.6(12), O1–P1–C1 113.2(6), O2–P2–C7 114.3(6).

Colourless needle-like crystals of **4** suitable for a single-crystal X-ray diffraction study were collected from a toluene solution at -30° C. The molecular structure of **4** contains typical values for phosphine oxides with an average P–O bond distance of 1.488 Å consistent with the average value for **1** of 1.492 Å and in the range of 1-diphenylphosphinoyl-1-alkene compounds (from 1.483 to 1.501 Å).[23] The HC–P–O average angle of 113.7° is in the literature range (112.6 to 114.6°) and is relatively close to the average value of **1** of 112.7° for the H_2C–P–O angle. Furthermore, other metric data of **4** are also in the literature range: C=C average bond distance of 1.325 Å in the range of 1.314 to 1.326 Å; P–C=C average angle of 119.4° just below the range of 120.5 to 124.9° and very close to the theoretical 120° for sp^2 carbon atoms; and C=C–C average angle of 129.4° just above the range of 124.0 to 127.4° for the reported 1-diphenylphosphinoyl-1-alkenes.[23]

In 2008, the Park group reported the kinetic resolution of a racemic mixture of β-hydroxy esters using the combination of a prolinol chiral ligand and a zinc base to selectively dehydrate one of the enantiomers. The process results, then, in an enantiomerically pure β-hydroxy ester and a trans-α-olefin (Equation 2.10).[22]

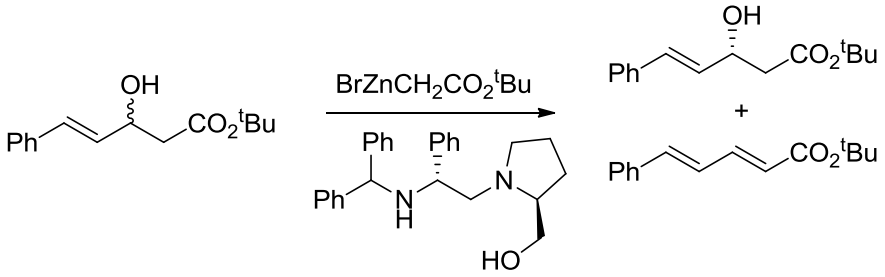

Equation 2.10. Asymmetric dehydration of a β-hydroxy ester through a chiral ligand and zinc

The Park group, prompted by unsuccessful attempts to increase enantioselectivity through the Reformatsky reaction (zinc-assisted condensation of aldehyde with ester to form a β-hydroxy),[24] have not reported mechanistic studies but it is understood that $BrZnCH_2CO_2{}^tBu$, in excess, acts as a stereoselective base when is bound to the N–H of the ligand.[25] The authors also noted that this kind of asymmetric dehydration was only observed when the ester chain had no substituents in the α-position and only a conjugated substituent in the β-position.[26] Similar dehydrations have been seen for products of the aldol reaction and for other phosphine oxides, generally using silyl or sulfonyl species.[27] The common feature for the dehydration, other than the ones already stated, is the presence of a carbonyl group. In our case, the π character of the bonding in an ester or an aldehyde is replaced by that of the phosphine oxide species, as is seen in Scheme 2.2.

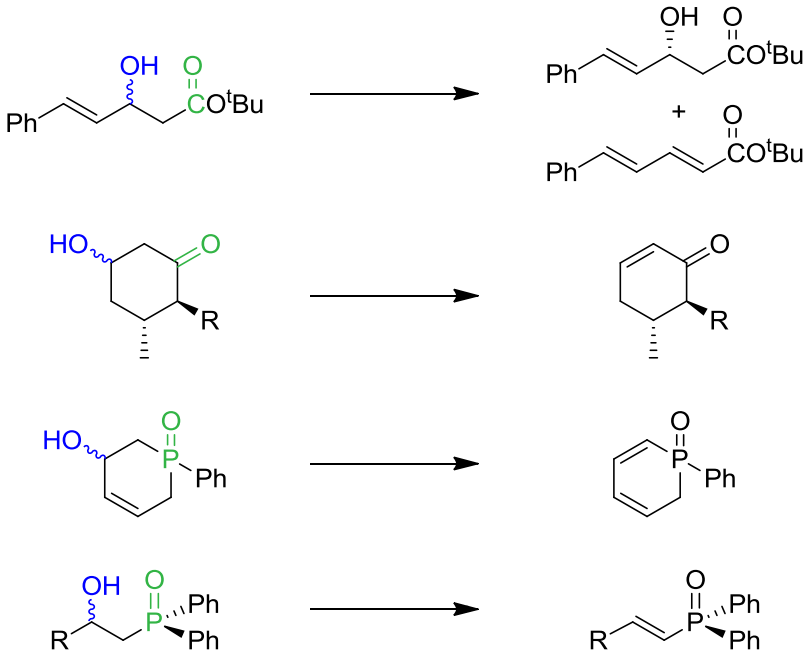

Scheme 2.2. Different types of dehydration of β-alkoxy compounds.[27]

The synthesis of (*E*)-3,3-dimethyl-1-diphenylphosphinoylbut-1-ene (**4**) has been achieved by the hydrophosphinylation of alkynes mediated by rhodium supported in a variety of ligands and even mesoporous materials, as depicted in Equation 2.11.[28]

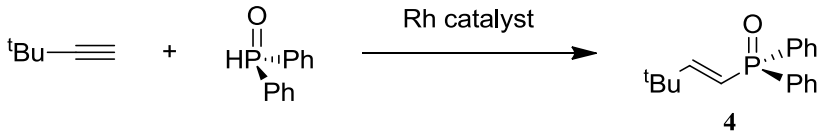

Equation 2.11. Preparation of 4 from phosphine oxide and alkyne

Santelli-Rouvier developed two methods for the dehydration of β-hydroxy phosphine oxides. One of them includes the direct elimination of water using thionyl chloride at room temperature, whilst the other requires the addition of silyl chloride forming first alkoxysilanes followed by a hydride at higher temperatures to recover the alkylvinyldiphenylphosphine oxide as is shown in Scheme 2.3.[29] Both methods were tested by Bartels *et al*. more recently, with effective results for various substrates using the latter one.[30] Another study, from the same group, reports compound **4** synthesised through its alkoxysilane.[31]

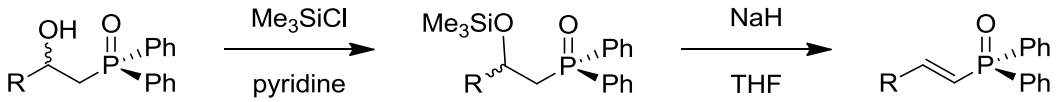

Scheme 2.3. Preparation of a vinylphosphine oxide through the formation of an alkoxysilane

Given these previous studies of the formation of the α,β-unsaturated phosphine oxide, a mechanism including zinc(bis(bis(trimethylsilyl)amide)) is proposed (see Scheme 2.4). The base, in this case the silylamide, performs a nucleophilic attack on the hydrogen in the α-carbon allowing the hydroxy group to leave through coordination to the zinc complex. This process yields the conjugated alkene; zinc is expected to precipitate as hydroxide.

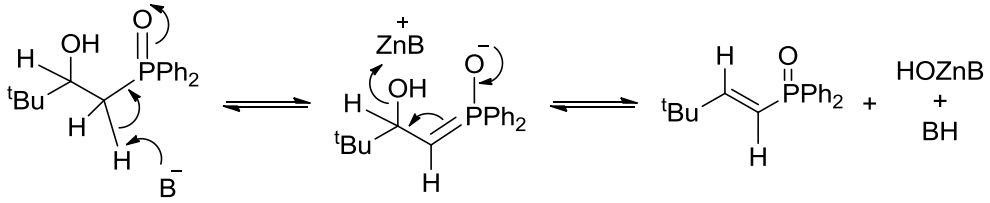

Scheme 2.4. Proposed mechanism for the dehydration of 1 with a zinc base

The difficulty of forming a metal complex from **1** was also observed when trying to synthesise its potassium complex producing an intractable mixture of compounds.[2] From the previous examples found in the literature and the variation of the Horner-Wittig reaction

postulated by the Warren group[32] we can suggest that one of the components of the resulting mixture between the β-hydroxyphosphine oxide and the potassium salts used as reagents (hydride, bis(trimethylsilyl)amide and *tert*-butoxide) was 3,3-dimethyl-1-butene and another diphenylphosphinic acid as is shown in Equation 2.12.

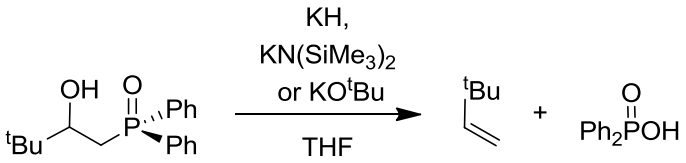

Equation 2.12. Reaction of 1 with potassium bases

2.6. Conclusion

Complexes $Zn(L^{tBu})_2$ (**LVIII**) and $Sn(L^{tBu})_2$ (**XI**) of bidentate phosphine oxide/alkoxide ligands are effective catalysts for the polymerisation of *rac*-lactide.[2] The cobalt analogue $Co(L^{tBu})_2$ (**3**) was synthesised and structurally characterised for comparison to **LVIII** and **XI** in topology and chemistry. Because the proligand HL^{tBu} (**X**) is expensive and its complexes sensitive to air and moisture, its more robust and inexpensive phenyl analogue HL^{Ph} (**1**) was synthesised and structurally characterised in two of its polymorphs. The proligand **1** has been used to prepare $\{Co(L^{Ph})_2\}_2$ (**LX**) and $\{Sn(L^{Ph})_2\}_2$ (**LXI**), but not their zinc counterpart.[2] Instead, the zinc compound used to attempt the synthesis of the complex acts as a base that produces dehydration of **1** into (*E*)-3,3-dimethyl-1-diphenylphosphinoylbut-1-ene (**4**), which was also structurally characterised. A proposed mechanism for the dehydration reaction is proposed. In addition, the complexes **LVIII**, **XI**, **3** and **LX** were tested for their reactivity towards CO_2 at low pressures (1 to 1.5 bar) with no formation of products. **LX** was also tested as a catalyst for the copolymerisation of CO_2 and propylene oxide or cyclohexene oxide at different pressures (from 1 to 50 bar). Limited conversion of the monomers into poly(cyclohexene carbonate) was achieved with and without PPNCl as cocatalyst (17 and 12%, respectively). The copolymers present molecular weights around 40000 Da with a wide distribution of molecular mass (PDI = 2.8). Finally, a mechanism of reaction for the copolymerisation is proposed based on previous studies using bimetallic catalysts[18,15,18] and reported evidence of the insertion of CO_2 into **LX** in the compound **LXIV**.[2]

2.7. References

[1] Arnold, P. L.; Buffet, JC.; Blaudeck, R. P.; Sujecki, S.; Blake, A. J.; Wilson, C. *Angew. Chem. Int. Ed.* **2008,** *47,* 6033-6036. 10.1002/anie.200801279

[2] Buffet, J.-C., PhD Thesis, The University of Edinburgh, UK (Edinburgh), **2009**.

[3] Genov, D. G.; Kresinski, R. A.; Tebby, J. C. *J. Org. Chem.* **1998,** *63,* 2574-2585. 10.1021/jo972036o.

[4] Inoue, S.; Koinuma, H.; Tsuruta, T. *Makromol. Chem.* **1969,** *130,* 210-220.

[5] Al-Resayes, S. I.; Hitchcock, P. B.; Nixon, J. F. *J. Chem. Soc., Chem. Commun.* **1991,** 78-79. Godfrey, S. M.; Kelly, D. G.; McAuliffe, C. A.; Pritchard, R. G. *J. Chem. Soc. Dalton Trans.* **1995,** 1095-1101. 10.1039/dt9950001095. Pérez-Lourido, P.; Romero, J.; García-Vázquez, J. A.; Sousa, A.; Zubieta, J.; Maresca, K. *Polyhedron* **1998,** *17,* 4457-4464. 10.1016/S0277-5387(98)00252-6. Jie, S.; Agostinho, M.; Kermagoret, A.; Cazin, C. S. J.; Braunstein, P. *Dalton Trans.* **2007,** 4472-4482. 10.1039/b706818b. Fessler, M.; Eller, S.; Bachmann, C.; Gutmann, R.; Trettenbrein, B.; Kopacka, H.; Mueller, T.; Brueggeller, P. *Dalton Trans.* **2009,** 1383-1395. 10.1039/b813720j. Bou-Moreno, R.; Cotton, S. A.; Hunter, V.; Leonard, K.; Platt, A. W.G.; Raithby, P. R.; Schiffers, S. *Polyhedron* **2011,** *30,* 2832-2836. 10.1016/j.poly.2011.08.005.

[6] Weast, R. C. (Ed.) "Crystal Ionic Radii." Handbook of Chemistry and Physics. CRC Press, Inc. USA. 61st Edition. 1980-1981. pp. F-216 – F-217.

[7] Kember, M. R.; White, A. J. P.; Williams, C. K. *Macromolecules* **2010,** *43,* 2291-2298. 10.1021/ma902582m.

[8] Nakano, K.; Kamada, T.; Nozaki, K. *Angew. Chem. Int. Ed.* **2006,** *45,* 7274-7277. 10.1002/anie.200603132.

[9] Noh, E. K.; Na, S. J.; Sujith, S.; Kim, S.-W.; Lee, B. Y. *J. Am. Chem. Soc.* **2007,** *129,* 8082-8083. 10.1021/ja071290n.

[10] Ren, W.-M.; Liu, Z.-W.; Wen, Y.-Q.; Zhang, R.; Lu, X.-B. *J. Am. Chem. Soc.* **2009,** *131,* 11509-11518. 10.1021/ja9033999.

[11] Ren, W.-M.; Zhang, X.; Liu, Y.; Li, J.-F.; Wang, H.; Lu, X.-B. *Macromolecules* **2010,** *43,* 1396-1402. 10.1021/ma902321g.

[12] Sugimoto, H.; Kuroda, K. *Macromolecules* **2008,** *41,* 312-317. 10.1021/ma702354s.

[13] Lu, X.-B.; Darensbourg, D. J. *Chem. Soc. Rev.* **2012,** *41,* 1462-1484. 10.1039/c1cs15142h.

[14] Soga, K.; Hyakkoku, K.; Ikeda, S. *Makromol. Chem.* **1978,** *179,* 2837-2843. 10.1002/macp.1978.021791203.

[15] Jutz, F.; Buchard, A.; Kember, M. R.; Fredriksen, S. B.; Williams, C. K. *J. Am. Chem. Soc.* **2011,** *133,* 17395-17405. 10.1021/ja206352x.

[16] Darensbourg, D. J. *Chem. Rev.* **2007,** *107,* 2388-2410. 10.1021/cr068363q. Darensbourg, D. J.; Mackiewicz, R. M. *J. Am. Chem. Soc.* **2005,** *127,* 14026-14038. 10.1021/ja053544f.

[17] Darensbourg, D. J.; Moncada, A. I. *Inorg. Chem.* **2008,** *47,* 10000-10008. 10.1021/ic801231p.

[18] Kember, M. R.; Jutz, F.; Buchard, A.; White, A. J. P.; Williams, C. K. *Chem. Sci.* **2012,** *3,* 1245-1255. 10.1039/c2sc00802e.

[19] Moore, D. R.; Cheng, M.; Lobkovsky, E. B.; Coates, G. W. *J. Am. Chem. Soc.* **2003,** *125,* 11911-11924. 10.1021/ja030085e.

[20] Cheng, M.; Moore, D. R.; Reczek, J. J.; Chamberlain, B. M.; Lobkovsky, E. B.; Coates, G. W. *J. Am. Chem. Soc.* **2001,** *123,* 8738-8749. 10.1021/ja003850n. Moore, D. R.; Cheng, M.; Lobkovsky, E. B.; Coates, G. W. *Angew. Chem. Int. Ed.* **2002,** *41(14),* 2599-2602. 10.1002/1521-3773(20020715)41:14<2599::AID-ANIE2599>3.0.CO;2-N.

[21] Darensbourg, D. J. *Inorg. Chem.* **2010,** *49,* 10765-10780. 10.1021/ic101800d.

[22] Choi, E. T.; Lee, M. H.; Kim, Y.; Park, Y. S. *Tetrahedron* **2008,** *64,* 1515-1522. 10.1016/j.tet.2007.11.026.

[23] Haynes, R. K.; Loughlin, W. A.; Hambley, T. W. *J. Org. Chem.* **1991,** *56(20),* 5785-5790. 10.1021/jo00020a018. Stockland Jr., R. A.; Lipman, A. J.; Bawiec III, J. A.; Morrison, P. E.; Guzei, I. A.; Findeis, P. M.; Tamblin, J. F. *J. Organomet. Chem.* **2006,** *691,* 4042-4053. 10.1016/j.jorganchem.2006.06.007. Yu, B.; Wang, X.-Q.; Shen, G.-Q.; Shen, D.-Z. *Acta Cryst.* **2007,** *E63* o2973. 10.1107/S1600536807023422. Doherty, S.; Smyth, C. H.; Harrington, R. W.; Clegg, W. *Organometallics* **2009,** *28,* 5273-5276. 10.1021/om9004862. Hu, J.; Zhao, N.; Yang, B.; Wang, G.; Guo, L.-N.; Liang, Y.-M.; Yang, S.-D. *Chem. Eur. J.* **2011,** *17,* 5516-5521. 10.1002/chem.201003561.

[24] Kim, D.; Lee, Y. M.; Choi, E. T.; Lee, M. H.; Park, Y. S. *Bull. Korean Chem. Soc.* **2009,** *30(5),* 1211-1214.

[25] Kim, Y.; Choi, E. T.; Lee, M. H.; Park, Y. S. *Tetrahedron Lett.* **2007,** *48,* 2833-2835. 10.1016/j.tetlet.2007.02.111.

[26] Lee, M. H.; Choi, E. T.; Kim, D.; Lee, Y. M.; Park, Y. S. *Eur. J. Org. Chem.* **2008,** 5630-5637. 10.1002/ejoc.200800807.

[27] Duce, S.; Jorge, M.; Alonso, I.; Ruano, J. L. G.; Cid, M. B. *Org. Biomol. Chem.* **2011,** *9,* 8253-8260. 10.1039/c1ob06356a. Quin, L. D.; Hughes, A. N.; Kisalus, J. C.; Pete, B. *J. Org. Chem.* **1988,** *53,* 1722-1729. 10.1021/jo00243a023.

[28] Han, L.-B.; Zhao, C.-Q.; Tanaka, M. *J. Org. Chem.* **2001,** *66,* 5929-5932. 10.1021/jo010337z. Huang, Y.; Hao, W.; Ding, G.; Cai, M.-Z. *J. Organomet. Chem.* **2012,** *715,* 141-146. 10.1016/j.jorganchem.2012.05.031.

[29] Santelli-Rouvier, C. *Synthesis* **1988,** 64-66.

[30] Bartels, B.; Clayden, J.; Martín, C. G.; Nelson, A.; Russell, M. G.; Warren, S. *J. Chem. Soc., Perkin Trans. 1* **1999,** 1807-1822. 10.1039/a902414j.

[31] Fox, D. J.; Medlock, J. A.; Vosser, R.; Warren, S. *J. Chem. Soc., Perkin Trans. 1* **2001,** 2240-2249 10.1039/b104436m.

[32] Buss, A. D.; Warren, S. *J. Chem. Soc. Perkin Trans. 1* **1985,** 2307-2325. 10.1039/p19850002307.

CHAPTER 3. SYNTHESIS OF METAL COMPLEXES OF CHELATING *N*-HETEROCYCLIC CARBENES AND THEIR USE AS POLYMERISATION INITIATORS

3.1. Introduction

In 1991 Arduengo reported the first isolable and stable carbene (**LXIX**) in the form of a di-*N*-substituted imidazole in which the carbene is formed at the C2 position, between the nitrogen atoms, as shown in Figure 3.1.[1] These compounds are known to bind with most of the metals in the periodic table and also with many small molecules.

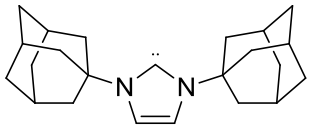

LXIX

Figure 3.1. First isolable and stable carbene.[1]

A number of metal complexes of *N*-heterocyclic carbenes (NHCs) have been used for the catalysis of different processes such as olefin metathesis,[2] diverse oxidations[3] and polymerisations.[4] Unsymmetrical NHCs have become a common feature as ligands having alkoxy and amino tethers are used to form bidentate ligands containing the carbene group, which has a pronounced σ-donor character. The Arnold group has synthesised numerous saturated and unsaturated NHCs and also their protonated precursors; alkoxy-tethered imidazol-2-ylidenes have generated complexes with more than a dozen metals, which include main group, transition and f-block metals; furthermore, even more metals are reported for the formation of amido-tethered NHC complexes.[5] Some of these complexes will be discussed further in comparison with the new compounds presented herein.

3.2. Cu^{I} complex of alkoxide/NHC ligand

Copper(II) complexes of an unsaturated alkoxide/NHC ligand were synthesised and tested as catalysts for the conjugate addition of alkyl anions to cyclohexenone with excellent conversion and up to 51% of stereoselectivity if an enantiomerically pure catalyst **LXX** is used (see Equation 3.1).[6]

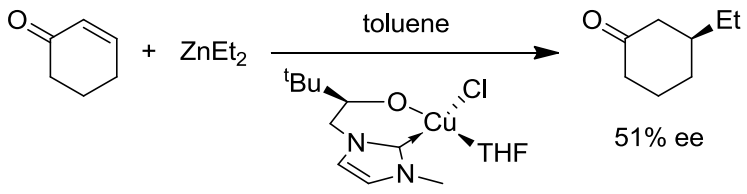

LXX

Equation 3.1. Example of conjugate addition using a copper(II) catalyst.[6]

Because **LXX** is a Cu^{II} complex, an analogous complex containing Cu^{I} (a softer ion) should have a stronger metal carbene bond. As the carbene centre is a softer base than the alkoxide, the alkoxide group may now be the more labile of the two functional groups, and available for further chemistries.

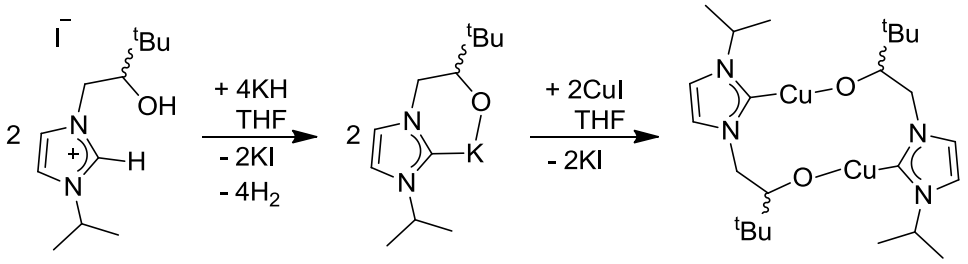

LXIII **5** **6**

Scheme 3.1. Synthesis of 6

The complex $(CuL)_2$ (**6**) was synthesised from the potassium complex (**5**) of the unsaturated hydroxyl-tethered NHC (**LXIII**) as is shown in Scheme 3.1. The potassium complex **5** was obtained through the reaction between **LXIII** and two equivalents of KH. Evolution of molecular hydrogen and a white precipitate of KI indicate the start of a reaction that requires two days to achieve a 60% yield of **5**. After removal of KI via filtration, an equivalent of copper(I) iodide was added to the solution of **5**, forming **6**, which was isolated by work-up from a 1:4 mixture of THF and hexane, as a beige-coloured powder in 60% yield. The ^{1}H NMR spectrum of **6** shows a single ligand environment with the CH_2 group at 4.33 ppm and the chiral CH group at 3.96 ppm. The singlet resonances of the backbone of the heterocycle were recorded at 7.26 and 7.23 ppm with respect to $SiMe_4$ as the internal standard. As expected, these resonances are at higher frequency than those of complex **5** (CH_2: 4.24 and 3.95, CH: 3.81, backbone: 7.13 and 7.12 ppm). The ^{13}C-{H} NMR spectrum of **6** shows the carbene frequency at 171.3 ppm and the frequencies of the CH groups from the backbone of the *N*-heterocycle at 120.7 and 118.3 ppm. The carbon in the chiral centre resonates at 83.7 and the CH_2 group at 59.4 ppm. Single crystals of **6** suitable for X-ray structural analysis were grown from a THF/hexane solution at -30° C. The molecular structure is dimeric in the solid state and shown in Figure 3.2.

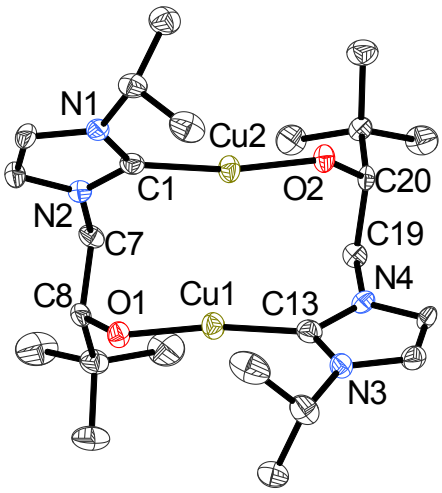

Figure 3.2. Displacement ellipsoid drawing of $(CuL)_2$ (6). 50% probability ellipsoids. All hydrogen atoms are omitted for clarity.

Selected distances (Å): Cu1–O1 1.821(2), Cu2–O2 1.821(2), Cu1–C13 1.870(4), Cu2–C1 1.868(4), Cu1…Cu2 2.9964(7); selected angles (°): O1–Cu1–C13 170.44(14), O2–Cu2–C1 169.03(13), N1–C1–N2 104.1(3), N4–C13–N3 104.3(13).

Copper(I) complexes of NHCs commonly form linear geometries for their metal centres; some examples are shown in Figure 3.3.[7] Diverse examples in the literature present two-coordinated copper centres as notoriously sensitive towards molecular oxygen and moisture;[8] this is also the case for complex **6**.

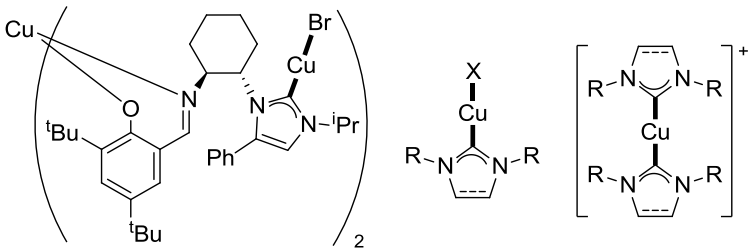

LXXI **LXXII** **LXXIII**

Figure 3.3. Examples of Cu^I complexes bearing a dicoordinated nucleus.[7]

Copper(I) complex **6** forms a dinuclear structure in which each ligand binds to two Cu^I atoms, as shown in Figure 3.2. The bond lengths from the carbene to the metal and from the metal to the alkoxy group are, in average, 1.869 and 1.821 Å, respectively; they are in agreement with the normal range of 1.85-1.87 and 1.79-1.88 Å, respectively, for linear dicoordinated Cu(I)-NHC.[7] Although in proximity, 2.9964(7) Å, there is no formal bond between the copper nuclei given that the distance is longer than the sum of the van der Walls radii of two copper atoms (~2.8 Å).[9] Nevertheless, an interaction is noticeable by the convergent angles O–Cu–NHC, measuring 169.74° in average. The structural geometry of

this complex is similar to that of the amino-tethered NHCs reported by the Danopoulos[10] and the Bellemin-Laponnaz[11] groups, a pyridine-tethered NHC (**LXXIV**) and an oxazoline-tethered NHC (**LXXV**), respectively. Table 3.1 contains representative bond lengths and angles of **6**, **LXXIV** and **LXXV**, all of which are dinuclear species of unsymmetrical Cu(I)NHC complexes with nucleophilic tethers (see Figure 3.4). Table 3.2 compares the same parameters for examples of the linear NHC–Cu–O motif such as that in a Dipp-substituted NHC copper *tert*-butoxide (**LXXVI**),[12] a mesityl-substituted NHC copper acetate (**LXXVII**)[13] and a Dipp-substituted NHC copper acetate (**LXXVIII**)[14] (see Figure 3.5). Finally, Table 3.3 compares the bond lengths and angles of **6** and three other species which contain a 12-member metallacycle and the dicoordinated linear cuprous ion (see Figure 3.6): an isopropyl-substituted, (**LXXIX**),[15a] and methyl-substituted dinuclear species (**LXXX**[9] and **LXXXI**[15b]).

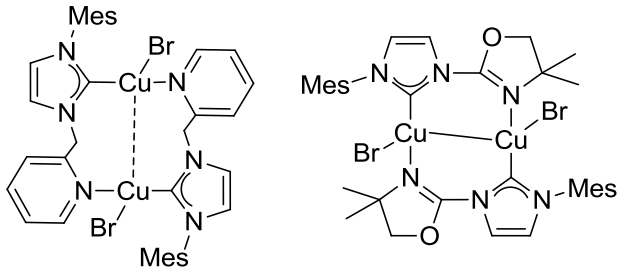

LXXIV **LXXV**

Figure 3.4. Copper(I) tethered-NHC complexes.[10,11]

Table 3.1. Comparison of selected bond lengths and angles of 6 against LXXIV and LXXV, which are similar complexes of tethered NHCs.

bond length/angle	**6**	**LXXIV**[10]	**LXXV**[11]
NHC–Cu (Å)	1.870(4) 1.868(4)	1.931(3)	1.904(4)
Cu–O/N (Å)	1.821(2) 1.821(2)	2.029(2)	1.998(3)
Cu–Cu (Å)	2.9964(7)	2.647(2)	2.7072(7)
NHC–Cu–O/N (°)	169.03(13) 170.44(14)	133.9(1)	142.8(1)

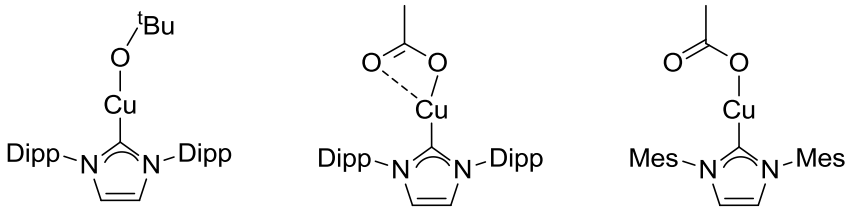

LXXVI **LXXVII** **LXXVIII**

Figure 3.5. Examples of compounds with linear NHC–Cu–O geometries.[12,13,14]

Table 3.2. Comparison of selected bond lengths and angles of 6 against LXXVI, LXXVII and LXXVIII, which are similar complexes containing the NHC–Cu–O geometries

bond length/angle	**6**	**LXXVI**[12]	**LXXVII**[a,13]	**LXXVIII**[14]
NHC–Cu (Å)	1.870(4) 1.868(4)	1.864(2)	1.854(4) [1.850(5)]	1.859(3)
Cu–O (Å)	1.821(2) 1.821(2)	1.810(1)	1.850(3) [1.924(5)], *2.868(4) [2.673(7)]*[b]	1.867(3)
NHC–Cu–O (°)	169.03(13) 170.44(14)	179.05(8)	177.19(18) [166.0(2)], *133.08(17) [143.4(2)]*	171.1(1)

a: The first measurement in each cell corresponds to a κ^1-carboxylate bound to copper; in square brackets are measurements of the second molecule in the unit cell, which features a κ^2-carboxylate. **b**: The measurements taking the more distant oxygen atom are expressed in italics.

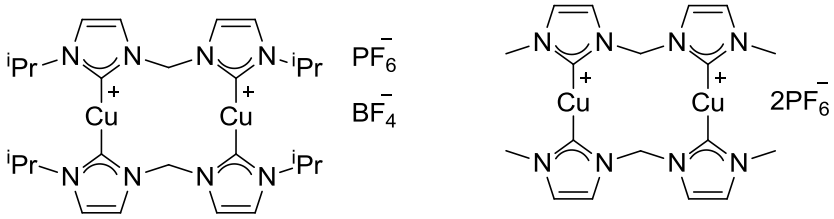

LXXIX **LXXX** **LXXXI** (with acetone and water)

Figure 3.6. Examples of 12-member metallacycles containing Cu(I)NHC.[9,15]

Table 3.3. Comparison of selected bond lengths and angles of 6 against LXXIX, LXXX and LXXXI, which are similar complexes bearing a 12-member ring and the NHC–Cu^{I} motif

bond length/angle	**6**	**LXXIX**[15]	**LXXX**[9]	**LXXXI**[15]
NHC–Cu (Å)	1.870(4) 1.868(4)	2.096(7)	1.918(9)	2.113(8)
Cu–O/NHC' (Å)	1.821(2) 1.821(2)	2.091(7)	1.927(9)	2.083(8)
Cu–Cu (Å)	2.9964(7)	3.2268(7)	2.903(2)	3.353(2)
NHC–Cu–O/NHC' (°)	169.03(13) 170.44(14)	171.4(3)	169.7(4)	167.6(3) 170.3(3)

The NHC–Cu and Cu–O bond lengths of **6** are in close agreement to those in complexes featuring a linear NHC–Cu–O motif such as **LXXVI**, **LXXVII** and **LXXVIII**, with the Cu–O bond being shorter throughout (see Table 3.2). It is interesting to note the similarities between **6** and the dinuclear compounds in both Table 3.1 and Table 3.3, especially when concerned with the NHC–Cu–X angle: **LXXIX**, **LXXX**, and **LXXXI** are definitely constrained because of the planarity in both chelating agents, although their NHC–Cu distances are considerably longer than for the other selected species. This might be a

consequence of spatial constrain imposed by the *N*-methyl and *N*-*iso*propyl groups. The importance of the *N*-mesityl groups is not that noticeable for compounds **LXXIV** and **LXXV**, which invites to think that the reason for the elongation in the NHC–Cu bond distance is purely due to the poor π-backbonding character of the NHCs.

Due to the ready availability of 2-bromo propane in the laboratory's stock, the bromide analogue **2** of proligand **LXIII** was also made, following the analogous procedure for the preparation of **LXIII** (Figure 3.7).[6] This precursor was also used for the synthesis of compound **5** and the subsequent preparation of **6** and other complexes. When comparing the overall yield for the formation of **2** against **LXIII**, the synthesis of **LXIII** is reportedly more effective with 82% yield against 70% for **2**. Also, the synthesis of **5** from **2** afforded a lower yield than that obtained using **LXIII** as precursor (52% for **2** against 60% for **LXIII**).

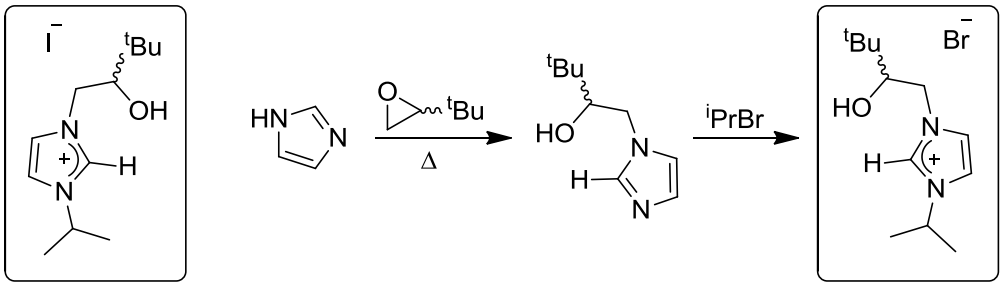

LXIII **2**

Figure 3.7. Analogous precursors of NHCs and preparation of 2.[6]

3.2.1. Reactivity of $(CuL)_2$ towards CO_2 and other small molecules

3.2.1.1. With CO_2

If the interaction between the NHC and the copper(I) ions in **6** is stronger than that between the alkoxide group and the metal, this would enable a chain-growth mechanism of polymerisation in which the alkoxide is the initiator. However, there are a number of reports in which NHCs react with carbon dioxide to form imidazolium-2-carboxylate zwitterions (Scheme 3.2);[16] this would represent an alternative mechanism for the polymerisation initiation. Accordingly, a solution of **6** was exposed to an atmosphere of CO_2 at 1.5 bar and temperatures from 25° C to 70° C in THF (Equation 3.2).

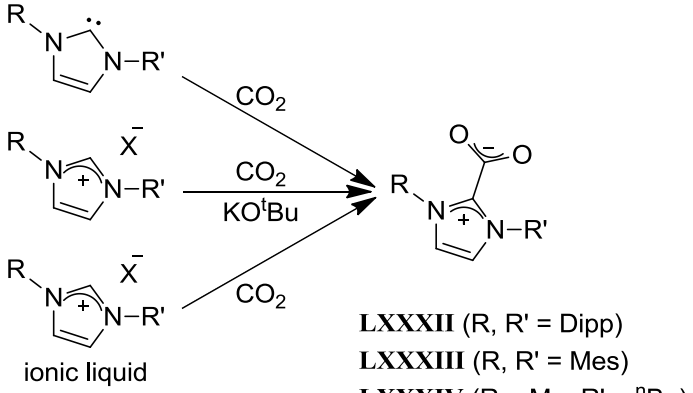

LXXXII (R, R' = Dipp)
LXXXIII (R, R' = Mes)
LXXXIV (R = Me, R' = ^{n}Bu)

Scheme 3.2. Formation of the NHC-CO_2 adduct.[16a,16d]

$$(CuL)_2 + CO_2\ (1.5\ bar) \xrightarrow[25^o\ C]{THF} (CuLCO_2)_2$$

6 **7**

Equation 3.2. Reaction of 6 with CO_2 to form 7

Upon addition of carbon dioxide, the yellow-coloured solution changed to an ocre suspension, and a compound characterised as $(CuLCO_2)_2$ (**7**) formed as a yellow precipitate. The precipitate, being very slightly soluble in THF, was isolated by filtration, washed with THF, and dried to afford pure **7** in 56% yield. The powder of **7** is slightly soluble in pyridine, allowing NMR spectroscopic analysis. The ^{1}H NMR spectrum of **7** shows a single ligand environment with the CH_2 group at 4.43 ppm and the chiral CH group at 4.37 ppm. The singlet resonances of the backbone of the heterocycle were recorded at 7.45 and 7.17 ppm with respect to $SiMe_4$ as the internal standard. These resonances are very similar to those of complex **6** (CH_2: 4.33, CH: 3.96, backbone: 7.26 and 7.23 ppm). The ^{13}C-{H} NMR spectrum of **7** shows the carbene frequency at 164.0 ppm and the frequencies of the CH groups from the backbone of the *N*-heterocycle at 122.5 and 117.1 ppm. The carbon in the chiral centre resonates at 83.7 and the CH_2 group at 54.8 ppm. Additionally, the resonance of the carbonate group appears at 156.7 ppm. The IR spectrum of **7** contains a C–O stretch at

1682 cm^{-1}. Unfortunately, it was not possible to grow single crystals of **7** suitable for X-ray structural analysis neither from the dissolution of the isolated **7** in pyridine, nor from the slowly diffusion of carbon dioxide into the frozen solution of **6** in THF.

Given that there is neither oxidation of the copper centre, ascertained by diamagnetic resonances in NMR spectroscopy experiments, nor the steric hindrance that a monomeric copper complex would impose; we suggest the compound is also dinuclear. Recently, a new compound from a reaction between a mononuclear tris(alkoxy-tethered NHC) scandium complex (**LXXXV**) and CO_2 was synthesised in our laboratory.[17] The insoluble compound is proposed as a 1D supramolecular polymer in which the alkoxy-tethered imidazolium carboxylates act as bridges between Sc nuclei (see **LXXXVI** in the reaction depicted in Equation 3.3). It is worth to mention that **LXXXVI** is, to our knowledge, the first and only example of imidazolium carboxylate bound to a metal through the carboxylate. Measured ^{13}C-NMR and IR spectroscopic data on **LXXXVI** and other examples of NHC–CO_2 adducts are compared against those of 7 in Table 3.4. Table 3.5 compares the same parameters with the data reported for diverse NHC compounds containing metal-carbonate and metal-carboxylate motifs. The compounds in Table 3.5 can be divided into three categories: copper organic carbonates with either phosphines or isocyanides as σ-donors (**LXXXVII**, **LXXXVIII**,[18] **LXXXIX** and **XC**[19]); NHC copper carbonates already mentioned (**LXXVII**[13] and **LXXVIII**[14]); and other metal carbonates such as zinc ethyl carbonates of pyrazolyl borate (**XCI** and **XCII**)[20] and organometallic tin methyl carbonate (**XCIII**).[21]

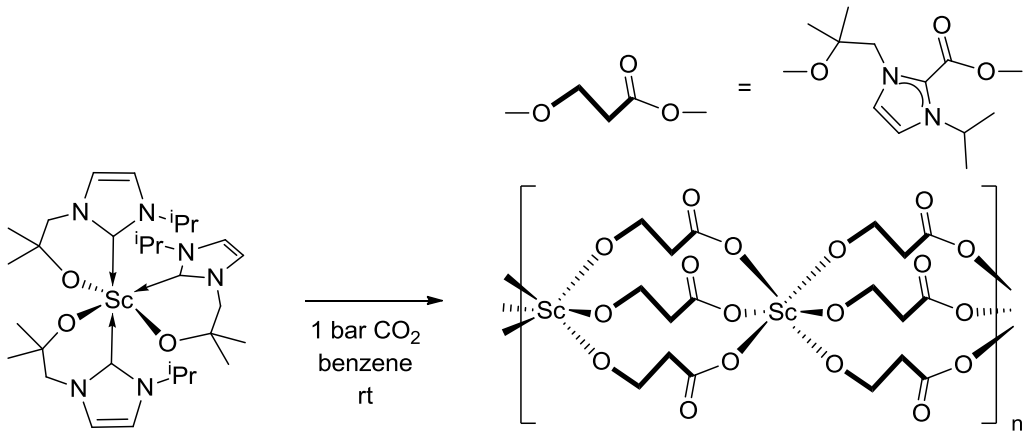

LXXXV **LXXXVI**

Equation 3.3. Reaction of mononuclear tris(alkoxy-tethered NHC) scandium complex and CO_2 at room temperature and pressure.[17]

Table 3.4. Selected spectroscopic data for 7 and other compounds containing imidazolium-carboxylates

structural motif	7[s]	LXXXVI[17]	LXXXII[16a]	LXXXIII[16a]	LXXXIV[16d]
δ_C NH<u>C</u>–CO_2 (ppm)	153.9[t]	145.0[v]	140.8[w]	147.6[y]	140.29[z]
δ_C NHC–<u>C</u>O_2 (ppm)	175.0[t]	156.1[v]	149.2[w]	152.3[y]	158.15[z]
vNHCC(O)–O (cm^{-1})	1694[u]	1672[u]	1675[x]	1678[x]	1662[x]

[s] Values in this column may or may not correspond to the structural motif stated, but are assigned as if they were for comparison, [t] in pyridine-d_5, [u] in Nujol, [v] in solid state, [w] in DMSO-d_6, [x] in KBr, [y] in CD_2Cl_2, [z] in D_2O

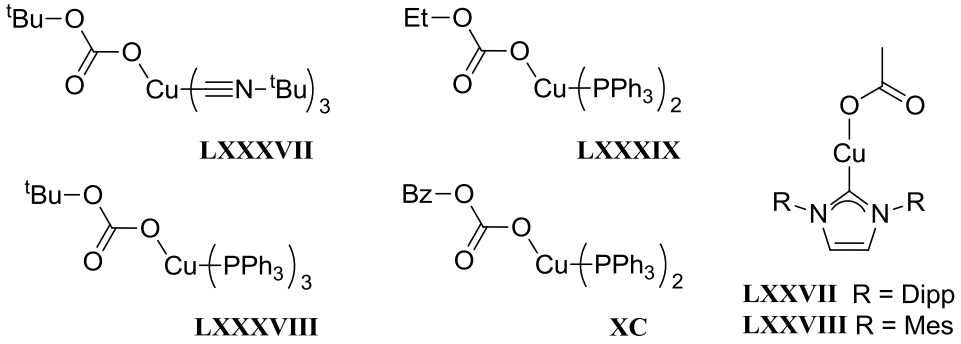

Figure 3.8. Copper(I) carbonate and carboxylate complexes.[13,14,18,19]

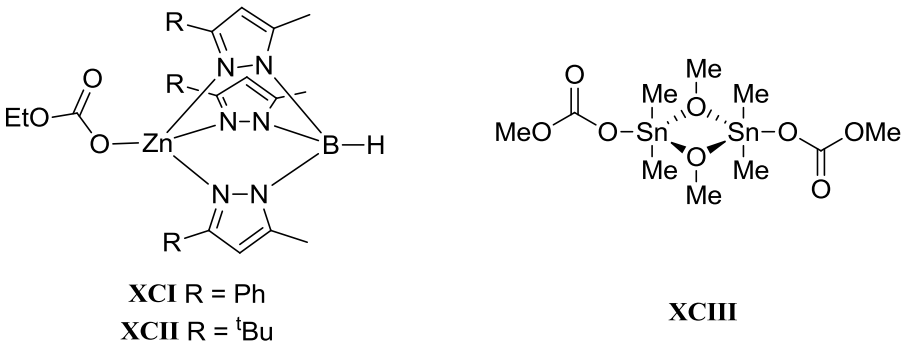

Figure 3.9. Metal-carbonate complexes.[20,21]

Table 3.5. Selected spectroscopic data for 7 and metal carbonate and carboxylate complexes

structural motif	7[a]	**LXXXVII** **LXXXVIII**[18]	**LXXXIX** **XC**[19]	**LXXVII**[13] **LXXVIII**[14]	**XCI** **XCII**[20]	**XCIII**[21]
δ_C CO–<u>C</u>(O)O–M (ppm)	153.9[b]			128.9[d] 130-120[d]	157.5[f] 157.7[f]	159.2[f]
δ_C NH<u>C</u>–M (ppm)	175.0[b]			182.6[d] 180.9[d]		
vCOC(O)–OM (cm^{-1})	1694[c]	1650, 1310, 1013.[c] 1646, 1305, 1017.[c]	1660, 1380, 1285. 1660, 1380, 1280.	1615[e] -	1719, 1268. 1681, 1295.	1682[g]

[a] Values in this column may or may not correspond to the structural motif stated, but are assigned as if they were for comparison, [b] in pyridine-d_5, [c] in Nujol, [d] in C_6D_6, [e] in KBr, [f] in $CDCl_3$, [g] in D_2O

Comparing the data in both Table 3.4 and Table 3.5 with the information we have from new complexes **6** and **LXXXVI**, we suggest that carbon dioxide inserts into the Cu–O bond, whilst the carbene remains bound to a copper(I) atom. For instance, in Table 3.4, complex **7** is regarded as containing the imidazolium-carboxylate functional group; compounds **LXXXII**, **LXXXIII** and **LXXXIV** are not metal complexes and the resonances from the imidazolium-carboxylate group understandably present a lower-frequency chemical shift to that of such a group bound to metal in **LXXXVI** and potentially in **7**. It is expected that the chemical shifts of both carbon atoms in the imidazolium-carboxylate groups of **LXXXVI** and **7** are very similar but the resonances of **7** are at a noticeable higher frequency. In addition, the infrared band of the carboxylate in **7** is not in the vicinity of the peaks presented by the compounds containing imidazolium-carboxylate groups. Table 3.5 shows some examples of carbonate and carboxylate complexes including complex **7**: compounds **XCI**, **XCII** and **XCIII** (metal carbonates) have chemical shifts for the carbonate group bound to metal which are very similar to the resonance of **7** at 154 ppm. In addition, ^{13}C NMR frequencies for NHCs bound to metal carboxylates (**LXXVII** and **LXXVIII**, for example) are comparable to the ^{13}C NMR frequency assigned to the carbene in **7** at 175 ppm. Finally, the IR frequencies of C–O in metal carbonates are comparatively higher than those assigned to imidazolium carboxylate groups and, hence, closer to the sharp frequency at 1694 cm^{-1} for C–O in **7**. These data are shown in the last rows of both Table 3.4 and Table 3.5. In further support of this assignment, Yamamoto *et al*. argue that if the C–O stretch is of high energy, the mode of coordination of the carbonate towards the copper nucleus is κ^1, which in their case, that corresponds to 1660 cm^{-1}.[19] For a carboxylate such as **LXXVII** both κ^1 and κ^2 binding modes coexist in the solid state; the energy of its C–O stretch is 1615 cm^{-1} and could be taken as the threshold between monodentate or bidentate carbonate.[13] In this case, given the frequency of its C–O stretch of 1694 cm^{-1}, we could say that a κ^1-carbonate is more likely to be present in **7**. Thus, the proposed structure of **7** is depicted in Figure 3.10, as was

suggested in Equation 3.2 above. As speculated in Section 3.2, Cu^{I}, being a soft acid, finds stronger affinity towards the carbene than towards the alkoxide (hard base) and allows the latter to react more easily with carbon dioxide. It would be interesting to see how a Cu^{II} complex such as **LXX** reacts with carbon dioxide under the same conditions.

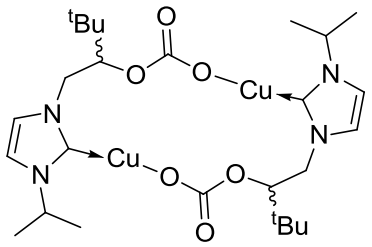

Figure 3.10. Proposed structure of 7

3.2.1.2. With CO_2 and chlorosilanes

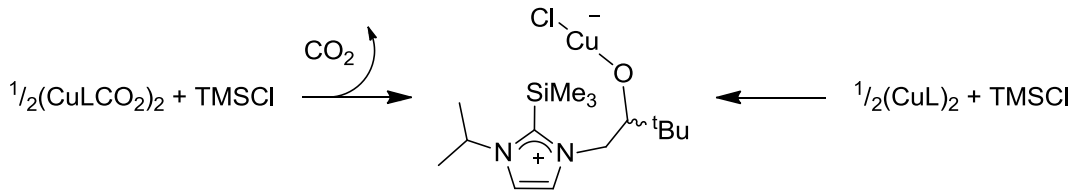

7 **8** **6**

Equation 3.4. Reaction of studied copper complexes and trimethylsilylchloride

In order to ascertain the structural characteristics of **7** and to understand its reactivity, it was treated with trimethylsilylchloride (TMSCl) forming complex **8** in which the trimethylsilyl group displaces the metal and carbon dioxide is released (see Equation 3.4), although no noticeable bubbling was observed. Compound **8** was characterised by ^{1}H and ^{13}C NMR spectroscopy as a diamagnetic copper(I) species. Copper complex **6** was also treated with two equivalents of TMSCl resulting in compound **8**, as evidenced by the identical ^{1}H NMR spectra, supporting the suggestion that CO_2 is not present in the product **8**. The ^{1}H NMR spectrum of a C_6D_6 solution of **8** contains a set of ligand resonances in the region 0-10 ppm, and no high-frequency resonances attributable to an imidazolium CH group, suggesting that **8** is a diamagnetic, i.e. copper(I) complex. Analysis of a C_6D_6 solution of **8** by ^{13}C NMR spectroscopy shows a resonance at 175.5 ppm, which is assigned to the C2 carbon in the heterocycle. This is similar to the C2 carbon resonance reported for analogous magnesium (174.6 ppm) and yttrium (174.9 and 174.7 ppm) complexes (compounds **XCIV**, **XCV** and **XCVI** in Figure 3.11) indicating the formation of a $Si–C_{imidazolium}$ bond.[22,23] The ^{13}C NMR spectral resonances of the NHC carbon bound to a metal are in the high-frequency portion of the spectra at 207.2 and 198.3 ppm for magnesium and zinc complexes, **XCVII** and **XCVIII**, respectively (Figure 3.12).[22] **XCVII** and **XCVIII** were prepared from analogous starting

materials to the ones used in the syntheses of **XCIV**, **XCV** and **XCVI**. Also, **XCVII** and **XCVIII** contain the –O–$SiMe_3$ motif. In addition, only one resonance for silicon was found in the ^{29}Si NMR spectrum of **8** at 18.3 ppm. It is interesting to note that the synthesis of compound **8** adds a univalent analogue to the existing divalent Mg (**XCIV**), and trivalent Y (**XCV**, **XCVI**), Ce and U complexes.[22,23] It is proposed that the formation of the metal-halide bond is the driving force for the reaction, which also works for the formation of C–P, C–B, and C–Sn bonds using halophosphines, boranes and stannanes, respectively, as reported by Turner *et al*.[23] It is worth mentioning that additional resonances in the ^{1}H and ^{13}C NMR spectra of some of the samples were identified as those of hexamethyldisiloxane, which is the hydrolysis product of TMSCl. The presence of water in the sample, then, might be the cause of the release of CO_2 from **7**, most likely driven by the formation of carbonate. Unfortunately, no further experiments were performed to this system to prove the mechanism of release of CO_2.

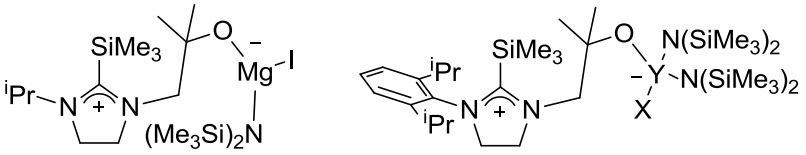

XCIV

XCV: X=I
XCVI: X=Cl

Figure 3.11. Examples of metal complexes with the Si–imidazolium motif.[22,23]

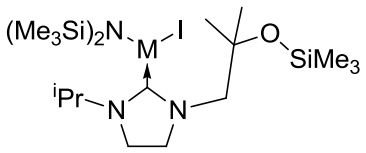

XCVII: Mg
XCVIII: Zn

Figure 3.12. Metal complexes with NHC and trimethylsilyl moieties.[22]

Compound **7** also decomposed in the presence of silanes to form a mixture of compounds which were not identified. Stoichiometric amounts of cyclohexene oxide were also probed as reactant with **7**, but no reaction took place.

3.2.1.3. With CS_2

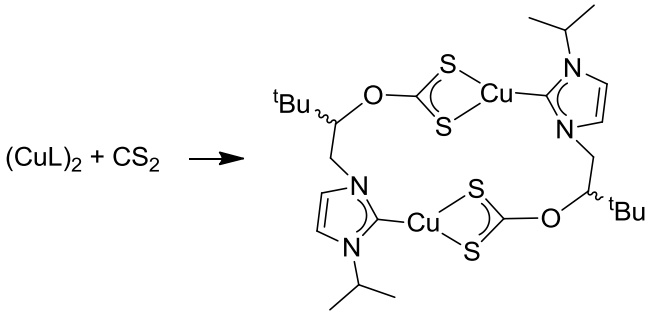

6 **9**

Equation 3.5. Reaction of 6 and carbon disulfide

Compound **6** was also treated with carbon disulfide; the yellow-coloured toluene solution of **6** produced a brown precipitate upon addition of CS_2. The precipitate, being washed with toluene, was isolated by filtration and dried to afford red-coloured **9** in 62% yield. The powder of **9** is soluble in pyridine, allowing NMR spectroscopic analysis. The ^{1}H NMR spectrum of **9** shows a single ligand environment with the CH_2 group at 5.03 ppm and the chiral CH group at 6.13 ppm. The singlet resonances of the backbone of the heterocycle were recorded at 7.47 and 7.13 ppm with respect to $SiMe_4$ as the internal standard. The resonances show higher frequency compared to those of complex **6** (CH_2: 4.33, CH: 3.96, backbone: 7.26 and 7.23 ppm). The ^{13}C-{H} NMR spectrum of **9** shows the carbene frequency at 183.5 ppm and the frequencies of the CH groups from the backbone of the *N*-heterocycle at 122.6 and 116.5 ppm. The carbon in the chiral centre resonates at 89.9 and the CH_2 group at 52.1 ppm. Additionally, the resonance of the dithiocarbonate group appears at 230.8 ppm. Unfortunately, it was not possible to grow single crystals of **9** suitable for X-ray structural analysis neither from the dissolution of the isolated **9** in benzene or pyridine, nor from the slowly diffusion of carbon disulfide into a THF solution of **6** through a buffer of pure THF.

Table 3.6 contains a number of related compounds (see Figure 3.13 and Figure 3.14) that have their CS_2 and NHC features compared with **9**. The compounds referred to are a cadmium complex featuring dithiocarbonates or xanthates, **XCIX**;[24] a copper(I) xanthate, **C**;[25] an imidazolium dithiocarboxylate adduct, **CI**;[26] a ruthenium complex with the same adduct as ligand, **CII**;[27] and a scandium carbene complex featuring the same adduct as a betaine, **CIII**.[17] The data shown in the table indicate that the ^{13}C NMR chemical shift of the CS_2 group in **9** at 230 ppm is in the range of both the xanthate and the imidazolium dithiocarboxylate functional groups. Nevertheless, the ^{13}C NMR chemical shift of the carbene in **7** is very different to that of the carbene groups forming adducts with CS_2 (**CI**, **CII**, and especially in **CIII**), hence discarding that **9** contains this adduct. The **CIII** complex, one of the Sc complexes with analogous ligands to **9** (see Figure 3.15), is particularly interesting

because it contains both a metal–carbene motif and an imidazolium dithiocarboxylate betaine.[17] Looking at the spectroscopic data only for **9** and **CIII** it can be argued that **9** might contain the same features as **CIII**; however, the ^{13}C NMR chemical shifts for the C–CS_2 group are not visible in the NMR spectrum of **9**. In conclusion, we believe that **9** is indeed a symmetric compound in which a carbene and a xanthate are, independently, bound to the metal centre. We attribute the differences between **CIII** and **9** to the fact that scandium is a harder metal centre and its alkoxide bond is stronger than its carbene interaction; consequently copper(I), being softer, has its alkoxide group more readily available for external reactions than the carbene bond. Further work would allow us to see where the threshold between hard and soft metal centres lays when complexed to carbon disulfide and alkoxy-tethered NHC ligands.

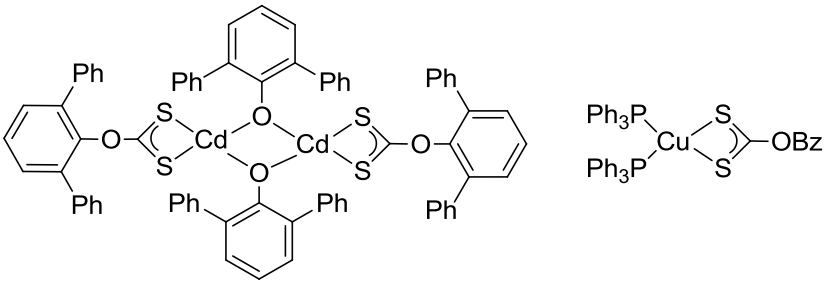

XCIX **C**

Figure 3.13. Metal complexes featuring xanthates.[24,25]

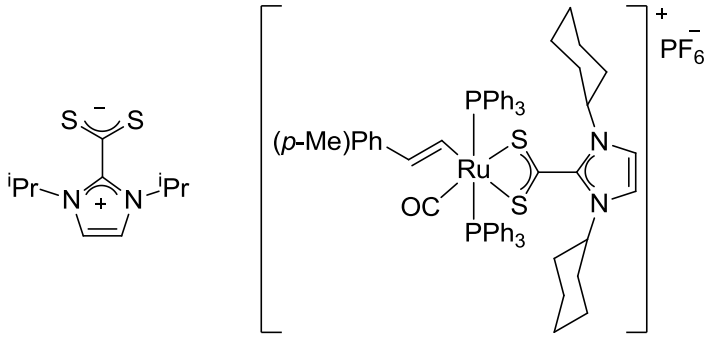

CI **CII**

Figure 3.14. Compounds containing the NHC–CS_2 adduct.[26,27]

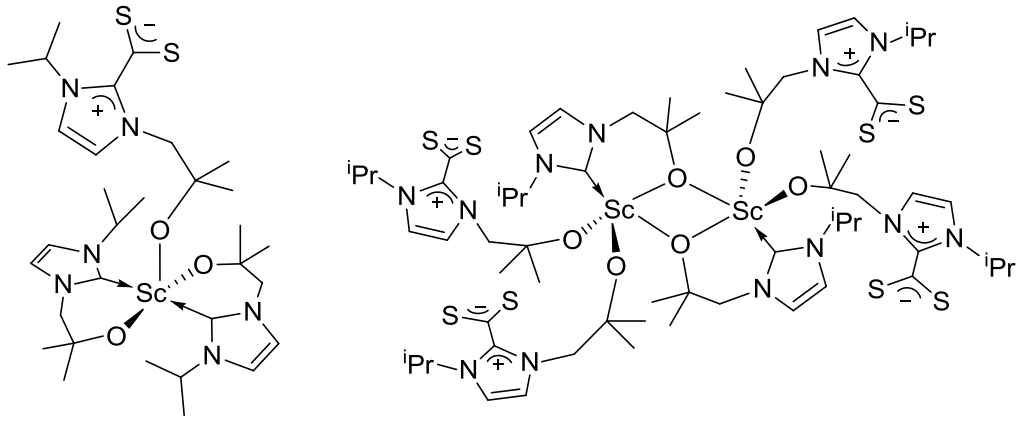

CIII **CIV**

Figure 3.15. Scandium complexes with imidazolium dithiocarboxylate adduct.[17]

Table 3.6. Selected spectroscopic data of 9 and compounds featuring either xanthates or the NHC–CS_2 adduct

structural motif	**9**	**XCIX**[24]	**C**[25]	**CI**[26]	**CII**[27]	**CIII**[17]
δ_C $\underline{C}S_2$ (ppm)	230.2[a]	231.4[b]	266.66[c]	225.7[c]	206.1[c]	226.7[b]
δ_C NH$\underline{C}$ (ppm)	182.2[a]			149.0[c]	141.6[c]	150.6[b,d], 189.9[b,e]

[a] In pyridine-d_5, [b] in C_6D_6, [c] in $CDCl_3$, [d] forming the NHC–CS_2 adduct, [e] Sc–carbene

3.2.2. Reactivity of $(CuL)_2$ as initiator of ring-opening polymerisation

The complex **6** was also tested as a catalyst for the ring-opening polymerisation of *rac*-lactide and ε-caprolactone, as well as for the copolymerisation of epoxides and carbon dioxide at different pressures.

3.2.2.1. Reactivity of $(CuL)_2$ as initiator of ring-opening polymerisation of *rac*-lactide

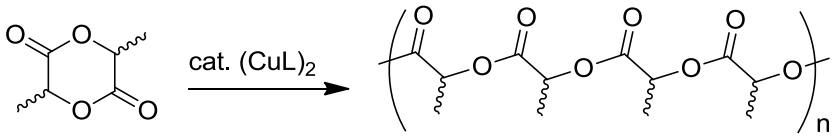

rac-lactide poly(lactic acid)

Equation 3.6. Polymerisation of *rac*-lactide initiated by $(CuL)_2$

In a typical polymerisation reaction, a DCM solution of *rac*-lactide was added through cannula to a Schlenk flask containing $(CuL)_2$, **6**, in DCM and stirred for 16 h at room temperature under atmosphere of N_2. At the end of the reaction time, an aliquot from the crude was taken to measure overall conversion of lactide using the integration data of the CH resonances of the polymer against those of the monomer in the ^1H NMR spectrum. Cold hexane was added to the bulk of the mixture to stop the reaction and separate the polymer through precipitation/centrifugation; the viscous solid was dried under reduced pressure and analysed using gel permeation chromatography (GPC). The samples of poly(lactic acid) obtained had low molecular weights and narrow polydispersities as shown in Table 3.7. Although compound **6** has two chiral centres, the present study did not include analysing tacticity data, which might be interesting for future investigations.

Table 3.7. Polymerisations of *rac*-lactide using 6

Entry	6 (mg)	solvent (mL)	Ratio cat:monom:solv	Time (h)	TON[a]	Yield %[b]	M_n[c]	PDI[d]
i[e]	50	4.2	1:50:750	60	50	>99	-	-
ii	25	2.75	1:100:1000	16	100	>99	8872	1.1
iii[f]	12.5	2.75	1:200:2000	16	200	>99	12145	1.0

Amount of monomer in all entries: 660 mg. Solvent in all entries: DCM. **a** Because the catalyst was not recovered at the end of the reaction, the turnover frequency is the molar ratio monomer/catalyst for a conversion of 100%. **b** Measured from the ^1H NMR spectrum in $CDCl_3$ of an aliquot taken right at the end of the reaction. **c** Measured using GPC with a polystyrene standard and a dn/dc of 0.051 mL/g. **d** Polydispersity index is the M_w/M_n ratio from GPC results. **e** The sample from Entry **i** was not measured by GPC. **f** Entry **iii** is a mixture of polymers: the minor trace is reported in the table. Data of the major trace: M_n=5195 Da; PDI= 2.0.

In the presence of catalyst **6**, the polymerisation of *rac*-lactide into poly(lactic acid) proceeded in DCM at room temperature and for catalyst loadings as little as 0.5% with relation to the cyclic monomer.

3.2.2.2. Reactivity of $(CuL)_2$ as initiator of ring-opening polymerisation of ε-caprolactone

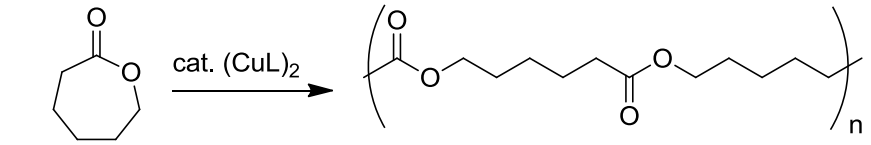

ε-caprolactone polycaprolactone

Equation 3.7. Polymerisation of ε-caprolactone initiated by $(CuL)_2$

In a typical polymerisation reaction, a DCM solution of ε-caprolactone was added through cannula to a Schlenk flask containing $(CuL)_2$, **6**, in DCM and stirred at room temperature under atmosphere of N_2. At the end of the reaction time, an aliquot from the crude was taken to measure overall conversion of caprolactone using the integration data of the proton resonances in the α carbon of the polymer against those of the monomer in the ^1H NMR spectrum. Cold hexane was added to the bulk of the mixture to stop the reaction and separate the polymer through precipitation/centrifugation; the viscous solid was dried under reduced pressure and analysed using gel permeation chromatography (GPC). The samples of poly(caprolactone) obtained presented high molecular weights and narrow polydispersities, as is shown in Table 3.8. The number of turnovers for these polymers is the molar ratio of monomer/catalyst because the remaining catalyst at the end of the reaction was not recovered. No evidence was found of another Cu(I) complex able to polymerise ε-caprolactone; copper(II) triflate, nevertheless, had been successful as a catalyst producing polymers with lower molecular weight (16400 g/mol) and higher polydispersity index (1.97).[28]

Table 3.8. Polymerisations of ε-caprolactone using 6

Entry	Ratio cat:monom:solv	Time (h)	TON	Yield %[a]	M_n[b]	M_w[b]	PDI[c]
iv[d]	1:100:1000	16	100	>99	89567	91638	1.0
iv'	1:100:1000	60	100	>99	13428	17300	1.3

Amount of **6** in all entries: 25 mg. Amount of monomer in all entries: 523 mg. Solvent in all entries: 2.75 mL of DCM. **a** Measured from the ^1H NMR spectrum in $CDCl_3$ of an aliquot taken right at the end of the reaction. **b** Measured using GPC with a polystyrene standard and a dn/dc of 0.079 mL/g. **c** Polydispersity index is the M_w/M_n ratio from GPC results. **d** The sample from Entry **iv** is a mixture of polymers: the major trace is reported in the table. Data of the minor trace: M_n=60434 Da; PDI= 1.2.

3.2.2.3. Reactivity of $(CuL)_2$ as initiator of copolymerisation of cyclohexene oxide with carbon dioxide

Finally, copolymerisation of cyclohexene oxide with carbon dioxide at 1.5 bar, 8 bar of 50 bar of the gas and catalyst molar load of 1.5% or 0.3%, respectively, was attempted.

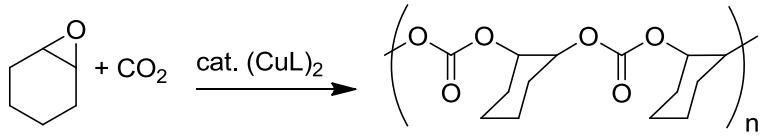

cyclohexene oxide — poly(cyclohexene oxide) carbonate

Equation 3.8. Attempted copolymerisation of cyclohexene oxide and carbon dioxide initiated by $(CuL)_2$

The reactions at 80° C were not successful even for the formation of polyesters. The copolymerisation of cyclohexene oxide and CO_2 was also tried at 50 bar of the gas with similar results; see Table 3.9 for the reaction conditions used. Given the energetic profile of the formation of copolymers and cyclic carbonates from epoxides and carbon dioxide, it is certain that the first activation energy was not overcome; thus, if the copper complex can indeed act as a catalyst for this kind of reactions, higher temperatures, molar load of catalyst and/or pressures are still needed for the coupling of the epoxide and carbon dioxide. These facts are consistent with the current literature, given that, to our knowledge, there is only one example of copper catalysing the coupling of epoxides and carbon dioxide in the formation of chloropropene carbonate with modest yields and poor selectivity.[29]

Table 3.9. Reaction conditions for the failed copolymerisation of CHO and CO_2 using 6

Entry	6 (mg)	CHO (g)	solvent (mL)	Ratio cat:monom:solv	CO_2 (bar)	solv.	temp (°C)	time (h)	conv. (%)
v	50	0.60	2	1:67:366	1.5	DCM	60	60	0
vi	50	0.58	1.4	1:65:188	1.5	THF	80	16	0
vii	50	2.91	2	1:324:269	8	THF	80	60	0
viii	163	14.55	1.5	1:496:62	50	THF	80	24	0

3.3. Zn^{II} complex of alkoxide/NHC ligands

Once we had investigated the behaviour of **6** toward CO_2 and other species, we wanted to understand how the same ligand reacts with other metals, especially harder Lewis acids.

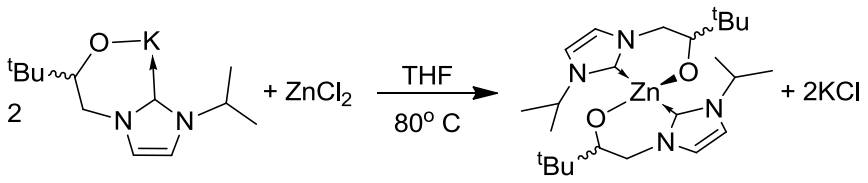

5 **10**

Equation 3.9. Reaction of $ZnCl_2$ and KL (5) to form $Zn(L)_2$ (10)

The reaction of two equivalents of KL (**5**) and $ZnCl_2$ afforded a mixture of compounds from which two sets of resonances, with an integration ratio of 62/38, were identified from ^1H NMR spectroscopy. The sets of resonances were assigned as diastereomers of $Zn(L)_2$ (**10**): the homochiral and the heterochiral complexes. The ^{13}C NMR spectrum also shows two resonances for each carbon, accounting for both diastereomers. Attempts to purify **10** were not successful; nevertheless, a crystal suitable for structural analysis was isolated, measured and modelled as shown in Figure 3.16.

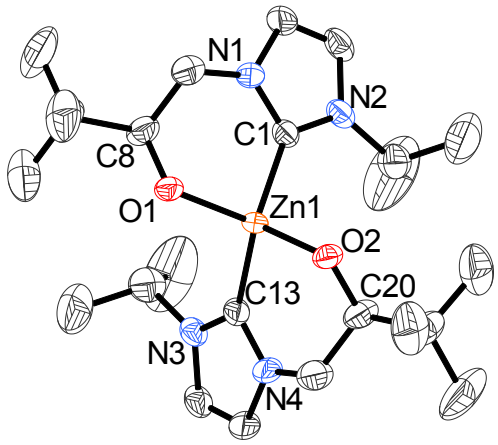

Figure 3.16. Displacement ellipsoid drawing of $Zn(L)_2$ (10). 50% probability ellipsoids. All hydrogen atoms are omitted for clarity.

Selected distances (Å): Zn1–O1 1.956(3), Zn1–O2 1.957(3), Zn1–C1 2.032(4), Zn1–C13 2.029(4); selected angles (°): O1–Zn1–C1 96.7(1), O2–Zn1–C13 96.9(1), O1–Zn1–O2 120.7(1), C1–Zn1–C13 127.0(2).

The metal cation in **10** has a distorted tetrahedral geometry. The distortion is derived from the cumbersome *tert*-butyl and *iso*-propyl groups. As a result, the bite angles of the ligand (96.7(1) and 96.9(1)°) are smaller in comparison to the C–Zn–O' angles where C and O' belong to different ligands (both at 108.8(1)°). The Zn–O average bond length (1.956 Å) is

within the literature range for zinc complexes of bidentate *O*-tethered NHC ligands (1.888 to 2.068 Å),[22,30] and it is just longer than the reported lengths for the similar compound $Zn(L^M)_2$ (**CV**) (1.941(3) and 1.932(4) Å) in which L^M contains an *N*-mesityl group instead of the *N*-*iso*-propyl group in the 3 position, the carbon atoms in the NHC backbone are saturated, and the alkoxy carbon atom is quaternary with two methyl groups (see Figure 3.17).[22] It is important to mention that one of the carbon atoms in a methylene group in the structure was refined isotropically due to the quality of the crystal measured; hence, the analyses based on the structural data from this compound should be taken with caution.

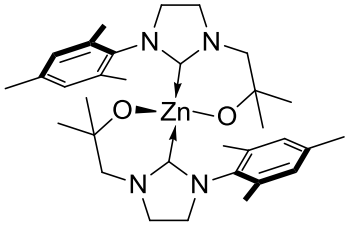

CV

Figure 3.17. Zinc complex of an alkoxy-tethered saturated NHC.[22]

The $Zn–C_{carbene}$ bond distances of 2.032(4) and 2.029(4) Å are in the lower part of the literature range for zinc complexes of bidentate tethered NHC ligands (2.02 to 2.10 Å).[22,30,31] The complex **CV** was successfully tested as a catalyst for the polymerisation of *rac*-lactide; a reaction with 1% of catalyst loading resulted in 92.5% of monomer conversion with experimental molecular weight of 20.5 kg/mol and a polydispersity index of 1.5.[22] This fact shows the possibility of **10** to act as a catalyst for ring-opening polymerisations; unfortunately, its isolation and purification were challenging and **10** could not be tested as catalyst.

In an effort to separate the mixture of products from the reaction of zinc chloride and **5**, a number of common solvents were used to wash the crude and extract the different species. Extraction with diethyl ether afforded a pale yellow solution of **10** that was concentrated and cooled to -30° C. Unfortunately, the solution was opened to air generating a compound that crystallised and was structurally characterised as $Zn(HL)_2\{O(Si(Me_2)O)_2\}$ (**15**). The siloxane group appears to have come from reaction with silicone grease in the glassware, and the alkoxide groups of the ligands have been reprotonated, but the Zn–NHC bonds are intact.

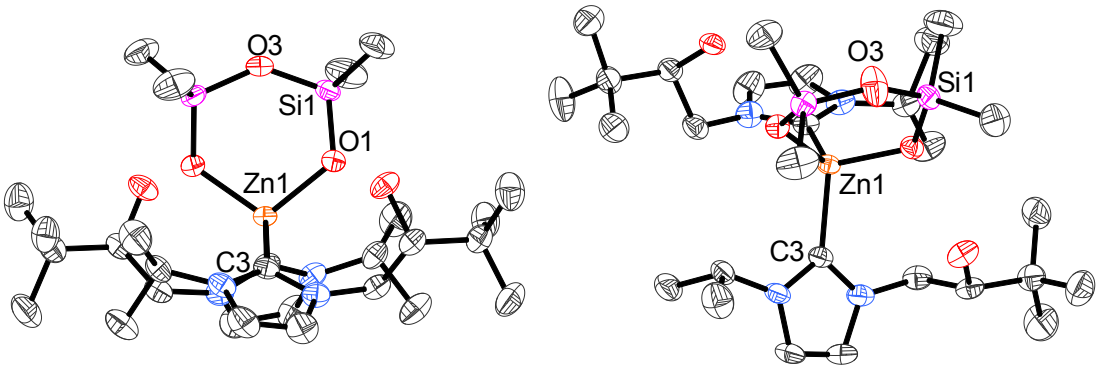

Figure 3.18. Two views of the displacement ellipsoid drawing of $Zn(L)_2\{O(Si(Me_2)O)_2\}$ (15). 50% probability ellipsoids. All hydrogen atoms are omitted for clarity.

Selected distances (Å): Zn1–O1 1.970(1), Zn1–C3 2.066(2), O1–Si1 1.604(1), O3–Si1 1.6312(8); selected angles (°): O1–Zn1–O1' 106.44(6), C3–Zn1–C3' 114.92(8).

There are a number of accounts of metal complexes performing polysilanol depolymerisation from the otherwise inert silicone grease used for keeping the glassware airtight.[32] Many of these, especially the earlier works in the 1970s, refer to the formation of dimethylcyclosiloxanes $(Me_2SiO)_n$, analogous to crown ethers.[33] The first publication of a structurally-characterised bidentate disiloxide, $\{OSi(Me_2)\}_2O$, from silicone grease was a samarium complex in which the disiloxide was bound to two different THF-solvated samarium bis(pentamethylcyclopentadienyl) moieties (compound **CVI** in Figure 3.19).[34] The authors also identified dimethylsilicones in the batch through gas chromatographic-mass spectral analysis, which suggests a significant breakdown of the Dow Corning silicone grease used in the reaction. A trinuclear tetrakis(2-pyridylmethyl)amide organozinc complex bearing a disiloxide (compound **CVII** in Figure 3.19) was also synthesised whilst observing the ligand exchange between an alkoxide and *tert*-butylamine of the dinuclear precursor. Kahnes *et al*. suggested that the base, which in this case is also the solvent, is responsible for the depolymerisation of the Wacker silicone grease.[35] There are four examples of metal complexes of NHCs and siloxides in the literature: a dimeric nickel NHC with disiloxides bridging between metal nuclei (compound **CIX** in Figure 3.20);[36] two nitride technetium complexes with either one (**CXI**) or two (**CX**) NHCs completing the coordination needs of the tetragonal pyramidal nucleus;[37] and a polymeric framework with siloxides bridging a pair of titanium-potassium metals per every three pairs of these atoms (**CXII** in Figure 3.20).[38]

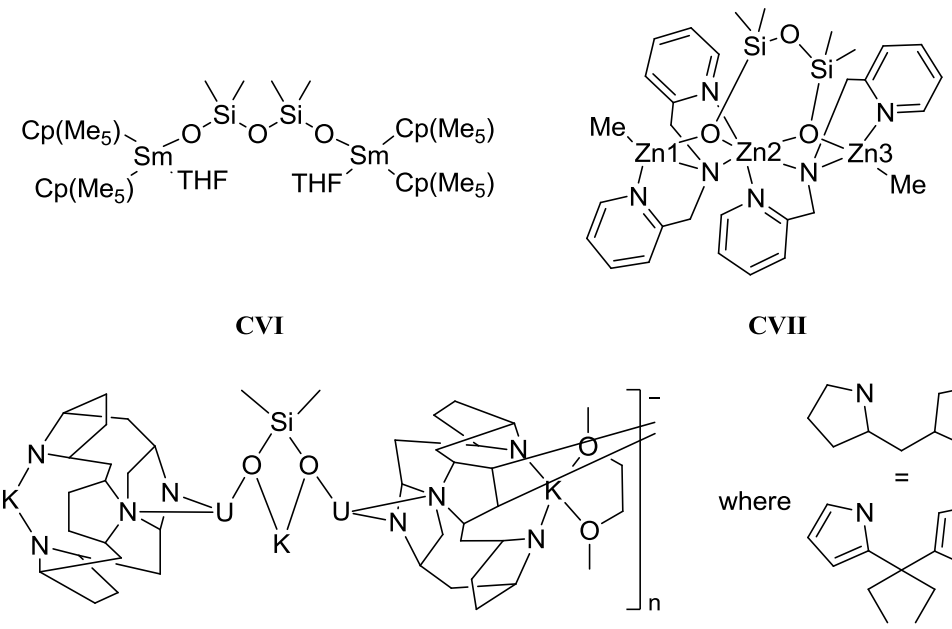

CVI **CVII**

CVIII

Figure 3.19. Selection of metal complexes with siloxide motifs from activated silicone grease.[34,35,40]

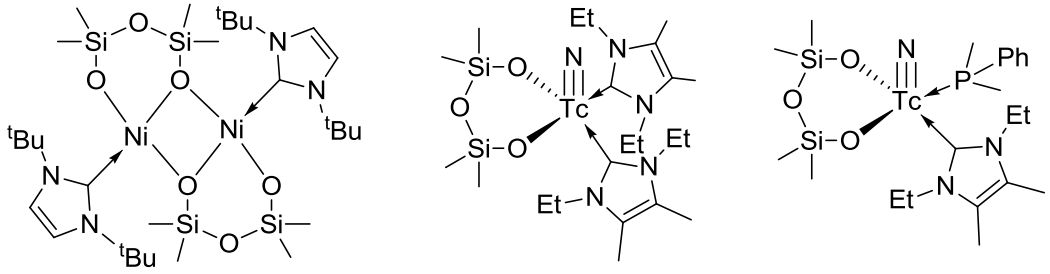

CIX **CX** **CXI**

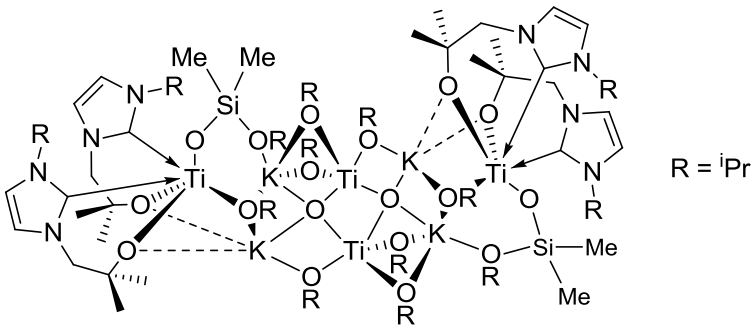

CXII

Figure 3.20. Metal complexes with siloxides and *N*-heterocyclic carbenes.[36,37,38]

The molecular structure of compound **15** presents a 2-fold symmetry down the *b* axis and a distorted tetrahedral coordination for zinc. The Zn–O bond length (1.970(1) Å), in comparison with compound **CVII** is more similar to those of the tetrahedral zinc nuclei (Zn1

and Zn3 in Figure 3.19) with 2.000(2) and 1.992(2) Å, respectively, than to the Zn2–O bond lengths in the same compound (2.104(2) and 2.160(2) Å).[35] When compared with the M–O bond distance of other metal complexes bearing NHCs, 1.970(1) Å is inside the range from 1.839 to 2.063 Å; interestingly, the M–O bond distance in **CXII**, in which the metal is bound to a very similar bidentate NHC, is the closest in magnitude to that of **15** with 1.969(2) Å.[38] The Si–O bond distances of **15** (1.604(1) and 1.6312(8) Å, for the chelating and the bridging oxygen atoms, respectively) are well in the range of the mentioned examples with bond distances going from 1.578 to 1.633 and from 1.628 to 1.656 Å for the chelating and the bridging oxygen atoms, respectively.[36,37] The NHC–Zn bond distance of 2.066(2) Å in **15** is low compared to the NHC–Ti distance of 2.308(3) Å in **CXII** but is in the range for other NHC/disiloxide complexes going from 1.883 to 2.134 Å.[38] Finally, the O–Zn–O angle of 106.44(6)° is close to the expected value for a tetrahedral coordination, with the only other reported examples being 104.9(1) and 99.50(8)° for a cobalt and an indium complexes, respectively.[39] In 2002, the Gambarotta group found an unexpected polymeric uranium complex by reacting a trivalent uranium [Et_8-calix[4]tetrapyrrole] complex with potassium naphthalenide. The anionic compound (**CVIII** in Figure 3.19) has cationic potassium tetrakis(1,2-dimethoxyethane) as counterions.[40] Gambarotta *et al*. claim that **CVIII** was generated by the attack of a transient, highly reactive polysilanol species from the silicone grease. They made more experiments to assess the reactivity of potassium naphthalenide and silicone grease in dimethoxyethane with no reaction even after a long time period.[40] Most of the published compounds containing disiloxides are formed in the presence of potassium or other alkali metals;[32] thus, it is possible that the presence of moisture is what initiates the depolymerisation by the formation of KOH which is known to decompose silicone grease. Other possible agents which cause the reaction are the other components of the Dow Corning high vacuum grease: silicon dioxide (7.0 to 13.0 wt %) and a silicone metalloid complex (5.0 to 10.0 wt %);[41] the latter, in the form of borates was found active for the polymerisation of gaseous diazomethane.[42]

3.3.1. Reactivity of $Zn(L)_2$ towards CO_2

$$\underset{\mathbf{10}}{Zn(L)_2} + CO_2\ (1.5\ bar) \xrightarrow[25^{o}\ C]{THF} \underset{\mathbf{16}}{[Zn(LCO_2)_2]}$$

Equation 3.10. Reaction of 10 with CO_2 to form 16

Compound $Zn(L)_2$ (**10**) was dissolved in THF and transferred to a Young's tap NMR tube before it was degassed and put under static vacuum. A pressure of 1.5 bar of CO_2 was added to the tube turning the colourless solution into a fine white suspension. The tube was allowed to stand over 72 hours and the solid separated by centrifugation and decanting. The

remaining solvent was evaporated and the solid dissolved in pyridine-d_5 and analysed by ^{1}H and ^{13}C NMR spectroscopy. The reaction was repeated using ^{13}C-labelled carbon dioxide. Comparisons of the ^{13}C NMR spectra of $(CuLCO_2)_2$ (**7**) (spectrum **i** in Figure 3.21), that of the polymeric scandium complex **LXXXVI** from Equation 3.3 (spectrum **ii**),[17] and those of "$Zn(LCO_2)_2$" (**16**) (spectra **iii** and **iv** for the unlabelled and ^{13}C-labelled compounds, respectively), enables a tentative structural assignment for **16**.

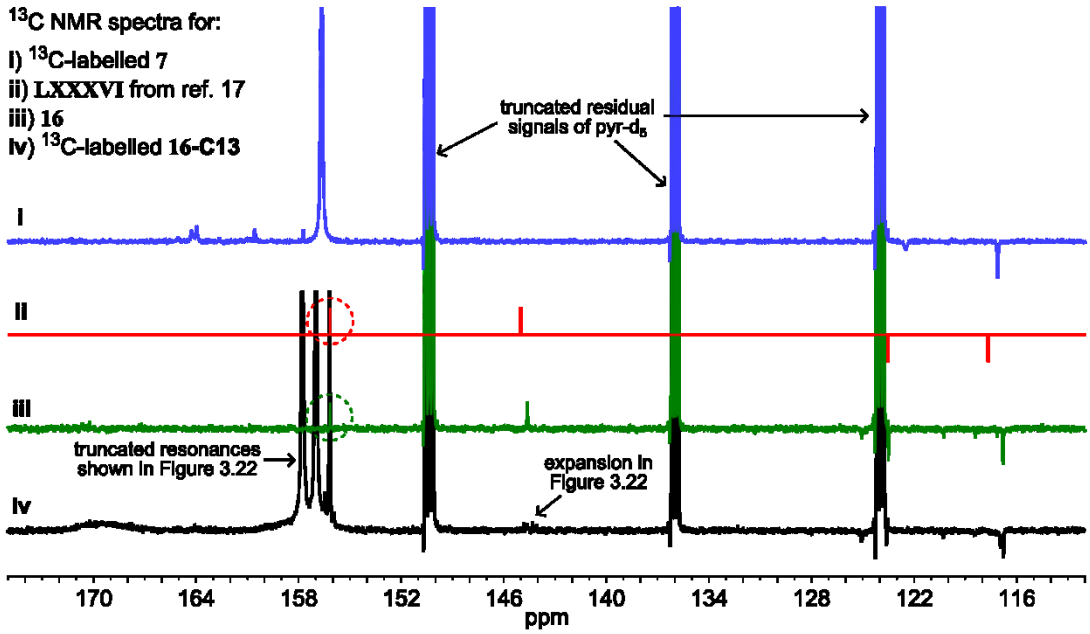

Figure 3.21. High-frequency region of the $^{13}C\{H\}$ DEPTQ* NMR spectra (125.76 MHz in pyridine-d_5) of: i) ^{13}C-labelled 7, ii) LXXXVI simulated,[17] iii) 16, and iv) ^{13}C-labelled 16-C13

From spectrum **iv**, we find three resonances for the CO_2 moiety in the complex at ~157 ppm, with other minor resonances at ~170, ~164, and ~144 ppm. None of the latter resonances correspond to free carbon dioxide which resonates at ~125 ppm in pyridine solution. Compound **7** (spectrum **i**) was identified as a compound with a carbonate motif and empirical formula $[CuLCO_2]$ (Figure 3.10). The resonance at 164.0 ppm in the ^{13}C NMR spectrum of **7** is assigned as the carbene carbon; there are resonances at a similar frequency in spectra **iii** and **iv** in Figure 3.21, although they are very small. However, resonances at 144.6 ppm in **iii** and around that frequency in **iv**, have a similar chemical shift to the resonance assigned to the imidazolium carbon of the imidazolium carboxylate in **LXXXVI** at 145.0 ppm. Therefore, we suggest that CO_2 inserts into **10** mainly by the formation of an imidazolium carboxylate group.

* Distortionless Enhancement by Polarisation Transfer with retention of Quaternaries experiment with the quaternary and secondary carbon resonances in one phase (up in this case) and the tertiary and primary carbon signals in the opposite phase.

Other evidence confirming this assignment are the absence of resonances in the range normally found for zinc carbonate complexes: ^{13}C NMR spectroscopy data of carbonate groups in zinc complexes ranging from 163.7 to 157.5 ppm (see Table 3.10 and Figure 3.24 for details);[20,43,44,45,46] the resonances corresponding to the CO_2 group in spectra **iii** and **iv** are mostly outside of this range. In spectrum **iv**, the most high-frequency resonance of the CO_2 moiety is at 157.7 ppm (see also Figure 3.22). Some very minor resonances at higher frequency than 160 ppm were deemed impurities.

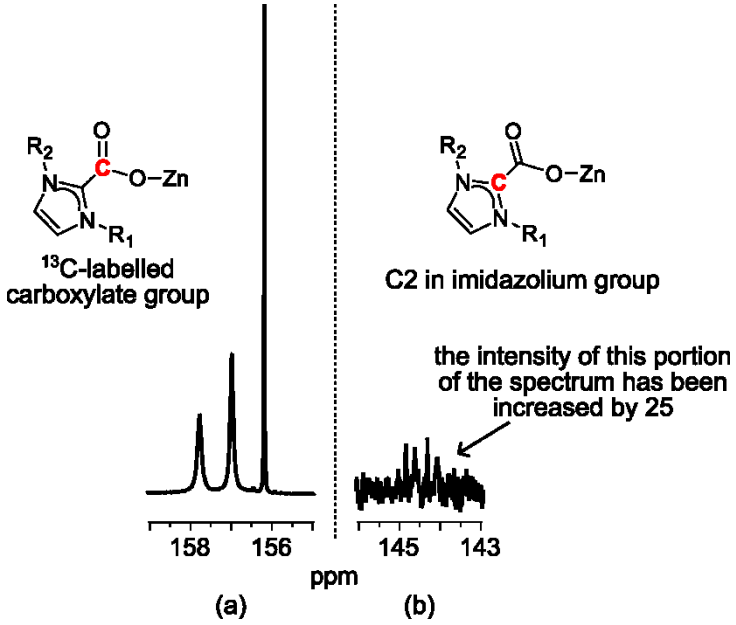

Figure 3.22. Selected expansions of the $^{13}C\{H\}$ DEPTQ NMR spectrum (125.76 MHz in pyridine-d_5) of 16 showing (a) the region for the carboxylate C resonance and (b) the region for the C2 imidazolium resonance for the ^{13}C-labelled 16-C13.

The three resonances of ^{13}C-labelled **16-C13** (spectrum **iv** in Figure 3.21, and Figure 3.22a) could be due to different environments of the CO_2 group either from the insertion position, the coordination of the carboxylate (κ^1 or κ^2-O_2C) to the metal, or from the presence of different diastereomers of ZnL_2 (**10**). The number of resonances for the C2 carbon in the imidazolium group has also increased in the ^{13}C-labelled spectrum (spectrum **iv** in Figure 3.21, and Figure 3.22b) from the unlabelled spectrum of **16** (spectrum **iii** in Figure 3.21). The rest of the low-frequency resonances in Figure 3.21 are similar to **7**; hence, from the NMR spectra we can only propose two structures for **16**: a discrete $Zn(LCO_2)_2$, **16a**, or a polymeric $[Zn(LCO_2)_2]_n$, **16b**, as suggested in Figure 3.23. No reactions were performed at a bigger scale because of the difficulty to purify **10**.

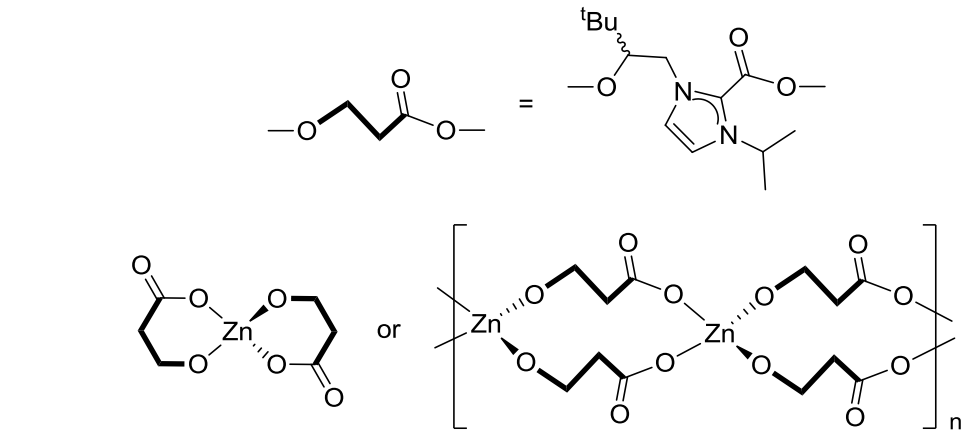

16a **16b**

Figure 3.23. Possible structures of the product of the reaction of 10 and CO_2: a discrete molecule (16a) and a polymeric chain (16b)

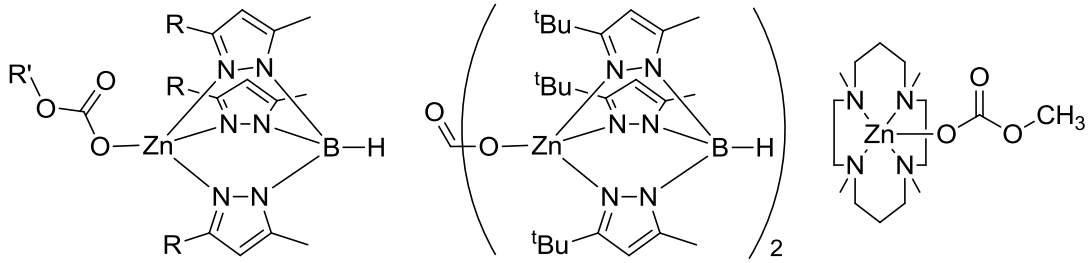

XCI: R=Ph, R'=Et
XCII: R=^{t}Bu, R'=Et
CXIII: R=^{t}Bu, R'=Me
CXIV: R=(*p*-^{i}Pr)Ph, R'=Me
CXV: R=(*p*-^{i}Pr)Ph, R'=Et
CXVI: R=Ph, R'=Me

CXVII **CXVIII**

Figure 3.24. Reported zinc carbonate complexes.[20,43,44,45,46]

Table 3.10. Reported ^{13}C NMR spectroscopic data of R–OCO_2–Zn motifs in $CDCl_3$

XCI[20]	XCII[20,43]	CXIII[43]	CXIV, CXV[44]	CXVI[45]	CXVII[43]	CXVIII[46]
157.5	157.7	158.4	158.0	157.8	163.7	158.8

3.4. Ti^{III} complex of alkoxide/NHC ligands

Other NHC complexes of more Lewis acidic metals such as aluminium, vanadium(III) and titanium(IV) have been used as catalysts for the polymerisation of ethylene.[47] After that, titanium(IV) complexes were prepared in the Arnold group containing amido-tethered and alkoxy-tethered NHCs.[48] More recently, the titanium(III) complex $Ti(L^m)_3$ (**CXIX** in Figure 3.25), in which L^m is an alkoxy-tethered NHC similar to L, but with two methyl groups instead of the *tert*-butyl group in the alkoxy-carbon atom, was synthesised.[49] The preparation of an analogue of $Ti(L^m)_3$ using L as ligand was desirable because it would help to compare the activities of studied complexes such as **6** and **10** with a complex of a more strongly Lewis acidic metal.

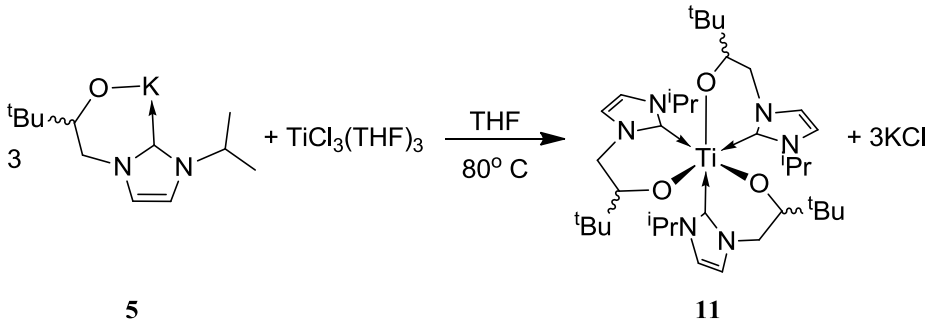

5 **11**

Equation 3.11. Synthesis of $[Ti(L)_3]$ (11) from 5 and $TiCl_3(THF)_3$

The reaction of three equivalents of KL (**5**) and $TiCl_3(THF)_3$ affords after work-up a compound with the empirical formula $[Ti(L)_3]$ (**11**) identified by elemental analyses. The bright orange powder was set to crystallise in toluene and hexane, but the formed crystals dried out very quickly losing crystallinity. Because of its empirical formula and colouration, it could be speculated that **11** is isostructural with **CXIX**, but because it shows a paramagnetic ^{1}H NMR spectrum, structural assignments are not possible without further analyses.

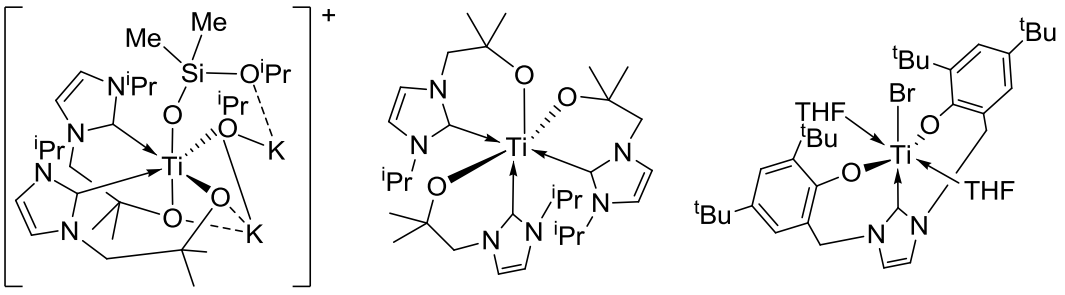

CXII **CXIX** **CXX**

Figure 3.25. Octahedral titanium(III) alkoxy-tethered NHC complexes.[38,52]

Only a few titanium(III) complexes of NHCs have been synthesised,[50] with examples of NHCs functionalised with π-coordinating aromatic groups,[51] a tridentate ligand (**CXX** in

Figure 3.25),[52] as well as the alkoxy-tethered NHCs mentioned earlier.[38,49] Of these, only **CXII**, **CXIX** and **CXX** present an octahedral geometry and the last two a *meridional* conformation (forced by rigidity of the tridentate ligand in **CXX**). The *mer* conformation of **CXIX** requires only one alkoxide being *trans* to an NHC ligand; in the case of **11** proving to be isostructural with **CXIX**, it would be interesting to compare their conformations. It is interesting to note that compound **CXX** has been tested as a catalyst for the polymerisation of ethylene in the presence of methylaluminoxane, cocatalyst, resulting in polymers with relatively lower molecular weight than those produced by analogous titanium(IV) complexes.[52] Studies on **CXII** and **CXIX** came to the conclusion that it is not possible to ascertain that there is a π-backbonding contribution from the NHC to the metal centre from modelling calculations or structural data.[38]

3.4.1. Reactivity of $[Ti(L)_3]$ (11) towards CO_2

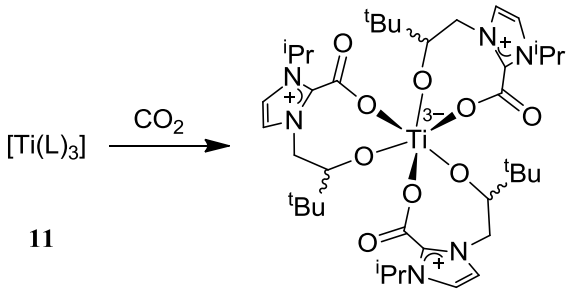

Equation 3.12. Expected reaction of 11 and carbon dioxide

Compound $[Ti(L)_3]$ (**11**) was dissolved in THF and transferred to a Young's tap NMR tube before it was degassed and sealed under static vacuum. A pressure of 1.5 bar of CO_2 was added to the tube turning the orange solution into a brown-coloured suspension. The tube was allowed to stand over 16 hours after which time the brown solid was separated by centrifugation and decanting. Elemental analyses on the solid after it had been dried had weight percentages of carbon, nitrogen and hydrogen a little over half of what was expected, which suggests decomposition in favour of an oxidised species or a mixture of compounds.

3.4.2. Reactivity of $[Ti(L)_3]$ as initiator of ring-opening polymerisation

Given that another Ti^{III} NHC complex was successfully probed as a polymerisation catalyst (**CXX**, ethylene polymerisation),[52] complex **11** was also tested as an initiator for the polymerisation of *rac*-lactide and the copolymerisation of cyclohexene oxide and carbon dioxide.

3.4.2.1. Reactivity of [Ti(L)$_3$] (11) as initiator for the polymerisation of *rac*-lactide

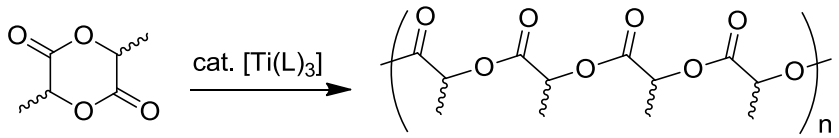

rac-lactide poly(lactic acid)

Equation 3.13. Attempted polymerisation of *rac*-lactide initiated by [Ti(L)$_3$]

A DCM solution of *rac*-lactide was added through cannula to a Schlenk flask containing [Ti(L)$_3$], **11**, in DCM at a catalyst load of 0.5% in relation to the cyclic monomer. The reaction mixture was stirred for 16 h at room temperature under atmosphere of N_2. At the end of the reaction time, an aliquot from the crude was taken to measure overall conversion of lactide, but it did not show conversion of the monomer in ^{1}H NMR spectroscopy.

3.4.2.2. Reactivity of [Ti(L)$_3$] (11) as initiator for the copolymerisation of cyclohexene oxide and carbon dioxide

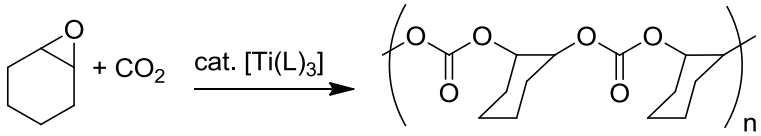

cyclohexene oxide poly(cyclohexene oxide) carbonate

Equation 3.14. Copolymerisation of cyclohexene oxide and carbon dioxide initiated by [Ti(L)$_3$]

In addition, copolymerisation of cyclohexene oxide with carbon dioxide at 50 bar of the gas was tried using a catalyst loading of 0.2% in relation to the epoxide. Two reactions were performed: the first with some THF to form a solution of the catalyst in the presence of CHO, and a second with PPNCl as cocatalyst in addition to THF; reaction conditions are summarised in Table 3.11. ^{1}H NMR spectroscopy of aliquots taken just after 24 h show a 2% conversion for Entry 1 and a 15% conversion for Entry 2 into PCC. Unfortunately, the polymers could not be precipitated and separated from the unreacted monomer and were not further studied. To the best of our knowledge there are no other examples in the peer-reviewed literature of titanium(III) complexes aiding in the formation of polycarbonates from CO_2 and epoxides; nevertheless, there is one patent, by the Williams group, that protects numerous complexes of their ligand (see for examples Figure 1.20) with Ti(III) among the metal centres.[53]

Table 3.11. Reaction conditions for the copolymerisation of CHO and CO_2 using 11

Entry	11 (mg)	CHO (g)	solvent (mL)[a]	Ratio cat:monom:solv:cocat[b]	Temp (°C)	Yield %[c]	TON[d]
1	202.7	14.55	4.5	1:494:185:-	80	2[e]	10
2	202.7	14.55	2	1:494:82:1	80	15[e]	74

a Copolymerisation reactions were performed for 24 h using 50 bar of CO_2 and THF as solvent. **b** Cocatalyst in Entry 2 was PPNCl. **c** Measured from the ^{1}H NMR spectrum in $CDCl_3$ of an aliquot taken right at the end of the reaction. **d** Because the catalyst was not recovered at the end of the reaction, the turnover frequency is the molar ratio monomer/catalyst for a conversion of 100%. **e** The polymer generated could not be isolated from the crude neither by evaporation of the components nor by precipitation with hexanes.

3.5. Tridentate complex of NHC (CNC) ligand

There have been a number of examples of tridentate ligands of the CNC form featuring flexible ethylene bridges (see Section 1.5) of Mg, Ti, Y, Zr, and Pd. Because of their somewhat flexible backbone, the ligands can accommodate metal centres with diverse geometries and even clusters of multiple nuclei (Figure 3.26).[54,55,56,57]

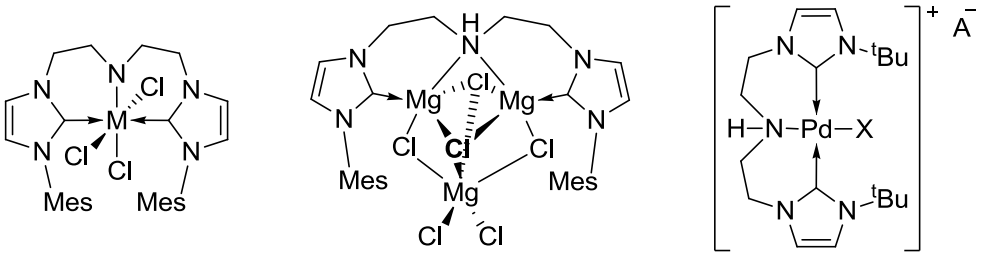

XXII: M=Ti
XXIII: M=Zr

XXV

CXXI: X=Cl, A=Cl
CXXII: X=MeCN, A=2BF_4

Figure 3.26. Examples of metal complexes of tridentate *N*-bridged bis(NHC) ligands.[54,55,56,57]

Because of the formation of magnesium complexes such as **XXV**, the similarity of the ionic radii of Mg and Zn, and the use of zinc catalysts for polymerisations, we targeted analogous zinc complexes using a similar tridentate ligand.

The proligand $H_4L^{CNC}Br_3$ (**CXXIII**) is reported by Fernández Perandones to be formed from the reaction of *N*-substituted benzimidazole and bis(2-bromoethyl)amine hydrobromide (Equation 3.15).[58]

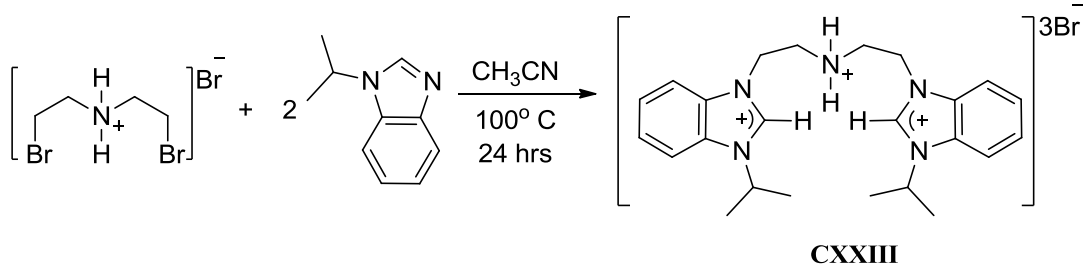

CXXIII

Equation 3.15. Synthesis of $H_4L^{CNC}Br_3$ (CXXIII)

3.5.1. Reactions of Zn(II) with tridentate CNC ligands

A solution of proligand **CXXIII** was treated with a solution of $Zn\{N(SiMe_3)_2\}_2$ in pyridine at room temperature for 24 h (Equation 3.16). After this time, volatiles were evaporated from the yellow-coloured solution under reduced pressure to afford a pale-yellow solid. This solid was recrystallised from a pyridine solution with hexane layered on top at room temperature and characterised as compound $ZnHL^{CNC}Br_2$ (**12**), isolated in 63% yield. Suitable crystals for single-crystal X-ray diffraction studies were obtained using this method; the molecular structure of **12** is depicted in Figure 3.27. The ^{1}H NMR spectrum of **12** shows a symmetric

environment for both NHC groups with the aromatic protons in the range of 8.67-7.27 ppm, and the frequencies of the CH_2 groups linking the amino and the NHC groups at 4.74 and 3.78 ppm. These resonances are at similar frequencies to those of the proligand **CXXIII** at 8.46-7.32 ppm for the aromatic protons and 5.39, 5.03, 4.06 and 3.41 ppm for the linking CH_2 groups, which exist in an asymmetric environment. The ^{13}C-{H} NMR spectrum of **12** shows the carbene frequency at 177.0 ppm and the frequencies of the quaternary aromatic carbon atoms from the backbone of the *N*-heterocycle at 135.4 and 130.9 ppm. The CH_2 groups linking the amino and the NHC groups are found at a frequency of 49.3 and 44.5 ppm.

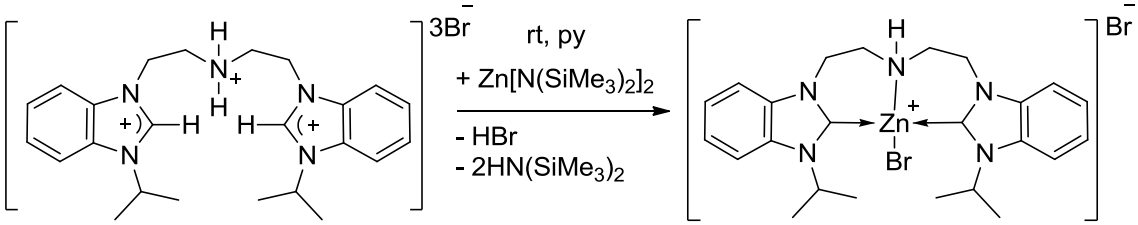

CXXIII **12**

Equation 3.16. Synthesis of $ZnHL^{CNC}Br_2$ (12)

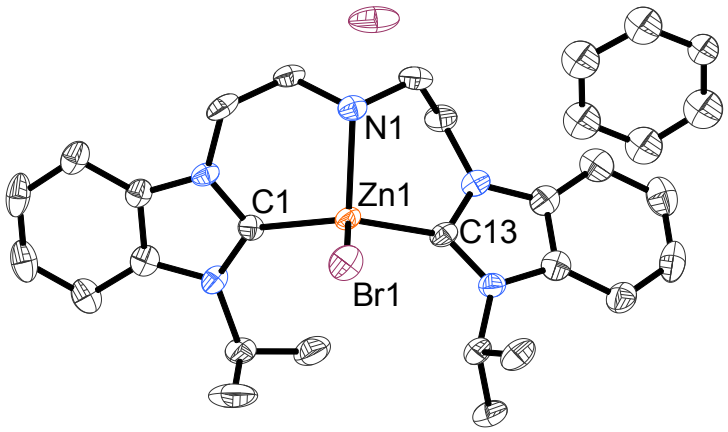

Figure 3.27. Displacement ellipsoid drawing of $Zn(HL^{CNC})Br_2$ (12). 50% probability ellipsoids. All hydrogen atoms are omitted for clarity.

Selected distances (Å): Zn1–N1 2.126(5), Zn1–C1 2.025(6), Zn1–C13 2.020(6), Zn1–Br1 2.3968(9); selected angles (°): C1–Zn1–C13 131.7(2), N1–Zn1–C1 97.3(2), N1–Zn1–C13 96.8(2).

The metal cation in **12** has a much distorted tetrahedral geometry, which could be considered distorted trigonal pyramidal, due to the rigidity of the tridentate ligand. In the molecular structure, the bound bromide group is located as far as possible from the ligand forming consistent angles with the other groups bound to the zinc centre: 110.7(1)° for the Br–Zn–N angle and 108.7(2) and 108.8(2)° for the Br–Zn–$C_{carbene}$ angles. The Zn–C average bond length (2.023 Å) is in the lower part of the literature range for zinc complexes of

tethered NHC ligands (2.02 to 2.10 Å) [22,30,31] and is most similar to the average bond distance of **10** at 2.030 Å. The Zn–C average bond distance of the only other structurally characterised zinc NHC complex with a nitrogen atom bound to the metal centre (compound **CXXIV** in Figure 3.28)[31] is longer than that of **12** at 2.052 Å (Zn–C bond distances for **CXXIV** are 2.049(6) and 2.055(6) Å). The Zn–N average bond distance at 2.483 Å (Zn–N bond distances for **CXXIV** are 2.557(6) and 2.408(5) Å) is high in comparison with 2.126(5) Å of the Zn–N distance in **12**; the difference is mostly due to the trigonal bipyramidal geometry of the zinc in which the pyridine groups are in the axial and farthest away position.

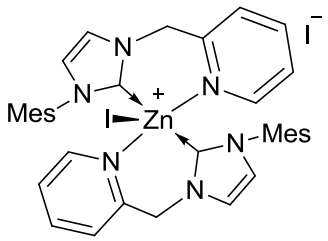

CXXIV

Figure 3.28. Zinc complex of pyridine-tethered NHCs.[31]

Only a handful of tridentate aminocarbene metal complexes with a secondary amine in the backbone have been synthesised (see **XXV**, **CXXI** and **CXXII** in Figure 3.26). From ^{1}H NMR spectroscopy, the resonances of NH have been assigned at 6.91, 8.33, 5.72, and 10.07 ppm for **12**, **CXXI**,[56] **CXXII**,[57] and **CXXIII** respectively. For the other complex of this type containing an NH group, **XXV**, the amino proton could not be located in its ^{1}H NMR spectrum.[55]

Most recently, two complexes with almost the same tridentate ligand of **12** have been reported by the Hazari group. They, however, made use of protecting groups to avoid possible oligomerisation of the backbone whilst preparing the ligand. The Ir (**CXXV**)[59] and Fe (**CXXVI**)[60] complexes are only bound by the NHCs and halogen ligands (Figure 3.29).

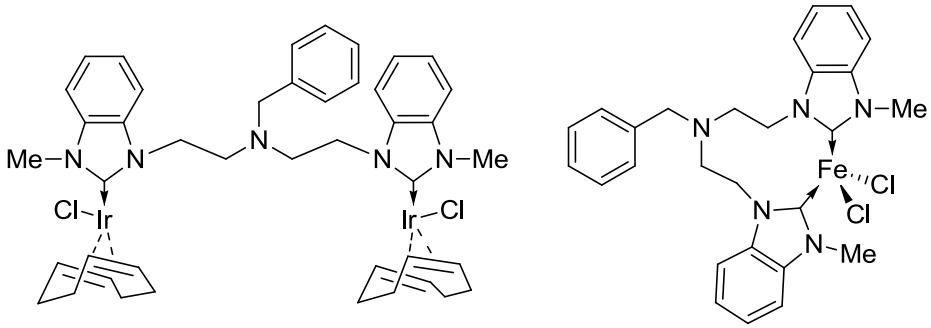

CXXV **CXXVI**

Figure 3.29. Metal complexes featuring a tridentate amino-bridged NHC ligand similar to CXXIII.[59,60]

3.5.2. Reactivity of $ZnHL^{CNC}Br_2$ towards CO_2

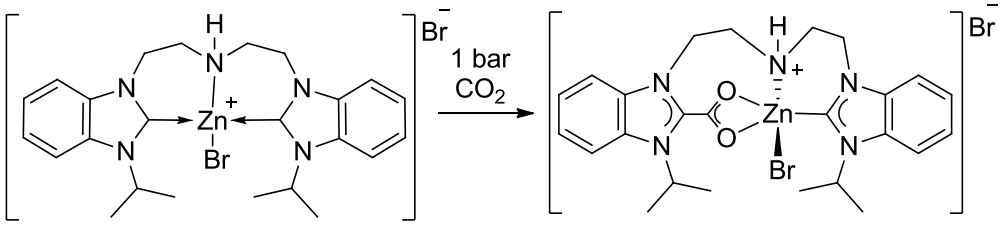

12

Equation 3.17. Proposed reaction of 12 with CO_2

Compound $Zn(HL^{CNC})Br_2$ (**12**) was dissolved in pyridine and transferred to a Young's tap NMR tube before it was degassed and put under static vacuum. A pressure of 1 bar of CO_2 was added to the tube and the tube was heated to 90 °C for 7 days. After the 1st, 3rd, 5th, and 7th days, ^{1}H NMR spectra were acquired to observe the progress of the reaction (see Figure 3.30). This work was carried out with the help of Mr Robert Maller.

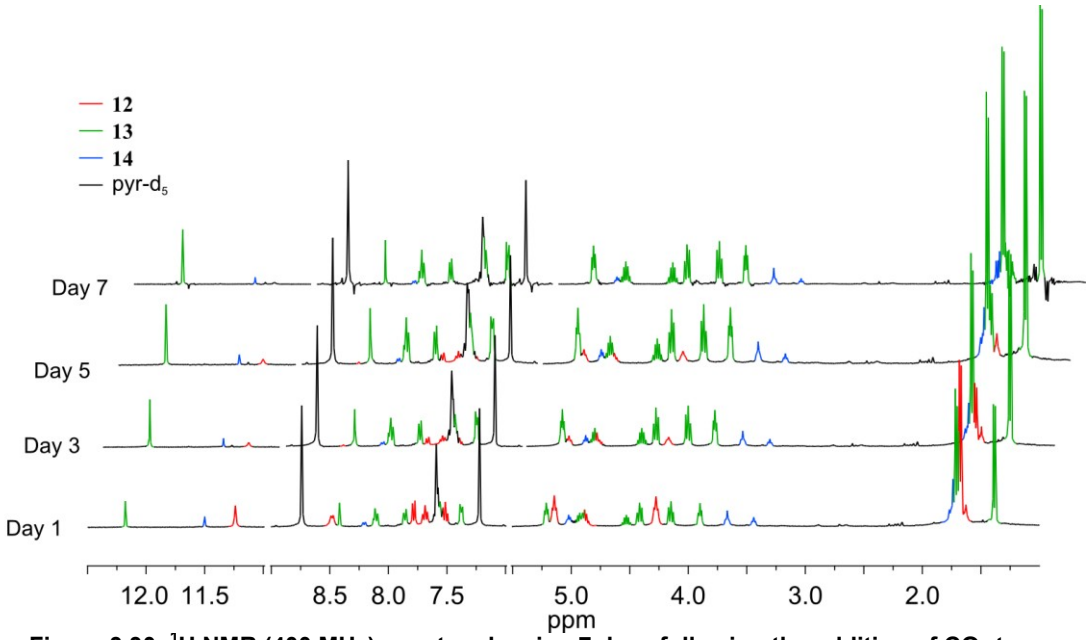

Figure 3.30. ^{1}H NMR (400 MHz) spectra showing 7 days following the addition of CO_2 to a pyridine-d_5 solution of 12. Resonances in each spectrum: black = solvent and baseline, red = starting material, green = main product, blue = by-product. No resonances found in the intervals from 11 to 9 and from 7 to 5.5 ppm.

There are a number of features to account for in the spectra in Figure 3.30:

a) The consumption of the starting material (resonances highlighted in red) is noticeable. The by-product (in blue) is present from the beginning of the reaction till the end with no appreciable change in concentration relative to the concentration of C_5D_4NH (in black).

b) The resonances observed have been assigned as follows: the singlets to high frequency as the NH groups in the backbone of the ligand; the resonances in the range from 9 to 7 ppm as those corresponding to the aromatic rings; the resonances in the range from 6 to 3 ppm as those corresponding to the bridging chain and the CH of the *iso*-propyl groups; and the most low-frequency resonances corresponding to the CH_3 of the *iso*-propyl groups.

c) For the most part, individual resonances account for both NHCs in the ligand; in the main product, however, the resonances for protons in the *iso*-propyl group and the backbone are split in two frequencies each. We propose that this fact is due to the presence of CO_2 inserted just in one side of the molecule and breaking its symmetry.

d) The starting material and the products of the reaction feature high-frequency resonances which are assigned to the NH groups; these resonances, however, are in the area where resonances of protons of imidazolium salts would appear; causing uncertainty about their correct assignment without additional NMR spectroscopic correlation experiments. Furthermore, the resonances assigned to the starting material do not match completely the recorded ^{1}H NMR spectrum of compound **12**; for instance, the NH proton resonance in **12** was assigned as broad at 6.91 ppm, but signals at this frequency do not appear in any of the spectra measured for the CO_2 reaction.

In conclusion, due to the fact that a reaction is occurring in the presence of CO_2, and that the product formed shows asymmetric environments unlike **12** or the original ligand in solution, we propose the formation of an imidazolium carboxylate only in one side of the complex with a remaining metal–carbene bond (compound **13**). Because of low concentration of the samples it was not possible to assign a resonance for the CO_2 group by ^{13}C NMR spectroscopy. Furthermore, we suggest that the by-product (**14**) shown in the ^{1}H NMR spectra in Figure 3.30 is formed by the decomposition of **12** into a doubly reprotonated ligand.

A colourless crystal of the doubly cationic form (containing a neutral secondary amino group) was isolated as a by-product in the reaction of **12** with CO_2 described above, and was studied by single-crystal X-ray diffraction (Figure 3.31).

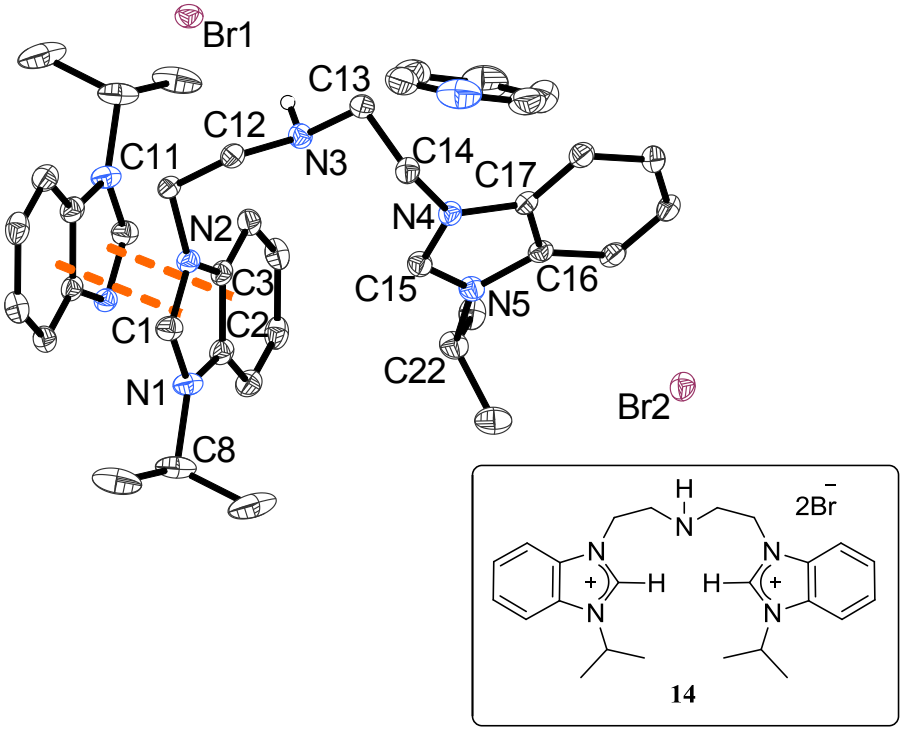

Figure 3.31. Displacement ellipsoid and geometric drawings of $H_3L^{CNC}Br_2$ (14). 50% probability ellipsoids. All hydrogen atoms are omitted for clarity except the one in the amino group. A fragment of a neighbouring molecule is added to show π–π interactions

Selected distances (Å): C1—N2 1.332(2), C1—N1 1.333(2), C15—N4 1.327(2), C15—N5 1.332(2), π–π interaction 3.527; selected angles (°): N2—C1—N1 110.32(15), N4—C15—N5 110.75(15), C12—N3—C13 112.12(13).

As expected, bond distances and angles of the imidazolium groups in **14** are different to those for the carbene in compound **12**. For instance, the average C–N distance for the imidazolium C2 carbon in **14** is 1.331 Å (1.332(2), 1.333(2), 1.327(2) and 1.332(2) Å), whilst that of the carbene in **12** is 1.351 Å (1.347(7), 1.358(7), 1.344(7) and 1.356(7) Å). In addition, the N–C–N average angle in **14** at 110.54° is bigger than 106.4° in **12** as expected due to the NHC being more nucleophilic. The other C–N average distances in the heterocycle are very similar with 1.392 Å in **14** (1.392(2), 1.387(2), 1.390(2) and 1.399(2) Å) and 1.395 Å in **12** (1.395(7), 1.388(7), 1.391(8) and 1.408(8) Å). Compared to other tridentate amino-bridged imidazolium proligands, the average C–N distance of **14** is well in the range from 1.301 to 1.344 Å; and the N–C–N average angle is also in the range from 108.7 to 110.7°.[54,57,59] Finally, as with other benzimidazole-containing compounds, molecules of **14** form π-π interactions with neighbouring molecules; distances as shown in Figure 3.31 are 3.527 Å long, with face-to-face distances of 3.626 Å compared to those of 3.741 Å in **12** and an average of 3.527 Å in similar complexes.[61]

3.6. Conclusion

We have synthesised a ditopic proligand of an alkoxide-tethered N-heterocyclic carbene (**2**) which has been used for the synthesis of potassium, copper, zinc, and titanium complexes. The potassium complex **5** was chosen as the starting material of other complexes because of its ease with which it can be purified on a large scale. A copper(I) complex, **6**, which is highly sensitive to moisture and oxygen, was structurally characterised and reactions with CO_2, CS_2, TMSCl, silanes and epoxides studied. Products were identified only for the reactions with CO_2, CS_2 and TMSCl. Complex **6** has two copper nuclei close to each other; no formal bond was proposed. The reaction of **6** with CO_2 afforded complex **7**, which was identified as the homoleptic complex of a carbonate-tethered NHC ligand. Complex **7**, as well as **6**, react with TMSCl to form a zwitterionic copper alkoxide with a pendant trimethylsilyl imidazolium group. **7** was also tested with silanes, with no identifiable product reported. The reaction of **6** with CS_2 resulted in complex **9**, which was identified as structurally similar to **7**: a homoleptic complex of a xanthate-tethered NHC ligand. Complex **6** was also tested as catalyst for the polymerisation of *rac*-lactide and ε-caprolactone requiring low molar loads and mild conditions to afford calculated quantitative yields. As a potential catalyst for the copolymerisation of CHO and CO_2, **6** was found not to be active under diverse conditions.

Zinc complex **10** was synthesised from **5** and zinc chloride as a homoleptic complex with zinc in a tetrahedral environment. We propose that in one of the attempts to prepare complex **10**, the potassium complex was hydrolysed and activated silicone grease to form compound **15**: a zinc complex containing disiloxide and two NHCs with pendant alcohols. Compound **10** was also treated with CO_2 at ambient pressures and the product, zinc complex **16**, was identified as either a bis(imidazolium carboxylate/alkoxide) or a polymeric compound in which each zinc nucleus is bound by two imidazolium carboxylates and two alkoxides, all from different ligands. A more exact assignment of the structure of **16** should be proposed from more characterising data, especially using variable-temperature NMR spectroscopy, elemental analysis and single-crystal X-ray diffraction.

Paramagnetic titanium complex **11** was prepared from **5** and $TiCl_3(THF)_3$ as a homoleptic tris(alkoxide-tethered NHC). It was treated with CO_2 in a THF solution, but the observed precipitate could not be characterised. **11** was also tested as a catalyst for the polymerisation of *rac*-lactide and the copolymerisation of CHO and CO_2. Formation of poly(lactic acid) did not occur under mild conditions. Complex **11** initiates the coupling of CHO and CO_2 with 15% conversion of CHO in the presence of the cocatalyst PPNCl. However, the polymer obtained was not separated and further analyses were not performed. It is worth mentioning that the present report contains examples of homoleptic complexes of

univalent, divalent and trivalent metal centres with the bidentate alkoxide-tethered NHC from **2**.

The tridentate amino-bridged bis(NHC) proligand **CXXIII** was treated with $Zn\{N(SiMe_3)_2\}_2$ to obtain complex **12**, which was structurally characterised. This compound in turn was treated with CO_2 for a week to afford one major product in an NMR-scale reaction. This product is tentatively identified as **13** from its ^1H NMR spectrum. Because of the asymmetric resonances in such a spectrum, **13** is proposed to have only one molecule of CO_2 inserted in the carbene–metal bond. During the reaction, another species was detected as a decomposition by-product (**14**). This compound was structurally identified as a protonated precursor of the tridentate *N*-bridged bis(NHC) ligand of **12**. **14** differs from the starting material of **12** by the loss of a HBr molecule.

3.7. References

[1] Arduengo, III, A. J.; Harlow, R. L.; Kline, M. *J. Am. Chem. Soc.* **1991,** *113(1),* 361-363. 10.1021/ja00001a054.

[2] Hong, S. H.; Sanders, D. P.; Lee, C. W.; Grubbs, R. H. *J. Am. Chem. Soc.* **2005,** *127,* 17160-17161. 10.1021/ja052939w. Despagnet-Ayoub, E.; Ritter, T. *Top. Organomet. Chem.* **2007,** *21,* 193-218. 10.1007/3418_037.

[3] Rogers, M. M.; Stahl, S. S. *Top. Organomet. Chem.* **2007,** *21,* 21-46. 10.1007/3418_025.

[4] Tekavec, T. N.; Louie, J. *Top. Organomet. Chem.* **2007,** *21,* 159-192. 10.1007/3418_036.

[5] References can be found all along the text of this Chapter.

[6] Arnold, P. L.; Rodden, M.; Davis, K. M.; Scarisbrick, A. C.; Blake, A. J.; Wilson, C. *Chem. Commun.* **2004,** 1612-1613. 10.1039/B404614E.

[7] a) Kaur, H.; Zinn, F. K.; Stevens, E. D.; Nolan, S. P. *Organometallics* **2004,** *23,* 1157-1160. 10.1021/om034285a. b) Díez-González, S.; Kaur, H.; Zinn, F. K.; Stevens, E. D.; Nolan, S. P. *J. Org. Chem.* **2005,** *70,* 4784-4796. 10.1021/jo050397v. c) Díez-González, S.; Stevens, E. D.; Scott, N. M.; Petersen, J. L.; Nolan, S. P. *Chem. Eur. J.* **2008,** *14,* 158-168. 10.1002/chem.200701013. d) Simonovic, S.; Whitwood, A. C.; Clegg, W.; Harrington, R. W.; Hursthouse, M. B.; Male, L.; Douthwaite, R. E. *Eur. J. Inorg. Chem.* **2009,** 1786-1795. 10.1002/ejic.200801152.

[8] Dance, I. G.; Scudder, M. L.; Fitzpatrick, L. J. *Inorg. Chem.* **1985,** *24,* 2547-2550. 10.1021/ic00210a016. Dance, I. G.; Fitzpatrick, L. J.; Craig, D. C.; Scudder, M. L. *Inorg. Chem.* **1989,** *28,* 1853-1861. 10.1021/ic00309a019. Medina, I.; Jacobsen, H.; Mague, J. T.; Fink, M. J. *Inorg. Chem.* **2006,** *45,* 8844-8846. 10.1021/ic061579q.

[9] Matsumoto, K.; Matsumoto, N.; Ishii, A.; Tsukuda, T.; Hasegawa, M.; Tsubomura, T. *Dalton Trans.* **2009,** 6795-6801. 10.1039/b822109j.

[10] Tulloch, A. A. D.; Danopoulos, A. A.; Kleinhenz, S.; Light, M. E.; Hursthouse, M. B.; Eastham, G. *Organometallics* **2001,** *20,* 2027-2031. 10.1021/om010014t.

[11] Schneider, N.; César, V.; Bellemin-Laponnaz, S.; Gade, L. H. *J. Organomet. Chem.* **2005,** *690,* 5556-5561. 10.1016/j.jorganchem.2005.06.044.

[12] Mankad, N. P.; Laitar, D. S.; Sadighi, J. P. *Organometallics* **2004,** *23,* 3369-3371. 10.1021/om0496380.

[13] Mankad, N. P.; Gray, T. G.; Laitar, D. S.; Sadighi, J. P. *Organometallics* **2004,** *23,* 1191-1193. 10.1021/om034368r.

[14] Goj, L. A.; Blue, E. D.; Delp, S. A.; Gunnoe, T. B.; Cundari, T. R.; Petersen, J. L. *Organometallics* **2006,** *25,* 4097-4104. 10.1021/om060409i.

[15] a) Venkatachalam, G.; Heckenroth, M.; Neels, A.; Albrecht, M. *Helv. Chim. Acta* **2009,** *92,* 1034-1045. 10.1002/hlca.200800406. b) Sabiah, S.; Lee, C.-S.; Hwang, W.-S.; Lin, I. J. B. *Organometallics* **2010,** *29,* 290-293. 10.1021/om9010406.

[16] a) Duong, H. A.; Tekavec, T. N.; Arif, A. M.; Louie, J. *Chem. Commun.* **2004,** 112-113. 10.1039/b311350g. b) Gurau, G.; Rodríguez, H.; Kelley, S. P.; Janiczek, P.; Kalb, R. S.; Rogers, R. D. *Angew. Chem. Int. Ed.* **2011,** *50,* 12024-12026. 0.1002/anie.201105198. c) Besnard, M.; Cabaço, M. I.; Chávez, F. V.; Pinaud, N.; Sebastião, P. J.; Coutinho, J. A. P.; Danten, Y. *Chem. Commun.* **2012,** *48,* 1245-1247. 10.1039/c1cc16702b. d) Tommasi, I.; Sorrentino, F. *Tetrahedron Lett.* **2006,** *47,* 6453-6456. 10.1016/j.tetlet.2006.06.106.

[17] Arnold, P. L.; Marr, I. H.; Zlatogorsky, S.; Bellabarba, R.; Tooze, R. P. *Dalton Trans.* **2014,** *43,* 34-37. 10.1039/c3dt52762.

[18] Tsuda, T.; Sanada, S.-I.; Ueda, K.; Saegusa, T. *Inorg. Chem.* **1976,** *15(10),* 2329-2332. 10.1021/ic50164a001.

[19] Yamamoto, T.; Kubota, M.; Yamamoto, A. *Bull. Chem. Soc. Jpn.* **1980,** *53(3),* 680-685. 10.1246/bcsj.53.680.

[20] Peter, A.; Vahrenkamp, H. *Z. Anorg. Allg. Chem.* **2005,** *631,* 2347-2351. 10.1002/zaac.200500196.

[21] Choi, J. C.; Sakakura, T.; Sako, T. *J. Am. Chem. Soc.* **1999,** *121,* 3793-3794. 10.1021/ja9900499.

[22] Arnold, P. L.; Casely, I. J.; Turner, Z. R.; Bellabarba, R.; Tooze, R. B. *Dalton Trans.* **2009,** 7236-7247. 10.1039/b907034f.

[23] Turner, Z. R.; Bellabarba, R.; Tooze, R. P.; Arnold, P. L. *J. Am. Chem. Soc.* **2010,** *132,* 4050-4051. 10.1021/ja910673q.

[24] Darensbourg, D. J.; Niezgoda, S. A.; Draper, J. D.; Reibenspies, J. H. *J. Am. Chem. Soc.* **1998,** *120,* 4690-4698. 10.1021/JA9801487.

[25] Rajput, G.; Singh, V.; Singh, S. K.; Prasad, L. B.; Drew, M. G. B.; Singh, N. *Eur. J. Inorg. Chem.* **2012,** *24,* 3885-3891. 10.1002/ejic.201200307.

[26] Siemeling, U.; Memczak, H.; Bruhn, C.; Vogel, F.; Träger, F.; Baio, J. E.; Weidner, T. *Dalton Trans.* **2012,** *41,* 2986-2994. 10.1039/c2dt11976e.

[27] Naeem, S.; Thompson, A. L.; White, A. J. P.; Delaude, L.; Wilton-Ely, J. D. E. T. *Dalton Trans.* **2011,** *40,* 3737-3747. 10.1039/c1dt10048c.

[28] Wang, Y.; Kunioka, M. *Macromol. Symp.* **2005,** *224,* 193-205. 10.1002/masy.200550617.

[29] Macias, E. E.; Ratnasamy, P.; Carreon, M. A. *Catal. Today* **2012,** *198,* 215-218. 10.1016/j.cattod.2012.03.034.

[30] Lee, Y.; Li, B.; Hoveyda, A. H. *J. Am. Chem. Soc.* **2009,** 131, 11625-11633. 10.1021/ja904654j.

[31] Jensen, T. R.; Schaller, C. P.; Hillmyer, M. A.; Tolman, W. B. *J. Organomet. Chem.* **2005,** *690,* 5881-5891. 10.1016/j.jorganchem.2005.07.070.

[32] Haiduc, I. *Organometallics* **2004,** *23,* 3-8. 10.1021/om034176w.

[33] Ritch, J. S.; Chivers, T. *Angew. Chem. Int. Ed.* **2007,** *46,* 4610-4613. 10.1002/anie.200701822.

[34] Evans, W. J.; Ulibarri, T. A.; Ziller, J. W. *Organometallics* **1991,** *10,* 134-142. 10.1021/om00047a040.

[35] Kahnes, M.; Richthof, J.; Görls, H.; Escudero, D.; González, L.; Westerhausen, M. *J. Organomet. Chem.* **2010,** *695,* 280-290. 10.1016/j.jorganchem.2009.09.041.

[36] Caddick, S.; Cloke, F. G. N.; Hitchcock, P. B.; Lewis, A. K. de K. *Angew. Chem. Int. Ed.* **2004,** *43,* 5824-5827. 10.1002/anie.200460955.

[37] Braband, H.; Abram, U. *Organometallics* **2005,** *24,* 3362-3364. 10.1021/om050245q.

[38] Arnold, P. L.; Zlatogorsky, S.; Jones, N. A.; Carmichael, C. D.; Liddle, S. T.; Blake, A. J.; Wilson, C. *Inorg. Chem.* **2008,** *47,* 9042-9049. 10.1021/ic801046u.

[39] Ackermann, H.; Weller, F.; Dehnicke, K. *Z. Naturforsch.* **2000,** *55b,* 448-451. Petz, W.; Kutschera, C.; Tschan, S.; Weller, F.; Neumüller, B. *Z. Anorg. Allg. Chem.* **2003,** *629,* 1235-1244. 10.1002/zaac.200300048.

[40] Korobkov, I.; Gambarotta, S.; Yap, G. P. A. *Angew. Chem. Int. Ed.* **2002,** *41,* 3433-3436. 10.1002/1521-3773(20020916)41:18<3433::AID-ANIE3433>3.0.CO;2-V.

[41] "Material Safety Data Sheet. Dow Corning® High Vacuum Grease." Dow Corning Corporation. 20 September 2013. <http://www2.dowcorning.com/DataFiles/090007b281c88dd4.pdf>.

[42] Kubota, H.; Morawetz, H. *J. Polym. Sci. Part A: Polym. Chem.* **1967,** *5,* 585-591. 10.1002/pol.1967.150050317.

[43] Alsfasser, R.; Ruf, M.; Trofimenko, S.; Vahrenkamp, H. *Chem. Ber.* **1993,** *126,* 703-710. 10.1002/cber.19931260322.

[44] Ruf, M.; Vahrenkamp, H. *Inorg. Chem.* **1996,** *35,* 6571-6578. 10.1021/ic960335a.

[45] Brombacher, H.; Vahrenkamp, H. *Inorg. Chem.* **2004,** *43,* 6042-6049. 10.1021/ic049179v.

[46] Kato, M.; Ito, T. *Inorg. Chem.* **1985,** *24,* 504-508 (10.1021/ic00198a015) and 509-514. (10.1021/ic00198a016).

[47] Zhou, H.; Campbell, E. J.; Nguyen, S. T. *Org. Lett.* **2001,** *3,* 2229-2231. 10.1021/ol0161110. McGuinness, D. S.; Gibson, V. C.; Steed, J. W. *Organometallics* **2004,** *23,* 6288-6292. 10.1021/om049246t.

[48] Mungur, S. A.; Blake, A. J.; Wilson, C.; McMaster, J.; Arnold, P. L. *Organometallics* **2006,** *25,* 1861-1867. 10.1021/om0508839.

[49] Jones, N. A.; Liddle, S. T.; Wilson, C.; Arnold, P. L. *Organometallics* **2007,** *26,* 755-757. 10.1021/om060486d.

[50] Lorber, C.; Vendier, L. *Organometallics* **2008,** *27,* 2774-2783. 10.1021/om800121g. Lorber, C.; Vendier, L. *Dalton Trans.* **2009,** 6972-6984. 10.1039/b905056f. Li, J.; Schulzke, C.; Merkel, S.; Roesky, H. W.; Samuel, P. P.; Döring, A.; Stalke, D. *Z. Anorg. Allg. Chem.* **2010,** *636,* 511-514. 10.1002/zaac.200900486.

[51] Downing, S. P.; Danopoulos, A. A. *Organometallics* **2006,** *25,* 1337-1340. 10.1021/om051017s. Downing, S. P.; Guadaño, S. C.; Pugh, D.; Danopoulos, A. A.;

Bellabarba, R. M.; Hanton, M.; Smith, D.; Tooze, R. P. *Organometallics* **2007,** *26,* 3762-3770. 10.1021/om700269u.

[52] Zhang, D.; Liu, N. *Organometallics* **2009,** *28,* 499-505. 10.1021/om800717h.

[53] Williams, C.; Kember, M.; Buchard, A.; Jutz, F. Method of Synthesising Polycarbonates in the Presence of a Bimetallic Catalyst and a Chain Transfer Agent. International Patent WO2013/034750 A2. 14 March 2013.

[54] Edworthy, I. S.; Blake, A. J.; Wilson, C.; Arnold, P. L. *Organometallics* **2007,** *26,* 3684-3689 10.1021/om0701874.

[55] Arnold, P. L.; Edworthy, I. S.; Carmichael, C. D.; Blake, A. J.; Wilson, C. *Dalton Trans.* **2008,** 3739-3746 10.1039/b803253j.

[56] Douthwaite, R. E.; Houghton, J.; Kariuki, B. M. *Chem. Commun.* **2004,** 698-699. 10.1039/b314814a.

[57] Houghton, J.; Dyson, G.; Douthwaite, R. E.; Whitwood, A. C.; Kariuki, B. M. *Dalton Trans.* **2007,** 3065-3073 10.1039/b703248j.

[58] Fernández Perandones, B. Laboratory Notebook, **2009**.

[59] Ashley, J. M.; Farnaby, J. H.; Hazari, N.; Kim, K. E.; Luzik Jr., E. D.; Meehan, R. E.; Meyer, E. B.; Schley, N. D.; Schmeier, T. J.; Tailor, A. N. *Inorg. Chim. Acta* **2012,** *380,* 399-410. 10.1016/j.ica.2011.11.034.

[60] Wu, J.; Dai, W.; Farnaby, J. H.; Hazari, N.; Le Roy, J. J.; Mereacre, V.; Murugesu, M.; Powell, A. K.; Takase, M. K. *Dalton Trans.* **2013,** *42,* 7404-7413. 10.1039/c3dt32551b.

[61] Liu, Q.-X.; Yu, J.; Zhao, X.-J.; Liu, S.-W.; Yang, X.-Q.; Li, K.-Y.; Wang, X.-G. *CrystEngComm* **2011,** *13,* 4086-4096. 10.1039/c1ce05134b.

CHAPTER 4. GENERAL CONCLUSIONS

4.1. Impact of the present research in a broader context

The main aim of the present work was the synthesis and identification of metal complexes for the polymerisation of renewable monomers. The utilisation of waste and resources other than fossil fuels for the creation of useful materials has become a promising area of study not only because of its importance to governments and industry, but also because of the variety of products, the processes to make them, and the methodologies followed by such processes. We focused our efforts on the ring-opening polymerisation methodology which yielded partial success and a large amount of new knowledge. For instance, we identified the soft metal complex $(CuL)_2$, **6**, capable of performing the single-site polymerisation of *rac*-lactide and ε-caprolactone under mild conditions with quantitative yield. The same compound was also tested as catalyst for the copolymerisation of CHO and CO_2 with no monomer conversion. On the other hand, a complex of a harder metal (Ti^{III}), **11**, with the same ligand was not effective for the polymerisation of esters but preliminary results show that it can copolymerise epoxides and CO_2, albeit in poor yield. We also studied the reactivity of $\{Co(L^{Ph})_2\}_2$, **LX**, a five-coordinated cobalt(II) complex, in the presence of CO_2 and diverse coordinating molecules. This complex was relatively successful in the copolymerisation of CHO and CO_2, granting mixtures of polymers with reasonable number-average molecular weights but in wide distributions.

From the results obtained, it is clear that the polymer quality and the rates of conversion into polycarbonate using the studied complexes are nowhere near the efficiency of other systems such as Williams's macrocycles, Darensbourg's salen complexes and Coates's β-diiminates; however, our complexes based on carbenes and phosphine oxides have room for improvement and, thus, the potential of becoming more effective catalysts:

a) **LX**, **6** and **11**, were the first from our library of active catalysts to be tested for this system at high pressures. For instance, **LX** did not show activity for pressures of 1 and 8 bar, but was successful for the formation of polycyclohexene carbonate under 50 bar of CO_2. The obtained results are very useful for the future design of new metal complexes or of adaptations to the existing ones in order to create more competitive catalysts.
b) All the catalysts tested had bidentate ligands, which provide structure, but lack rigidity. The use of metal complexes of tridentate ligands, such as $ZnHL^{CNC}Br_2$ **12**, would be a suitable test as catalysts for the formation of polycarbonate, for the assessment of a rigid structure against a more flexible one.

c) The successful catalysts used contained metals which are not regarded as active for the copolymerisation of epoxides with CO_2 (no known examples of Ti^{III} catalysts and just a few Co^{II} complexes have been reported). Future work should focus on experiments using zinc(II) and cobalt(III) complexes to assess the true potential of complexes of NHC and phosphine oxide.

Currently, our laboratory does not have a high-pressure reactor, but collaborations with other research groups allows the opportunity to test our complexes in an already proven set up, providing good comparisons with other literature reported systems. On the other hand, when using other laboratories, we need to adapt our complexes to the experiment conditions set in said laboratories. For instance, when testing our catalysts using the reactors in the Williams's group at Imperial College London, the procedure required that the catalysts were soluble in CHO but we had to add THF to the reaction mixture, changing the conditions away from standard. Adding substituents to the ligands would change the solubility of the complex in future experiments using the same reactors.

Recently, the Edinburgh and St Andrews School of Chemistry inaugurated the Joseph Black Laboratory for Carbon Dioxide Chemistry for the study of capture, storage and utilisation of CO_2 in an interdisciplinary environment. The advances and conclusions from the present investigation are the starting point of the research carried out at the Laboratory. There is also a contribution to the regional academic, industrial, and political fields because the Laboratory is part of the Scottish Centre for Carbon Capture and Storage which is very active in the development of technologies and policies concerning CO_2.

Furthermore, the preparation of PLA and PCL by **6** is important given that, to our knowledge, it is the first example of a copper(I) complex as catalyst of polymerisations of renewable monomers. Cu^{I} has been extensively used for the Huisgen coupling of azides and alkynes in "click chemistry" procedures, even for the formation of block copolymers,[1] but not as an initiator for the polymerisation of esters.

Finally, the expertise of the Arnold group in the synthesis and reactivity of phosphine oxides and *N*-heterocyclic carbenes could be utilised for the development of organocatalysts for the copolymerisation of epoxides and CO_2 based on the reports of Lu and Kakuchi for the formation of cyclic carbonates from CO_2,[2] and the polymerisation of the former,[3] as depicted in Scheme 4.1.

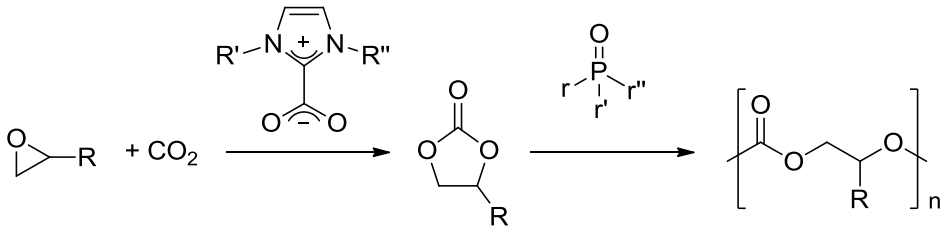

Scheme 4.1. Proposed formation of polycarbonates from epoxides and CO_2 using organocatalysts

4.2. Characteristics of the new compounds and their reactivity

The syntheses of compounds HL^{Ph}, **1**, and H_2LBr, **2**, were based on previous reports by Buffet[4] and Arnold,[5] with the crystallisation of two polymorphs of **1** as an interesting highlight. Compounds $Co(L^{tBu})_2$ (**3**), and (*E*)-3,3-dimethyl-1-diphenylphosphinoylbut-1-ene (**4**), were synthesised following the same procedure but with different metals and analogous ligands. Compound **3** fits nicely in the series of homoleptic complexes of divalent metals first reported by Buffet (see Table 2.2).[4] Compound **4** was first identified by NMR studies as a zinc complex analogous to **LX**; from integration of ^1H NMR spectra, the missing proton resonance was thought as hidden among the resonances of the original proligand in the crude. Compound **4**, thought as a zinc complex, was then tested as a catalyst for the ring-opening polymerisation of *rac*-lactide and the copolymerisation of propylene oxide and carbon dioxide with obvious inactivity. Later, **4** was correctly identified from single-crystal X-ray diffraction as an alkene. Compound **6** was firstly synthesised from **2**, CuI and $LiN(SiMe_3)_2$ resulting in a mixture of compounds. KL, **5**, was then prepared as starting material for the rest of the reported compounds. The reactivity of **5**, **6**, ZnL_2 (**10**) and **11** towards CO_2 is noticed immediately with a precipitate; unfortunately, only derivatives from compounds **6** and **10** were identified (compounds **7** and **16**, respectively, see Scheme 4.2). Structural characterisation of **7** and **16** would reinforce the belief that Cu^I is soft enough to insert CO_2 into its alkoxide bond and Zn^{II} is hard enough to favour the formation of imidazolium carbonate. Compound **9** also follows this trend for Cu^I. However, the insertion of silicon-based ligands into both complexes produces counterintuitive hard/soft acid/base interactions: in the formation of compound **8**, trimethylsilyl is bound to the imidazolium carbon whilst the copper centre binds to the alkoxide motif of the ligand; and in the molecular structure of compound **15** the zinc centre is bound to the carbene, leaving the alcohol tether free (see Figure 4.1).

Experiments with the tridentate CNC ligand and zinc produced compound **12**, which in turn was treated with CO_2 at ambient pressure. The formation of an asymmetric complex was identified as the insertion of CO_2 into the carbene–metal bond resulting in **13**. Decomposition of **12** gave place to the structurally-characterised proligand **14** which differs

from the starting material in the loss of an HBr equivalent (See Section 3.5). Because of the similarity in the ionic radii of divalent Mg and Zn, it would be interesting to synthesise complexes using the tridentate ligand of **XXIV** and **XXV**,[6] to compare structural features and the amino/amido interaction of the nitrogen atom with the metal centre. As stated before, we found it very difficult to synthesise the tridentate proligand **CXXIII** in high yield. Fortunately, recent reports show the preparation of a very similar ligand using a protecting group to prevent oligomerisation of the amino group, and carrying out the reflux reaction in dioxane.[7] The utilisation of **CXXIII** is also interesting for the potential formation of cobalt(II) complexes which could then be oxidised without the need for additional ligands. As mentioned earlier, cobalt(III) complexes are well known catalysts for the copolymerisation of epoxides and CO_2.

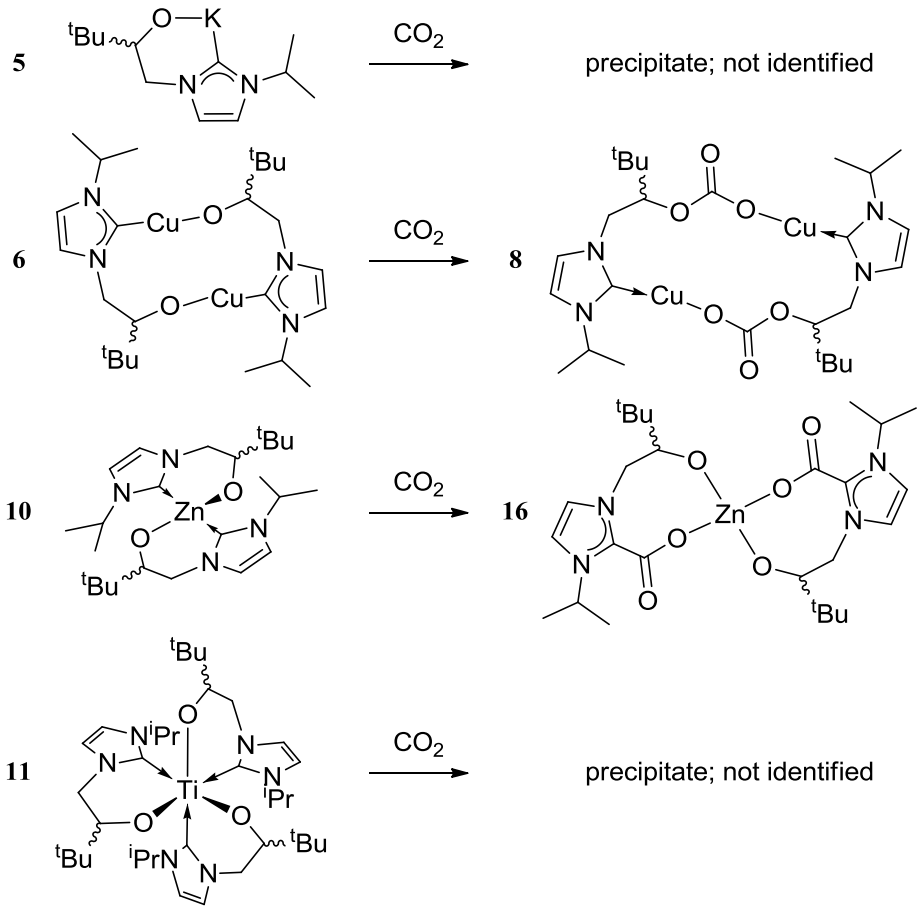

Scheme 4.2. Reactivity of NHC metal complexes with CO_2

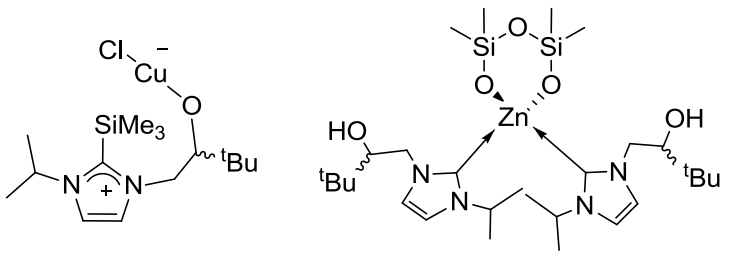

8 **15**

Figure 4.1. Metal complexes 8 and 15

Finally, it is notable that these polymerisation catalysts were derived from asymmetric ligands containing chiral centres; whilst we have not explored the effect of asymmetry in this work, it is expected to affect the tacticity of the resulting polymers. A detailed analysis on this issue should be a priority for the future development of more active and selective catalysts and to measure the overall efficiency of the metal complexes studied as initiators of polymerisations.

4.3. References

[1] Vora, A.; Singh, K.; Webster, D. C. *Polymer* **2009,** *50,* 2768-2774. 10.1016/j.polymer.2009.03.054

[2] Zhou, H.; Zhang, W.-Z.; Liu, C.-H.; Qu, J.-P.; Lu, X.-B. *J. Org. Chem.* **2008,** *73,* 8039-8044. 10.1021/jo801457r.

[3] Makiguchi, K.; Ogasawara, Y.; Kikuchi, S.; Satoh, T.; Kakuchi, T. *Macromolecules* **2013,** *46,* 1772-1782. 10.1021/ma4000495.

[4] Buffet, J.-C., PhD Thesis, The University of Edinburgh, UK (Edinburgh), **2009**.

[5] Arnold, P. L.; Rodden, M.; Davis, K. M.; Scarisbrick, A. C.; Blake, A. J.; Wilson, C. *Chem. Commun.* **2004,** 1612-1613. 10.1039/B404614E.

[6] Arnold, P. L.; Edworthy, I. S.; Carmichael, C. D.; Blake, A. J.; Wilson, C. *Dalton Trans.* **2008,** 3739-3746 10.1039/b803253j.

[7] Blakemore, J. D.; Chalkley, M. J.; Farnaby, J. H.; Guard, L. M.; Hazari, N.; Incarvito, C. D.; Luzik, Jr.; E. D.; Suh, H. W. *Organometallics* **2011,** *30,* 1818-1829. 10.1021/om100890q.

CHAPTER 5. EXPERIMENTAL PROCEDURES

5.1. Instrumentation and reagents

All manipulations were carried out using standard Schlenk techniques, or a Vacuum Atmospheres Omni-Lab double glovebox, under an atmosphere of dry dinitrogen. Hexane, toluene, dichloromethane (DCM), and tetrahydrofuran (THF) were dried by passage through activated alumina towers and degassed before use. Solvent 1,2-dimethoxyethane (DME) was distilled from potassium under an atmosphere of dry nitrogen. All solvents were stored over potassium mirrors (with the exception of THF and DME which were stored over activated 4 Å molecular sieves). Deuterated solvents were distilled from potassium, degassed by three freeze-pump-thaw cycles and stored under nitrogen.

Lithium bis(trimethylsilyl)amide, $LiN(SiMe_3)_2$, purchased from Sigma Aldrich, was sublimed prior to use. Zinc chloride was dried using trimethylsilyl chloride (TMSCl) and stored under nitrogen. The epoxide 3,3-dimethyl-epoxybutane, purchased from Alfa Aesar was used as received. Cyclic *rac*-lactide was purchased from Alfa Aesar, recrystallised from hot toluene, washed with diethyl ether, and sublimed (10^{-4} torr, 110 °C) prior to use. The starting materials: 1*N*-isopropyl-2*N*-(2-hydroxy-3,3-dimethylbutane) imidazolium iodide (**LXIII**),[1] HL^{tBu} (**X**),[2] $Co\{N(SiMe_3)_2\}_2{\cdot}(THF)_2$,[3] $Zn\{N(SiMe_3)_2\}_2$,[4] $Y\{N(SiMe_3)_2\}_3$,[5] $TiCl_3(THF)_3$,[6] $Zn(L^{tBu})_2$ (**LVIII**),[7] $Sn(L^{tBu})_2$ (**XI**),[11] and $\{Co(L^{Ph})_2\}_2$ (**LX**)[11] were synthesised according to literature procedures.

5.1.1. NMR spectroscopy

NMR spectra (^1H and ^{31}P) were recorded at 298 K on a Bruker AVA400 spectrometer, operating frequencies at 399.9 MHz (^1H), 155.518 (^{29}Si) and 161.9 (^{31}P); $^{13}C\{^1H\}$ NMR spectra were recorded on a Bruker AVA500 operating at 125.76 MHz. Chemical shifts are quoted in parts per million (ppm) and are relative to external $SiMe_4$ or H_3PO_4.

5.1.2. Mass spectrometry

Mass spectra were recorded by Dr. Logan McKay at the University of Edinburgh SIRCAMS facility.

5.1.3. Infrared spectroscopy

Infrared spectra were recorded on a Jasco 410 spectrophotometer using Nujol mull as dispersing agent.

5.1.4. Elemental analyses

Elemental analyses were carried out by Mr Stephen Boyer at London Metropolitan University.

5.1.5. Gel Permeation Chromatography

Gel permeation chromatography was performed on a Malvern Instruments Viscotek 270 GPC Max triple detection system (refractive index, viscometer and light scattering) with 2 × mixed bed styrene/DVB columns (300 × 7.5 mm). GPC analyses were carried out in HPLC-grade THF at a flow rate of 1 mL/min, at 35 ˚C. Absolute molecular weights were obtained using dn/dc values of 0.051 mL/g for poly(lactic acid),[8] 0.079 mL/g for polycaprolactone,[8] and 0.1855 mL/g for polycarbonate.[9] Samples were prepared weighing out 20 mg of the polymer before dissolving it in HPLC-grade THF overnight. The solution was filtered through a 0.2-micron filter before it was injected into the chromatograph.

5.2. Syntheses and reactions of organic ligands and other precursors

5.2.1. Preparation of $(Ph)_2P(O)CH_2CH(^tBu)OH$, HL^{Ph} (1)

Due to the clear indication of impurities in this starting material, chlorodiphenylphosphine was distilled at 160 °C and low pressure.[10] A solution of 5 g (45.3 mmol, 220.638 g/mol) of the colourless compound in 30 mL THF was mixed with 2.58 g of $LiAlH_4$ (68.0 mmol, 37.955 g/mol) in 30 mL THF at 0 °C to form a pale-yellow solution containing Ph_2PH after 12 h and filtration. 34 mL of ^nBuLi (1.6M, 64.056 g/mol) were added dropwise to the solution changing its colour to bright orange before 6.97 mL of 3,3-dimethyl-1,2-epoxybutane (54.4 mmol, 100.160 g/mol) were added to the mixture. Finally, 10.3 mL of H_2O_2 (30% w/m, 34.014 g/mol) were added to oxidise the phosphine and to form the alcohol. 3,3-dimethyl-1-(diphenyl phosphinoyl)-butan-2-ol, **1,** was obtained out of crystallisation in toluene. 6.5 g of ligand were isolated (47% overall yield)

^{1}H-NMR δ(400 MHz, $CDCl_3$): 7.7-7.4 (m, 10H, aromatics), 4.38 (s, 1H, OH), 3.6 (t, 1H, CH), 2.3 (m, 2H, CH_2), 0.8(s, 9H, $(–CH_3)_3$) ppm. ^{1}H-NMR δ(400 MHz, C_6D_6): 7.77-7.57, 7.07-6.95 (m, 10H, aromatics), 5.26 (s, 1H, OH), 3.84 (dd, J=3.2, 9.0, 1H, CH), 2.23 (m, 2H, CH_2), 0.92 (s, 9H, $(–CH_3)_3$) ppm.^{13}C{H}-NMR δ(125.76 MHz, $CDCl_3$): 130.5 (aromatics), 74.2 (C–OH), 35.2 (CMe_3), 30.8 (CH_2), 25.5 (CH_3) ppm. ^{31}P-NMR δ(161.9 MHz, $CDCl_3$): 36.7 ppm. ^{31}P NMR (C_6D_6): 33.82 ppm. IR data (Nujol): 3136 (s, OH), 1150 (m, P=O) cm^{-1}.

5.2.2. Synthesis of 3*N*-*iso*-propyl-1*N*-(2-hydroxy-3,3-dimethylbutane) imidazolium bromide, H_2LBr (2)

A high-pressure glass ampoule filled with 6.8 g of imidazole (100 mmol) and 10 g of 3,3-dimethyl-1,2- epoxybutane (100 mmol) was heated overnight at 50° C forming a melt after 6 hrs. Acetonitrile (20 mL) was added to the ampoule and the mixture heated and stirred for dissolution before 12.3 g of 2-bromo propane (100 mmol) were added. Temperature was raised to 80° C and kept for 4 hrs. The solvent was evaporated and the white product was purified by recrystallisation from a 1:1 mixture of acetone and ethyl acetate. Yield: 70%.

^{1}H-NMR δ(400 MHz, $CDCl_3$): 10.04 (s, 1H, NC*H*N), 7.40 (s,1H, C*H*CH), 7.32 (s, 1H, CHC*H*), 4.73 (sept, 1H, C*H*($C(CH_3)_3$), J=6.6Hz), 4.36 (s, 1H, C*H*(OH)), 4.34 (d, 1H, NC*H*H, $^2J_{HH}$=5.2Hz), 3.64 (dd, 1H, NCH*H*, $^2J_{HH}$=4.2Hz, $^3J_{HH}$=4.4Hz), 1.62 (d, 6H, CH(CH_3)$_2$, J=6.7Hz), 1.01 (s, 9H, C(CH_3)$_3$) ppm. ^{13}C{H}-NMR δ(125.76 MHz, $CDCl_3$): 135.6 (NCN), 122.8 (N*C*CN), 119.3 (NC*C*N), 78.2 (CH_2), 52.3 (*C*H(CH_3)$_2$), 49.7 (CH(O)), 25.8 ($C(CH_3)_3$), 22.8 (CH(*C*H_3)$_2$) ppm.

5.3. Syntheses and reactions of metal complexes with alkoxide/phosphine oxide ligands

5.3.1. Synthesis of $Co(L^{tBu})_2$ (3)

A 10 mL THF solution of 125 mg of **X** (0.48 mmol, 262.371 g/mol) was added to an ampoule filled with 90.5 mg of $Co\{N(SiMe_3)_2\}_2 \cdot (THF)_2$ (0.24 mmol, 379.707 g/mol) in 10 mL of THF. The solution turned purple upon addition and was stirred and heated at 70° C for 16 h. After, the solvent and $HN(SiMe_3)_2$ were removed under vacuum at 65° C for 4 h. Remaining ligand was separated by sublimation and the pure compound crystallised in hexane at -30° C. The compound is purple in solution and green in the solid state. 100 mg of **3** recovered (71% yield).

^{1}H-NMR δ(400 MHz, C_6D_6) prominent paramagnetic resonances: 27.9, -5.2, -9.3 ppm.

5.3.2. Synthesis of (*E*)-3,3-dimethyl-1-diphenylphosphinoylbut-1-ene (4)

A 15 mL toluene solution of 3 g of **1** (9.92 mmol, 302.352 g/mol) was added to an ampoule filled with 1.9 g of $Zn\{N(SiMe_3)_2\}_2$ (4.96 mmol, 386.16 g/mol) in 15 mL of toluene. The colourless solution was stirred and heated at 70° C for 16 h with the formation of a white precipitate. After filtration, the solvent and $HN(SiMe_3)_2$, formed by the decomposition of the zinc base, were removed under vacuum at 65° C for 4 h. Pure **4** was recovered from recrystallisation from ethyl acetate/hexanes solution in a 1:1 mixture. 1.45 g of **4** recovered (51% yield).

^{1}H-NMR δ(500 MHz, $CDCl_3$): 7.75-7.63, 7.55-7.38 (aromatic, 10H), 6.76 (dd, $^3J_{HH}$=17.3, $^2J_{HP}$=20.5Hz, 1H), 6.11 (dd, $^3J_{HH}$=17.3, $^3J_{HP}$=24.5Hz, 1H), 1.10 (s, 9H) ppm. ^{13}C{H}-NMR δ(125.76 MHz, $CDCl_3$): 162.5, 133.5 (J_{CP}=102.2Hz), 131.8, 131.5 (J_{CP}=9.7Hz), 128.6 (J_{CP}=12.1Hz), 127.8 (J_{CP}=13.3Hz), 116.6 (J_{CP}=104.1Hz), 35.4 (J_{CP}=14.7Hz), 28.8, 25.5 ppm. m.p. 156-157° C.

5.4. Synthetic procedures concerning metal complexes with alkoxide/phosphine oxide ligands

5.4.1. Attempted reactions of alkoxide/phosphine oxide metal complexes and carbon dioxide

In a typical reaction 30 mg of $Sn(L^{tBu})_2$ (**XI**),[11] **3** or $\{Co(L^{Ph})_2\}_2$ (**LX**)[11] in a 1.5 mL C_6D_6 solution were placed in a Young's tap NMR tube. The tube was subjected to three freeze-degas-thaw cycles to remove all nitrogen and, subsequently, carbon dioxide was let into the tube at 1 or 1.5 bar. The solution was left at room temperature with occasional shaking or heated to a set temperature for a particular time. Specific reaction conditions and results are summarised in Section 2.4.1.

5.4.2. Attempted copolymerisations of epoxides and carbon dioxide with alkoxide/phosphine oxide metal complexes

Compound **LX** was tested as a catalyst for the copolymerisation of carbon dioxide and propylene oxide or cyclohexene oxide. Reaction conditions in these attempts varied widely in terms of catalyst load ratio, solvents, temperature, time of reaction and pressures. The specific data is found in Table 5.1 and Table 5.2.

a. Typical reaction at 1 bar: An appropriate solution of **LX** and the epoxide was placed into a high-pressure ampoule before it was subjected to three freeze-degas-thaw cycles to remove all nitrogen. Then, 1 bar of CO_2 was added to the ampoule and the mixture stirred at a set temperature and for the applicable amount of time. Once the reaction was deemed complete, carbon dioxide was let escape through a mercury bubbler with the addition of nitrogen. A small aliquot of the crude solution was taken with pipette to study the conversion of the epoxide into the copolymer using ^{1}H and ^{13}C NMR spectroscopy. All reactions at this pressure were unsuccessful.

b. Typical reaction at 8 bar: A 30 mL Büchi mini-clave reactor with an oven-dried glass round-bottom flask equipped with a stirring bar is placed under vacuum for 1 h. An image of the reactor is in Figure 5.1. For Entry **v** in Table 5.2, after filling it with nitrogen at ambient pressure, an appropriate solution of **LX** and cyclohexene oxide (CHO) was added into it *via* cannula. The reaction vessel was degassed three times. For Entry **viii** in Table 5.2, the reactor was filled with CO_2 at ambient pressure and an appropriate solution of **LX** and CHO was added into it *via* cannula also under CO_2 atmosphere. For both experiments, a pressure of 8 bar of CO_2 was added to the reactor whilst stirring and heating. The pressure increased to 9.5 bar in the first hour of reaction and stayed at about 9 bar for the remaining of the

procedure. At the end of the reaction, CO_2 was gently let out and an aliquot was retrieved for ^{1}H and ^{13}C NMR spectroscopy studies. Both reactions at this pressure were unsuccessful.

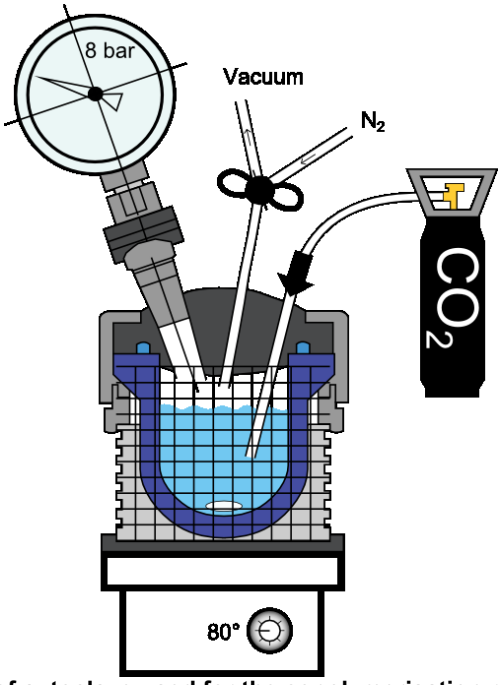

Figure 5.1. Arrangement of autoclave used for the copolymerisation reactions of epoxides with CO_2 at 8 bar

c. Typical reaction at 50 bar: These reactions were attempted in the Williams Laboratory at Imperial College London, where a reactor is set for procedures at up to 50 bar of carbon dioxide (Figure 5.2). The set of conditions described have been reported for other catalysts.[12] A 100-mL Parr reaction vessel, equipped with a motorised 4-fold-bladed impeller for stirring, was placed in an oven at 140° C overnight, after which it was subject to vacuum for 3 h. The vessel was subjected to a pressure of 50 bar of CO_2 to check for leaks and then a continuous flow of the gas went through it for the next step. The flow of CO2, before reaching the Parr reaction vessel, passes through a set of adsorptive materials manufactured by Valco Instruments Co. Inc. (VICI). A solution of 394 mg of **LX** (0.3 mmol, 1323.241 g/mol), and 172 mg of PPNCl (0.3 mmol, 574.03 g/mol) for Entry **vii** in Table 5.2, in 15 mL of CHO was formed under CO_2 atmosphere and transferred using a syringe to the Parr reactor. Whilst stirring, the temperature of reaction was increased to 80° C and the pressure of CO_2 to 50 bar. After 20 minutes, the pressure, which had dropped due to CO_2 solubility in CHO, was taken to 50 bar again and the reaction continued for 24 h. At the end, an aliquot was taken to study the conversion of the epoxide into the copolymer using ^{1}H and ^{13}C NMR spectroscopy. The remaining solution was transferred to a vial washing with DCM. The crude solution had its solvent evaporated and remaining CHO evaporated under low pressure overnight. Both reactions at this pressure were successful.

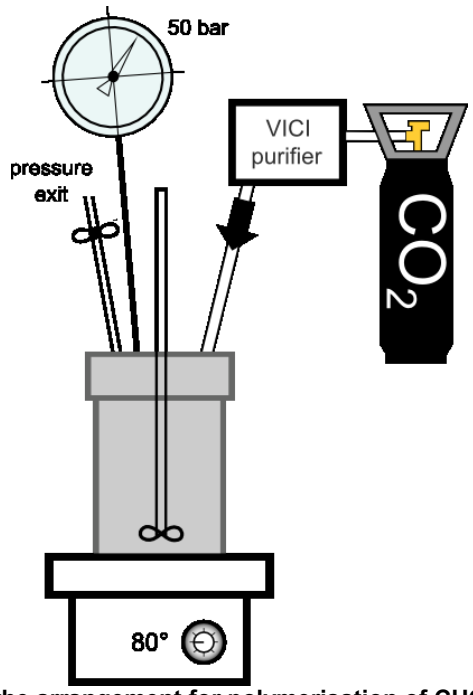

Figure 5.2. Schematic of the arrangement for polymerisation of CHO and CO_2 at 50 bar in the Williams laboratory at Imperial College London

The summary of the conditions and results of the coupling of propylene oxide (PO) and cyclohexene oxide (CHO) with CO_2 in the presence of **LX** is found in Table 5.1 and Table 5.2.

Table 5.1. Reaction conditions for the copolymerisation of PO and CO_2 using LX as catalyst

Entry	LX (mg)	PO (g)	CO_2 (bar)	Molar ratio cat:epox:solv	Solvent	Temp. (°C)	Time (h)
i	30	1.3	1	1:1000:500	C_6D_6	70	16
ii	30	1.3	1	1:1000:3000	THF	70	16
iii	200	8.8	1	1:1000:400	THF	40	16

All reactions were unsuccessful for the conversion of PO

Table 5.2. Reaction conditions for the copolymerisation of CHO and CO_2 using LX as catalyst

Entry	LX (mg)	CHO (g)	CO_2 (bar)	Molar ratio cat:epox:solv[a]	Solv[a]	Temp (°C)	TOF (h^{-1})[b]	M_n /1000[c]	PDI[c]
iv[d]	50	0.3	1	1:80:500	DCM	85	-	-	-
v[d]	100	0.6	8	1:80:500	DCM	60	-	-	-
vi[e]	397	14.55	50	1:500:0	-	80	2.5	39	2.8
vii[e]	397	14.55	50	1:500:1	PPNCl	80	3.5	37	2.8
viii[e]	100	1.48	8	1:200:0	-	80	-	-	-

a Solvent in entry **vii** is in fact a cocatalyst: PPNCl. **b** Because the catalyst was not recovered at the end of the reaction, the turnover frequency is the molar ratio monomer/catalyst for a conversion of

100% per hour. **c** Measured using GPC with a polystyrene standard and a dn/dc of 0.1855 mL/g. Polydispersity index, from the weight average molecular weight-to-number average molecular weight ratio. **d** Time of reaction: 16 h. **e** Time of reaction: 24 h.

5.4.3. Attempted oxidation of LX into a cobalt(III) species

a. Using $AgBF_4$: A high-pressure ampoule was filled with a 5 mL solution of 100 mg of **LX** (151 µmol, 661.620 g/mol) in THF. Whilst stirring at room temperature, a 5 mL solution of 45.7 mg of **1** (151 µmol, 302.352 g/mol) in THF was added to the purple solution before a 5 mL suspension of 29.4 mg of $AgBF_4$ (151 µmol, 194.673 g/mol) in THF was finally added. There was no apparent change in the suspension and the reaction mixture was heated at 60° C for 16 h with stirring. Although a gray mirror is observed at the bottom of the ampoule, the remaining solution was a mixture of compounds in the diamagnetic region of the ^{1}H NMR spectrum.

b. Using I_2: A Schlenk flask was charged with 100 mg of **LX** (151 µmol, 661.620 g/mol), 45.7 mg of **1** (151 µmol, 302.352 g/mol) and 19.0 mg of I_2 (75 µmol, 253.80 g/mol) in 15 mL of THF. The solution turned from purple to green upon addition and was stirred overnight. After evaporating the solvent under reduced pressure, the green solid was dissolved in the minimum amount of toluene, but it did not crystallise out. The ^{1}H NMR spectrum in C_6D_6 shows diamagnetic resonances for the proligand **1** and paramagnetic resonances from 80 to -70 ppm.

5.5. Syntheses and reactions of metal complexes with NHC

5.5.1. Synthesis of KL (5)

In a Schlenk flask 16.5 g of H_2LI (48.8 mmol, 338.228 g/mol) were mixed with 50 mL of THF whilst stirring vigorously. The suspension was cooled down to -78° C. A 30 mL suspension of 6 g of KH (146.4 mmol, 40.1062 g/mol) in THF was added dropwise to the Schlenk flask over 10 min. Evolution of H_2 was noticeable. Stirring continued for 16 h whilst temperature rose to ambient conditions. Pure KL was obtained after precipitation using hexane as anti-solvent once the iodide salts had been discarded by filtration. 7.27 g recovered of 5 (yield: 60%).

^{1}H-NMR δ(500 MHz, pyr-d_5): 7.13 (s,1H, C*H*CH), 7.12 (s, 1H, CHC*H*), 4.61 (m, 1H, C*H*(C(CH_3)$_3$), J=6.8Hz), 4.24 (d, 1H, NCH*H*, J=12.1Hz) , 3.95 (d, 1H, NC*H*H, J=8.9Hz), 3.81 (dd, 1H, C*H*(O), $^3J_{HH}$=8.9Hz, $^3J_{HH}$=12.1Hz), 1.51 (dd, 6H, CH(CH_3)$_2$, $^2J_{HH}$=6.8Hz, $^3J_{HH}$=14.7Hz), 1.12 (s, 9H, C(CH_3)$_3$) ppm. ^{13}C{H}-NMR δ(125.76 MHz, pyr-d_5): 208.9 (N*C*N), 120.2 (*C*HCH), 116.9 (CH*C*H), 86.6 (CHO), 60.1 (*C*(CH_3)$_3$), 52.4 (N*C*H(CH_3)$_2$), 37.5 (NCH_2), 28.1 (C(*C*H_3)$_3$), 25.1 (NCH(*C*H_3)(CH_3)), 24.8 (NCH(CH_3)(*C*H_3)) ppm.

5.5.2. Synthesis of $(CuL)_2$ (6)

In a high-pressure ampoule 1 g of CuI (5.2 mmol, 190.450 g/mol) were mixed with 15 mL of THF whilst stirring vigorously. A 10 mL suspension of 1.3 g of KL (5.2 mmol, 248.406 g/mol) in THF was added to the ampoule. Stirring continued for 16 h after the temperature was increased to 70° C. Pure $(CuL)_2$ is obtained after precipitation using hexane as anti-solvent once the iodide salts had been discarded by filtration. 851 mg recovered of **6** (yield: 60%).

^{1}H-NMR δ(500 MHz, pyr-d_5): 7.26 (s,1H, C*H*CH), 7.23 (s, 1H, CHC*H*), 4.58 (s, 1H, C*H*(C(CH_3)$_3$)), 4.33 (s, 2H, NCH_2), 3.96 (s, 1H, C*H*(O)), 1.31 (s, 6H, CH(CH_3)$_2$), 1.26 (s, 9H, C(CH_3)$_3$) ppm. ^{13}C{H}-NMR δ(125.76 MHz, pyr-d_5): 171.3 (N*C*N), 120.7 (*C*HCH), 118.3 (CHC*H*), 83.7 (*C*HO), 59.4 (N*C*H_2), 53.3 (N*C*H(CH_3)$_2$), 36.1 (*C*(CH_3)$_3$), 27.2 (C(*C*H_3)$_3$), 24.1 (NCH(*C*H_3)(CH_3)), 24.0 (NCH(CH_3)(*C*H_3)) ppm. Anal. Calcd for $C_{24}H_{42}Cu_2N_4O2$: C 52.82, H 7.76, N 10.27. Found: C 52.62, H 7.65, N 10.13. IR data (Nujol in cm^{-1}): 1561m, 1419s, 1282s, 1136s (C–O), 682m, 541m.

5.5.3. Synthesis of $(CuLCO_2)_2$ (7)

In a high-pressure ampoule 200 mg of $(CuL)_2$ (0.37 mmol, 545.708 g/mol) were dissolved in 10 mL of THF. After performing three freeze-degas-thaw cycles, 1.5 bar of CO_2 at room temperature were added to the ampoule. Stirring continued for 16 h with the formation of a light yellow precipitate; the ampoule was replenished with CO_2 to the same

pressure for the stirring to continue for another 16 h. Pure $(CuLCO_2)_2$ was obtained after washing several times with THF. 131 mg recovered of **7** (yield: 56%).

^{1}H-NMR δ(500 MHz, pyr-d_5): 7.45 (s,1H, C*H*CH), 7.17 (s, 1H, CHC*H*), 4.80 (s, 1H, C*H*$(CH_3)_2$), 4.43 (s, 2H, NC*H*$_2$), 4.37 (s, 1H, C*H*(O)), 1.33 (s, 6H, CH(C*H*$_3)_2$), 1.17 (s, 9H, C(C*H*$_3)_3$) ppm. ^{13}C{H}-NMR δ(125.76 MHz, pyr-d_5): 164.0 (N*C*N), 156.7 (O*C*O$_2$), 122.5 (*C*HCH), 117.1 (CH*C*H), 83.7 (*C*HO), 54.8 (N*C*H$_2$), 53.6 (N*C*H$(CH_3)_2$), 35.5 (*C*$(CH_3)_3$), 27.1 (C(*C*H$_3)_3$), 24.1 (NCH(*C*H$_3)_2$) ppm. Anal. Calcd for $C_{26}H_{42}Cu_2N_4O_6$: C 49.28, H 6.68, N 8.84. Found: C 49.40, H 6.72, N 8.78. IR data (Nujol in cm^{-1}): 1682b (CO_2), 1561m, 1423s, 1414s, 1371s, 1346s, 1291s 1125s (C–O) 1071s, 1043s 982s, 880m, 684m, 622m.

5.5.4. Reaction of $(CuLCO_2)_2$ and Me_3SiCl to form $ClCuLSiMe_3$ (8)

In a Young's tap NMR tube, 10.3 mg of tetramethylsilyl chloride (TMSCl, 95 µmol, 1087.64 g/mol) were added to a suspension of 15 mg of **7** (24 µmol, 633.732 g/mol) in pyridine-d_5. Immediately, the suspension became a yellow solution that was characterised by NMR spectroscopy.

^{1}H-NMR δ(400 MHz, pyr-d_5): 7.27 (s,1H, C*H*CH), 7.23 (s, 1H, CHC*H*), 4.91 (m, 1H, C*H*$(CH_3)_2$, $^3J_{HH}$=6.4Hz), 4.41 (d, 1H, NC*H*H), 4.18 (dd, 1H, C*H*(O)), 3.98 (d, 1H, NCH*H*), 1.39 (t, 6H, CH(C*H*$_3)_2$), 0.97 (s, 9H, C(C*H*$_3)_3$), -0.02 (s, 9H, Si(C*H*$_3)_3$) ppm. ^{1}H-NMR δ(500 MHz, C_6D_6): 6.28 6.19 (d,2H, $^3J_{HH}$=1.5Hz, C*H*C*H*), 4.33 (m, 1H, $^3J_{HH}$=6.7Hz, C*H*$(CH_3)_2$), 3.98 (ddd, 1H, $^2J_{HH}$=24.3, $^3J_{HH}$=3.2Hz, $^3J_{HH}$=13.5Hz, NC*HH*), 3.34 (dd, 1H, $^3J_{HH}$=3.2, $^3J_{HH}$=13.5Hz, C*H*(O)), 1.00 (dd, 6H, $^2J_{HH}$=7.9, $^3J_{HH}$=6.7Hz, CH(C*H*$_3)_2$), 0.92 (s, 9H, C(C*H*$_3)_3$), -0.17 (s, 9H, Si(C*H*$_3)_3$) ppm. ^{13}C{H}-NMR δ(125.76 MHz, pyr-d_5): 178.7 (N*C*N), 123.4 (*C*HCH), 117.4 (CH*C*H), 81.9 (*C*HO), 54.8 (N*C*H$_2$), 53.9 (N*C*H$(CH_3)_2$), 35.5 (*C*$(CH_3)_3$), 26.9 (C(*C*H$_3)_3$), 24.2 (NCH(*C*H$_3$CH$_3$)), 24.1 (NCH(CH$_3$*C*H$_3$)), 1.0 (3*C*H$_3$) ppm. ^{13}C{H}-NMR δ(125.76 MHz, C_6D_6): 175.5 (N*C*N), 123.0 (*C*HCH), 116.2 (CH*C*H), 81.9 (*C*HO), 54.6 (N*C*H$_2$), 53.6 (N*C*H$(CH_3)_2$), 35.0 (*C*$(CH_3)_3$), 26.5 (C(*C*H$_3)_3$), 23.8 (NCH(*C*H$_3$CH$_3$)), 23.4 (NCH(CH$_3$*C*H$_3$)), 0.5 (3*C*H$_3$) ppm. ^{29}Si-NMR δ(155.518 MHz, pyr-d_5): 18.3 ppm.

An additional portion of 10 mg of TMSCl (95 µmol) was added to the tube. Only the resonances of TMSCl changed. Extra resonances in the NMR spectra (^{1}H-NMR: 0.15 ppm in pyr-d_5 and 0.10 ppm in C_6D_6; ^{13}C{H}-NMR: 2.5 ppm in pyr-d_5 and 2.1 ppm in C_6D_6) are identified as the product of the hydrolysis of TMSCl: hexamethyldisiloxane.

Control reaction: A solution of 20 mg of **6** (37 µmol, 545.714 g/mol) in 1.5 mL of pyridine-d_5 was placed in a Young's tap NMR tube. 15.9 mg of TMSCl (147 mmol) were added to the solution.

5.5.5. Synthesis of $(CuLCS_2)_2$ (9)

A Schlenk flask was filled with 199 mg of $(CuL)_2$, **6** (364 µmol, 545.714 g/mol), and 10 mL of toluene. Whilst swirling, 55.5 mg of CS_2 (729 µmol, 76.143 g/mol) were added to the orange solution generating immediately a dark brown precipitate. The suspension was kept stirring for 16 h and then filtered. The solid was washed with toluene and then dried under low pressure overnight. 158 mg recovered of **9** (yield: 62%).

^{1}H-NMR δ(500 MHz, C_6D_6): 7.07 (s,1H, C*H*CH), 6.61 (s,1H, C*H*CH), 5.87 (m, 1H, C*H*$(CH_3)_2$), 4.92 (s, 1H, C*H*(O)), 4.78 (s, 1H, NC*H*H), 4.10 (s, 1H, NCH*H*), 1.18 (d, 6H, CH(C*H*$_3)_2$), 1.01 (s, 9H, C(C*H*$_3)_3$) ppm. ^{1}H-NMR δ(500 MHz, pyr-d_5): 7.47 (s,1H, C*H*CH), 7.13 (s,1H, C*H*CH), 6.13 (s, 1H, C*H*(O)), 5.18 (m, 1H, C*H*$(CH_3)_2$), 5.03 (dd, $^2J_{HH}$=13.8Hz, 2H, NC*H*H), 5.03 (dd, $^2J_{HH}$=13.8Hz, $^3J_{HH}$=9.5Hz, 2H, NC*H*H), 1.39 (dd, J_{HH}=6.4Hz, J_{HH}=23.2Hz, 6H, CH(C*H*$_3)_2$), 1.11 (s, 9H, C(C*H*$_3)_3$) ppm. ^{13}C{H}-NMR δ(125.76 MHz, C_6D_6): 230.2 (CS_2), 182.2 (N*C*N), 122.4 (*C*HCH), 116.6 (CH*C*H), 90.7 (*C*HO), 53.1 (N*C*H$(CH_3)_2$), 51.9 (N*C*H_2), 35.7 (*C*$(CH_3)_3$), 26.7 (C(*C*$H_3)_3$), 24.2 23.9 (NCH(*C*$H_3)_2$) ppm. ^{13}C{H}-NMR δ(125.76 MHz, pyr-d_5): 230.8 (CS_2), 183.5 (N*C*N), 122.6 (*C*HCH), 116.5 (CH*C*H), 89.9 (*C*HO), 53.3 (N*C*H$(CH_3)_2$), 52.1 (N*C*H_2), 35.9 (*C*$(CH_3)_3$), 26.8 (C(*C*$H_3)_3$), 24.2 24.0 (NCH(*C*$H_3)_2$) ppm. Anal. Calcd for $C_{26}H_{42}Cu_2N_4O_2S_4$: C 44.74, H 6.07, N 8.03. Found: C 44.57, H 5.96, N 7.94.

5.5.6. Synthesis of $Zn(L)_2$ (10)

A 15-mL high-pressure ampoule was charged with 28.3 mg of $ZnCl_2$ (207 µmol, 136.30 g/mol) and 3 mL of THF; a 3 mL THF solution of 103 mg of **5** (415 µmol, 248.409 g/mol) were added to the ampoule whilst stirring. White precipitate appeared upon addition but the stirring continued for 16 h at 80° C. After filtering, the yellow solution was concentrated and left at -30° C for 5 days. Crystals suitable for single-crystal X-ray diffraction studies were isolated. No yield recorded.

^{1}H-NMR δ(500 MHz, pyr-d_5): 7.21 *7.17 7.10* 7.06 (s, 2H, NC*H*C*H*N), 5.45 *4.99* (m, 1H, C*H*$(CH_3)_2$), 4.70 *4.61* (t, 1H, C*H*(O)), 4.27 *4.11 3.79* 3.76 (d, 2H, NC*H*$_2$), *1.50* 1.40 (s, 6H, CH(C*H*$_3)_2$), *1.17* 1.14 (s, 9H, C(C*H*$_3)_3$) ppm. There are two frequency values corresponding to two sets of resonances in a 62/38 ratio; the minor resonances are in italics. ^{13}C{H}-NMR δ(125.76 MHz, pyr-d_5): *177.8* 177.7 (N*C*N), *123.3* 123.0 (*C*HCH), 116.3 *116.0* (CH*C*H), *84.5* 83.5 (*C*HO), 57.6 *56.9* (N*C*H_2), *52.8* 52.4 (N*C*H$(CH_3)_2$), *37.3* 37.1 (*C*$(CH_3)_3$), *27.7* 27.6 (C(*C*$H_3)_3$), 24.5 *23.2* (NCH(*C*$H_3)_2$) ppm.

5.5.7. Synthesis of $[Ti(L)_3]$ (11)

An ampoule was charged with 425 mg of $TiCl_3(THF)_3$ (1.38 mmol, 307.56 g/mol) and 10 mL of THF to form a turquoise solution; a 10 mL THF solution of 1 g of **5** (4.14 mmol, 248.409 g/mol) was added to the ampoule whilst stirring turning the suspension from yellow

to deep red. Stirring continued for 60 h at room temperature. After filtering, a pure compound was obtained from evaporating the solvent under reduced pressure. Compound **11** is soluble in toluene and hexane. Crystals deemed suitable for single-crystal X-ray diffraction studies dried out very quickly and lost their crystallinity. 700 mg of **11** were recovered (yield: 75%). Anal. Calcd for $C_{36}H_{63}TiN_6O_3$: C 63.98, H 9.40, N 12.44. Found: C 63.94, H 9.52, N 12.36.

5.5.8. Synthesis of $ZnHL^{CNC}Br_2$ (12)

In a high-pressure ampoule 122 mg of $Zn\{N(SiMe_3)_2\}_2$ (316 µmol, 386.16 g/mol) were added to a 5 mL pyridine suspension of 200 mg of the tridentate proligand $H_4L^{CNC}Br_3$, **CXXIII**, (316 µmol, 632.280 g/mol). The reaction mixture was stirred at room temperature for 24 h and then the solvent and $HN(SiMe_3)_2$ were evaporated under vacuum and 40° C. Suitable crystals for single-crystal X-ray diffraction studies were obtained after two weeks through slow diffusion of hexane layered into a concentrated pyridine solution at room temperature. 122 mg recovered of **12** (yield: 63%).

^{1}H-NMR δ(400 MHz, $CDCl_3$): 8.67-7.27 (aromatic, 8H), 5.17 (s, J_{HH}=7.4Hz, 2H, C*H*$(CH_3)_2$), 4.74 (m, 4H, N–C*H*$_2$), 3.78 (m, 4H, N–C*H*$_2$), 1.74 (dd, J=7.4Hz, 12H, CH(C*H*$_3)_2$) ppm. ^{1}H-NMR δ(400 MHz, pyr-d_5): 7.94-7.40 (aromatic, 8H), 6.91 (b, 1H, NH), 5.47 (d, $^3J_{HH}$=6.4Hz, 2H, C*H*$(CH_3)_2$), 4.88 (m, 4H, N–C*H*$_2$), 3.82 (m, 4H, N–C*H*$_2$), 1.80 (dd, $^3J_{HH}$=6.4Hz, 12H, CH(C*H*$_3)_2$) ppm. ^{13}C{H}-NMR δ(125.76 MHz, $CDCl_3$): 177.0 (2C, carbene), 149.8 (2C, aromatic, CH), 135.4 130.9 (4C, aromatic C), 124.1 113.2 (6C, aromatic, CH), 54.5 (2C, *C*H$(CH_3)_2$), 49.3 (2C, CH_2), 44.5 (2C, CH_2), 22.1 (4C, CH_3) ppm.

5.5.9. Attempt to prepare $ZnHL^{CNC}(CO_2)Br_2$ (13)

A Young's tap NMR tube was charged with a 2 mL pyridine-d_5 solution containing 100 mg of **12** (0.16 mmol, 614.73 g/mol). The freeze-degas-thaw technique was applied three times before the tube was filled with CO_2 at 1 bar and heated at 90° C for 7 days. The solution was analysed by ^{1}H NMR spectroscopy after 1, 3, 5 and 7 days. Two sets of resonances were identified in the mixture; major resonances were assigned to **13**.

For starting material: ^{1}H-NMR δ(400 MHz, pyr-d_5): 11.24 (1H, NH), 8.53-7.48 (aromatic, 8H), 5.14 (t, $^3J_{HH}$=6.9Hz, 2H, C*H*$(CH_3)_2$), 4.88 (m, 4H, N–C*H*$_2$), 4.28 (m, 4H, N–C*H*$_2$), 1.67 (dd, $^3J_{HH}$=6.9Hz, 12H, CH(C*H*$_3)_2$) ppm.

For main product: ^{1}H-NMR δ(400 MHz, pyr-d_5): 12.18 (1H, NH), 8.43-7.34 (aromatic, 8H), 5.21 3.90 (m, 4H, N–C*H*$_2$), 4.93 (t, $^3J_{HH}$=6.4Hz, 1H, C*H*$(CH_3)_2$), 4.53 (t, $^3J_{HH}$=6.4Hz, 1H, C*H*$(CH_3)_2$), 4.41 (m, 2H, N–C*H*$_2$), 4.15 (m, 2H, N–C*H*$_2$), 1.71 (d, $^3J_{HH}$=6.4Hz, 6H, CH(C*H*$_3)_2$), 1.39 (d, $^3J_{HH}$=6.4Hz, 6H, CH(C*H*$_3)_2$) ppm.

5.5.10. Formation of $H_3L^{CNC}Br_2$ (14)

From the reaction in Section 5.5.9, a product formed in lower quantity than **13** was identified by single-crystal X-ray diffraction as $H_3L^{CNC}Br_2$ (**14**). This compound barely changed its concentration throughout the experiment.

^{1}H-NMR δ(400 MHz, pyr-d_5): 11.50 (s, 1H, NH), 11.24 (s, 1H, NC*H*N), 8.24-7.46 (aromatic, 8H), 5.02 (m, 2H, C*H*(CH_3)$_2$), 3.66 (m, 4H, N–CH_2), 3.44 (m, 4H, N–CH_2), 1.74 (12H, CH(CH_3)$_2$) ppm.

5.6. Synthetic procedures concerning metal complexes containing NHC ligands

5.6.1. Reaction of $(CuL)_2$ and cyclohexene oxide

A Young's tap NMR tube was filled with 60 mg of $(CuL)_2$, **6** (110 μmol, 545.714 g/mol), and 2 mL of pyridine-d_5; 50 μL of CHO (440 μmol, 98.144 g/mol) were added dropwise to the amber solution. Upon addition, some precipitate appeared but disappeared after shaking gently. The solution was heated at 50° C for 4 h with no apparent change in the ^{1}H NMR spectrum. After heating at 120° C for 16 h, there was still no noticeable reaction.

5.6.2. Reaction of $(CuLCO_2)_2$ with 3,3-dimethyl epoxybutane

A Young's tap NMR tube was charged with 15.5 mg of $(CuLCO_2)_2$, **7** (24.4 μmol, 633.732 g/mol), in 1.5 mL of pyridine-d_5. Four equivalents of 3,3-dimethyl epoxybutane (10 mg, 0.1 mmol, 100.160 g/mol) were added to the suspension with no apparent change. The tube was heated at 90° C for 60 h. The mixture became a dark red solution, which was found to be a mixture of products, including resonance of a hydrogenated ylidene at 9.49 ppm.

5.6.3. Reaction of $(CuLCO_2)_2$ with HBBN

A Young's tap NMR tube was filled with 27.5 mg of **7** (43.4 μmol, 633.732 g/mol) and 1.5 mL of pyridine-d_5; 10.6 mg of 9-borabicyclo[3.3.1]nonane (HBBN, 87 μmol, 122.017 g/mol) were added to the tube. After heating at 80° C for 16 h an intractable mixture of compounds was formed with a species with a resonance at 9.49 ppm in the ^{1}H NMR spectrum, corresponding to a hydrogen atom in the C2 position of the imidazolium cation. This species was also identified in the ^{1}H NMR spectrum of the reaction of **7** with 3,3-dimethyl epoxybutane.

5.6.4. Reaction of $(CuLCO_2)_2$ and silanes

A Young's tap NMR tube was filled with 21.8 mg of **7** (34.4 μmol, 633.732 g/mol) and 1.5 mL of pyridine-d_5. Two equivalents of $PhSiH_3$ (7.4 mg, 68.8 μmol, 108.21 g/mol) were added to the tube and a dark suspension formed, being an intractable mixture of compounds unidentified by ^{1}H NMR spectroscopy.

A Young's tap NMR tube was filled with 22.2 mg of **7** (35 μmol, 633.732 g/mol) and 1.5 mL of pyridine-d_5. Two equivalents of $BzSi(CH_3)_3$ (11.5 mg, 70 μmol, 164.322 g/mol) were added to the tube with no apparent change. From ^{1}H NMR spectroscopy, we found an unidentified mixture of compounds.

5.6.5. Reaction of $(CuLCO_2)_2$ and cyclohexene oxide

A Young's tap NMR tube was filled with 15.5 mg of $(CuLCO_2)_2$, **7** (24.4 μmol, 633.732 g/mol), and 1.5 mL of pyridine-d_5; 10 mg of CHO (440 μmol, 98.144 g/mol) were added dropwise to the amber solution. Upon addition, some precipitate appeared but disappeared after shaking gently. The solution was heated at 50° C for 4 h with no apparent change in the ^{1}H NMR spectrum. After heating at 120° C for 16 h, there is still no noticeable reaction.

5.6.6. Activation of grease whilst forming $Zn(L)_2$. Synthesis of $Zn(HL)_2\{O(Si(Me_2)O)_2\}$ (15)

An ampoule was charged with 28.3 mg of $ZnCl_2$ (207 μmol, 136.30 g/mol) and 3 mL of THF; a 3 mL THF solution of 103 mg of **5** (415 μmol, 248.409 g/mol) were added to the ampoule whilst stirring. A white precipitate appeared upon addition but the stirring continued for 16 h at 80° C. After filtering, the yellow solution was dried under reduced pressure and the white solid washed with diethyl ether. The washings were concentrated slowly under air and crystals suitable for single-crystal X-ray diffraction studies were recovered. No yield recorded.

5.6.7. Product of reaction of $Zn(L)_2$ and CO_2, compound 16

In a typical reaction, 30 mg of $Zn(L)_2$ (**10**) in a 1.5 mL THF solution were placed in a Young's tap NMR tube. The tube was subjected to three freeze-degas-thaw cycles to remove all nitrogen and, subsequently, carbon dioxide was let into the tube at 1.5 bar. The solution was left at room temperature with occasional shaking for four hours and then left standing for separation of phases over the weekend. Because the phases did not separate by gravity, the solid was subjected to three cycles of precipitation and washing using a centrifuge for 5 minutes at 4000 revolutions per minute.

^{1}H-NMR δ(500 MHz, pyr-d_5): 7.78 (s, 1H, NC*H*CHN), 7.47 (s, 1H, NCHC*H*N), 5.99 (m, 1H, $^3J_{HH}$=6.6Hz, C*H*(CH_3)$_2$), 5.17 (dd, 1H, $^2J_{HH}$=2.3, $^3J_{HH}$=13.3Hz, NC*H*H), 4.47 (dd, 1H, $^3J_{HH}$=10.8, $^3J_{HH}$=13.3Hz, NC*H*(O), 3.98 (m, 1H, $^2J_{HH}$=2.3, $^3J_{HH}$=13.3Hz, NCH*H*), 1.31 (dd, 6H, $^2J_{HH}$=16.0, $^3J_{HH}$=6.6Hz, CH(C*H*$_3$)$_2$), 1.11 (s, 9H, C(C*H*$_3$)$_3$) ppm. ^{13}C{H}-NMR δ(125.76 MHz, pyr-d_5): 156.1 (*C*O_2), 144.6 (N*C*N), 123.4 (*C*HCH), 116.7 (CH*C*H), 78.6 (*C*HO), 52.7 (N*C*H$_2$), 51.5 (N*C*H(CH_3)$_2$), 35.5 (*C*(CH_3)$_3$), 26.4 (C(*C*H$_3$)$_3$), 23.1 (NCH(*C*H$_3$)$_2$), 22.9 (NCH(*C*H$_3$)$_2$) ppm.

5.6.8. Attempted reaction of $[Ti(L)_3]$ (11) and CO_2

In a typical reaction, 30 mg of $Ti(L)_3$ (**11**) in a 1.5 mL THF solution were placed in a Young's tap NMR tube. The tube was subjected to three freeze-degas-thaw cycles to remove all nitrogen and, subsequently, carbon dioxide was let into the tube at 1.5 bar. The

solution was left at room temperature with occasional shaking for four hours and then left standing overnight. The solid was subjected to five cycles of precipitation and washing using a centrifuge for 5 minutes at 4000 revolutions per minute. Elemental analysis of the dry solid does not match with a species resulting from carbon dioxide insertion.

5.6.9. Polymerisation of *rac*-lactide with $(CuL)_2$ and $[Ti(L)_3]$

A Schlenk flask was charged with an appropriate quantity of either **6** or **11** in DCM; for specific reaction conditions see Table 5.3 and Sections 3.2.2.1 and 3.4.2.1. A 2 mL DCM solution of 660.1 mg of *rac*-lactide (4.58 mmol, 144.13 g/mol) were added to the original vessel from another Schlenk flask through cannula. All reactions were carried out at room temperature and with continuous stirring. Once the reaction time had finished, an aliquot of the crude suspension was obtained to characterise the mixture using ^{1}H NMR spectroscopy. Hexane was added to the bulk of the mixture to stop the reaction and separate the polymer through precipitation. Reactions using **11** as initiator did not show any conversion of the monomer in ^{1}H NMR spectroscopy.

Table 5.3. Polymerisations of *rac*-lactide using 6

Entry	6 (mg)	solvent (mL)	Ratio cat:monom:solv	Time (h)	TON[a]	Yield %[b]	Mn[c]	PDI[d]
i[e]	50	4.2	1:50:750	60	50	>99	-	-
ii	25	2.75	1:100:1000	16	100	>99	8872	1.1
iii[f]	12.5	2.75	1:200:2000	16	200	>99	12145	1.0

Amount of monomer in all entries: 660 mg. Solvent in all entries: DCM. **a** Because the catalyst was not recovered at the end of the reaction, the turnover frequency is the molar ratio monomer/catalyst for a conversion of 100%. **b** Measured from the ^{1}H NMR spectrum in $CDCl_3$ of an aliquot taken right at the end of the reaction. **c** Measured using GPC with a polystyrene standard and a dn/dc of 0.051 mL/g. **d** Polydispersity index is the Mw/Mn ratio from GPC results. **e** The sample from Entry **i** was not measured by GPC. **f** Entry **iii** is a mixture of polymers: the minor trace is reported in the table. Data of the major trace: M_n=5195 Da; PDI= 2.0.

5.6.10. Attempt to polymerise ε-caprolactone with $(CuL)_2$

A Schlenk flask was charged with 25 mg of **6** (46 µmol, 545.714 g/mol) in 1 mL of DCM. A 1.75 mL DCM solution of 523 mg of ε-caprolactone (4.58 mmol, 114.14 g/mol) were added to the original vessel from another Schlenk flask through cannula. All reactions were carried out at room temperature and with continuous stirring; for specific times, see Table 5.4. Once the reaction time had finished, an aliquot of the crude suspension was obtained to characterise the mixture using ^{1}H NMR spectroscopy. Hexane was added to the bulk of the mixture to stop the reaction and separate the polymer through precipitation.

Table 5.4. Polymerisations of ε-caprolactone using 6

Entry	Ratio cat:monom:solv	Time (h)	TON	Yield %[a]	Mn[b]	Mw[b]	PDI[c]
iv[d]	1:100:1000	16	100	>99	89600	91600	1.0
iv'	1:100:1000	60	100	>99	13400	17300	1.3

Amount of **6** in all entries: 25 mg. Amount of monomer in all entries: 523 mg. Solvent in all entries: 2.75 mL of DCM. **a** Measured from the ^{1}H NMR spectrum in $CDCl_3$ of an aliquot taken right at the end of the reaction. **b** Measured using GPC with a polystyrene standard and a dn/dc of 0.079 mL/g. **c** Polydispersity index is the Mw/Mn ratio from GPC results. **d** The sample from Entry **iv** is a mixture of polymers: the major trace is reported in the table. Data of the minor trace: M_n=60434 Da; PDI= 1.2.

5.6.11. Attempt to copolymerise carbon dioxide and CHO using $(CuL)_2$ and $Ti(L)_3$

Compounds **6** and **11** were tested as catalysts for the copolymerisation of carbon dioxide and cyclohexene oxide. Reaction conditions in these attempts varied in terms of catalyst load ratio, solvents, temperature, time of reaction and pressures. The specific data is found in Table 5.5 and Table 5.6.

a. Typical reaction at 1.5 bar: A high-pressure ampoule was charged with 50 mg of **6** (91.6 μmol, 545.71 g/mol) in an appropriate amount of solvent (see corresponding conditions in Table 5.5). Then, 600 mg of CHO (6.13 mmol, 98.144 g/mol) were added to the ampoule before it was subjected to three freeze-degas-thaw cycles to remove all nitrogen. Then, 1.5 bar of CO_2 was added to the ampoule and the mixture stirred at a set temperature and for the applicable amount of time. Once the reaction was deemed completed, carbon dioxide was let escape through a mercury bubbler with the addition of nitrogen. A small aliquot of the crude solution was taken with pipette to study the conversion of CHO into the copolymer using ^{1}H and ^{13}C NMR spectroscopy. All reactions at this pressure were unsuccessful.

b. Reaction at 8 bar: A 30 mL Büchi mini-clave reactor with an oven-dried glass round-bottom flask equipped with a stirring bar was placed under vacuum for 1 h (Figure 5.1). After filling the vessel with nitrogen at ambient pressure, a suspension of 50 mg of **6** (91.6 μmol, 545.71 g/mol) and 2.91 g of CHO (29.6 mmol, 98.144 g/mol) in 2 mL of THF was added into it *via* cannula. The reaction vessel was gently degassed three times. Then, a pressure of 8 bar of CO_2 was added to the reactor whilst stirring and heating at 80° C. The pressure increased to 9.5 bar in the first hour of reaction and stayed at about 9 bar for another 59 h. At the end of the reaction, CO_2 was gently let out and an aliquot was retrieved for ^{1}H and ^{13}C NMR spectroscopy studies. The reaction at this pressure was unsuccessful.

c. Typical reaction at 50 bar: These reactions were attempted in the Williams Laboratory at Imperial College London (Figure 5.2). A 100 mL Parr reaction vessel, equipped with a motorised 4-fold-bladed impeller for stirring, was placed in an oven at 140° C overnight, after which it was under vacuum for 3 h. The vessel was subjected to a pressure

of 50 bar of CO_2 to check for leaks and then a continuous flow of the gas went through it for the next step. A solution of 0.3 mmol of the catalyst in THF was added to 15 mL of CHO to form a solution to be transferred under a CO_2 atmosphere, using a syringe, to the Parr reactor (see Table 5.5 and Table 5.6 for specific conditions). In the case of Entry **xi** in Table 5.6, 0.3 mmol of PPNCl (172.2 mg, 574.03 g/mol), which acts as a cocatalyst, were also added to the reaction mixture. Once the reactor was closed, stirring began; the temperature of reaction was increased to 80° C and the pressure of CO_2 to 50 bar. After 20 minutes, the pressure, which had dropped due to CO_2 solubility in CHO, was taken to 50 bar again and the reaction continued for 24 h. At the end, an aliquot was taken to study the conversion of the epoxide into the copolymer using ^{1}H NMR spectroscopy. The remaining solution was transferred to a vial washing with DCM. No epoxide/carbon dioxide coupling was observed in the reaction with $(CuL)_2$ and very little copolymer was found using $[Ti(L)_3]$ (**11**), both with and without PPNCl as cocatalyst (see Table 5.6 for results).

Table 5.5. Reaction conditions for the failed copolymerisation of CHO and CO_2 using 6

Entry	6 (mg)	CHO (g)	solvent (mL)	Ratio cat:monom:solv	CO_2 (bar)	solvent	temp (°C)	time (h)
v	50	0.60	2	1:67:366	1.5	DCM	60	60
vi	50	0.58	1.4	1:65:188	1.5	THF	80	16
vii	50	2.91	2	1:324:269	8	THF	80	60
viii	163	14.55	1.5	1:496:62	50	THF	80	24

Table 5.6. Reaction conditions for the copolymerisation of CHO and CO_2 using 11

Entry	11 (mg)	CHO (g)	solvent (mL)[a]	Ratio cat:monom:solv:cocat[b]	Temp (°C)	Yield %[c]	TON[d]
x	202.7	14.55	4.5	1:494:185:-	80	2[e]	10
xi	202.7	14.55	2	1:494:82:1	80	15[e]	74

a Copolymerisation reactions were performed for 24 h using 50 bar of CO_2 and THF as solvent. **b** Cocatalyst in Entry **xi** was PPNCl. **c** Measured from the ^{1}H NMR spectrum in $CDCl_3$ of an aliquot taken right at the end of the reaction. **d** Because the catalyst was not recovered at the end of the reaction, the turnover frequency is the molar ratio monomer/catalyst for a conversion of 100%. **e** The polymer generated could not be isolated from the crude neither by evaporation of the components nor by precipitation with hexanes.

5.7. X-ray crystallography

Crystal data for the structures described within are presented in Table 5.16 and Table 5.17. The molecular structure of **14** was collected on an Agilent Technologies SuperNova diffractometer with Cu–Kα radiation (λ=1.5418 Å) and X-ray mirror optics at 100 K. All other data sets were collected at 170 K on an Oxford Diffraction Excalibur diffractometer using graphite monochromated Mo-Kα radiation (λ=0.71073 Å) equipped with an Eos CCD detector. Absorption corrections were carried out using the multi-scan procedure CrysAlisPro.[13] Structures were solved either using SHELXS-97 direct methods[14] or Olex2,[15] and refined using a full-matrix least square refinement on $|F|^2$ using SHELXL-97.[14] All programs, except Olex2, were used within the WinGX suite[16] or the ShelXle interface.[17] All non-hydrogen atoms were refined with anisotropic displacement parameters and H-parameters were constrained to parent atoms and refined using a riding model unless otherwise stated.

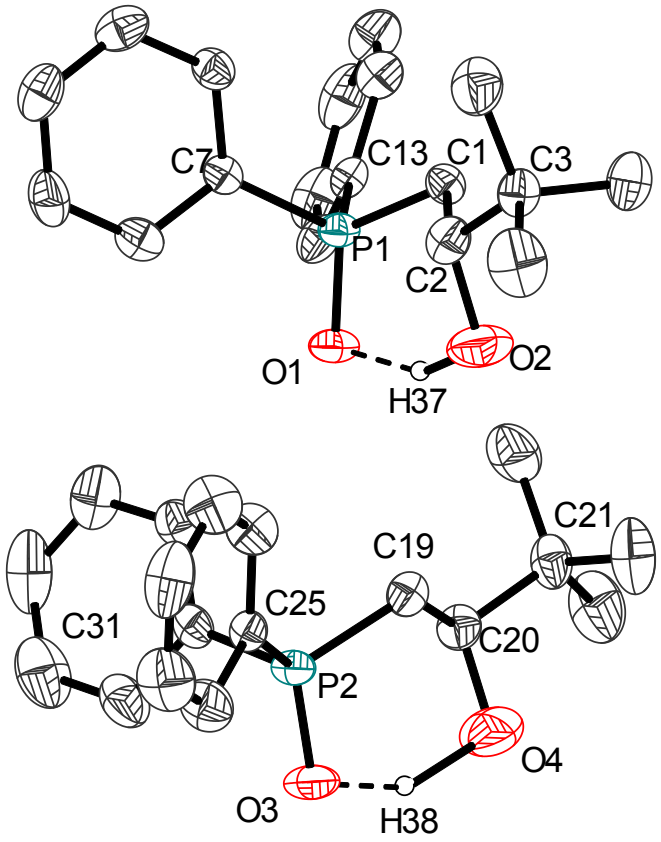

Figure 5.3. Displacement ellipsoid drawing of one morphology of 3,3-dimethyl-1-(diphenyl phosphinoyl)-butan-2-ol, HL^{Ph} (1a). 50% probability ellipsoids. All hydrogen atoms are omitted for clarity with the exception of those of the alcohol units, which were modelled from existing electronic density

Table 5.7. Selected bond distances (Å) and angles (°) for 1a

O1—P1	1.496 (3)	O1—P1—C1	111.47 (18)
O3—P2	1.499 (3)	O3—P2—C19	112.41 (19)
C2—O2	1.442 (5)	C2—C1—P1	110.3 (3)
C20—O4	1.410 (5)	C20—C19—P2	112.6 (3)
C1—P1	1.793 (4)	O2—C2—C1	108.9 (4)
C19—P2	1.791 (4)	O4—C20—C19	111.4 (4)
C1—C2	1.534 (6)	P1—O1—H37	101.0 (15)
C19—C20	1.523 (6)	P2—O3—H38	102.0 (14)
O2—H37	1.50 (4)	C2—O2—H37	100.8 (14)
O4—H38	1.63 (4)	C20—O4—H38	103.6 (12)
O1…H37	1.47 (4)	O2—H37…O1	147.1 (25)
O3…H38	1.336 (16)	O4—H38…O3	147.7 (23)
C7—P1	1.798 (4)		
C13—P1	1.810 (4)		
C25—P2	1.813 (4)		
C31—P2	1.807 (4)		
C2—C3	1.517 (6)		
C20—C21	1.531 (6)		

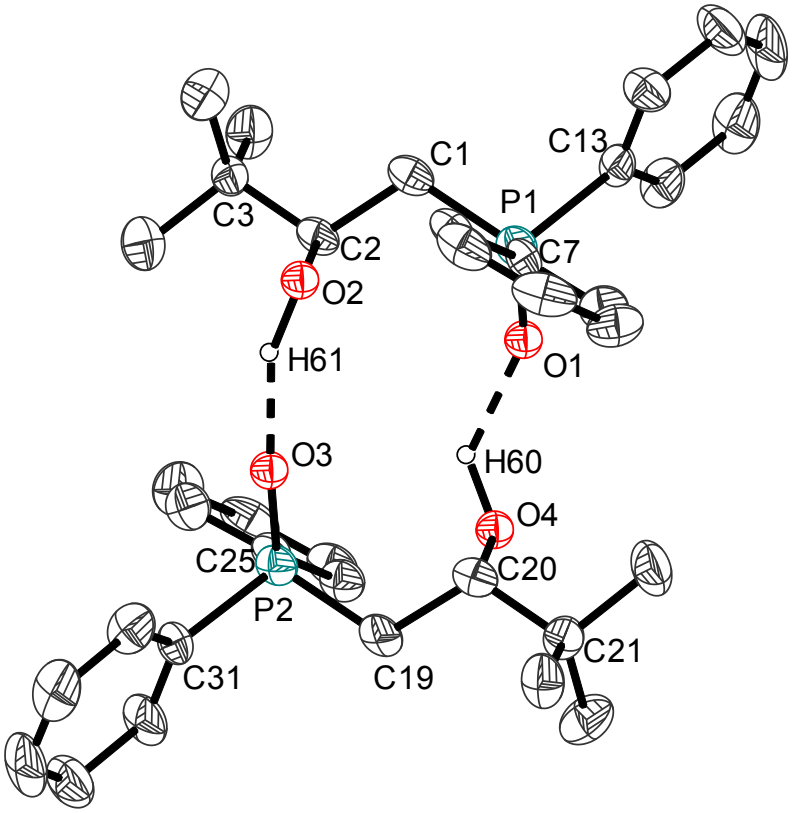

Figure 5.4. Displacement ellipsoid drawing of one morphology of 3,3-dimethyl-1-(diphenyl phosphinoyl)-butan-2-ol, HL^{Ph} (1b). 50% probability ellipsoids. All hydrogen atoms are omitted for clarity with the exception of those of the alcohol units, which were modelled from existing electronic density

Table 5.8. Selected bond distances (Å) and angles (°) for 1b

P1—O1	1.477 (4)	O1—P1—C1	113.4 (3)
P2—O3	1.496 (5)	O3—P2—C19	113.6 (3)
O2—C2	1.436 (5)	C2—C1—P1	114.0 (4)
O4—C20	1.440 (5)	C20—C19—P2	115.5 (4)
P1—C1	1.803 (5)	O2—C2—C1	105.7 (4)
P2—C19	1.785 (5)	O4—C20—C19	107.2 (4)
C1—C2	1.537 (7)	P1—O1…H60	146.3 (11)
C20—C19	1.532 (7)	P2—O3…H61	150.9 (11)
O2—H61	1.138 (17)	C2—O2—H61	99.3 (26)
O4—H60	1.085 (19)	C20—O4—H60	112.1 (26)
O1…H60	1.81 (3)	O2—H61…O3	152.6 (26)
O3…H61	1.60 (4)	O4—H60…O1	147.7 (23)
P1—C13	1.820 (6)		
P1—C7	1.821 (5)		
P2—C25	1.801 (5)		
P2—C31	1.811 (6)		
C3—C2	1.535 (6)		
C20—C21	1.540 (6)		

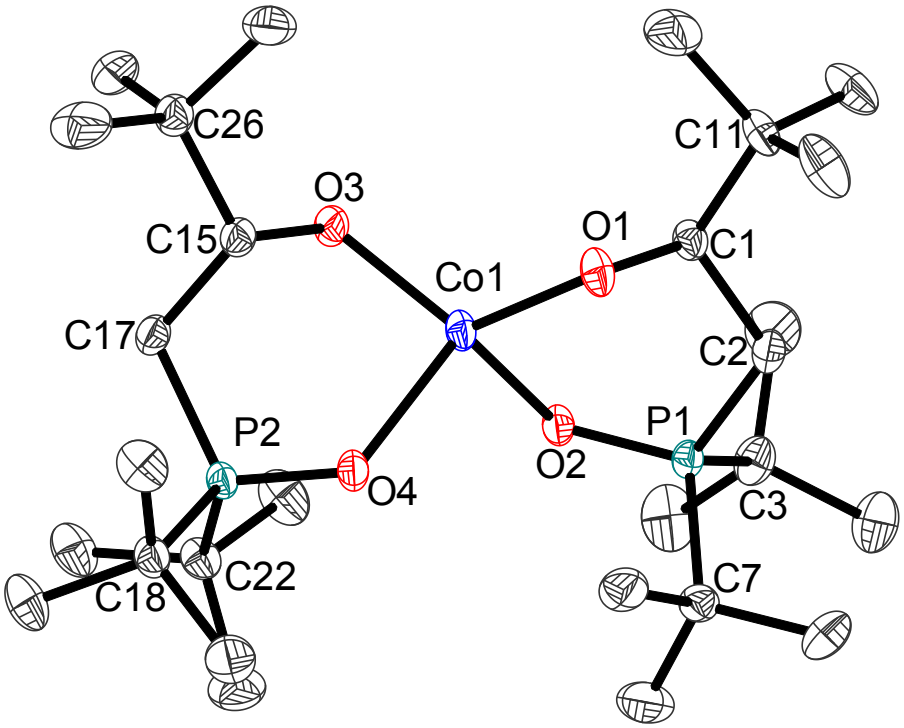

Figure 5.5. Displacement ellipsoid drawing of Co(L^{tBu})$_2$ (3). 50% probability ellipsoids. All hydrogen atoms are omitted for clarity

Table 5.9. Selected bond distances (Å) and angles (°) for 3

O1—Co1	1.897 (2)	O2—Co1—O1	93.61 (10)
O2—Co1	2.046 (2)	O3—Co1—O1	119.37 (11)
O3—Co1	1.897 (2)	O3—Co1—O2	128.03 (10)
O4—Co1	2.060 (2)	O4—Co1—O1	127.73 (10)
O2—P1	1.512 (2)	O4—Co1—O2	95.55 (9)
O4—P2	1.507 (2)	O4—Co1—O3	93.78 (10)
C1—O1	1.395 (4)	Co1—O1—C1	113.7 (2)
C15—O3	1.396 (4)	Co1—O2—P1	125.14 (14)
C1—C2	1.548 (5)	Co1—O3—C15	114.0 (2)
C15—C17	1.539 (5)	Co1—O4—P2	125.24 (14)
C2—P1	1.816 (4)	C3—P1—C2	107.74 (17)
C3—P1	1.843 (4)	C7—P1—C2	106.24 (17)
C7—P1	1.850 (4)	C7—P1—C3	113.92 (17)
C17—P2	1.814 (4)	O2—P1—C2	111.91 (15)
C18—P2	1.849 (4)	O2—P1—C3	107.42 (15)
C22—P2	1.852 (4)	O2—P1—C7	109.69 (15)
C1—C11	1.552 (5)	C18—P2—C17	107.88 (16)
C15—C26	1.561 (5)	C22—P2—C17	106.85 (17)
		C22—P2—C18	113.66 (17)
		O4—P2—C17	111.70 (15)
		O4—P2—C18	107.13 (15)
		O4—P2—C22	109.69 (15)

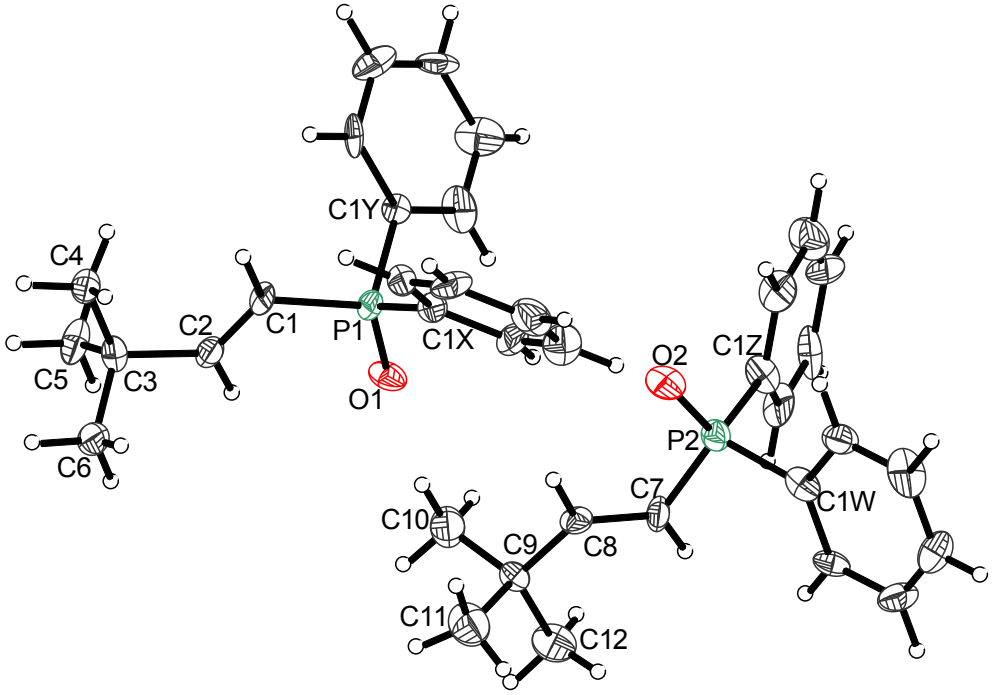

Figure 5.6. Displacement ellipsoid drawing of (*E*)-3,3-dimethyl-1-diphenylphosphinoylbut-1-ene (4). 50% probability ellipsoids.

Table 5.10. Selected bond distances (Å) and angles (°) for 4

P1—O1	1.478 (13)	O1—P1—C1	113.2 (6)
P2—O2	1.498 (14)	O2—P2—C7	114.3 (6)
P1—C1	1.805 (12)	C2—C1—P1	117.7 (9)
P2—C7	1.765 (14)	C8—C7—P2	121.0 (11)
C2—C1	1.323 (19)	C1—C2—C3	126.2 (12)
C8—C7	1.328 (18)	C7—C8—C9	132.6 (12)
P1—C1Y	1.807 (7)	O1—P1—C1Y	109.6 (5)
P1—C1X	1.813 (8)	O1—P1—C1X	112.7 (5)
P2—C1W	1.817 (8)	O2—P2—C1W	111.2 (5)
C1Z—P2	1.830 (7)	O2—P2—C1Z	112.5 (5)
C2—C3	1.54 (2)	C1—P1—C1Y	107.4 (5)
C8—C9	1.45 (2)	C1—P1—C1X	107.8 (5)
C3—C4	1.498 (19)	C7—P2—C1W	108.1 (6)
C3—C5	1.51 (2)	C7—P2—C1Z	105.0 (6)
C3—C6	1.52 (2)		
C10—C9	1.54 (2)		
C11—C9	1.55 (2)		
C9—C12	1.57 (2)		

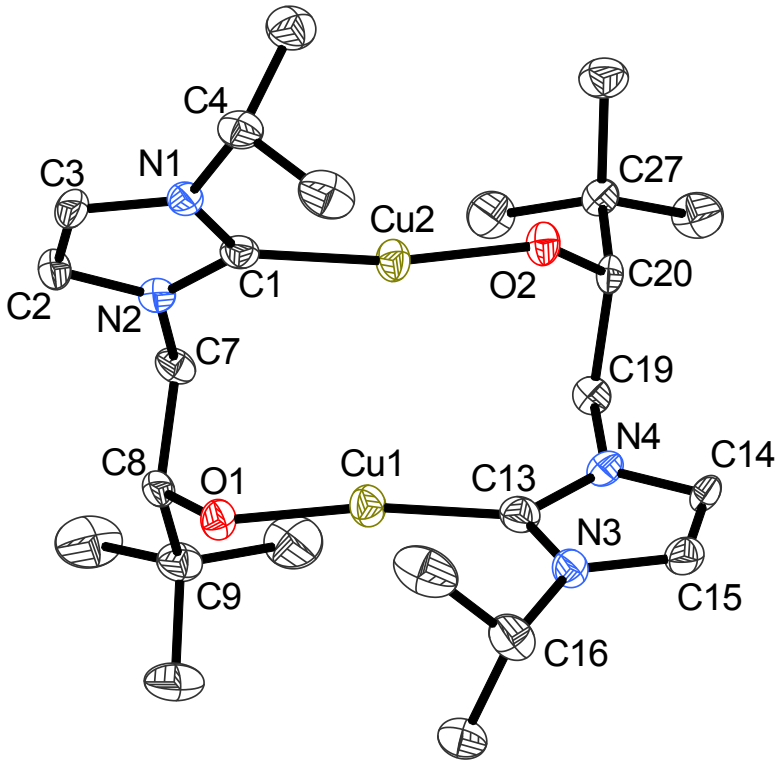

Figure 5.7. Displacement ellipsoid drawing of $(CuL)_2$ (6). 50% probability ellipsoids. All hydrogen atoms are omitted for clarity

Table 5.11. Selected bond distances (Å) and angles (°) for 6

Cu1—O1	1.821 (2)	O1—Cu1—C13	170.44 (14)
Cu2—O2	1.821 (2)	O2—Cu2—C1	169.03 (13)
Cu1—C13	1.870 (4)	N1—C1—N2	104.1 (3)
Cu2—C1	1.868 (4)	N4—C13—N3	104.3 (3)
N1—C1	1.352 (4)	C8—O1—Cu1	125.7 (2)
N2—C1	1.364 (4)	C20—O2—Cu2	125.05 (19)
N4—C13	1.360 (4)	C1—N1—C3	111.5 (3)
C13—N3	1.364 (4)	C1—N2—C2	110.5 (3)
N4—C14	1.379 (4)	C13—N3—C15	110.7 (3)
N3—C15	1.385 (4)	C13—N4—C14	110.9 (3)
N1—C3	1.379 (4)	N2—C7—C8	112.7 (3)
C2—N2	1.377 (4)	N4—C19—C20	112.4 (3)
C2—C3	1.339 (5)		
C14—C15	1.339 (5)		
O1—C8	1.385 (4)		
O2—C20	1.382 (4)		
N4—C19	1.452 (4)		
N2—C7	1.455 (4)		
C7—C8	1.541 (5)		
C19—C20	1.533 (4)		
Cu1...Cu2	2.9964 (7)		

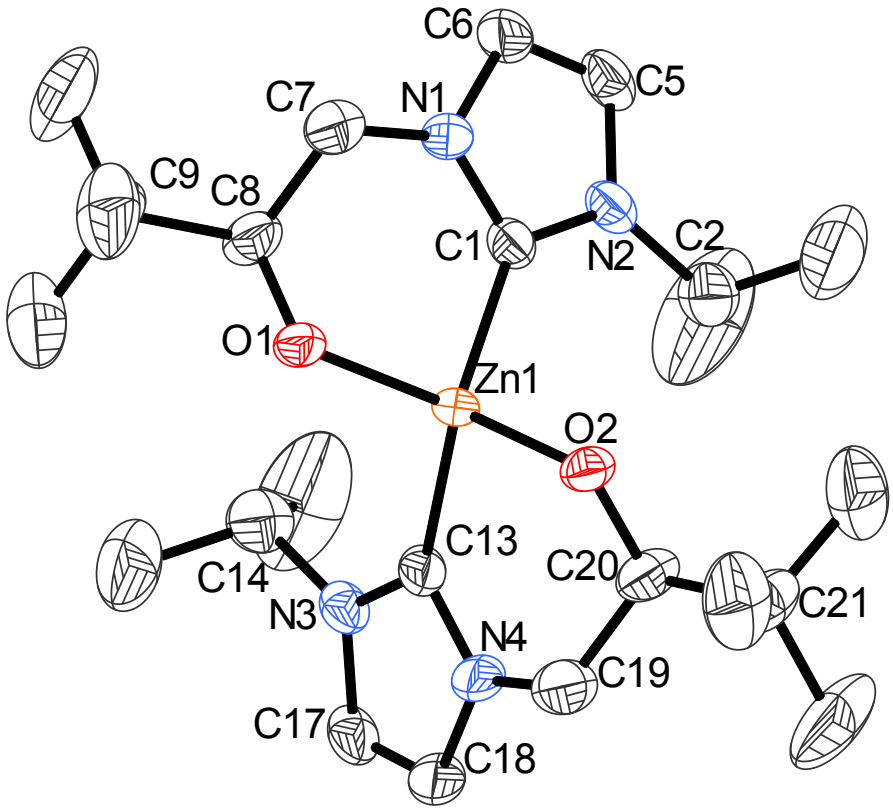

Figure 5.8. Displacement ellipsoid drawing of $Zn(L)_2$ (10). 50% probability ellipsoids. All hydrogen atoms are omitted for clarity

Table 5.12. Selected bond distances (Å) and angles (°) for 10

Zn1—O1	1.956 (3)	O1—Zn1—O2	120.74 (12)
Zn1—O2	1.956 (3)	O1—Zn1—C13	108.74 (14)
Zn1—C13	2.029 (4)	O2—Zn1—C13	96.95 (14)
Zn1—C1	2.033 (4)	O1—Zn1—C1	96.74 (14)
O1—C8	1.378 (5)	O2—Zn1—C1	108.81 (14)
O2—C20	1.374 (5)	C13—Zn1—C1	127.01 (17)
N3—C13	1.351 (5)	N2—C1—N1	104.9 (3)
N4—C13	1.369 (5)	N3—C13—N4	104.8 (3)
N2—C1	1.355 (5)	C8—O1—Zn1	115.9 (2)
N1—C1	1.358 (5)	C20—O2—Zn1	116.0 (2)
N1—C6	1.380 (5)	C8—C7—N1	112.0 (4)
N2—C5	1.382 (5)	C20—C19—N4	111.9 (4)
N3—C17	1.386 (5)	C1—N1—C6	110.5 (4)
N4—C18	1.381 (5)	C1—N2—C5	110.9 (4)
C5—C6	1.350 (7)	C13—N3—C17	111.0 (4)
C17—C18	1.351 (7)	C13—N4—C18	110.4 (4)
N1—C7	1.510 (6)		
N4—C19	1.501 (6)		
C8—C7	1.488 (7)		
C19—C20	1.501 (7)		

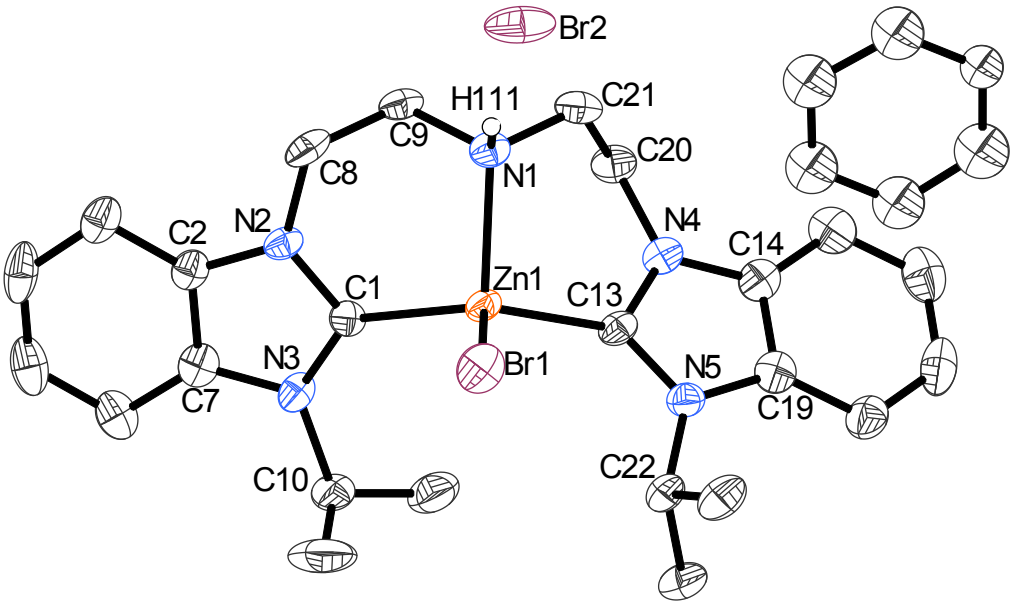

Figure 5.9. Displacement ellipsoid drawing of Zn(HL^{CNC})Br$_2$ (12). 50% probability ellipsoids. All hydrogen atoms are omitted for clarity except the one in the amino group.

Table 5.13. Selected bond distances (Å) and angles (°) for 12

C1—Zn1	2.025 (5)	C1—Zn1—N1	97.3 (2)
C13—Zn1	2.020 (6)	C13—Zn1—Br1	108.80 (16)
N1—Zn1	2.126 (5)	C1—Zn1—Br1	108.75 (16)
Zn1—Br1	2.3968 (9)	N1—Zn1—Br1	110.66 (13)
C1—N3	1.347 (7)	N3—C1—N2	106.4 (5)
C1—N2	1.358 (7)	N4—C13—N5	106.5 (5)
C13—N4	1.344 (7)	C1—N3—C7	110.3 (5)
C13—N5	1.356 (7)	C1—N2—C2	110.8 (5)
C7—N3	1.395 (7)	C13—N4—C14	111.0 (5)
C2—C7	1.390 (8)	C13—N5—C19	110.2 (5)
C2—N2	1.388 (7)	C21—N1—C9	110.6 (5)
C8—N2	1.462 (7)	Zn1—N1—H111	110 (5)
C8—C9	1.501 (9)		
C9—N1	1.475 (7)		
C21—N1	1.473 (8)		
C20—C21	1.524 (9)		
C20—N4	1.463 (7)		
C14—N4	1.391 (8)		
C14—C19	1.387 (9)		
C19—N5	1.408 (8)		
N1—H111	0.90 (2)		

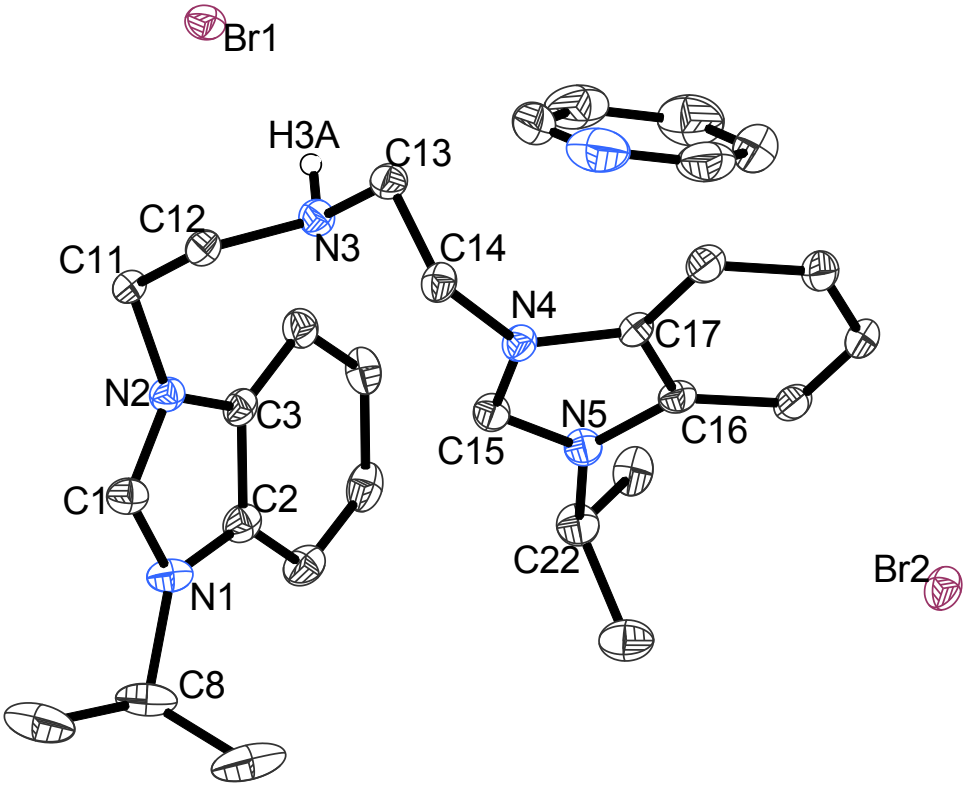

Figure 5.10. Displacement ellipsoid drawing of $H_3L^{CNC}Br_2$ (14). 50% probability ellipsoids. All hydrogen atoms are omitted for clarity except the one in the amino group.

Table 5.14. Selected bond distances (Å) and angles (°) for 14

C1—N2	1.332 (2)	N2—C1—N1	110.32 (15)
C1—N1	1.333 (2)	N4—C15—N5	110.75 (15)
C15—N4	1.327 (2)	C1—N1—C2	108.21 (14)
C15—N5	1.332 (2)	C1—N2—C3	108.56 (14)
C8—N1	1.489 (2)	C15—N4—C17	108.30 (14)
C2—N1	1.392 (2)	C15—N5—C16	108.01 (13)
C2—C3	1.400 (2)	C12—N3—C13	112.12 (13)
C3—N2	1.387 (2)	C12—N3—H3A	108.7 (14)
C11—N2	1.4765 (19)	C13—N3—H3A	108.9 (14)
C11—C12	1.514 (2)		
C12—N3	1.462 (2)		
C13—N3	1.463 (2)		
C14—C13	1.522 (2)		
C14—N4	1.469 (2)		
C17—N4	1.390 (2)		
C16—C17	1.397 (2)		
C16—N5	1.399 (2)		
C22—N5	1.490 (2)		
N3—H3A	0.83 (2)		

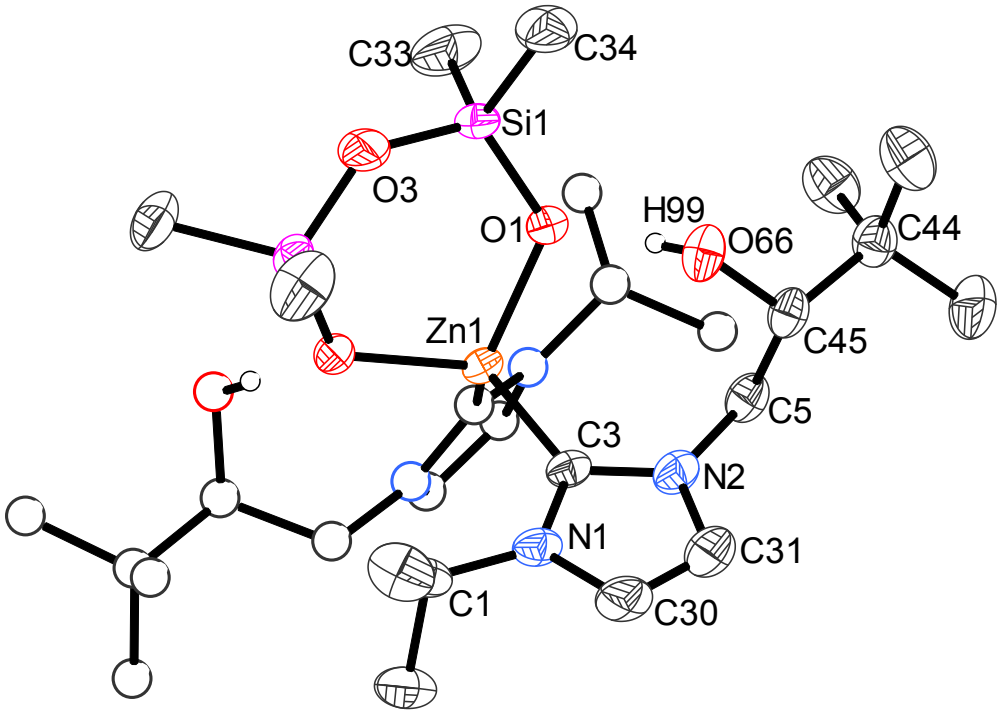

Figure 5.11. Displacement ellipsoid drawing of $Zn(L)_2\{O(Si(Me_2)O)_2\}$ (15). 50% probability ellipsoids. All hydrogen atoms are omitted for clarity except the one in the alcohol group. The NHC ligand in the background, which is equivalent to the one in the foreground, is faded.

Table 5.15. Selected bond distances (Å) and angles (°) for 15

Zn1—O1	1.9703 (13)	O1—Zn1—O1	106.43 (8)
Zn1—C3	2.066 (2)	O1—Zn1—C3	105.71 (7)
Si1—O1	1.6042 (15)	O1—Zn1—C3	111.92 (7)
Si1—O3	1.6310 (10)	C3—Zn1—C3	114.92 (11)
Si1—C33	1.859 (3)	Si1—O1—Zn1	122.16 (8)
Si1—C34	1.860 (2)	O1—Si1—O3	111.71 (9)
N2—C3	1.355 (3)	Si1—O3—Si1	136.79 (15)
N1—C3	1.356 (3)	C33—Si1—C34	109.51 (13)
N1—C30	1.387 (3)	N2—C3—N1	104.11 (17)
C31—C30	1.328 (3)	C3—N1—C30	111.00 (19)
N2—C31	1.380 (3)	C3—N2—C31	110.87 (19)
N2—C5	1.463 (3)	C45—O66—H99	112 (2)
C5—C45	1.526 (3)		
O66—C45	1.407 (3)		
O66—H99	0.83 (3)		
C16—C17	1.397 (2)		
C16—N5	1.399 (2)		
C22—N5	1.490 (2)		
N3—H3A	0.83 (2)		

Table 5.16. X-ray crystallography experimental details for compounds 1, 3 and 4

	1a	**1b**	**3**	**4**
Crystal data				
Chemical formula	$C_{36}H_{46}O_4P_2$	$C_{36}H_{46}O_4P_2$	$C_{28}H_{60}CoO_4P_2$	$C_{18}H_{21}OP$
M_r	604.67	604.67	581.654	284.32
Crystal system	Orthorhombic	Monoclinic	Monoclinic	Monoclinic
space group	*Pbcn*	$P2_1$	$P2_1/n$	*Pc*
Temperature (K)	171	170	170	170
***a* (Å)**	18.6742 (13)	8.1166 (8)	10.8618 (5)	16.9861 (18)
***b* (Å)**	16.1673 (7)	22.173 (2)	19.9939 (10)	5.8568 (3)
***c* (Å)**	22.3474 (9)	9.9718 (10)	15.2286 (6)	18.771 (3)
β (°)	90	112.467 (11)	99.308 (4)	123.414 (9)
***V* (Å^3)**	6746.9 (6)	1658.4 (3)	3263.6 (3)	1558.8 (3)
Z	8	2	1	4
μ (mm^{-1})	0.17	0.17	0.65	0.17
Crystal size (mm)	0.22 × 0.18 × 0.14	0.55 × 0.14 × 0.09	0.39 × 0.20 × 0.16	0.34 × 0.15 × 0.12
Data collection				
No. of measured, independent and observed reflections	28689, 5746, 3337 [$I > 2\sigma(I)$]	18658, 7570, 3912 [$I > 2\sigma(I)$]	30977, 7158, 4383 [$I \geq 2u(I)$]	10895, 4731, 3071 [$I > 2\sigma(I)$]
R_{int}	0.097	0.085	0.090	0.039
(sin θ/λ)$_{max}$ (Å^{-1})	0.588	0.686	0.705	0.588
Refinement				
$R[F^2 > 2\sigma(F^2)]$, $wR(F^2)$, S	0.076, 0.200, 1.02	0.071, 0.140, 0.96	0.059, 0.171, 0.95	0.045, 0.112, 1.01
No. of reflections	5746	7570	7158	4731
No. of parameters	385	392	335	320
No. of restraints	2	5	0	2
$\Delta\rho_{max}$, $\Delta\rho_{min}$ (e Å^{-3})	0.94, -0.36	0.39, -0.41	0.91, -0.76	0.30, -0.31

Table 5.17. X-ray crystallography experimental details for compounds 6, 10, 12 and 14

	6	**10**	**12**	**14**
Crystal data				
Chemical formula	$C_{24}H_{42}Cu_2N_4O_2$	$C_{24}H_{42}N_4O_2Zn$	$C_{30}H_{37}Br_2N_5Zn$	$C_{29}H_{38}Br_2N_6$
M_r	545.69	483.98	692.84	630.47
Crystal system	Triclinic	Monoclinic	Triclinic	Monoclinic
space group	$P\bar{1}$	$P2_1/c$	$P\bar{1}$	$P2_1/n$
Temperature (K)	293	293	293	293
***a* (Å)**	10.0722 (8)	22.4015 (4)	7.2367 (3)	13.82290 (8)
***b* (Å)**	11.4743 (8)	11.2408 (2)	10.7549 (6)	11.25132 (9)
***c* (Å)**	12.3324 (6)	10.5037 (2)	20.1089 (10)	19.25116 (14)
α (°)	79.692 (5)	90	81.298 (4)	90
β (°)	71.218 (6)	90.022 (2)	86.301 (4)	90.5401 (6)
γ (°)	87.347 (6)	90	79.424 (4)	90
***V* (Å^3)**	1327.50 (16)	2644.94 (8)	1519.69 (13)	2993.92 (4)
Z	2	4	2	4
μ (mm^{-1})	1.63	0.95	3.47	3.64
Crystal size (mm)	0.38 × 0.18 × 0.10	0.26 × 0.25 × 0.15	0.26 × 0.18 × 0.12	0.21 × 0.19 × 0.13
Data collection				
No. of measured, independent and observed reflections	20108, 4376, 3105 [$I > 2s(I)$]	39101, 5842, 4431 [$I > 2s(I)$]	26358, 5691, 3972 [$I > 2s(I)$]	29159, 5984, 5674 [$I > 2s(I)$]
R_{int}	0.073	0.041	0.071	0.022
(sin θ/λ)$_{max}$ (Å^{-1})	0.581	0.641	0.610	0.623
Refinement				
$R[F^2 > 2\sigma(F^2)]$, $wR(F^2)$, S	0.044, 0.076, 1.03	0.061, 0.188, 0.92	0.061, 0.149, 1.03	0.024, 0.059, 0.98
No. of reflections	4376	5842	5691	5984
No. of parameters	299	290	316	338
No. of restraints	0	0	1	0
$\Delta\rho_{max}$, $\Delta\rho_{min}$ (e Å^{-3})	–	1.30, -0.60	1.92, -0.89	0.58, -0.44

Table 5.18. X-ray crystallography experimental details for compound 15

	15
Crystal data	
Chemical formula	$C_{14}H_{28}N_2O_{2.50}SiZn_{0.50}$
M_r	325.16
Crystal system	Monoclinic
space group	*C*2/*c*
Temperature (K)	170
***a* (Å)**	17.3086 (6)
***b* (Å)**	9.1354 (3)
***c* (Å)**	23.5771 (8)
α (°)	90
β (°)	102.672 (3)
γ (°)	90
***V* (Å^3)**	3637.2 (2)
Z	8
μ (mm^{-1})	0.78
Crystal size (mm)	0.99 × 0.73 × 0.61
Data collection	
No. of measured, independent and observed reflections	20503, 3862, 3298
R_{int}	0.039
$(\sin \theta/\lambda)_{max}$ (Å^{-1})	0.633
Refinement	
$R[F^2 > 2\sigma(F^2)]$, $wR(F^2)$, S	0.038, 0.085, 1.10
No. of reflections	3862
No. of parameters	192
No. of restraints	0
$\Delta\rho_{max}$, $\Delta\rho_{min}$ (e Å^{-3})	0.28, -0.31

5.8. References

[1] Arnold, P. L.; Rodden, M.; Davis, K. M.; Scarisbrick, A. C.; Blake, A. J.; Wilson, C. *Chem. Commun.* **2004,** 1612-1613. 10.1039/B404614E.

[2] Arnold, P. L.; Buffet, JC.; Blaudeck, R. P.; Sujecki, S.; Blake, A. J.; Wilson, C. *Angew. Chem. Int. Ed.* **2008,** *47,* 6033-6036. 10.1002/anie.200801279.

[3] Bradley, D. C.; Fisher, K. J. *J. Am. Chem. Soc.* **1971,** *93,* 2058-2059. 10.1021/ja00737a041.

[4] Bürger, H.; Sawodny, W.; Wannagat, U. *J. Organomet. Chem.* **1965,** *3,* 113-120. 10.1016/S0022-328X(00)84740-3.

[5] Bradley, D. C.; Ghotra, J. S.; Hart, F. A. *J. Chem. Soc., Dalton Trans.* **1973,** 1021-1023. 10.1039/dt9730001021.

[6] Jones, N. A.; Liddle, S. T.; Wilson, C.; Arnold, P. L. *Organometallics* **2007,** *26,* 755-757. 10.1021/om060486d.

[7] Buffet, J.-C., PhD Thesis, The University of Edinburgh, UK (Edinburgh), **2009**.

[8] Allan, L. E.N.; Briand, G. G.; Decken, A.; Marks, J. D.; Shaver, M. P.; Wareham, R. G. *J. Organomet. Chem.* **2013,** *736,* 55-62. 10.1016/j.jorganchem.2013.03.009.

[9] "Light Scattering dn/dc Values." American Polymer Standards Corporation. 19 September 2013. <http://www.ampolymer.com/dndc.html>.

[10] Weinberg, K. G. *J. Org. Chem.* **1975,** *40,* 3586-3589. 10.1021/jo00912a027.

[11] Buffet, J.-C., PhD Thesis, The University of Edinburgh, UK (Edinburgh), **2009**.

[12] Kember, M. R.; White, A. J. P.; Williams, C. K. *Macromolecules* **2010,** *43,* 2291-2298. 10.1021/ma902582m. Jutz, F.; Buchard, A.; Kember, M. R.; Fredriksen, S. B.; Williams, C. K. *J. Am. Chem. Soc.* **2011,** *133,* 17395-17405. 10.1021/ja206352x.

[13] CrysAlis PRO, Oxford Diffraction Ltd. UK, 2007.

[14] Sheldrick, G. M. *Acta Cryst.* **2008,** *A64,* 112-122. 10.1107/S0108767307043930.

[15] Dolomanov, O. V.; Bourhis, L. J.; Gildea, R. J.; Howard, J. A. K.; Puschmann, H. *J. Appl. Cryst.* **2009**, *42*, 339-341. 10.1107/S0021889808042726.

[16] Farrugia, L. J. *J. Appl. Cryst.* **1999,** *32,* 837-838. 10.1107/S0021889899006020.

[17] Hübschle, C. B.; Sheldrick, G. M.; Dittrich, B. *J. Appl. Cryst.* **2011,** *44,* 1281-1284. 10.1107/S0021889811043202.

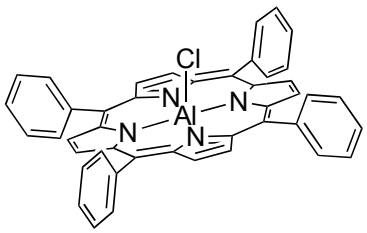

I

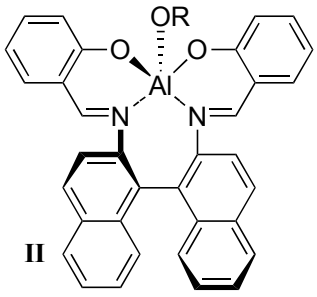

II

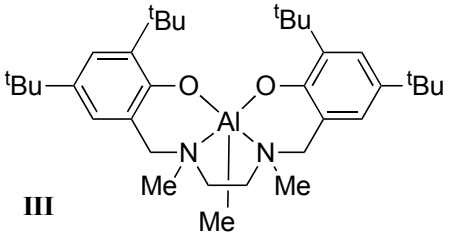

III

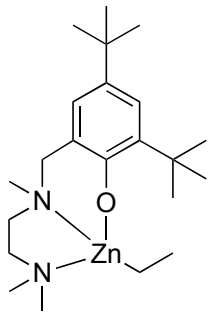

IV

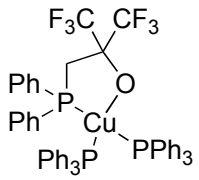

V

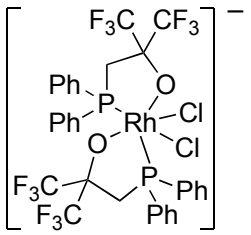

VI

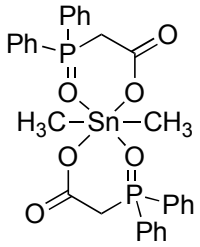

VII

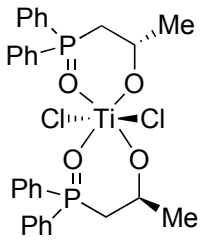

VIII

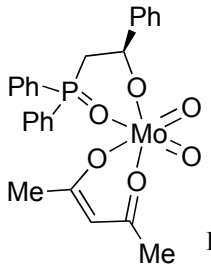

IX

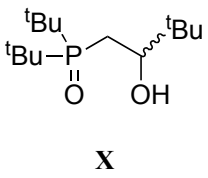

X

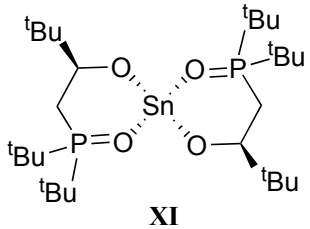

XI

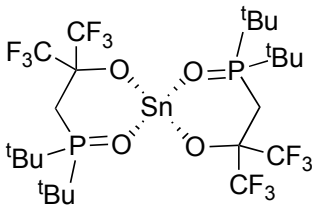

XII

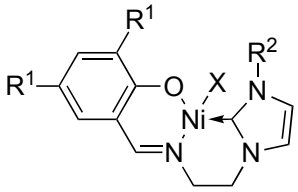

XIII

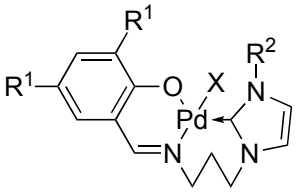

XIV

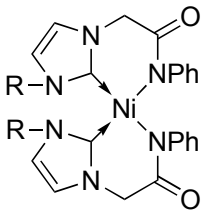

XV

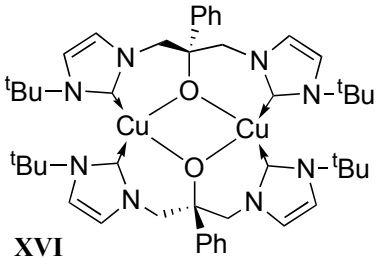

XVI

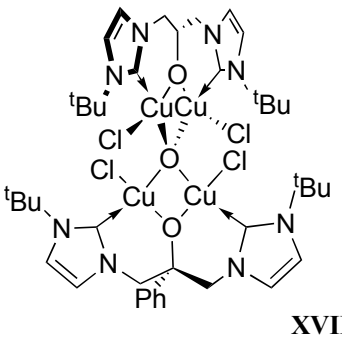

XVII

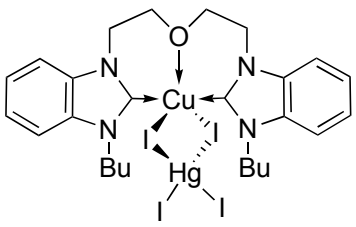

XVIII

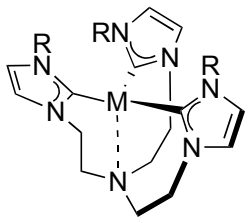

XIX

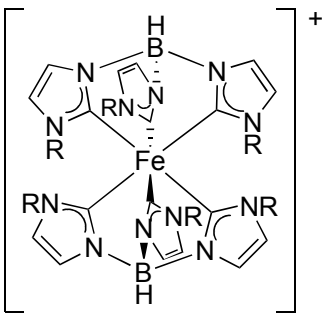

XX

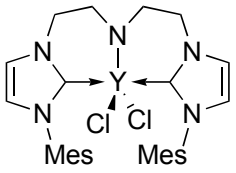

XXI

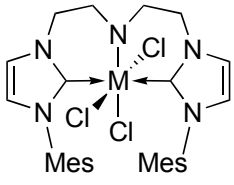

M = Ti, Zr

XXII, XXIII

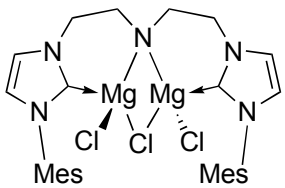

XXIV

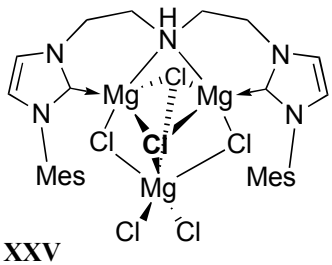

XXV

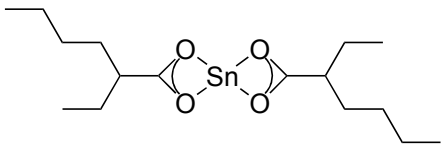

XXVI

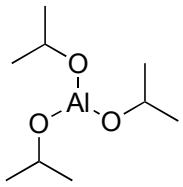

XXVII

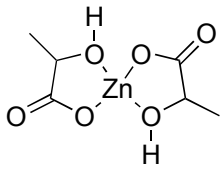

XXVIII

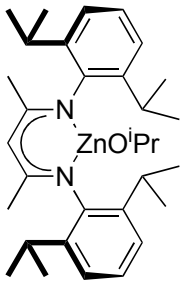

XXIX

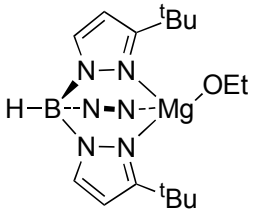

XXX

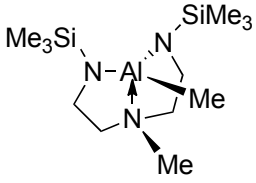

XXXI

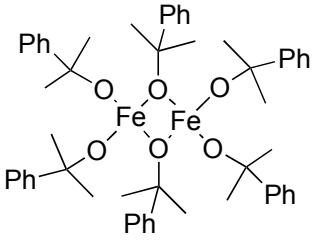

XXXII

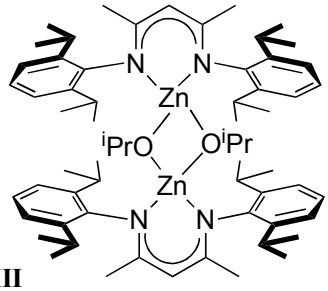

XXXIII

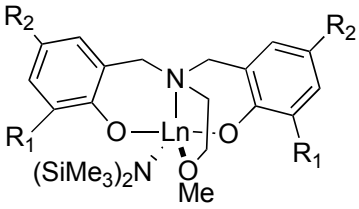

XXXIV

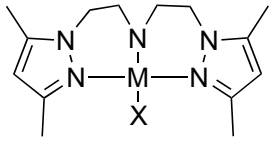

XXXV

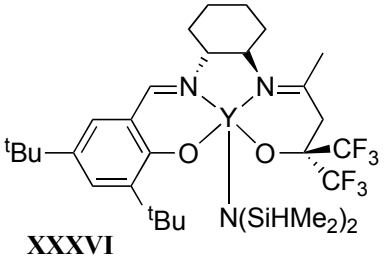

XXXVI

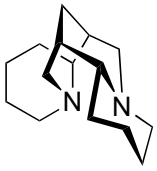

XXXVII

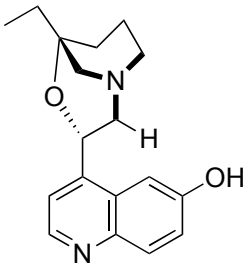

XXXVIII

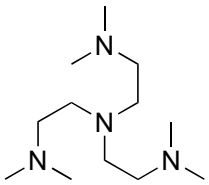

XXXIX

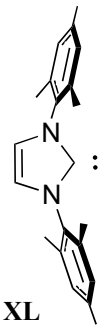

XL

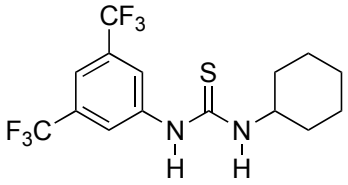

XLI

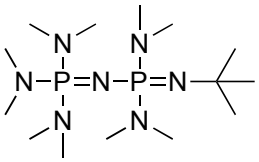

XLII

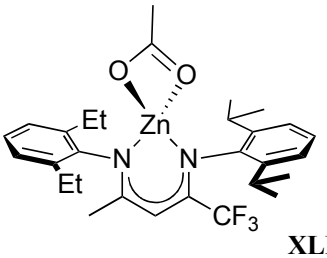

XLIII

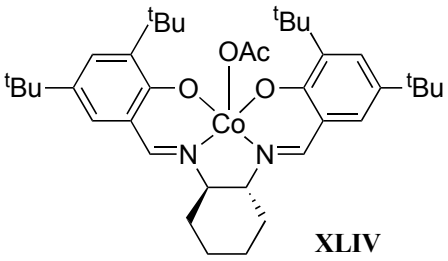

XLIV

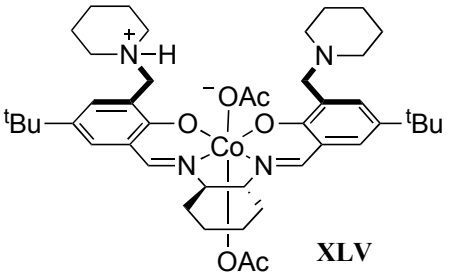

XLV

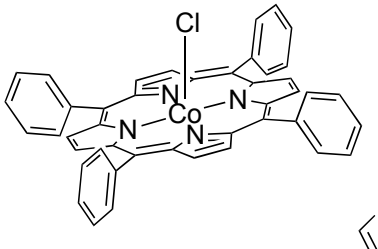

XLVI

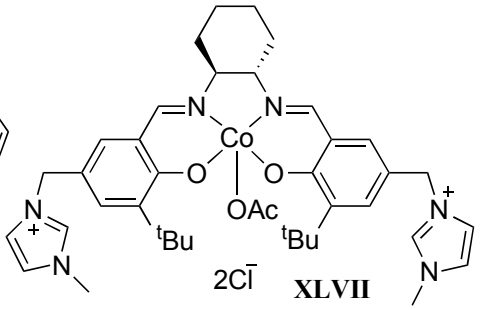

XLVII

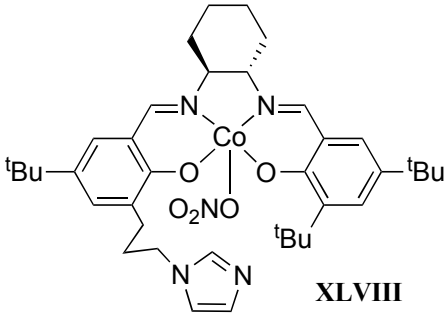

XLVIII

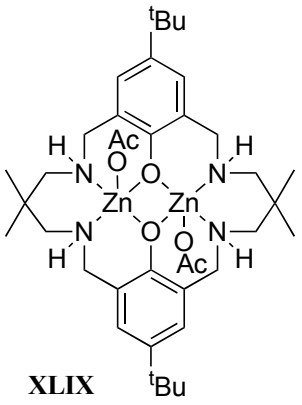

XLIX

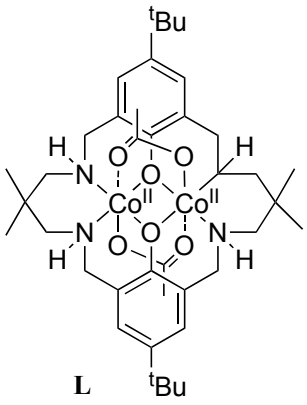

L

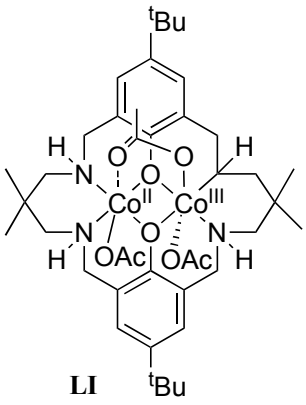

LI

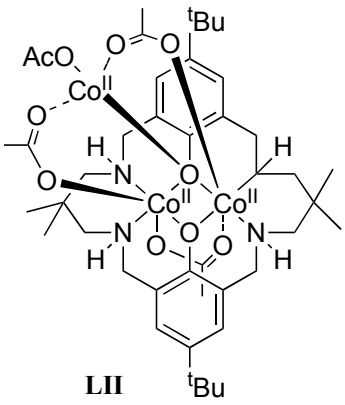

LII

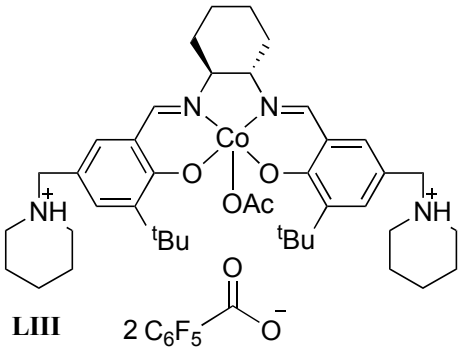

LIII

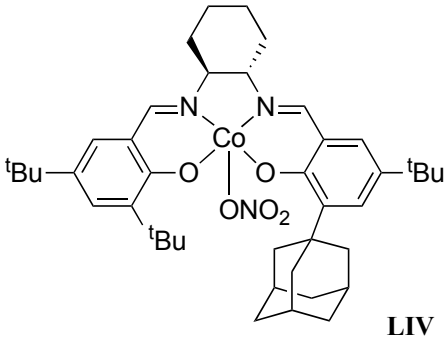

LIV

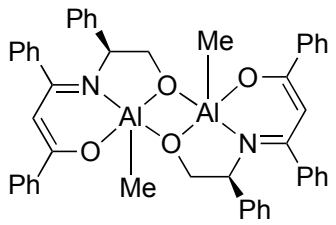

LV

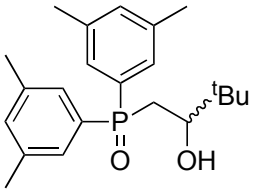

LVI

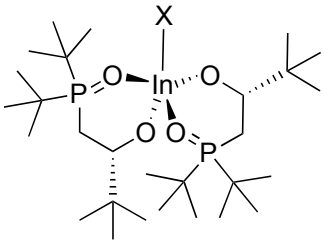

LVII

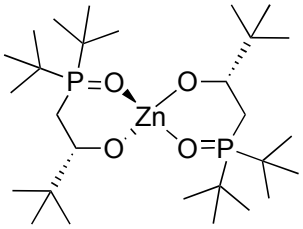

LVIII

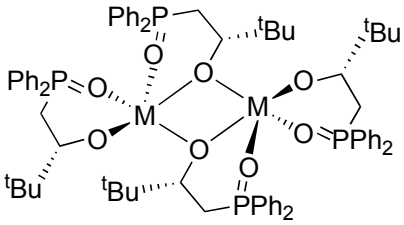

M = Mg (**LIX**), Co (**LX**), Sn (**LXI**)

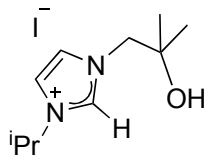

LXII

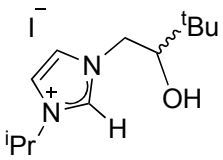

LXIII

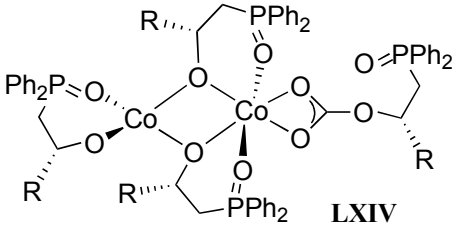

LXIV

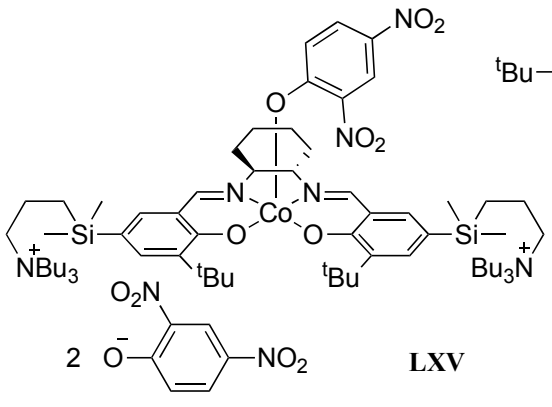

LXV

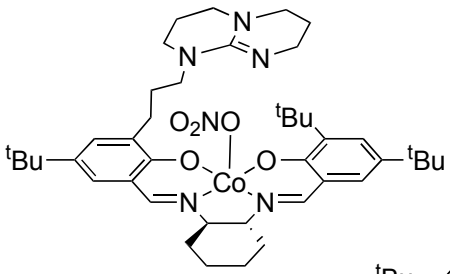

LXVI

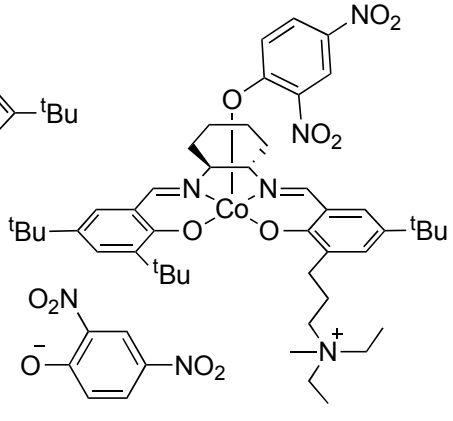

LXVII

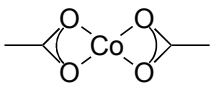

LXVIII

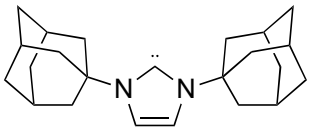

LXIX

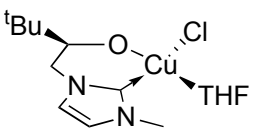

LXX

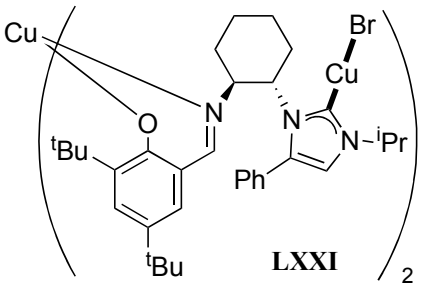

LXXI

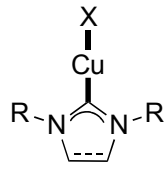

LXXII

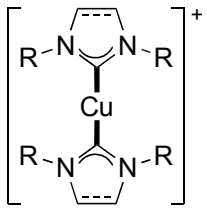

LXXIII

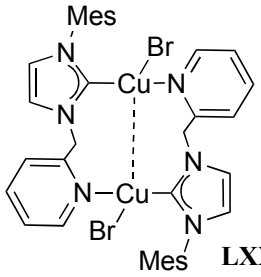

LXXIV

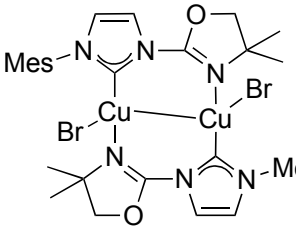

LXXV

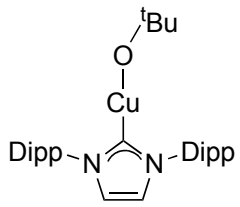

LXXVI

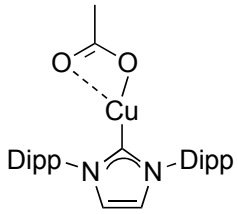

LXXVII

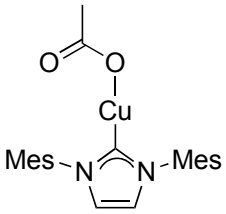

LXXVIII

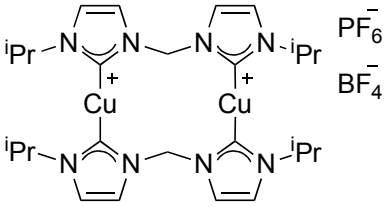

LXXIX

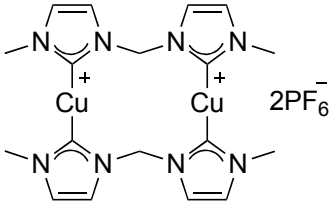

LXXX

LXXXI (with acetone and water)

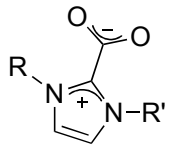

LXXXII (R, R' = Dipp)
LXXXIII (R, R' = Mes)
LXXXIV (R = Me, R' = ^{n}Bu)

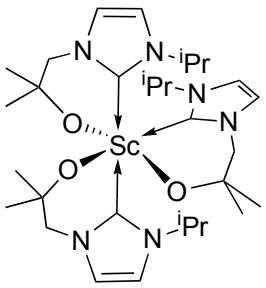

LXXXV

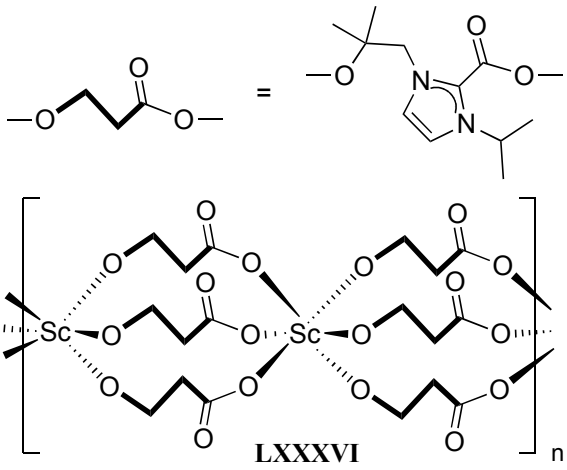

LXXXVI

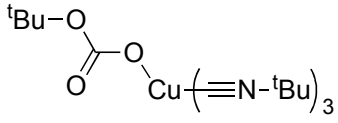

LXXXVII

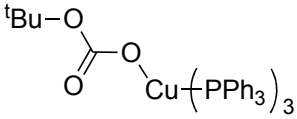

LXXXVIII

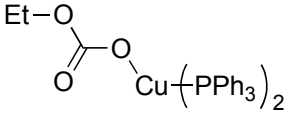

LXXXIX

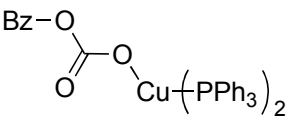

XC

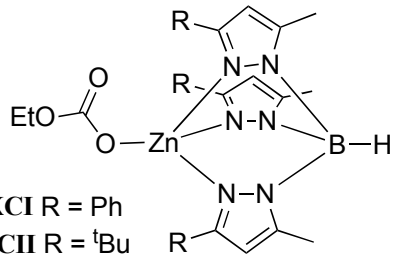

XCI R = Ph
XCII R = ^{t}Bu

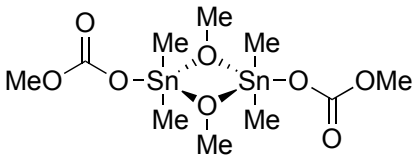

XCIII

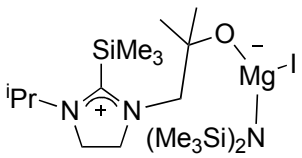

XCIV

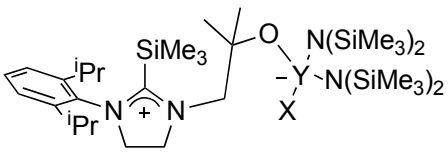

XCV: X=I
XCVI: X=Cl

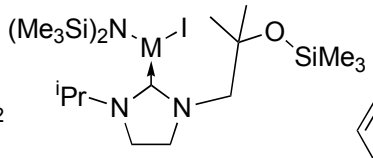

XCVII: Mg
XCVIII: Zn

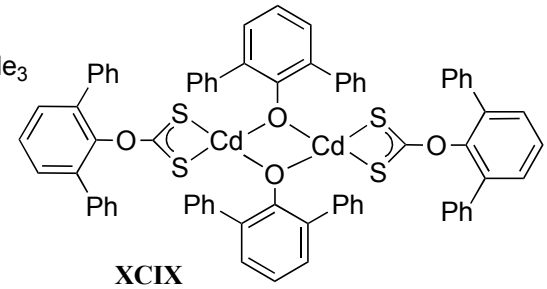

XCIX

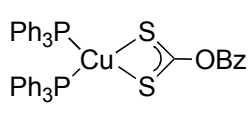

C

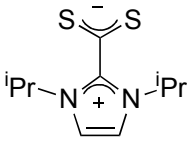

CI

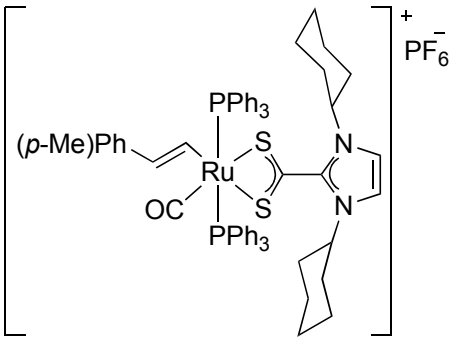

CII

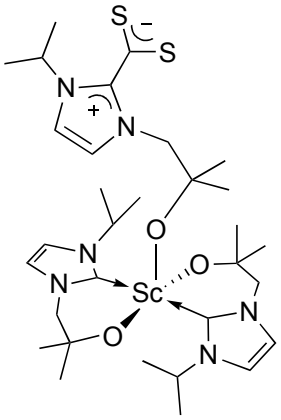

CIII

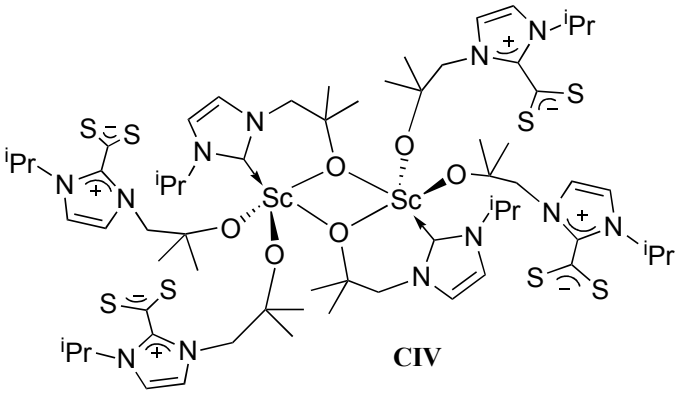

CIV

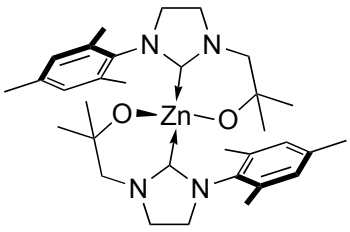

CV

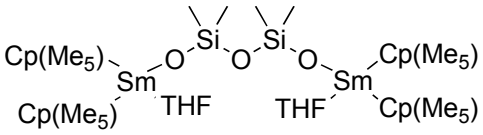

CVI

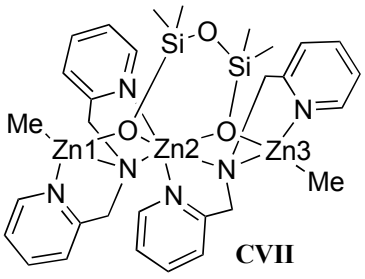

CVII

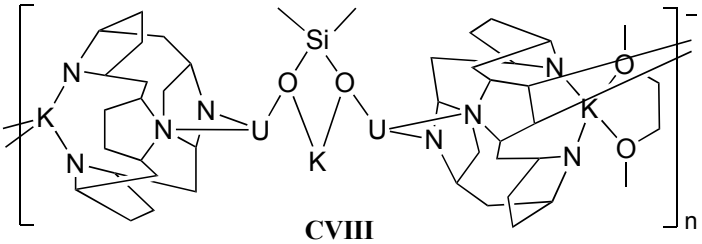

CVIII

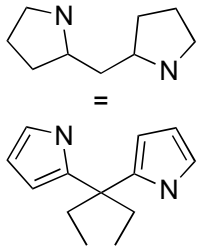

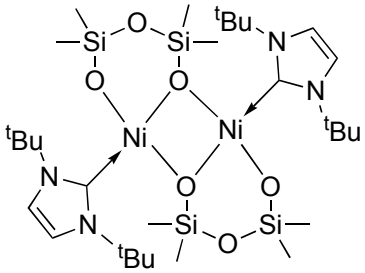

CIX

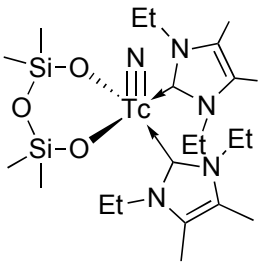

CX

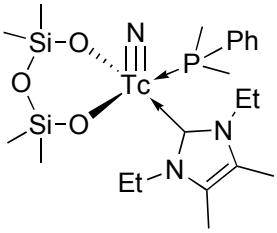

CXI

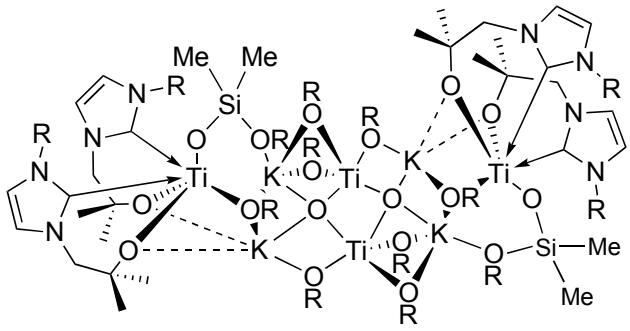

CXII

R = ^{i}Pr

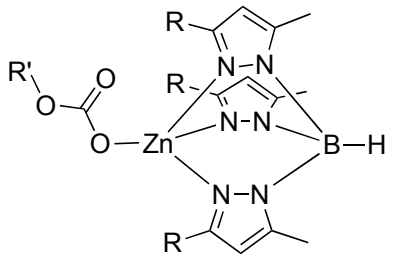

CXIII: R=^{t}Bu, R'=Me
CXIV: R=(*p*-^{i}Pr)Ph, R'=Me
CXV: R=(*p*-^{i}Pr)Ph, R'=Et
CXVI: R=Ph, R'=Me

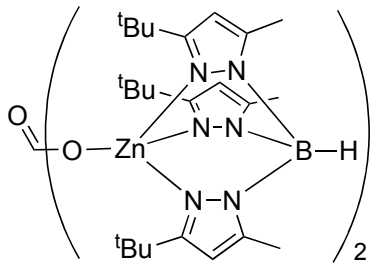

CXVII

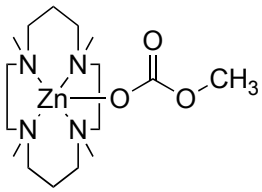

CXVIII

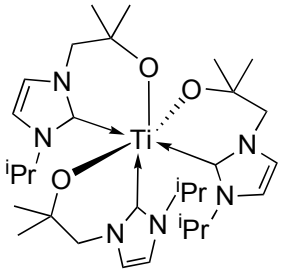

CXIX

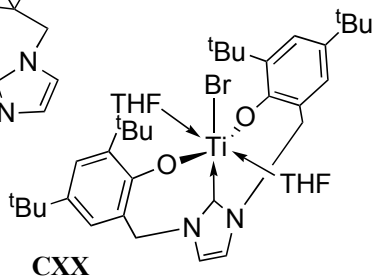

CXX

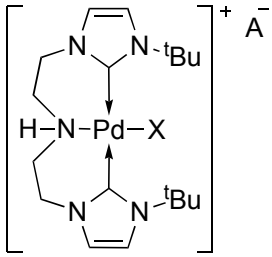

CXXI: X=Cl, A=Cl
CXXII: X=MeCN, A=2BF_4

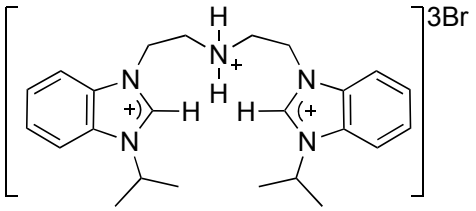

CXXIII

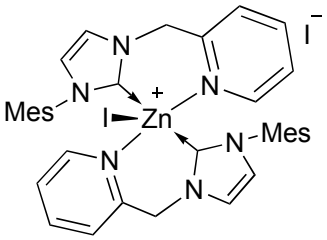

CXXIV

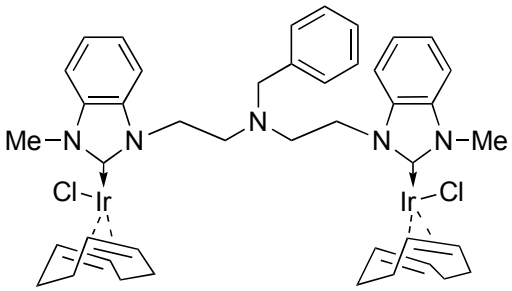

CXXV

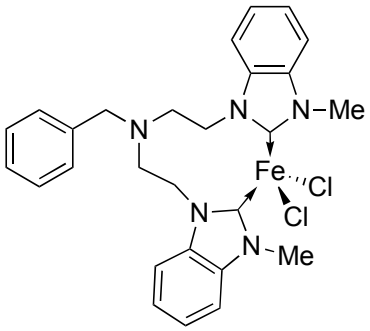

CXXVI

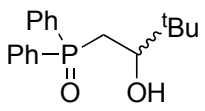

1

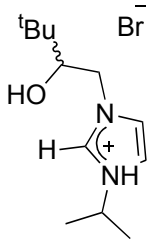

2

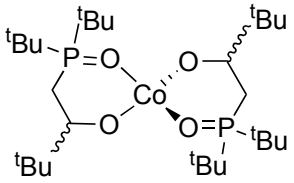

3

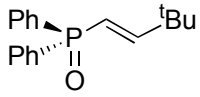

4

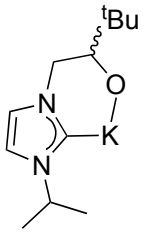

5

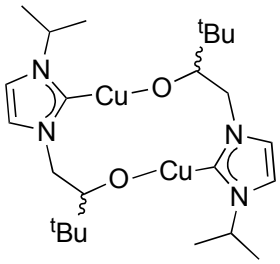

6

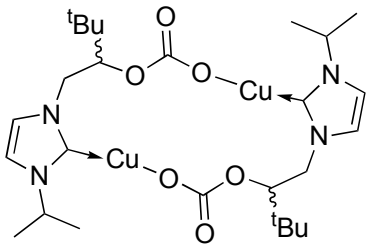

7

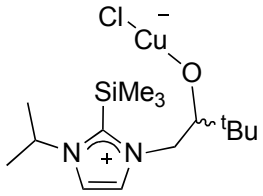

8

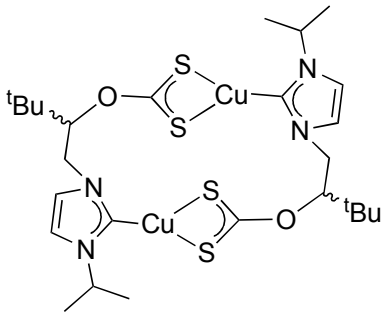

9

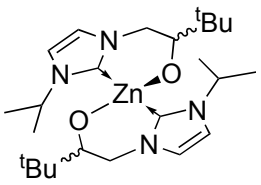

10

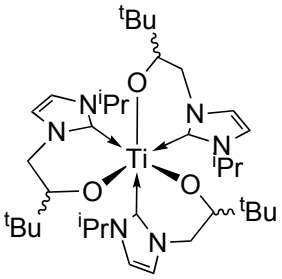

11

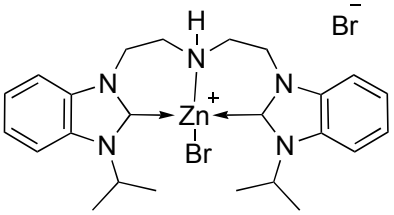

12

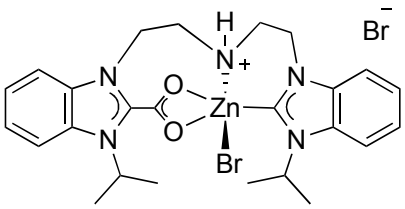

13

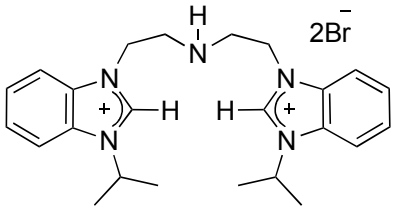

14

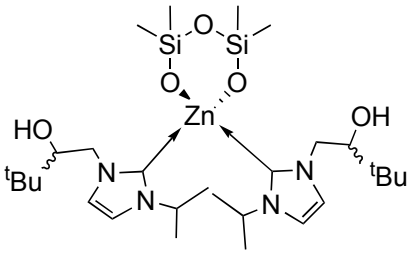

15

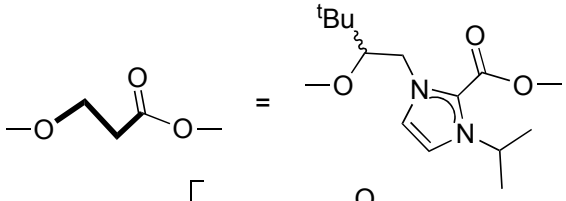

16a

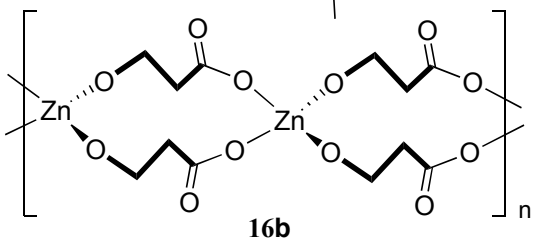

16b